THE DEVELOPMENT OF A WATER QUALITY MODEL FOR BALTIMORE HARBOR, BACK RIVER, AND THE ADJACENT UPPER CHESAPEAKE BAY

Prepared by

Harry V. Wang, Hui Liu and Kyeong Park

A Report to the

Maryland Department of the Environment
Technical and Regulatory Service Administration
Montgomery Business Park
1800 Washington Boulevard, Suite 540
Baltimore, MD 21230

Special Report No. 386
in Applied Marine Science and Ocean Engineering

School of Marine Science/Virginia Institute of Marine Science
The College of William and Mary in Virginia
Gloucester Point, VA 23062

May 2004

TABLE OF CONTENTS

LIST OF TABLES AND FIGURES

TABLES Page

FIGURES Page

*CBP: Chesapeake Bay Program, US EPA office

*MDE: Maryland Department of the Environment

I. INTRODUCTION

A. Background

Eutrophication, defined as the over-enrichment of systems by excess allochthonous nutrient inputs and autochthonous recycling of nutrients, has increasingly become an issue in many coastal and estuarine systems of the world. Excessive nutrient input can cause degradation of water quality and disruption of a healthy ecosystem. In the Chesapeake Bay, for example, the impacts have been documented which include: (1) increase of phytoplankton production (Boynton, 1982; Malone et al., 1988; Jordan et al., 1991a,b), (2) decrease of dissolved oxygen (Taft et al., 1980; Officer et al., 1984), (3) demise of submerged aquatic vegetation (Kemp et al., 1984), and (4) declines of commercially and recreationally important organisms (Nixon, 1981; Kemp et al., 1984). Due to its wide spread effects, the eutrophication and the associated degradation of water quality have received considerable attention from federal, state, regional and local agencies. It also poses a challenge to the scientific community as an intricate problem that requires multi-discipline approach, such as marine ecology, chemistry, biology, geology, and physics.

For several decades, the Upper Chesapeake Bay and its tributaries such as Baltimore Harbor and Back River often show signs of eutrophication and nutrient over-enrichment (Magnien et al., 1993; Robertson, 1977; Boynton et al., 1998). Examples of persistent anoxic/hypoxic conditions were observed regularly at the deep channel waters in the Upper Chesapeake Bay and Baltimore Harbor, while some of the highest chlorophyll-a concentrations were observed in the Back River. In order to better understand the processes that cause the low dissolved oxygen and the high chlorophyll in the region, a water quality model framework was developed for Baltimore Harbor, Back River and the adjacent Upper Chesapeake Bay. The modeling framework consists of a three-dimensional hydrodynamic model CH3D, water quality model, CE-QUAL –ICM,

and a sediment process model. The models, when properly calibrated, can provide a systematic, rational, and descriptive framework for the analysis of existing problems as well as predictive capability that cannot be achieved by measurements alone. Furthermore, the modeling framework can provide environmental managers a proper tool for proposing appropriate management, planning and remedial actions.

B. Description of Study Area and Previous Works

(1) The Upper Chesapeake Bay

The Upper Chesapeake Bay is defined as the region extending from the mouth of the Susquehanna River seaward to the mouth of the Patuxent River (Fig. 1). It consists of the mainstem bay, a host of tributaries and embayments. The mainstem is roughly 130 km long, 5 to 20 km wide, and the depth ranges from 2 to 29 m.

The depletion of dissolved oxygen at waters beneath the pycnocline during late spring and summer is a well-known phenomenon for the mainstem of the Upper Chesapeake Bay. The bottom water hypoxia or anoxia occurs at recurrent, predictable time intervals (Taft et al., 1980; Officer et al., 1984; Seliger et al., 1985). A summary report concluded the volume of anoxic bay water increased by an order of magnitude from 1950 to 1980 (Flemer et al., 1983). While the bay itself has a natural propensity for oxygen depletion due to the basin morphology and estuarine circulation (Boicourt, 1992; Malone et al., 1988), it is widely accepted that excess phytoplankton growth beyond the assimilation capacity of the Bay has caused a worsening of oxygen depletion (Harding et al., 1992b; Boynton et al., 1982; Kemp and Boynton, 1984).

The phytoplankton bloom is also a well-known, recurrent phenomenon in the Chesapeake Bay, where considerable research in recent years has been devoted to understanding the spatial, and temporal variations of phytoplankton and nutrient dynamics (Boynton et al., 1982; Malone et al., 1983; Malone et al., 1988; Fisher et al., 1988; Conley and Malone, 1992; Glibert et al., 1995; Fisher et al., 1999). The spring

blooms dominated by diatoms are found as a common feature of the annual phytoplankton cycle in the temperate aquatic system including the Chesapeake Bay (Malone et al., 1983; Fisher et al., 1988; Glibert et al., 1995). In Chesapeake Bay, the amount of accumulated chlorophyll a is highly related to the nitrogen loading mostly from the Susquehanna River (Boynton et al., 1982; Malone et al., 1988). In late spring, a typically rapid transition from a diatom-dominated community to a cyanobacteria- and microflagellate- dominated summer community has been documented (Malone et al., 1988). Both phosphorus and silicon limitation is suggested to be responsible for the collapse of the spring bloom (Fisher et al., 1992; Conley and Malone, 1992).

The spring bloom in the Chesapeake Bay usually commences in February, reaches a maximum in April, and ends in May (Malone et al., 1988; Cerco and Cole, 1994). In some years, high chlorophyll a concentrations have been documented near the bottom rather than the surface of the water column. For example, Malone et al. (1988) found most chlorophyll were located in the bottom layer below the euphotic zone during the spring blooms in 1985 and 1986. Also, concentrations of chlorophyll a in near-bottom waters exceeded those of the surface layer in the 1990 spring bloom (Glibert et al., 1995). So far, the mechanism that causes the occurrence of viable algae at great depth, in the absence of light, still remains unexplained except for the suggestion that much of the chlorophyll a was advected by an upstream flow of bottom water (Malone, 1988).

(2) Baltimore Harbor

Baltimore Harbor is located on the west side of Upper Chesapeake Bay about 160 miles from the Virginia Capes at the entrance to the Bay (Fig. 1). It is part of the 15 miles tidal region of the lower Patapsco River. Natural water depths in the Harbor are generally less than 20 feet except for the main navigation channel maintained by the U.S. Army Corps of Engineers at the depth of 50 feet. The tidal range in the Harbor is approximately one foot. The only other sizable streams that enter the Harbor directly are Jones Falls and Gwynns Falls. The earliest comprehensive report (Garland, 1952) concluded water circulation and exchange within the region are generally regulated by

local wind forces which overwhelm the real currents driven by river and tidal forces. The existence of a three-layered circulation in Baltimore Harbor was inferred by Pritchard and Carpenter (1960), based on salinity and dye distributions. Later, a hydrodynamic study done by Boicourt et al. (1982) confirmed the existence of the three-layer density-driven circulation within Baltimore Harbor. Several recent studies in Baltimore Harbor have been concentrated on contaminant distributions at the bottom sediments and the associated pathway (Sinex and Helz, 1982; Bieri et al., 1982; Sanford et al., 1996).

Relatively few studies have been carried out focusing on the water quality in Baltimore Harbor. The Chesapeake Bay Water Quality Monitoring Program has recorded measurements in the Patapsco River indicating anoxic and hypoxic events occur during summer months (Weaver, 1995; Wang et al., 2001). Increased algal blooms have been found to occur every warm season of the year in the water column (Wang et al., 2001). Sellner et al. (2001) also documented high phytoplankton biomass in the Patapsco River estuary (Baltimore Harbor) with more than 60% of the phytoplankton assemblage comprised of dinoflagellates during the summer months. He concluded that it is high nutrient concentrations, low turbulence and minimal berbivory that help autotrophic dinoflagellates be selected in the system.

(3) Back River

Back River is a relatively smaller estuary located further north along the western shoreline (Fig. 1). Average depths of the Back River estuary are approximately 25 feet (near the mouth), 9 feet (middle estuary), and 5 feet (upper estuary). The tidal range in the estuary is approximately 1.2 feet (Maryland Environmental Service, 1974).

For decades, clear indications of extreme eutrophication in the Back River were documented (Robertson, 1977). Some of the highest chlorophyll a concentrations observed in the entire Chesapeake system was recorded in Back River (Boynton et al., 1998). For example, chlorophyll a concentrations can reached 325.0 μg/l at the surface water and 400 μg/l at the bottom water in the upstream portion of the Back River (Wang

et al., 2001). Although large diel excursion of DO was documented, hypoxia/anoxia are rarely occurred in Back River (Boynton et al., 1998).

Based on recent environmental evaluation of Back River system conducted by Boynton et al. (1994,1997), it indicated that the nutrient fluxes released from the sediment in Back River are high to very high compared with other areas of the Chesapeake (Boynton et al., 1998). The released dissolved inorganic phosphorus fluxes, in particular, are large enough to be comparable to those observed in regions of the main Bay during the warm months of the year where bottom waters are hypoxic (Boynton et al., 1998). This is counter-intuitive to the conventional wisdom that major phosphate flux release from the sediment is closely related to the anoxic conditions in the water column (Mortimer, 1941 and1942). Does it imply that there are other triggering mechanisms that cause a large phosphorus release from the sediment in the Back River? Was the phosphorus cycle in the Back River unusual?

C. Requirement for the Present Study

Supported by EPA Chesapeake Bay program and Army Corps of Engineering, a Chesapeake Bay-wide hydrodynamic and water quality model has been developed (Cerco and Cole,1994). Their efforts provide a credible representation of the historical and contemporary water quality condition in the Bay and tributaries. Despite their success, the limitation for use in the Upper Bay, Baltimore Harbor and Back River are apparent. First, the resolution of the Bay-wide grid is not sufficient to resolve important features in the locals such as Back River geometry, the Hart-Miller Island, the deep channel in the Baltimore Harbor, to name a few. Secondly, there are specific technical issues identified in the Upper Bay, Baltimore Harbor, and Back River that require special attention and additional modeling efforts. The three technical issues identified are described as follows:

(1) The seasonal high chlorophyll a concentration in the bottom water of the Upper Chesapeake Bay.

In the mainstem proper of the Upper Chesapeake Bay (from Patuxent River mouth up to the Bay Bridge near Annapolis), there is convincing evidence indicating subsurface chlorophyll a maximum occurring regularly during each spring season (see section III-1 "analysis of observation data"). While it is not uncommon to find spring algal bloom at the surface layer, it is highly unusual to find high chlorophyll a concentration at the bottom where light is limited. We make the assumption that while some of the chlorophyll was advected from the downstream stations of Chesapeake Bay, the settling phytoplankton from the surface layer of the water column resuspended by the bottom shear stress is another source contributing to the high chlorophyll a concentrations at the bottom in spring.

(2) The low DO condition in the Baltimore Harbor.

It is well known that the anoxic water exists in the main Bay each summer. In Baltimore Harbor, anoxic conditions also occur each year at the bottom of the deep ship channel as well as all the tributaries such as the Inner Harbor and the Middle Branch. The period of the Harbor anoxic condition generally starts in the early spring and ends in the late fall, which is longer than that in the main Bay (for example, comparison with the corresponding station at CB3.2). This leads to the hypothesis that the origin of the low DO in the Harbor is not resulting from the intrusion of the Bay anoxic water, but rather it is an internal process of the Harbor.

(3) The abnormally high algal bloom in the Back River.

In the Back River, abnormally high chlorophyll a concentrations occur. Concentrations (usually as high as 200-300 μg/l) were observed in the upstream stations, which are among the highest in the entire Chesapeake Bay. In contrast, the chlorophyll a level in Baltimore Harbor located just 10 km south is only 50-100 μg/l, although the latter is already relatively high as compared to those in the Chesapeake Bay. Why is chlorophyll a so high in the Back River? Based on the nutrient flux measurements, we found that the phosphorus flux from the sediment is very high which is the potential source for fueling the phytoplankton production. A more intriguing question is why the phosphorus flux

from the sediment can be high when the overlying oxygen concentration never falls below 4 mg/l? After examining the observed pH value, we made the hypothesis that the high pH value in the overlying water enhances the sediment phosphorus release, which in turn supports the recurrent abnormally high algal bloom.

Given the technical issues illustrated above, following are hypothesis that are made and envisioned to meet the technical challenge:

I. In the Upper Chesapeake Bay, high chlorophyll a concentrations were advected from the downstream, as well as falling from the surface and resuspended from the bottom.
II. The anoxic condition in Baltimore Harbor is caused by the internal eutrophication process rather than from intrusion of the Bay water.
III. In the Back River, the high chlorophyll a concentrations is the result of enhanced aerobic sediment phosphorus release triggered by high pH values.

The further development of hydrodynamic/water quality models follows Cerco and Cole (1994)'s general direction. It is based on formulated ideas, and set up for simulation by the high speed computer. The model results were calibrated and verified by the observation data, and used further for testing and verifying of above hypotheses. The organization of the rest of the report starts with Approach in Chapter II, Model Kinetics in Chapter III, Water Quality Model Calibration in Chapter IV, Sensitivity Analysis in Chapter V. The Discussion and Conclusion are in Chapter VI, Chapter VII, respectively.

II. APPROACH

A. Analysis of Observation Data

(1) Water Quality Monitoring Data

EPA Chesapeake Bay Program Office has been collecting monitoring data since June 1984 from stations throughout the Chesapeake Bay. Surveys have been conducted

semi-monthly in March through October and monthly in the remaining months. Of Bay-wide stations, forty stations fall inside the present modeling domain (Fig. 2) including one station in Baltimore Harbor and one in Back River. Chesapeake Bay Program monitoring data from these forty stations in 1992-97 are referred to as CBP Monitoring Data in this paper. The water quality parameters used in the present study are listed in Table 1.

Additionally, Maryland Department of the Environment (MDE) provided spatially intensive field data for both Baltimore Harbor and Back River. The water column data at twenty-four stations were collected from February 1994 to May 1995 by the Maryland Department of the Environment, and twenty-seven data stations from June to December 1997 were monitored by the Baltimore City Department of Public Works (Environmental Resources Management, 1997 and 1999) (Fig. 3). The intensive water column data set is referred to as MDE Monitoring Data. The description of conventions used in figures can be found in Appendix A.

Upper Chesapeake Bay

A temporal distribution of chlorophyll a for surface and bottom from station CB4.4 upstream to CB3.2 in the Upper Chesapeake Bay is shown in Fig. 4. The surface chlorophyll a concentration time series is characterized as having multiple peaks, often prolonged in warmer seasons. Most of the time, the magnitude of the surface chlorophyll a concentrations are less than 30 μg/l except CB3.3 where the surface chlorophyll a reached as high as 123.7 μg/l. Spatially, the magnitude of the surface chlorophyll a maximum seemed to decrease both downstream and upstream of CB3.3.

The temporal variation patterns of chlorophyll a at the bottom are, however, quite different from those of the surface. For example, at station CB4.4, the bottom high chlorophyll a usually commences in February, reaches the maximum in March, and drops precipitously in April. The bottom chlorophyll a values are characterized by a singular distinguished spike just in a very short time with the peak as high as 46 μg/l; but in other seasons the chlorophyll a concentration are almost zero. The same patterns also hold for

other stations such as CB4.3C, CB4.2C, CB4.1C, CB3.3C, and CB3.2. Spatially, the magnitude of bottom chlorophyll a peaks are strongest at CB3.3 (shown by data from 1992, 1995, and 1996), with a gradually decreasing downstream trend and a suddenly decreasing upstream trend (as shown in CB3.2). Also, compared with those of the surface, the bottom chlorophyll a concentration is much higher from March to April, and much lower from May to October.

Baltimore Harbor

In Baltimore Harbor, the data from the long-term monitoring station WT5.1 (Fig. 2) shows the surface chlorophyll a concentrations ranged from 0.3 to 273.4 μg/l from 1992 to 1997 (Fig. 5). Most of the time, chlorophyll a concentrations were less than 100 μg/l in the surface water with only a few values higher than 100 μg/l in 1994 and 1995. Surface chlorophyll a appeared to have a strong seasonal pattern: high during the warm season and low during the cold season. From 1992 to 1995, the surface chlorophyll a were characterized by prolonged, multiple peaks from late spring to late fall. In 1996 and 1997, the surface chlorophyll a were characterized by two distinguished peaks: one in spring and the other one in fall. The bottom chlorophyll a concentrations ranged from 0.3 to 83.4 μg/l and were generally much lower compared with surface chlorophyll a concentrations, except in 1995 and 1996 when the bottom chlorophyll a spiked around April. The seasonality was not obvious for the bottom chlorophyll a in Baltimore Harbor. The chlorophyll a both at the head and at the mouth (Fig. 6) appeared to have the same trend as the middle portion of the Harbor (WT4.1): high in the surface and low in the bottom.

The dissolved oxygen data at station WT5.1 ranged from 6.8 to 17.7 mg/l in the surface water and from zero to 12.8 mg/l in the bottom water. Seasonality was identified both in the surface water and the bottom water, but a more evident seasonal variation was observed in the bottom water with winter peaks and summer minimum for every year. The bottom water hypoxia/anoxia condition usually commenced in May and ended in October for the middle portion of Baltimore Harbor (Fig. 5). However, the anoxic conditions were more severe at the head portion of the Harbor. Fig. 6 shows that in the

Inner Harbor (M28), the hypoxia started as early as February and did not end until October. At the same time, anoxic conditions even extended to the surface water in the summer. Fig. 6 also shows that the anoxic condition at the mouth of the Harbor (M08) was less severe than that in the Inner Harbor.

Back River

At station WT4.1 of the Back River (Fig. 7), the surface and bottom chlorophyll a generally exhibit the same variational pattern due to the shallowness of the river. Chlorophyll a concentrations ranged from 6.0 to 272.0 μg/l with the average value of 90.1 μg/l. Chlorophyll a concentrations appear to have a seasonal pattern: high during the warm season and low during the cold season. For most of the year, annual chlorophyll a appeared to have two blooms: one in spring and the other in summer or fall. The spring bloom is characterized by the first singular peak of the year, and the summer/fall blooms were characterized by multiple peaks and prolonged time interval. Also from Fig. 7, dissolved oxygen concentrations in the Back River (WT4.1) ranged from 3.9 to 18.8 mg/l in both surface and bottom water. Seasonal variation of DO was not as strong as in Baltimore Harbor and the adjacent Upper Chesapeake Bay. Hypoxia was not found over the period of 6 years.

The MDE monitoring data provide supplemental information about the spatial distribution of chlorophyll a in Back River (Fig. 8). The extremely high chlorophyll a is identified again in the upstream of the Back River. For example, at the most upstream portion (M05) of the Back River, the chlorophyll a ranged from 9.3 to 373.4 μg/l with the average of 160 μg/l. At the station a little downstream of M05 (M04), the data ranged from 6.0 to 341.2 μg/l with the average of 130 μg/l. The chlorophyll a concentrations were lower at the downstream portion of WT4.1. For example, the chlorophyll a concentrations at the station further downstream of WT4.1 (M02) ranged from 9.5 to 293 μg/l with the average value of 92.2 μg/l, and the data at the mouth of the Back River ranged from 2.7 to 146.6 with an average of 35.0 μg/l (M02 and M01 shown in Fig. 8). Overall, the chlorophyll a concentrations decreased from upstream to downstream in the Back River.

(2) Benthic Flux Data

The sediment flux data collected for Baltimore Harbor and Back River by Boynton et al. (1998) is referred to as Benthic Flux Data. Measurements were made for three stations in Back River and six stations in Baltimore Harbor in 1994, 1995 and 1997 (Fig. 3). A detailed description of field surveys can be found in Boynton et al. (1998). Figs. 9 and 10 show the measured sediment-water exchange rates for dissolved oxygen, ammonium, nitrate, dissolved phosphate and dissolved silica at Witch Coat Point (WCPT) in the Back River and Curtis Bay (CTBY) in Baltimore Harbor, respectively. Although all the data were collected in the warmer season from June to November, the relatively smaller values in November versus those in August most likely indicate the seasonal variation of the sediment release.

Table 2 shows some simple statistical results for the sediment fluxes. The negative values indicate that the fluxes go to the sediment from the water column, such as nitrate and sediment oxygen demands; the positive values means the nutrients come from the sediment such as ammonia, phosphate, and dissolved silica. The mean ammonia flux in Back River indicated the increased trend from the downstream station WCPT to the upstream station DPCK, whereas the mean value of phosphate flux indicated the decreased trend from downstream to upstream. Also, the mean values of all the fluxes in Back River are equal or larger than those for most of the stations of the Baltimore Harbor except the station in the Inner Harbor (INHB).

B. Point and Non-Point Source Loading

Point Source Loads

The Maryland Department of the Environment provided monthly loading data from 1992-97 for twenty-two major point source facilities (municipal and industrial) discharging wastewater into the present modeling domain. The outfall locations are shown in Fig. 11. Currently, among the 28 point source outfalls in the Upper Bay, there are five major facilities discharging wastewater into Baltimore Harbor (the Bethlehem

Steel facility has seven outfalls PP7-PP13), and two discharging into the Back River. For each of twenty-eight point sources and each of the variables, the loads are evenly distributed in the vertical of the adjacent water cells.

Non-point Source Loads

When overlapped with the present modeling domain, the watershed model maintained by EPA Chesapeake Bay Program Office has four segments contributing to fall-line loads and nineteen segments contributing to below-fall-line nonpoint source loads (Fig. 12). Since the Maryland Department of the Environment has a refined watershed model for Baltimore Harbor and Back River, the non-point source loads from MDE's watershed model is used for Back River and Baltimore Harbor instead. Both of the watershed model provided daily outputs from 1992 to 1997.

Annual mean fall-line loads from four rivers (Susquehanna, Patapsco, Gunpowder and Choptank) are shown in Fig. 13. The Susquehanna River, which contributes 62% of the gauged freshwater inflow to Chesapeake Bay (Cerco and Cole, 1994), is by far the most dominant source of fall-line loads for carbon, nitrogen, phosphorus and suspended solids. For each of the below fall-line watershed model segments, the loads are evenly distributed into adjoining surface cells of the water quality model.

Loading Characteristics

For the entire Upper Chesapeake Bay, fall-line loading (FL) is the most important source of carbon, nitrogen, phosphorus, and suspended solids (Fig. 14). Both point (PS) and below fall-line non-point source (NPS) loadings are important sources for carbon and nitrogen, while below-fall-line non-point source loadings is the second most important source for phosphorus and total suspended solids. Relatively, atmospheric (ATM) deposition is negligible.

In contrast, from Figs. 15 and 16, it is clear that, for the Back River and Baltimore Harbor, point source loadings is the dominant source for carbon, nitrogen, and phosphorus. Point source, below fall-line non-point sources, and fall-line loadings are

important for TSS in Baltimore Harbor. In Back River, both point source and below-fall-line non-point sources are important.

C. Model Framework

The three-dimensional time-variable eutrophication model package (CE-QUAL-ICM), which is internally coupled with a benthic sediment process model and externally linked to a hydrodynamic model (CH3D-WES), is described in this section.

(1) Hydrodynamic Model

The three-dimensional, time-variable hydrodynamic model CH3D-WES (Curvilinear Hydrodynamic in Three Dimensions) was developed at the US Army Engineer Waterways Experiment Stations. As its name indicated, CH3D-WES makes hydrodynamic computations on a curvilinear or boundary-fitted planform grid that provides enhancement to fit the deep navigation channel and the irregular shoreline. The numerical grid employed in the present study domain is shown in Fig. 12. There are 3,758 active horizontal cells and a maximum of 19 vertical layers, resulting in 16,149 computational cells. The grid resolution is 1.52 m in the vertical, approximately 0.2 km laterally and 0.4 km longitudinally. Physical processes that are modeled include tides, wind, density effects (salinity and temperature), freshwater inflows, turbulence, and the effect of the earth's rotation. The inputs require spatial distribution of salinity and temperature fields as initial conditions, time series of tidal elevation, salinity, temperature, and river discharge as the open boundary conditions and the meteorological forcings at the free surface. The outputs include three dimensional velocities, water surface elevation, salinity, temperature, and the turbulent mixing coefficients, which in turn are used to drive the water quality model. The detailed description can be found in Johnson et al. (1991).

(2) Water Column Eutrophication Model

A three-dimensional time-variable eutrophication model package including water column eutrophication and benthic sediment process models, the Corps of Engineers

Water Quality Integrated Compartment Model (CE-QUAL-ICM) (Cerco and Cole, 1994), originally developed for the Chesapeake Bay, is further modified and employed in the present study. In the water column, the present model has twenty-t The total phosphorus wo model state variables (Table 3), which constitute five interacting systems: i.e., phytoplankton dynamics, nitrogen cycle, phosphorus cycle, silicate cycle, and oxygen dynamics. The water column eutrophication model solves the mass-balance equation for each state variable and for each model cell. A detailed description of the water column eutrophication model can be found in Cerco and Cole (1994).

(3) Sediment Flux Model

The sediment flux model developed by DiToro and Fitzpatrick (1993) and coupled with CE-QUAL-ICM for Chesapeake Bay water quality modeling is used in the present model application. The model state variables and the resulting fluxes in this sediment flux model are listed in Table 4. Complete model documentation of the sediment flux model can be found in DiToro and Fitzpatrick (1993). A brief description of the model is given in this section with emphasis on the coupling with the water column eutrophication model.

The sediments in this model are represented by two layers: the upper aerobic layer (Layer 1) and the lower anoxic layer (Layer 2). The sediment process model is coupled with the water column eutrophication model through depositional and sediment fluxes. Firstly, the sediment model is driven by net settling of particulate organic matter from the overlying water column to the sediments (depositional flux). Then, the mineralization of particulate organic matter in the lower anoxic sediment layer produces soluble intermediates, which are quantified as diagenesis fluxes. The intermediates react in the upper oxic and lower anoxic layers, and portions are returned to the overlying water column as sediment fluxes. Computation of sediment fluxes requires mass-balance equations for ammonium, nitrate, phosphate, sulfide/methane, and available silica. Mass-balance equations are solved for these variables for both the upper and lower layers.

(4) Linkage Between Hydrodynamic and Water Quality Models

The hydrodynamic model CH3D is externally linked with the water column eutrophication CE-QUAL-ICM model. Physical transport processes computed by the hydrodynamic model are processed and stored in binary files, which are subsequently used by the water quality model to compute advective and turbulent diffusive transport terms. Of the stored information, time-invariant geometric information includes the surface areas, the horizontal box dimensions in both directions, the cross-sectional areas of all flow faces and the box volumes beneath the surface layer. Time-varying information includes the cross-sectional areas of flow faces in the surface layer, diffusivities through all vertical flow faces, horizontal and vertical flow rates through all flow faces, and external volume inflows. In the present model application, two-hour averages of time-varying parameters are processed and transferred to the water quality model. The validity of the linkage is demonstrated by comparing the salinities computed by hydrodynamic model with those by water quality model. A detailed description of the theory can be found in Dortch (1990) and Dortch et al. (1992).

III. MODEL KINETICS

A. Dissolved Oxygen

The central issues in the eutrophication model are computation of dissolved oxygen and algal biomass. Dissolved oxygen is considered as an indicator of the health of estuarine systems and also is necessary to support the life functions of higher organisms. Phytoplankton productivity provides the major source of food energy for most of the marine ecosystem through its primary production of carbon. Excessive primary production, however, is detrimental since its decomposition in the water and sediments consumes oxygen and hence degrades the water quality of the living condition. The dissolved oxygen process and phytoplankton kinetics are detailed in the following sections. Formulation of the remaining eutrophication processes can be found in Cerco and Cole (1994) and Park et al. (1995).

(1) Dissolved oxygen process

Effects of algae on dissolved oxygen

Algae produce oxygen during photosynthesis and consume oxygen through respiration. The quality produced during photosynthesis depends on the form of nitrogen taken up. Since oxygen is released in the reduction of nitrate (NO_3), more oxygen is produced, per unit of carbon fixed, when NO_3 is the algal nitrogen source than when ammonia NH_4 is the source. When NH_4 is the nitrogen source, one mole of oxygen is produced per mole carbon dioxide fixed. When NO_3 is the nitrogen source, 1.3 moles oxygen are produced per mole carbon dioxide fixed. The equation that describes the effect of algae photosynthesis on DO in the model is:

$$\frac{\delta DO}{\delta t} = \sum_x \left(\left(1.3 - 0.3\,PN_x\right) P_x \right) AOCR \cdot B_x \qquad \text{(IV-1)}$$

PN_x = algal group x preference for ammonium uptake
P_x = production rate of algae group x (day^{-1})
AOCR = DO-to-carbon ratio in respiration (2.67 g O_2 per g C)
B_x = algal biomass (g C m^{-3})

As employed here, basal metabolism is the sum of all internal processes that decrease algal biomass. A portion of the metabolism is respiration and may be viewed as reversal of production. In respiration, carbon and nutrients are returned to the environment accompanied by the consumption of DO. Respiration cannot proceed in the absence of DO. Basal metabolism cannot decrease in proportion to oxygen availability. Formulation of this process is described as:

$$\frac{\delta DO}{\delta t} = \sum_x \left(-\frac{DO}{KHR_x + DO} BM_x \right) AOCR \cdot B_x \qquad \text{(IV-2)}$$

KHR_x = half-saturation constant of DO for algal DOC exudation (g O_2 m^{-3})

BM_x, = basal metabolism rates for algae group x (day^{-1})

Effects of nitrification on dissolved oxygen

Nitrification is a process mediated by specialized groups of autotrophic bacteria that obtain energy through the oxidation of ammonia to nitrite and oxidation of nitrite to nitrate. A simplified expression for complete nitrification is:

$$NH_4^+ + 2O_2 \rightarrow NO_3^- + H_2O + 2H^{2+} \quad \text{(IV-3)}$$

The equation indicates that two moles of oxygen are required to nitrify one mole of ammonia into nitrate. The simplified equation is not strictly true, however. Cell synthesis by nitrifying bacteria is accomplished by the fixation of carbon dioxide so that less than two moles of oxygen are consumed per mole ammonium utilized (Wezernak and Gannon, 1968). In this study, nitrification is modeled as a function of available ammonium, dissolved oxygen, and temperature:

$$NT = \frac{DO}{KHONT + DO} \frac{NH4}{KHNNT + NH4} f(T) \cdot NTM \quad \text{(IV-4)}$$

NT = nitrification rate (gm N m^{-3} day^{-1})
NTM = maximum nitrification rate at optimal temperature (gm N m^{-3} day^{-1})
KHONT = half-saturation constant of DO required for nitrification (gm DO m^{-3})
KHNNT = half-saturation constant of NH4 required for nitrification (gm N m^{-3})

Therefore, the effect of nitrification on DO is described as follow:

$$\frac{\delta DO}{\delta t} = -AONT \cdot NT \quad \text{(IV-5)}$$

AONT = mass DO consumed per mass ammonia nitrified (4.33 gm DO gm^{-1} N)

Effects of surface reaeration on dissolved oxygen

Reaeration occurs only in the model cells that form the air-water interface. The effect of reaeration is:

$$\frac{\delta DO}{\delta t} = \frac{K_R}{\Delta z_s}(DO_S - DO) \qquad \text{(IV-6)}$$

K_R = reaeration coefficient (m day $^{-1}$)

Δz_s = model layer thickness (m)

DO_S = dissolved oxygen saturation concentration (gm DO m^{-3})

Saturation dissolved oxygen concentration DO_S is computed (Genet et al., 1974):

$$DO_S = 14.5532 - 0.38217\ T + 0.0054258\ T^2 - \frac{S}{1.80655}\left(0.1665 - 5.866\ 10^{-3}\ T + 9.796\ 10^{-5}\ T^2\right) \qquad \text{(IV-7)}$$

S = salinity (ppt).

Effects of Chemical Oxygen demand on Dissolved Oxygen

In the present model, chemical oxygen demand represents the reduced materials that can be oxidized through inorganic means. The source of chemical oxygen demand is sulfide in saline water and methane in fresh water released from benthic sediment process model. The released chemical oxygen demand is oxidized upon contact with dissolved oxygen in the water column. The kinetic equation showing the effect of chemical oxygen demand (bottom cells only) is:

$$\frac{\delta DO}{\delta t} = - \frac{DO}{KHO_{COD} + DO} K_{COD} \cdot COD \qquad \text{(IV-8)}$$

COD = chemical oxygen demand concentrations (g O_2-equivalents m^{-3})
KHO_{COD} = half-saturation constant of DO for oxidation of COD (g O_2 m^{-3})
K_{COD} = oxidation rate of COD (day^{-1})
BF_{COD} = sediment flux of COD (g O_2-equivalents m^{-2} day^{-1}).

$$K_{COD} = K_{CD} \cdot \exp\left(KT_{COD}[T - TR_{COD}]\right) \tag{IV-9}$$

K_{CD} = oxidation rate of COD at reference temperature TR_{COD} (day^{-1})
KT_{COD} = effect of temperature on oxidation of COD ($°C^{-1}$)
TR_{COD} = reference temperature for oxidation of COD (°C).

Overall, the internal sources and sinks of dissolved oxygen include algal photosynthesis and respiration, atmospheric reaeration (surface cells only), heterotrophic respiration, nitrification, and oxidation of COD.

The complete kinetic equation showing sediment oxygen demand (bottom cells only) is:

$$\begin{aligned}\frac{\delta DO}{\delta t} = & \sum_x \left((1.3 - 0.3 \cdot PN_x) P_x - \frac{DO}{KHR_x + DO} BM_x \right) AOCR \cdot B_x \\ & + \lambda_1 \frac{K_R}{\Delta z_S} (DO_S - DO) - \frac{DO}{KHO_{DOC} + DO} AOCR \cdot K_{DOC} \cdot DOC \\ & - AONT \cdot NIT - \frac{DO}{KHO_{COD} + DO} K_{COD} \cdot COD + \lambda_2 \frac{SOD}{\Delta z}\end{aligned} \tag{IV-10}$$

B. Phytoplankton Kinetics

Release 1 of the water quality model had three functional groups for algae: cyanobacteria, diatoms, and greens. The cyanobacteria (blue-green algae) in the original model were to represent the bloom-forming species found in the tidal, freshwater Potomac River. The present modeling domain does not include the Potomac River.

Dinoflagellates instead are considered as a group to represent the bloom observed in the Patapsco River and north of the Bay Bridge in summer (Tyler and Seliger, 1978). They are characterized by high optimum temperature for growth. As in Release 1, diatoms are used to represent the spring bloom species characterized by their requirement of silica as a nutrient and by high settling velocity. Green algae include all algae that do not fall into the preceding two groups and are subject to relatively high grazing pressure. In the following equations, the subscript, **x**, is used to denote three algal groups: **f** for dinoflagellates, **d** for diatoms, and **g** for greens. The internal sources and sinks included are production (growth), basal metabolism (respiration and exudation), predation, and settling. The kinetic equations for algae are:

$$\frac{\delta B_x}{\delta t} = \left(P_x - BM_x - PR_x\right) B_x - WS_x \frac{\delta B_x}{\delta z} \qquad \text{(IV-11)}$$

B_x = algal biomass (g C m^{-3})

P_x, BM_x, PR_x = production, basal metabolism and predation rates of algae, respectively (day^{-1})

WS_x = algal settling velocity (m day^{-1}).

(1) Growth (Production)

Algal growth depends on nutrient availability, ambient light, and temperature. The effects of these processes are considered to be multiplicative as follow:

$$P_x = PM_x \cdot f(N) \cdot f(I) \cdot f(T) \qquad \text{(IV-12)}$$

PM_x = maximum production rate under optimum conditions (day^{-1})

f(N), f(I), f(T) = effect of sub-optimal nutrient, light intensity, and temperature, respectively.

Effect of nutrient on growth

$$f(N) = \text{minimium}\left\{\frac{NH4 + NO3}{KHN_x + NH4 + NO3}, \frac{PO4d}{KHP_x + PO4d}, \frac{SAd}{KHS_d + SAd}\right\} \quad \text{(IV-13)}$$

NH4, NO3 = ammonium and nitrate nitrogen concentrations, respectively (g N m^{-3})

PO4d = dissolved phosphate concentration (g P m^{-3})

SAd = dissolved silica concentration (g Si m^{-3})

KHN_x = half-saturation constant for algal nitrogen uptake (g N m^{-3})

KHP_x = half-saturation constant for algal phosphorus uptake (g P m^{-3})

KHS_d = half-saturation constant for silica uptake by diatoms (g Si m^{-3})

Effects of light on growth

$$f(I) = \frac{1}{KESS \cdot \Delta z} \ln\left(\frac{IH_x + I_{TOP}}{IH_x + I_{BOT}}\right) \quad \text{(IV-14)}$$

Where:

$$I_{TOP} = I_{SFC}\, e^{-KESS \cdot Z_T} \quad \text{(IV-15)}$$

$$I_{BOT} = I_{SFC}\, e^{-KESS(Z_T + \Delta z)} \quad \text{(IV-16)}$$

$$I_{SFC} = \frac{I_{TOTAL}}{FD}\frac{\pi}{2}\sin\left(\pi\frac{t_D - t_U}{FD}\right) \quad \text{(IV-17)}$$

$$KESS = KE_B + KE_{CHL} \cdot \sum_x \frac{B_x}{CCHL_x} + KE_{TSS} \cdot TSS \quad \text{(IV-18)}$$

KESS = light extinction coefficient (m^{-1})

Z_T = distance from surface to the top of model layer (m)

IH_x = half-saturation light intensity for algal growth (langleys day^{-1})

I_{TOP}, I_{BOT} = light intensities at the top and bottom of model layer, respectively (langleys day^{-1})

I_{SFC} = light intensity at surface at time t (langley day^{-1})

I_{TOTAL} = total daily light intensity at surface (langley day^{-1})

FD = fractional daylength

t_D = time of day (in fractional days)

t_U = time of sunrise (in fractional days)

KE_B = background light extinction coefficient (m^{-1})

KE_{CHL} = light extinction coefficient for chlorophyll a (m^{-1} per mg CHL m^{-3})

$CCHL_x$ = carbon-to-chlorophyll ratio in algae (g C per g CHL)

KE_{TSS} = light extinction coefficient due to TSS (m^{-1} per g m^{-3})

The effect of light on algal growth in Release 1 was simulated using the Steele function, which always results in photo-inhibition at the surface under high light intensity. To relieve photo-inhibition, a Monod-type function with half-saturation light intensity is used in present model (IV-14). Now that the present model has the total suspended solids state variable, the light extinction coefficient is expressed to consist of three terms: background extinction, algal self-shading and extinction due to total suspended solids (IV-18).

Effect of temperature on growth

$$\begin{aligned} f(T) &= \exp\left(-KTG1_x\,[T - TM_x]^2\right) \quad \text{when } T \le TM_x \\ &= \exp\left(-KTG2_x\,[TM_x - T]^2\right) \quad \text{when } T > TM_x \end{aligned} \qquad \text{(IV-19)}$$

TM_x = optimal temperature for algal growth (°C)

$KTG1_x$ = effect of temperature below TM_x on algal growth ($°C^{-2}$)

$KTG2_x$ = effect of temperature above TM_x on algal growth ($°C^{-2}$).

(2) Basal Metabolism

Basal metabolism is commonly considered to be an exponentially increasing function of temperature:

$$BM_x = BMR_x \cdot \exp\left(KTB_x [T - TR_x]\right) \quad \text{(IV-20)}$$

BMR_x = metabolic rate at reference temperature TR_x (day $^{-1}$)
KTB_x = effect of temperature on metabolism ($C^{\circ -1}$)
TR_x = reference temperature for metabolism (C°)

(3) Predation

The predation formulation is identical to basal metabolism. The difference in predation and basal metabolism lies in the distribution of the end products of these processes.

$$PR_x = BPR_x \exp\left(KTB_x (T - TR_x)\right) \quad \text{(IV-21)}$$

where BPR_x = predation rate at TR_x (day $^{-1}$)
KTB_x = effect of temperature on predation ($C^{\circ -1}$)
TR_x = reference temperature for predation (C°)

(4) Settling velocity

Species comprising the algal population of the Bay vary according to season and location. In late winter and early spring, diatom population in the Bay and lower tributaries is characterized by large species of diatom with high settling velocities. In late spring and summer, large species are replaced by populations of smaller individuals with lower settling velocities. Reported algal settling rates typically range from 0.1 to 5 m d^{-1} (Bienfang et al., 1982; Riebesell, 1989; Waite et al., 1992). In part, this variation is a function of physical factors related to algal size, shape, and density (Hutchinson, 1967). The variability also reflects regulation of algal buoyancy as a function of nutritional status (Bienfang et al., 1982; Richardson and Cullen, 1995) and light (Waite et al., 1992).

The algal settling rate employed in the model represents the total effect of all physiological and behavioral processes that result in the downward transport of phytoplankton. The settling rate employed, from 0.1 m d^{-1} to 0.9 m d^{-1}, was used in the model to optimize agreement of predicted and observed algae.

C. Sediment Flux Release and pH Dependent Function

Since the existing model under-predicted the abnormally high chlorophyll a concentrations, a hypothesis was made that the high pH value can enhance the phosphorus to release from the sediment. A literature review revealed evidence of the relationship between the pH and the phosphorus release from the sediment, as shown in Fig. xxxxx (Seitzinger, 1986). This led to the derivation of an exponential function between phosphate flux and the pH of the overlying water, given as follows:

$$BF(t) = BF_{BFM} * \{ EXP [K_{PH} * (PH(t)-PHR)\}$$

where:
t: time in Julian days;
BF: enhanced phosphorus release (g P m^{-2} day^{-1});
BF_{BFM}: calculated phosphorus release without pH impact (g P m^{-2} day^{-1});
K_{PH}: the effect of pH on phosphorus exchange rate;
PH: pH value of the overlying water;
PHR: reference pH value of the overlying water column.

IV. WATER QUALITY MODEL CALIBRATION

The general procedure for calibration is to assign the literature-available values for various coefficients and parameters initially, and then perform a series of iterative comparison between model and data. This process continues through the adjustment and tuning of the model parameters and coefficients until it is judged that a reasonable reproduction of the observed data is attained. The initial parameters used following the

values used in the Chesapeake Bay (Cerco and Cole, 1994). Later in the study, changes were made when it is deems justified and backed up by the sound technical basis. The section starts with model input, initial and boundary condition, followed by calibration for Upper Chesapeake Bay, Baltimore Harbor, and Back River, and ends with the statistical summary.

A. Model Inputs, and Initial and Boundary Conditions

(1) Input Parameters

The water quality model incorporated 138 parameter inputs and the sediment model required 99 parameter inputs. The values of the kinetic parameters found from the water quality model (Cerco and Cole, 1994) and sediment flux model (DiToro and Fitzpatrick, 1993) applied to the Chesapeake Bay serve as a starting point for the present model application. Some of the water column and sediment parameters are adjusted in the present application within the feasible range, which was determined by observation/experiments, or employed in similar models. Values of the water column parameters employed in the present study are listed in Tables 5 -10. They are related to algae, organic carbon, nitrogen, phosphorus, silica, chemical oxygen demand, and dissolved oxygen, respectively. Values for the sediment flux model parameters are listed in Table 11.

(2) Initial and Boundary Conditions

Water Column Initial Conditions

Water column initial conditions are estimated using the CBP Monitoring Data in January of 1992. The CBP Monitoring Data exist for forty stations in the present modeling domain. Linear interpolation is employed between forty monitoring stations to construct a matrix table with contributing fractions of forty stations for each model cell. The matrix table of contributing fractions is applied to the January data in 1992 to estimate initial conditions for each model cell and each water column state variable. For some shallow cross-section stations where no measurements were made at the time (e.g.,

CB4.3E, CB4.3W, CB4.2E, CB4.2W, CB4.1E, CB4.1W, CB3.3E and CB3.3W), laterally uniform initial conditions are assumed for the lower portion of the main Bay.

Sediment Initial Conditions

Because of the relatively longer time scales involved in kinetic processes occurring in benthic sediments, the effects of initial conditions in the sediment model would persist longer for sediment state variables than for water column state variables. In principle, the initial conditions should reflect the past history of the depositional fluxes and overlying water column conditions. In practice, no such data exist for the earlier years. Initial conditions hence are derived from a "stand-alone" application of the model, as suggested in DiToro and Fitzpatrick (1993). That is, the steady-state conditions for 1992, the first year of the present simulation, are found from the stand-alone sediment model application and are used as initial conditions.

Boundary Conditions

Open boundary conditions are estimated using the CBP Monitoring Data at Station CB4.4. Linear interpolations are employed in the vertical and lateral directions uniformly. In time, linear interpolation also are used in time based on the interval of the measurements (bi-weekly or monthly). The Upper Chesapeake Bay model has four river boundaries including Susquehanna River, Chester River, Choptank River, and the Chesapeake and Delaware Canal. The state variables specified at the river boundary include temperature, dissolved oxygen, algae, and dissolved silica obtained from CBP Monitoring Data at station CB1.1 for the Susquehanna and ET5.1 for the Choptank. Concentrations of salinity, chemical oxygen demand, and particulate biogenic silica are considered to be zero. Concentrations of total suspended solids, carbon, nitrogen, and phosphorus are set to zero, since their fall-line loads are specified directly. For the Chesapeake and Delaware Canal, the same boundary condition for Susquehanna River are used, and for Chester River, the same boundary condition for Choptank River are used. River boundary conditions are specified at the same intervals as open boundary conditions (bi-weekly or monthly), which is linear interpolation in time.

Given the model framework, the specified initial condition, boundary condition, and the external loads described above, The model was run from January 1992 to 1997 for all state variables. It is calibrated from 1992 to 1995, and verified for 1996 and 1997. The data used come from (1) the CBP Monitoring Data over the entire modeling period and (2) the MDE Monitoring Data from February 1994 to May 1995, and 1997. Time-series plots are used to compare weekly means of model results with the observations data at the surface and the bottom. Comparisons are made for the following state variables: salinity (S), temperature (T), total suspended solids (TSS), chlorophyll (CHL), dissolved oxygen (DO), total organic carbon (TOC), particulate carbon (PC), dissolved organic carbon (DOC), total nitrogen (TN), particulate nitrogen (PN), total dissolved nitrogen (TDN), ammonia (NH_4), nitrate+nitrite (NO_3), total phosphorus (TP), particulate phosphorus (PP), total dissolved phosphorus (TDP), dissolved phosphate (PO_4d) and available silica (SA). Time series from three stations: CB4.1C, WT5.1 and WT4.1. The description of station naming conventions, symbol for observed data, model output convention used in figures etc. can be found in Appendix A.

B. Upper Chesapeake Bay Calibration Results

(1) Time Series comparison

Three stations CB4.1C, CB3.2 and CB2.1 located in the lower, middle and upper portion of the Upper Chesapeake Bay (see Figure 17) were selected for illustrating time series comparison. Comparisons were made both at the surface and at the bottom, and the horizontal axis on each plot extends 6 years with origin at January 1, 1992. The model and data comparisons for CB4.1C were shown in Figures 18-26. Figure 18 shows a well-defined seasonal cycle of temperature; the model, given a properly formulated air-sea interaction, catches the trend very well. For salinity, one can easily detect the salinity drop during spring freshet, in particular, the surface salinity. During year 1993, 1994,and 1996, when the freshwater inputs from Susquehanna River are large, the variation of salinity are obvious. The hydrodynamic model was able to describe the variability reasonably accurate. Phytoplankton blooms in the spring and thus higher chlorophyll-a

concentration was observed during the period, as shown in Figure 19. In many cases, the high chlorophyll-a concentrations (exceeding 20 mg/l) were measured at the bottom; this is counter-intuitive because phytoplankton population supported by the light usually stays in the euphotic zone near the surface. An in-depth study using numerical model was conducted to investigate the cause of it. With the investigation, diatom, one of the dominant species' sinking velocity was adjusted and the resuspension of diatoms from the bottom was considered. After including the above mechanisms, the model results emerge to revel that it was able to simulate the bottom chlorophyll-a maximum quite well (see VI discussion section A for the details). For the dissolved oxygen, the observation data in CB4.1C shows the well-known summer anoxic condition at the bottom water. The model predicted the re-occurring anoxic event each year with right timing and magnitude. Both data and model for total phosphorus were shown to be higher in concentration in the summer when compares with stations CB3.2 and CB2.1. This is attributed to the anoxic condition occurred in the deep channel of this station, which in turn triggering the release of phosphorus from the sediment. The model calculation confirms the coupling mechanism between water column and sediment processes is working robust and properly. For station CB3.2 located in the main Upper Bay outside of Baltimore Harbor, the results are shown in Figures 27-35. The salinity there occasionally can reach to zero value during the spring freshet and then bounce back gradually afterwards. The model, having proper advection and turbulence mixing scheme, was able to mimic the event, its downturn and upturn. The data and model comparison for all other variables are generally in good agreement, except the particular form of nitrogen and phosphorus, which has slightly larger discrepancy. These discrepancies are attributed to the resuspension events capable of bringing the particulate matter into the water column. This process requires a full-blown sediment transport model and thus needs a substantial improvement. For station CB2.1, this is the nearest station to the Susquehanna and the results are shown in Figures 27-35. The model results are in general satisfactory as compared to the observation. Among the variables, the nitrogen species, the nitrate and nitrate, are much higher as compared to the other two stations presumably due to the

proximity to source in Susquehanna River. The other high concentration TSS and silica might have to do with the turbidity maximum zone located near the station.

(2) Longitudinal Transect

Additional to the temporal variation shown above, it is important also to examine the spatial variability along a transect of Upper Bay for the water quality variables. The longitudinal transect used is along the main channel, as shown in Figure 45. The observation and model results in the cells along the transect are averaged over seasons for winter, spring, summer and fall. In 1994 (The year 1994 was chosen because the data are the most abundant for all other 6 years). Arithmetic mean and the range of observation are presented; so is the arithmetic mean of model result and the range for maximum and minimum values (red lines show the mean, and the two lines above and below it are maximum and minimum). The horizontal axis represents kilometers from the mouth, and the number of measurements used for averaging is shown above the observations. The plots of longitudinal transects for temperature, salinity, chlorophyll-a, dissolved oxygen, total nitrogen, and total phosphorus are presented in Figures 46-51. As shown in Figure 46, the spatial distribution of temperature in each of the season is quite uniform, with the deep water slightly lower than the shallow water in the upper portion of the Bay. The spatial distribution of salinity clearly marks the limit of salt intrusion moving around river kilometer 100-120 km. The modeled salinity values match quite well with the salinity observation along the transect and also the location for the limit of salt intrusion. In Figure 48, the anoxic condition for bottom dissolved oxygen concentration in the summer is quite obvious up to rive kilometer 75. Again, the model reproduces the spatial extent and magnitude of the anoxic condition correctly. For nutrient, total nitrogen and total phosphorus are shown in Figures 50-51. The general trend of total nitrogen concentration decrease as it goes downstream. The largest slope lies in the upper portion region. For total phosphorus, there is an increase of concentration at the bottom between river kilometer 50 to 100, an indication of additional source from the sediment in the middle portion of the region.

C. Baltimore Harbor Calibration Results

(1) Time series comparison

Station WT5.1 was selected for illustrating the time series model-data comparison in Baltimore Harbor, as designated in Figure 52. The station, located in the middle portion of the Harbor, is MDE's major monitoring station (M16) and is also a long-term monitoring station for EPA Chesapeake Bay program. As the major rivers, Patapsco River, Jones Falls and Gwynns Falls, have limited freshwater discharged into the Harbor, the salinity and temperature are strongly influenced by the bay station CB3.2 located outside the Baltimore Harbor. Since the model domain of the Harbor used in this study extends further out to the Upper Bay, it did not invoke the boundary condition at the mouth of the Harbor. The simulation therefore reflects the true nature of the interaction between the Bay and the Harbor, and thus a realistically salinity prediction was obtained. The surface chlorophyll-a peaked around 50 ug/l inside the Harbor, which is about twice higher than that of CB3.2; the bottom chlorophyll-a, on the other hand, is much lower in the Harbor as compared to that of CB3.2. This is has to do with the larger size of diatom in the Bay versus smaller size dinoflagellate in the Harbor. The water quality model differentiates the species composition and thus makes the right prediction consistent with the observation. The duration of anoxic condition for bottom DO inside the Harbor is longer than that in CB3.2. The factors identified as the main reason driving the anoxic condition in the Harbor are: the stratification and the SOD. The low DO water from the Bay, may aggravate the low DO condition already existing in the Harbor, but is not the direct cause for the formation of anoxic water. It is also found that total organic carbon, ammonia and total phosphorus all are more than 50% higher in the Harbor than in CB3.2. This is attributed to the metropolitan urban run-off through the non-point source loading. The model was doing very decent prediction on all these variable due partly to the superb watershed modeling conducted by MDE. The TSS in the Harbor is about the same magnitude as those in the CB3.2, indicating that Harbor may not be a source for the sediments.

(2) Longitudinal transect

The longitudinal transect from the mouth of the Harbor to the Inner Harbor is used to present the spatial distribution of water quality variables, as shown in Figure 62. The observation and model results in the cells along the transect are averaged seasonally and presented for 1994. Arithmetic mean and the range for observation and the model result are the same as described previously The number of measurements used for averaging is also shown above each observation point. The plots for longitudinal transects are presented for temperature, salinity, chlorophyll-a, dissolved oxygen, total nitrogen, and total phosphorus in Figures 63-68, respectively.

As shown in figure 63, the spatial distribution of temperature is quite uniform across the Harbor. In Figure 64, the spatial distribution of salinity shows that the surface salinity increases while the bottom salinity decrease as it goes from the Harbor mouth into the Harbor. This salinity pattern is different from that in the classical estuarine circulation where both surface and bottom salinity decrease as it is going upstream. Instead, the inverse of salinity gradient at the surface actually set up a circulation pattern, dubbed as a three-layer circulation. The model results accurately depict the patterns both in salinity and circulation (not shown). Figure 65 shows that both the data and model shows the extent of summer anoxic condition extends the entire harbor in the summer. For chlorophyll-a distribution (see Figure 66), the surface values in the summer obviously are much higher than in the spring. This is the result of dominant species in the Harbor is the dinoflagellate rather than the diatom. The model, having both species and their kinetics included, reflect the observational fact quite well. Figures 67 shows that both modeled and data for total nitrogen has a slightly higher value inside the Harbor than at the mouth. Figure 68 shows that there is a very high phosphorus concentration consistently observed at the bottom in the inner Harbor. The model does catch the trend, but in certain individual case, model underestimates the magnitude of the peak values.

(3) Sediment-water flux

Sediment water flux measurements were part of MDE Sediment Water Exchange of Oxygen and Nutrient Flux Program (Boyton et al. 1998). The program provides observation of sediment oxygen demand, ammonium, nitrate, and phosphate exchange, and data was collected in 1994, 1995 and 1997. Since the sediment water flux observation were sparse such that individual observations were plotted against modeled flux in the single cell that contain the flux observation station. The vertical axis indicates sediment water flux and the horizontal axis on each plot indicates time extends 6 years with the origin at January 1, 1992. The weekly-averaged modeled fluxes were output with positive flux is from sediment to water and negative fluxes from water to sediment. Figures 69-72 show the comparison at four station in the Harbor: Curtis Bay at CTBY, Curtis Bay at Fairfied Outfall (FFOF), Bear Creek at Humphrey's Creek (HMCK) and Middle Branch at Ferry Bar (FYBR). For all time, ammonia always shows the positive flux, namely released from the sediment to the water column. Its average quantity is on the order of 0.1 g/m2/d. Nitrite and nitrate flux alternates. Sediment flux goes from water column into the sediment during the spring when nitrogen was discharged into the water column; sediment flux goes from sediment into water column where the nitrogen was limited in the summer. The averaged flux is on the order of 0.02 –0.04 g/m2/d. Phosphorus flux generally is released from sediment into water column with the magnitude ranges from 0.02 – 0.04 g/m2/d. The flux tens to be in spike during the anoxic condition. For the stations compared, model and data are all on the same order of magnitude. One exception was found in Curtis Bay at FFOF where occasionally high value of NH4 and NO3 did occur. For example, nitrite and nitrate flux in 1997 show several order of magnitudes larger than the normal.

D. Back River Calibration Results

(1) Time series comparison

In the Back River, station WT4.1 located in the middle portion of the Back River were selected for illustrating time series model-data comparison (Figure 73). Station WT4.1, is MDE's major monitoring station and is also a long-term monitoring station for

EPA Chesapeake Bay program. The depth at the station is only about 5 feet and the system is vertically well mixed. Thus only one depth was presented in the vertical direction. The results for temperature, salinity and total suspended sediment are presented in Figure 74. The prediction of seasonal cycle for temperature is similar to the Upper Bay and Baltimore Harbor, and the model has a reasonable prediction for salinity. The one variable which model did not predict satisfactorily is TSS. The model underestimates the observation data presumably because very soft mud with very low critical shear stress is existing in the system and thus very sensitive to the sediment resuspension dynamics.

Although freshwater discharge from the watershed is limited, the point source discharge from Back River Waste Water sewage Treatment Plant (WWTP) with 100 mgd daily flow is significant input to the River. In order to calibrate salinity properly, both forcing from the Upper Bay and the upstream discharge (including discharge from WWTP) are important. Similar to the Baltimore Harbor, the domain of Back River in the model is connected to the Upper Bay, and thus the interaction between the Upper Bay and Back River was internally linked and resulted in a good prediction for salinity. The chlorophyll-a in the Back river with peak value at 250 ug/l is the highest among all the Upper Bay stations. This is about 8 times higher than Upper Bay at CB3.2 and 5 times higher than the Baltimore Harbor at WT5.1. In the Initial model calibration, when the conventional parameter values were used, there is no way the model can predict the chlorophyll-a high value. The simple reason is that given the existing nitrogen and phosphorus concentration and the stoichiometric relationship, they cannot support chlorophyll-a beyond 120 mg/l. As described in VI in detail, we eventually found that the pH value in Back River was abnormally high (up to 10) and that make the phosphorus release from sediment without the need of anoxic condition. As chlorophyll increases due to release of phosphorus from the sediment into a system that is phosphorus limited, phytoplankton increases rapidly and depletes the carbon, which in turn increases the pH. The higher the pH, the more phosphorus is released; the more the phosphorus is released, the more the phytoplankton grow; the higher the pH it becomes; it thus triggers a positive feed back in the system. Once the role of pH was identified, a pH dependent function

was added for the phosphorus cycle, and the model predicted peak value of up to 250 mg/l chlorophyll-a emerged, which is consistent with the observation, as shown in Figure 75. The nutrients in the Back River system such as carbon, nitrogen, and phosphorus are all higher than those in Baltimore Harbor and Upper Bay by at least a factor of two to five. Back River obviously is a highly eutrophic system that possesses high nutrients and supports high phytoplankton biomass. The model results as compared with the observations were doing a fairly decent prediction on most of the nutrient variables, indicating that the model has a wide range of application.

(2) Longitudinal transect

The longitudinal transect from the mouth to the head of the Back River (see Figure 73) is used to present the spatial distribution of water quality variables. The observation and model results in the cells along the transect are seasonally averaged and presented for 1994. The plots for longitudinal transects are presented in Figures 80-85 for temperature, salinity, chlorophyll-a, dissolved oxygen, total nitrogen, and total phosphorus. As shown in Figure 80, the spatial distribution of temperature is quite uniform across the Back River. Spatial distribution of salinity structure show that the salinity decrease as it goes into the River as a result of the major discharge is from WWTP in the Back River. The model results, having included the flow from WWTP and connected to the Upper Bay, accurately simulate the pattern (see Figure 81). The oxygen in the River generally is high due partly to the shallowness of the depth and partly to the high production of oxygen by the phytoplankton. Both the model and data did not show an anoxic or hypoxic condition (see Figure 82). For the chlorophyll–a distribution, the values are both high in the spring and in the summer, indicative that WWTP supplies sufficient nutrient for phytoplankton growing. Figures 84 - 85 shows that total nitrogen and total phosphorus are much high as compared with Upper Bay and Baltimore Harbor stations; it is about 5 times higher than those of Upper Bay and 3 time higher than those of harbor stations. Both total nitrogen and total phosphorus concentration show the highest concentration near kilometer 9 where WWTP located and gradually decreases as it go downstream. The model tracks the trend of the data in satisfaction.

(3) Sediment-water flux

Sediment water flux measurements were part of MDE Sediment Water Exchange of Oxygen and Nutrient Flux Program (Boyton et al., 1998). The program provides observation of sediment oxygen demand, ammonium, nitrate, and phosphate exchange, and data was collected in 1994, 1995 and 1997. Since the sediment water flux observation were sparse such that individual observations were plotted against modeled flux in the single cell that contain the flux observation station. The vertical axis indicates sediment water flux and the horizontal axis on each plot indicates time extends 6 years with the origin at January 1, 1992. The weekly-averaged modeled fluxes were output with positive flux is from sediment to water and negative fluxes from water to sediment. Figures 86 - 88 show the comparison at three stations in the Back River: Witch Coat Point (WCPT), Muddy Gut (MDGT), and Deep Creek (DPCK). Because of large quantity of nitrite and nitrate input from WWTP with denitrification occurred in the sediment, most of the NO3 flux in the Back River go from water column into sediment. This is in contrast with Baltimore Harbor where the sediment-water flux direction takes turns in different seasons. Among the three stations, DPCK, which is located closest to WWTP, has the highest sediment-water flux for NH4, NO3, and PO4. The peak values for NH4 flux reaches 0.9 g/m**2/day (release from the sediment), NO3 flux 0.4 g/m**2/day (mostly go into the sediment), and PO4 0.2 g/m**2/day (release from the sediment). These indeed are very high number for the sediment water exchange. Since the observation data are very sparse, the comparison is difficult. The model results, however, catches the right trend with the correct flux direction and the right order of magnitude.

E. Regional Basin Calibration Results for Upper Bay, Baltimore Harbor and Back River

For the TMDL scenarios runs, the aggregated transect comparisons were conducted for additional basins, such as (1) Baltimore Harbor mouth to middle branch transect, (2) Baltimore Harbor mouth cross section, (3) Bear Creek, (4) Curtis Creek, and

(5) Back River. In the regional basin calibration, two periods SN1 and SN2 were defined: SN1 represents the growing period from May 1 to October 31, and SN2 for non-growing season, which is all other period in the year. 1994 data were used for DO, Chlorophyll a, TN and TP comparison. Figures 89-90 shows the longitudinal transect of Upper Bay (Figure 45) aggregated over SN1 and SN2. Their trends are similar to the spring and summer season combined. Figure 91 shows the transect for Baltimore Harbor from the mouth to the Middle branch transect; the model and data comparison results are shown in Figures 92-93. The difference of this transect versus the one from the mouth to the inner Harbor transect (see Figures 94-95) is that TN and TP at the most upstream station is now within the normal range rather than those of abnormally high values. Figure 96 shows the cross-section transect at the Harbor mouth. The results shown in Figures 97 reveal that DO and CHL is not uniform across the Harbor, especially at the bottom. TN and TP results shown in Figure 98, on the other hand, indicated both variables are more or less uniform across the cross-section of the Harbor. Figure 99 shows the model grid for the Bear Creek transact. Figures 100-101 indicates that there is slightly increase of chlorophyll, TN and TP in the middle of the transect during the growing season. Figure 102 shows the model grid for the Curtis Creek transact and Figures 103-104 indicate bottom DO and the surface chlorophyll in the growing season are the concerns. For the Back River transect (Figure 73), Figures 105 and 106 shows that DO, TN do not differ much between SN1 and SN2. However, the chlorophyll a in the growing season is about twice as high in concentration as compared with non-growing season. Again, the model calculations reflect the variation in the observation data.

F. Statistical Summary of Calibration

In the previous portion of the section, comparison between observed water quality and the model computations were presented. Some quantitative assessments of model performance are desirable to render the evaluation of the model application. Six variables: Salinity, Temperature, Chlorophyll-a, oxygen, total nitrogen and total phosphorus are presented in Figures 107- 109, 110-112 and 113 - 115 for Upper Bay,

Baltimore Harbor and Back River respectively. Three measures of errors for model-data comparison are utilized in this study. The mean difference (MD) is defined as:

$$(1)\quad MD = \frac{1}{N}\sum_{n=1}^{N}(P_n - O_n)$$

Positive MD indicates the model's overestimation of the data on the average and negative MD indicates the model's underestimation of the data on the average, with zero MD being ideal. The R square (RSQ) is defined as:

$$(2)\quad RSQ = \frac{n(\sum op) - (\sum o)(\sum p)}{\sqrt{\left[n\sum o^2 - (\sum o)^2\right]\left[n\sum p^2 - (\sum p)^2\right]}}$$

RSQ returns the square of the Pearson product moment correlation coefficient through data points in known O's and known P's. The R-squared value can be interpreted as the proportion of the variance in P attributable to the variance in O. The RMS (root-mean-square error) is defined as:

$$(3)\ RMQ = \sqrt{\frac{\sum(p-o)^2}{n}}$$

The root mean square error is an indicator of the deviation between predictions and observations. The root-mean-square error is an alternative to the MD.
In addition to above three measures of errors, SDM and SDD representing standard deviation for model and for data separately were also provided.

G. Supplementary Calibration -- Primary Production and Nutrient Limitation

In addition to the temporal and spatial variation of the water quality variables, the net primary production for Upper Bay, Baltimore Harbor and Back River were also calculated. For comparison with observation, model net primary production was integrated over the depth of the photic zone. The photic zone was defined as the depth of

1% light penetration, based on light attenuation as computed in the model. Primary production measurement for carbon-14 fixation in the surface water sample in Upper Bay (station CB2.2) and Baltimore Harbor (station WT5.1) were provided by MDE. Figure 116 shows the comparison of instantaneous measurement of net primary production with the daily averaged model calculation (red lines show the daily mean, and the two lines above and below are maximum and minimum). For Back River, the data was not available. The nutrient limitations vary with season and location, as shown in Figure 117. Computed limitations to algal growth are presented at the three stations: CB3.2 located near the turbidity maximum, WT5.1 in the middle section of the Baltimore Harbor, and WT4.1 in the center of the Back River. In the spring, when runoff is high, phosphorus and silica tend to be more limiting than nitrogen. During the summer, when runoff is low and oceanic water intrudes, nitrogen becomes the most limiting nutrient.

V. SENSITIVITY ANALYSIS

The success of water quality model calibration in the Upper Bay, Baltimore Harbor, and Back River depends on several key factors: (1) properly calibrated hydrodynamic and watershed model results, (2) improved the resuspension formula for simulating the subsurface chlorophyll a maximum in the Upper Bay, (3) understanding the processes causing the low DO concentration in the Baltimore Harbor, and (4) implementation of a pH dependent phosphorus flux formula for simulating algal bloom in the Back River. In this section, (2), (3) and (4) listed above will be further investigated in terms of sensitivity analysis. The results of the analysis will provide an improved understanding of the processes and lead to better model calibration and performance.

A. Sensitivity Analysis to the Phytoplankton Settling Velocity

In order to study the bottom chlorophyll a maximum in the Upper Bay, we assume (1) while diatoms are the main component of the spring bloom in the spring, they do not stay at the surface very long after the bloom (instead they sink to the bottom fast), and (2) some of the diatoms will be suspended or resuspended by the strong tidal current.

While the phytoplankton in the Chesapeake Bay consists of many different species, the main components during the spring bloom are the three diatom families: Cerataulina, Rhizosolina, and Thalassisosira (Malone et al., 1988; Cerco and Cole, 1994). The reported settling rates observed for these diatoms vary widely over several orders of magnitude. In part, this variation is a function of physical factors related to algal size, shape, and density and also as the function of light, nutrients, and other factors (Collins and Wlosinski, 1983; Cerco & Cole, 1994). Therefore, settling rates in the model usually are determined by calibration. As part of the sensitivity test, the settling velocity for diatoms in the water column was increased from 0.3 m/day to 0.9 m/day. At the same time, the maximum growth rates for diatoms were increased from 2.5 to 3.0 per day in order to maintain the surface chlorophyll a concentration level. This is not unreasonable in part because the maximum growth rate original reported for the Bay model was subject to the in-situ nutrient limitations whereas the growth rates employed by the model were for nutrient-unlimited situations (Canale and Vogel, 1974; Collins and Wlosinski, 1983). From Fig. 118, the value of the 3.0 at reference temperature 20°C still within the range of the expected maximum growth rate (Eppley, 1972).

We assumed that the bottom resuspension due to tidal mixing is important and implemented a simplified "resuspension" formula. In the mass balance equation, we applied to the sediment-water interface cell the following sediment concentration equation:

$$\frac{\delta C}{\delta t} = [transport] + [kinetics] + \frac{WS}{\Delta z} C_{up} - \frac{WS_{net}}{\Delta z} C$$

C=concentration of particulate constituent (g m^{-3})

WS=settling velocity in water column (m day^{-1})

WS_{net}= net settling velocity to the sediment (m day^{-1})

C_{up} =constituent concentration two cells above sediments (g m^{-3})

Δz=cell thickness (m)

From the equation above, the difference between the specified water column settling velocity and the net settling velocity toward the sediment imply resuspension or suspension. When the algae get back from the sediment after they reach the bottom, it may imply resuspension. Otherwise, it may imply the suspension or retention of the particles in the water column due to the strong current before they reach the bed.

After implementing the above formula, it was revealed that the model is capable of predicting the bottom chlorophyll a peaks, and inter-annual variation was also surprisingly well predicted, as shown in Fig. 119. The one-to-one scatter plot of the model versus data for the whole mesohaline region of the Upper Chesapeake Bay is also shown in Fig. 120. As a consequence, other state variables, such as particulate carbon, particulate nitrogen, and particulate phosphorus also show significant improvements (Liu, 2002).

B. Sensitivity Analysis to Physical Parameters (vertical stratification and mixing)

Although the model results in the main stem of Baltimore Harbor and the Upper Chesapeake Bay are very good, the dissolved oxygen in the two local branches (i.e., Middle Branch and Inner Harbor) were over-predicted. After re-examining the geometry and the circulation pattern, it was decided that the cause of over-predicting bottom DO is due to excessive mixing between surface and bottom water. The root cause of it is the misrepresentation of the narrow, deep channel by a shallower, averaged depth, which in return under-estimated the vertical stratification and over-predicted the vertical mixing. To fix this problem, the maximum value instead of the average value of the various depths within each grid will be assigned as the depth of the grid.

In so doing, the deep ship channel is manifested and provides the conduit for importing the salty water. In the Inner Harbor, a depth of 35 feet was assigned wherever there is a channel, and 15 feet was assigned in the Middle Branch. The model results before and after applying the new geometry are shown from Figs. 121-122 for the Middle Branch. It is obvious that dissolved oxygen was much better simulated after using the

new geometry. All the other water quality variables (especially chlorophyll a, nitrogen, and particulate organic matter) were also improved significantly (Liu, 2002).

C. Sensitivity Analysis of Sediment Phosphorus Release to pH function (in Back River)

The same set of parameters employed in the main Bay and Baltimore Harbor was used in the Back River. The results of the prediction were marginal, especially the concentration of chlorophyll a, which was systematically underestimated. This suggests that the Back River is a very different system from Baltimore Harbor and the upper Chesapeake Bay. Firstly, the model results (calculated from equation IV-13) indicate that, for most of the time, Back River is a phosphorus-limited system (Fig. 117). Secondly, the benthic flux measurements from WCPT and DPCK indicate that the phosphorus sediment flux is very high whereas our model prediction is too low. Thirdly, the bottom pH values measured in the Back River are significantly higher than those in Baltimore Harbor; the value of bottom pH in Back River can reach as high as 10.7 in the water column and have an increased trend over the last several years (Fig. 124). These three factors suggest there is an association between high chlorophyll a, high phosphorus sediment flux, and high pH in the Back River.

After the pH function is implemented, the sediment flux model also shows the phosphorus flux is much increased (Figs. 125-126). The water quality model results show a dramatic increase of chlorophyll a in the upper portion of the Back River (Figs. 127-128). The magnitude was correctly predicted and the seasonal cycle was also captured, based on observed data. The statistic measure was shown in Fig. 129 by a one-to-one scatter plot. At the same time, model predictions for particulate organic nitrogen, ammonia, nitrate, particulate organic phosphorus, and dissolved phosphate were also significantly improved.

VI. DISCUSSION

A. Upper Chesapeake Bay

In the mesohaline reach of the Upper Chesapeake Bay, phytoplankton blooms occur in both spring and summer. This was first identified from the field data (Fig. 4) and then successfully simulated by the model (Fig. 64).

The formation of the spring blooms was controlled by several factors: 1) the large supply of nutrients, especially nitrate, and silica, transported by the high spring discharge from the Susquehanna River; 2) the increased amounts of light and temperature, which in turn increase the growth rate while maintaining a moderate predation as compared to the summer condition. For example, at CB4.2, shown in Figs. 65-68, both the seasonal peak and the inter-annual variation can be related to the increase of freshwater discharge, nitrate, and silica concentrations in the spring. The formation of the summer phytoplankton bloom, on the other hand, was supported by the increased productivity due to higher light availability, higher temperature, and by nutrient regeneration from the sediment. For example, the summer chlorophyll a maximum at CB4.2 is related to the release of bottom ammonia, and bottom phosphate occurring in the summer as shown in Figs. 69 -70.

The decline of the spring and summer blooms also differ due to varied nutrient limitations. The collapse of the spring phytoplankton bloom is due primarily to the limitations of phosphorus and/or silica. The limitation in summer, on the other hand, tends to be nitrogen, as shown in Fig. 117. These model results are consistent with previous studies by Boynton et al. (1982), Malone et al. (1983), Malone et al. (1988), Fisher et al. (1988), Conley and Malone (1992), Glibert et al. (1995) and Fisher et al. (1999).

One of the distinct features of the phytoplankton blooms in the Upper Chesapeake Bay is the chlorophyll a subsurface maximum. Previous investigators suggested that the chlorophyll a maximum at the bottom is the result of the phytoplankton biomass being accumulated in the lower Chesapeake Bay and advected upstream (Seliger et al., 1981; Malone, 1992). Our studies partially support the above hypotheses but suggest that there are other mechanisms that can contribute to this phenomenon.

First, we want to show that the large sub-surface chlorophyll a maximum in the Upper Bay does not necessarily come as the result of the blooms in the Lower Bay. For example, displayed in Figs. 130-131 are the chlorophyll a time series data collected from 1992-2001 at stations from the Upper Bay to the Lower Bay. In the 1998 to 2001 period, although we see no spring bloom in the Lower Bay, we do see high chlorophyll a concentrations at Upper Bay stations CB3.2, CB3.3 and CB4.2C with a decreasing trend toward the lower Bay.

Second, the high chlorophyll a concentration from the lower bay does not automatically produce the high chlorophyll a sub-surface peak. Before resuspension was implemented, we did try to use the chlorophyll a concentration from the monitoring data as a southern open boundary condition to drive the water quality model. Shown in the upper panel of Fig. 28 are the surface and bottom chlorophyll a predictions at CB4.1. It has the indication of producing some degree of high sub-surface chlorophyll a levels, but the magnitude is significantly under-computed. Since studies have shown that phytoplankton species distributions in the Upper Chesapeake Bay are dominated by diatoms such as Cerataulina, Rhizosolina, and Thalassiosira in the spring, the large size diatoms must have played a significant role. It was also reported that nearly 50% of the chlorophyll a biomass was larger than 20 μm in size and silicate limitation could also result in large increases of sinking rates for diatoms (Titman and Kilham, 1976; Bienfang et al., 1982). A conviction leads to the following hypothesis:

(1) Given diatoms are the main component of the spring bloom, they do not stay at the surface very long after the bloom (instead they sink quickly to the bottom),

(2) The diatoms can be suspended or resuspended by the strong tidal current.

After implementing the above hypothesis, the model result, shown at the bottom panel in Fig. 28, was vastly improved. This confirms that the size and species of the phytoplankton, the sinking, and its suspension or resuspension upon reaching the bottom

also play important roles in regulating the bottom chlorophyll a distribution. Once the bottom chlorophyll a was accurately simulated, the nutrient concentration predictions at the bottom were also improved. This implies that other nutrient concentrations at the bottom are closely related to the bottom chlorophyll a concentration.

So far, the predictions have been focused on the water quality parameters at the surface and the bottom. It is instructive to examine the distribution of the vertical profiles. Two parameters (chlorophyll a and dissolved phosphate) were selected for examination at station CB4.2 during 1996, when a large spring run-off occurred. Fig. 132 shows the time-depth chlorophyll a contour. It is clear that sub-surface chlorophyll a maximum existed in the spring and it was extended about 7-8 m above the bottom. The pattern shifted around day 150, after which chlorophyll was higher at the surface than at the bottom. Fig. 133 shows the companion plot for dissolved phosphate, indicating the source is from the sediment to the surface. Given the large algal bloom in the spring, the detritus provided the potential source for re-generated phosphorus. The vertical profile also indicates that the phosphorus can be mixed significantly into the water column.

B. Baltimore Harbor

In the sensitivity analysis, the reassignment of the depths in the Inner Harbor and the Middle Branch dramatically improved water quality model results. Both of these areas are characterized by having the shallow shoaling area intertwined with the narrow shipping channels, and connected to the main shipping channel outside. In a customary modeling practice, the depth value assigned to a grid is the averaged depth within the grid cell. For example, a shipping channel and a shoal area can both fall within a grid. Taking the average depth means smoothing out the deep channel because the grid has a limited resolution. When the deep channel was not well represented by the model grid, the salt simulated can no longer freely flow into and out of the basin and therefore the prediction of the salinity suffered. Examples of under-predicted salinity are shown in the upper panel of Fig. 50.

What was decided to remedy the aforementioned problem was the use of maximum depth values within the grid cell to represent the depth value of the grid. This essentially allows the deep shipping channel to manifest and enables the salt to be transported through it. The prediction of salinity and the vertical stratification are thus better, as shown in Fig. 50 (lower panel). Simultaneous predictions of other water quality parameters are also improved.

The modification of the assigned depth in the Inner Harbor and Middle Branch underscores the impact of physical processes on the bio-chemical processes. The improved salinity prediction is an indication of more accurate calculation of the transport. As a consequence, other water quality variables also show dramatic improvement. Since biological and chemical processes are coupled with the physical process, the physics must be described as accurately as possible before the subtle biological and chemical processes can be assessed.

Unlike the mesohaline reach of the Upper Chesapeake Bay, the bottom chlorophyll a in Baltimore Harbor is less pronounced in terms of the spring peak. The surface chlorophyll a in Baltimore Harbor, however, has higher values compared to Upper Chesapeake Bay, as shown in Fig. 77. The cause of the high chlorophyll a in Baltimore Harbor is of interest. The nitrate and dissolved silicate levels are very similar between Baltimore Harbor (WT5.1) and CB3.3 (Figs. 79-80). The light attenuation coefficient is slightly higher in Baltimore Harbor (Fig. 78). For surface phosphate and ammonia levels, Baltimore Harbor has considerably higher values (Figs. 81-82). These excessive nutrients plus the lower grazing and the turbulence level were reasons for supporting high dinoflagellates standing stock in the Baltimore Harbor (Sellner et al., 2001).

C. Back River

As shown in Figs. 7 and 8, the chlorophyll a levels in Back River can reach 200-300 μg/l in the early summer season, which is 4-6 times higher than those of Baltimore Harbor or the Upper Chesapeake Bay. Given the Back River Waste Water Treatment plant loadings (point source) and the non-point source loadings provided by MDE, the

initial model simulation severely under-calculated the chlorophyll a levels (see upper panel of Figs. 56 and 57). Obviously, Back River phytoplankton dynamics work very differently from either Baltimore Harbor or Upper Chesapeake Bay.

The important clues are obtained from the nutrient flux measurements by Boynton et al. (1998). They showed that the releases of phosphorus from the sediment in the Back River are high to very high in comparison with other areas of the Chesapeake Bay and even the rest of the world. Boynton estimated that sediment release of phosphorus in the Back River in the summer of 1997 amounted to about three times the external loads (Boynton et al., 1998). Therefore, there is little doubt that sediment phosphorus fluxes must play an important role in contributing to phosphorus availability in the water column.

However, the presence of a large sediment phosphorus flux in the Back River posed a dilemma: why and how does the phosphorus release from the sediment? Boynton did not provide an answer. In the Chesapeake Bay proper, the mechanism for the release of phosphorus is strongly influenced by DO levels in overlying waters (Mortimer, 1941, 1942; Ditoro et al., 2001). Usually a barrier to phosphate exists in the aerobic layer of the sediment due to the formation of iron oxyhydroxide precipitate ($Fe_2O_3(H_2O)_n$ with n= 1 to 3) (Dzombak and Morel, 1990) via the oxidation of ferrous iron. This particulate species strongly sorbs phosphate and prevents its escape to the overlying water via diffusion until the overlying oxygen level falls below 2 mg/l. But based on monitoring data, the oxygen never falls below 4 mg/l in the Back River, even during the summer. Then the question is what caused the high sediment flux of phosphorus under the aerobic conditions such as the Back River? Was there some significant gap in our understanding of the phosphorus cycle in the Bay?

In a number of studies in shallow eutrophic lakes, it was demonstrated to varying degrees that the occurrence of high algal blooms could be the result of a positive feedback loop involving phosphorus flux. In this loop, photosynthesis increases water column pH, thereby increasing phosphorus release from the sediments, and further

increasing photosynthesis. For example, some lake studies have shown a correlation between high pH and high phosphorus concentrations in the water column (Anderson, 1971). Additionally, other studies have incubated lake sediments in the laboratory and demonstrated an increase in phosphorus release from non-calcareous sediments at high pH (Kamp-Nielsen, 1974; Istvanovics, 1988).

Based on observation data shown in Fig. 51, the bottom pH values in the Back River are much higher than those in Baltimore Harbor. A pH value that exceeds 8.5 is not uncommon from year 1990 on. A study by Stumm and Morgan (1981) showed that phosphate sorption to iron hydroxides decreases with increasing pH. The Potomac River data collected by Seitzinger (1986) indicated that sediment phosphorus release quadrupled when pH exceeded 9.5. Could it be the pH in the Back River would trigger the large release of phosphorus?

In the sensitivity study described in the previous section, a pH function for phosphorus release was implemented in the model and forced by the long-term pH data measured in the Back River. The model results catch the right magnitude of the measured sediment fluxes. Figs. 54 and 55 (lower panel) shows the comparison of phosphorus sediment fluxes calculated by the model versus measurements of its values at station DPCK and MDGT. In turn, the sediment phosphorus release leads to the high chlorophyll a simulation occurring in the water column. The results for the chlorophyll a prediction were improved dramatically, as shown in Figs. 56 and 57 (lower panel). We believe that this mechanism provides logical answers as to why and how the phosphorus is released from the sediment and its consequence of fueling the high chlorophyll a in the Back River. There are still remaining questions as to what causes the pH to get above normal in the Back River and how the positive feedback works, which requires a more in-depth investigation.

VII. CONCLUSIONS

This is the first systematic water quality modeling study for Baltimore Harbor, Back River, and the adjacent Upper Chesapeake Bay. The model framework used consists of

the hydrodynamic model CH3D, which provides a detailed, three-dimensional hydrodynamic transport with 3-minute time step to the water quality model CE-QUAL-ICM. Non-point loads from the large watershed adjacent to the Upper Chesapeake Bay and the urban point source from the Baltimore Metropolitan area are both included. The model was calibrated with the long term EPA monitoring data and MDE intensive survey data for the period from 1992-1997. The three focused subjects that were investigated are summarized as follows:

(1) The seasonally high chlorophyll a concentration at the bottom water of the Upper Chesapeake Bay

This is a phenomenon that was under-computed since the earliest phase of the Chesapeake Bay Bay-wide water quality simulation (Cerco and Cole, 1994). We made the model modification based on the hypothesis that the rapid sinking of the diatoms and the subsequent resuspension of the phytoplankton by the strong current from the bottom should be considered important mechanisms. It was found that the combination of the advection from the lower Bay, settling from the surface, and the resuspension due to high bottom current, indeed do vastly improve the model prediction of high bottom chlorophyll a concentration in the deep channel of the Upper Chesapeake Bay.

(2) The low DO condition in the Baltimore Harbor

The low DO condition in the deep channel portion of the Baltimore Harbor was well simulated using the original model set up. This was consistent with the notion that the formation of low DO is the result of stratification, which prevents the penetration of oxygen-rich surface water into the deep zone, and the bottom oxygen demand exerted by the sediment in Baltimore Harbor. The anoxic condition inside the Harbor thus is not imported by the intrusion of anoxic water from the Bay.

What was further improved were the prediction of the low DO condition in tributaries of the Harbor such as Inner Harbor and Middle Branches. These are relatively narrow tributaries, which are the branches of the main shipping channel. Based on the grid

construction criterion, the depth assigned initially was the average depth of the deep channel and the intertwined shallow shoals adjacent to it. The model results using this averaged depth failed to show the low DO condition in these areas. We resorted to assign the maximum depth within the grid to represent the channel configuration. Although this over-specified the overall depth distribution, the model results were much improved not only for the stratification but also for DO and almost all the nutrients. This highlights the important roles played by topography and the stratification in regulating the hypoxia/anoxia in the tributaries of Baltimore Harbor.

(3) The abnormally high algal bloom in the Back River.

Back River has one of the highest chlorophyll a concentrations in the Chesapeake Bay region; it can reach 200 to 300 μg/l during its peak in the early summer season. The available sediment flux data indicated that the phosphorus released from the sediment is significant and is the major source for inorganic phosphorus fueling the high chlorophyll a. The effect of pH value was explored and identified as an important factor for controlling the phosphate release from sediment under aerobic conditions in Back River. Using historical Potomac River data, we constructed a pH-dependent sediment release function and implemented it in the model. The bi-weekly measured pH data from the Back River was used as a forcing function. The model simulates with reasonable success the phosphorus flux from the sediment. This sediment-released phosphorus in turn generates extremely high chlorophyll in the Back River.

Region-by-region calibrations were also conducted, which includes basins in the Baltimore Harbor such as: Harbor Mouth, Old Road Bay, Rock Creek, Stony Creek, Harbor Channel, Bear Creek, Curtis Creek, Middle Branch, Inner Harbor, and the Back River. Based on DO and chlorophyll criteria, Baltimore Harbor was impaired mainly by low DO and intermittent high chlorophyll, while Back River was impaired by very high chlorophyll. The model simulation result catches the trend and matches nutrient data in most places. DO calibration were excellent everywhere. Chlorophyll calibrations are good in most areas, except in Rock Creek and Stony Creek where the model was slightly

under-predicted. For Back River the DO and Chlorophyll calibration were generally quite satisfactory. Statistical examination conducted for the model results support the model evaluation.

Table 1. Water quality parameters in CBP* and MDE** monitoring data.

Parameters	Symbol	unit	period
Temperature	T	centigrade	CBP: 92-97; MDE: 94-95, 97
Salinity	S	ppt	CBP: 92-97; MDE: 94-95, 97
Dissolved Oxygen	DO	mg/l	CBP: 92-97; MDE: 94-95, 97
Chlorophyll-a	CHL	μg/l	CBP: 92-97; MDE: 94-95, 97
Total Suspended Solids	TSS	mg/l	CBP: 92-97; MDE: 94-95, 97
Secchi Depth		m	CBP: 92-97; MDE: 94-95, 97
Particulate Carbon	PC	mg/l	CBP: 92-97; MDE: 94-95, 97
Dissolved Organic Carbon	DOC	mg/l	CBP: 92-97; MDE: 94-95, 97
Particulate Nitrogen	PN	mg/l	CBP: 92-97; MDE: 94-95, 97
Total Dissolved Nitrogen	TDN	mg/l	CBP: 92-97; MDE: 94-95, 97
Ammonium Nitrogen	NH_4	mg/l	CBP: 92-97; MDE: 94-95, 97
Nitrate+Nitrite Nitrogen	NO_3	mg/l	CBP: 92-97; MDE: 94-95, 97
Particulate Phosphorus	PP	mg/l	CBP: 92-97; MDE: 94-95, 97
Total Dissolved Phosphorus	TDP	mg/l	CBP: 92-97; MDE: 94-95, 97
Dissolved Phosphate	PO_4d	mg/l	CBP: 92-97; MDE: 94-95, 97
Particulate Inorganic Phosphorus	PIP	mg/l	CBP: 92-97; MDE: 94-95, 97
Particulate Biogenic Silica	SU	mg/l	CBP: 92-97; MDE: 94-95, 97
Dissolved Silica	SA	mg/l	CBP: 92-97; MDE: 94-95, 97

* CBP: Chesapeake Bay program, US Environmental Protection Agency
** MDE: Maryland Department of the Environment

Table 2. Statistics of benthic flux data from Back River and Baltimore Harbor (Boynton et al., 1998).

	$BFNH_4$ ($g/m^2/day$)				$BFNO_3$ ($g/m^2/day$)			
STATION	MIN	MAX	MEAN	NUMBER	MIN	MAX	MEAN	NUMBER
WCPT*	0.02	0.25	0.13	15	-0.10	0.03	-0.01	13
MDGT*	0.04	0.26	0.14	8	-0.02	0.01	0.00	8
DPCK*	0.04	0.32	0.17	15	-0.16	0.03	-0.06	15
RVBH	0.01	0.10	0.05	6	-0.03	0.05	-0.01	6
HMC	0.05	0.24	0.14	9	-0.06	-0.01	-0.02	8
CTBY	0.00	0.19	0.08	6	-0.05	0.01	-0.02	6
FFOF	0.06	0.23	0.14	8	-0.08	-0.01	-0.05	9
FYBR	0.01	0.13	0.08	6	-0.03	0.00	-0.01	6
INHB	0.14	0.73	0.46	6	-0.05	0.00	-0.02	6

	$BFPO_4$ ($g/m^2/day$)				BFSI ($g/m^2/day$)			
STATION	MIN	MAX	MEAN	NUMBER	MIN	MAX	MEAN	NUMBER
WCPT*	0.00	0.13	0.05	15	0.08	0.53	0.27	14
MDGT*	0.01	0.05	0.03	6	0.14	0.27	0.18	8
DPCK*	0.00	0.04	0.02	15	0.03	0.53	0.26	14
RVBH	0.00	0.01	0.01	6	0.13	0.33	0.23	6
HMCK	0.00	0.05	0.01	7	0.08	0.24	0.17	9
CTBY	0.00	0.08	0.02	6	0.10	0.36	0.21	6
FFOF	0.00	0.06	0.02	9	0.14	0.34	0.23	9
FYBR	0.00	0.02	0.01	6	0.12	0.25	0.22	6
INHB	0.00	0.10	0.06	6	0.10	0.30	0.23	6

	SOD ($g/m^2/day$)			
STATION	MIN	MAX	MEAN	NUMBER
WCPT*	-3.31	-0.82	-2.16	15
MDGT*	-3.07	-1.17	-1.94	9
DPCK*	-2.78	-1.12	-1.98	15
RVBH	-4.12	-0.85	-2.18	6
HMCK	-2.04	-1.71	-1.84	9
CTBY	-3.12	-0.71	-1.34	6
FFOF	-2.18	-1.63	-1.88	9
FYB	-1.63	-0.67	-1.09	6
INHB	-1.82	-0.38	-0.85	6

* WCPT, MDGT, DPCK are in Back River, the other stations are in Baltimore Harbor.

Table 3. Model state variables in the eutrophication water quality model.

Parameter	symbol
Temperature	T
Salinity	S
Total Suspended Solids	TSS
Dinoflagellates	B_f
Diatoms	B_d
Green Algae	B_g
Refractory Particulate Organic Carbon	RPOC
Labile Particulate Organic Carbon	LPOC
Dissolved Organic Carbon	DOC
Refractory Particulate Organic Nitrogen	RPON
Labile Particulate Organic Nitrogen	LPON
Dissolved Organic Nitrogen	DON
Ammonium Nitrogen	NH_4
Nitrate+nitrite Nitrogen	NO_3
Refractory Particulate Organic Phosphorus	RPOP
Labile Particulate Organic Phosphorus	LPOP
Dissolved Organic Phosphorus	DOP
Total Phosphate	PO_4t
Particulate Biogenic Silica	SU
Available Silica	SA
Chemical Oxygen Demand	COD
Dissolved Oxygen	DO

Table 4. Model state variables and fluxes in the benthic sediment flux model.

Parameters
particulate organic carbon in Layer 2 (G_1, G_2 and G_3 classes)
particulate organic nitrogen in Layer 2 (G_1, G_2 and G_3 classes)
particulate organic phosphorus in Layer 2 (G_1, G_2 and G_3 classes)
particulate biogenic silica in Layer 2
sulfide (salt water) or methane (fresh water) in Layer 1 and 2
ammonium nitrogen in Layer 1 and 2
nitrate nitrogen in Layer 1 and 2
phosphate phosphorus in Layer 1 and 2
available silica in Layer 1 and 2
ammonium nitrogen flux
nitrate nitrogen flux
phosphate flux
silica flux
sediment oxygen demand
release of chemical oxygen demand
sediment temperature

Table 5. Parameters related to algae in the water column.

parameter	description	value	unit
PM_f	maximum growth rate of algae group 1	2.5	day^{-1}
PM_d*	maximum growth rate of algae group 2	2.5	day^{-1}
PM_g	maximum growth rate of algae group 3	2.5	day^{-1}
KHN_x	half-saturation constant of N uptake by algae	0.01	g N m^{-3}
KHP_x	half-saturation constant of P uptake by algae	0.001	g P m^{-3}
KHS	half-saturation constant of Si uptake by diatoms	0.05	g Si m^{-3}
KHRx	half-saturation constant of DO for algal excretion of DOC	0.5	g O_2 m^{-3}
IH_f	half-saturation light intensity for algal group 1growth	50	langley day^{-1}
IH_d	half-saturation light intensity for algal group 2 growth	30	langley day^{-1}
IH_g	half-saturation light intensity for algal Group 3 growth	40	langley day^{-1}
KE_B	background light attenuation coefficient	0.12 - 0.15	m^{-1}
KE_{CHL}	light attenuation coefficient due to self-shading of algae	0.017	m^2 per mg CHL
KE_{TSS}	light attenuation coefficient due to TSS	0.07	m^2 per g TSS
$CCHL_x$	C-to-CHL ratio in algae	60.0	g C per g CHL
TM_f	optimum T for algal group 1 growth	25.0	°C
TM_d	optimum T for algal group 2 growth	20.0	°C
TM_g	optimum T for algal group 3 growth	22.5	°C
$KTG1_f$	effect of T below optimum T on algal group1 grow	0.006	$°C^{-2}$
$KTG2_f$	effect of T above optimum T on algal group1 grow	0.006	$°C^{-2}$
$KTG1_d$	effect of T below optimum T on algal group2 growth	0.004	$°C^{-2}$
$KTG2_d$	effect of T above optimum T on algal group2 growth	0.006	$°C^{-2}$
$KTG1_g$	effect of T below optimum T on algal group3 growth	0.012	$°C^{-2}$
$KTG2_g$	effect of T above optimum T on algal group3 growth	0.007	$°C^{-2}$

Table 5 (con't)

BMR_f	basal metabolism rate of algae group 1 at reference T	0.05	day^{-1}
BMR_d	basal metabolism rate of algae group 2 at reference T	0.05	day^{-1}
BMR_g	basal metabolism rate of algae group 3 at reference T	0.05	day^{-1}
PRR_f	predation rate of algae group 1 at reference T	0.05	day^{-1}
PRR_d	predation rate of algae group 2 at reference T	0.05	day^{-1}
PRR_g	predation rate of algae group 3 at reference T	0.20	day^{-1}
KTB_x	effect of T on basal metabolism of algae	0.069	$°C^{-1}$
TR_x	reference T for basal metabolism of algae	20.0	°C
WS_f	settling velocity for algal group 1	0.1	m day^{-1}
WS_d**	settling velocity for algal group 2	0.3	m day^{-1}
WS_g	settling velocity for algal group 3	0.1	m day^{-1}

PM_d* : 3.0 day^{-1} in sensitivity analysis.
WS_d**: 0.9 m day^{-1} in sensitivity analysis.

Table 6. Parameters related to organic carbon in the water column.

Parameters	description	value	unit
FCRP	fraction of predated algal C produced as RPOC	0.35	none
FCLP	fraction of predated algal C produced as LPOC	0.55	none
FCDP	fraction of predated algal C produced as DOC	0.10	none
FCD_x	fraction of metabolized C by algae produced as DOC	0.0	none
KHR_x	half-saturation constant of DO for algal excretion of DOC	0.5	g O_2 m^{-3}
KHO_{DOC}	half-saturation constant of DO for oxic respiration of DOC	0.5	g O_2 m^{-3}
K_{RC}	minimum respiration rate of RPOC	0.005	day^{-1}
K_{LC}	minimum respiration rate of LPOC	0.075	day^{-1}
K_{DC}	minimum respiration rate of DOC	0.020	day^{-1}
K_{Rcalg}	constant relating respiration of RPOC to algal biomass	0.0	day^{-1} per g C m^{-3}
K_{Lcalg}	constant relating respiration of LPOC to algal biomass	0.0	day^{-1} per g C m^{-3}
K_{Dcalg}	constant relating respiration of DOC to algal biomass	0.0	day^{-1} per g C m^{-3}
KT_{HDR}	effect of T on hydrolysis/ mineralization of POM/DOM	0.069	$°C^{-1}$
KT_{MNL}	effect of T on hydrolysis/ mineralization of POM/DOM	0.069	$°C^{-1}$
TR_{HDR}	reference T for hydrolysis of POM	20.0	°C
TR_{MNL}	reference T for mineralization of DOM	20.0	°C
$KHNDN_N$	half-saturation constant of NO_{23} for Denitrification	0.1	g N m^{-3}
AANOX	ratio of denitrification to oxic DOC respiration rate	0.5	none

Table 7. Parameters related to nitrogen in the water column.

Parameters	description	Value	unit
FNRP	fraction of predated algal N produced as RPON	0.35	none
FNLP	fraction of predated algal N produced as LPON	0.55	none
FNDP	fraction of predated algal N produced as DON	0.10	none
FNIP	fraction of predated algal N produced as NH4	0.00	none
FNR	fraction of metabolized algal N produced as RPON	0.0	none
FNL	fraction of metabolized algal N produced as LPON	0.0	none
FND	fraction of metabolized algal N produced as DON	1.0	none
FNI	fraction of metabolized algal N produced as NH4	0.0	none
ANC_x	N-to-C ratio in algae	0.167	g N per g C
ANDC	mass of NO_{23}-N consumed per mass DOC oxidized	0.933	g N per g C
K_{RN}	minimum hydrolysis/mineralization rate of RPON	0.005	day^{-1}
K_{LN}	minimum hydrolysis/mineralization rate of LPON	0.075	day^{-1}
K_{DN}	minimum hydrolysis/mineralization rate of DON	0.015	day^{-1}
K_{Rnalg}	constant relating hydrolysis/mineralization of RPON to algal biomass	0.0	day^{-1} per g N m^{-3}
K_{Lnalg}	constant relating hydrolysis/mineralization of LPON to algal biomass	0.0	day^{-1} per g N m^{-3}
K_{Dnalg}	constant relating hydrolysis/mineralization of DON to algal biomass	0.0	day^{-1} per g N m^{-3}
$KHDO_{NIT}$	half-saturation constant of DO for nitrification	1.0	g O_2 m^{-3}
KHN_{NIT}	half-saturation constant of NH_4 for nitrification	1.0	g N m^{-3}
NT_M	maximum nitrification at optimum T	0.007	day^{-1}
KT_{NT1}	effect of T below optimum T on		

Table 7 (con't)

	nitrification rate	0.0045	$°C^{-2}$
KT_{NT1}	effect of T above optimum T on nitrification rate	0.0045	$°C^{-2}$
TM_{NT}	optimum T for nitrification rate	27.0	°C

Table 8. Parameters related to phosphorus in the water column.

Parameter	description	Value	unit
FPRP	fraction of predated algal P produced as RPOP	0.1	none
FPLP	fraction of predated algal P produced as LPOP	0.2	none
FPDP	fraction of predated algal P produced as DOP	0.5	none
FPR_x	fraction of metabolized P by algae produced as RPOP	0.0	none
FPL_x	fraction of metabolized P by algae produced as LPOP	0.0	none
FPD_x	fraction of metabolized P by algae produced DOP	0.5	none
APCMIN	minimum P-to-C ratio in algae	0.01	g P per g C
APCMAX	maximum P-to-C ratio in algae	0.024	g P per g C
PO4DMAX	maximum PO4d beyond which APC = APCMAX	0.01	g P m^{-3}
K_{RP}	minimum hydrolysis/mineralization rate of RPOP	0.005	day^{-1}
K_{LP}	minimum hydrolysis/mineralization rate of LPOP	0.075	day^{-1}
K_{DP}	minimum hydrolysis/mineralization rate of DOP	0.1	day^{-1}
K_{Rpalg}	constant relating hydrolysis/ mineralization of RPOP to algal biomass	0.0	day^{-1} per g P m^{-3}
K_{Lpalg}	constant relating hydrolysis/ mineralization of LPOP to algal biomass	0.0	day^{-1} per g P m^{-3}
K_{Dpalg}	constant relating hydrolysis/ mineralization of DOP to algal biomass	0.0	day^{-1} per g P m^{-3}

Table 9. Parameters related to silica in the water column.

Parameter	description	Value	unit
FSA	fraction of predated diatom Si produced as SA	0.0	none
ASC_d	Si-to-C ratio in diatoms	0.5	g Si per g C
K_{SU}	dissolution rate of SU at reference T	0.025	day^{-1}
KT_{SUA}	effect of T on dissolution of SU	0.092	$°C^{-1}$
TR_{SUA}	reference T for dissolution of SU	20.0	°C

Table 10. Parameters related to chemical oxygen demand and dissolved oxygen in the water column.

Parameters	description	Value	unit
KHO_{COD}	half-saturation constant of DO for oxidation of COD	1.5	g O_2 m^{-3}
K_{CD}	oxidation rate of COD at reference temperature	20.0	day^{-1}
KT_{COD}	effect of T on oxidation of COD	0.041	$°C^{-1}$
TR_{COD}	reference T for oxidation of COD	20.0	°C
K_{RDO}	reaeration coefficient	2.4	m day^{-1}
AOCR	mass DO consumed per mass C respired by algae	2.67	g O_2 per g C
AONT	mass DO consumed per mass NH_4-N nitrified	4.33	g O_2 per g N

Tables 11. Parameters used in the sediment flux model.

parameter	description	value	unit
HSEDALL	depth of sediment	10	cm
DIFFT	heat diffusion coefficient between water column and sediment	0.0018	cm^2 sec^{-1}
SALTSW	salinity for dividing fresh and saltwater for SOD kinetics (sulfide in saltwater or methane in freshwater) and for PO_4 sorption coefficients	1.0	ppt
SALTND	salinity for dividing fresh or saltwater for nitrification/denitrification rates (larger values for freshwater)	1.0	ppt
FRPPH1(1)	fraction of POP in algal group No 1 routed into G_1 class	0.65	none
FRPPH1(2)	fraction of POP in algal group No 1 routed into G_2 class	0.255	none
FRPPH1(3)	fraction of POP in algal group No 1 routed into G_3 class	0.095	none
FRPPH2(1)	fraction of POP in algal group No 2 routed into G_1 class	0.65	none
FRPPH2(2)	fraction of POP in algal group No 2 routed into G_2 class	0.255	none
FRPPH2(3)	fraction of POP in algal group No 2 routed into G_3 class	0.095	none
FRPPH3(1)	fraction of POP in algal group No 3 routed into G_1 class	0.65	none
FRPPH3(2)	fraction of POP in algal group No 3 routed into G_2 class	0.255	none
FRPPH3(3)	fraction of POP in algal group No 3 routed into G_3 class	0.095	none
FRNPH1(1)	fraction of PON in algal group No 1 routed into G_1 class	0.65	none
FRNPH1(2)	fraction of PON in algal group No 1 routed into G_2 class	0.28	none
FRNPH1(3)	fraction of PON in algal group No 1 routed into G_3 class	0.07	none
FRNPH2(1)	fraction of PON in algal group No 2 routed into G_1 class	0.65	none
FRNPH2(2)	fraction of PON in algal group No 2 routed into G_2 class	0.28	none

Table 11 (con't)

FRNPH2(3)	fraction of PON in algal group No 2 routed into G_3 class	0.07	none
FRNPH3(1)	fraction of PON in algal group No 3 routed into G_1 class	0.65	none
FRNPH3(2)	fraction of PON in algal group No 3 routed into G_2 class	0.28	none
FRNPH3(3)	fraction of PON in algal group No 3 routed into G_3 class	0.07	none
FRCPH1(1)	fraction of POC in algal group No 1 routed into G_1 class	0.65	none
FRCPH1(2)	fraction of POC in algal group No 1 routed into G_2 class	0.255	none
FRCPH1(3)	fraction of POC in algal group No 1 routed into G_3 class	0.095	none
FRCPH2(1)	fraction of POC in algal group No 2 routed into G_1 class	0.65	none
FRCPH2(2)	fraction of POC in algal group No 2 routed into G_2 class	0.255	none
FRCPH2(3)	fraction of POC in algal group No 2 routed into G_3 class	0.095	none
FRCPH3(1)	fraction of POC in algal group No 3 routed into G_1 class	0.65	none
FRCPH3(2)	fraction of POC in algal group No 3 routed into G_2 class	0.255	none
FRCPH3(3)	fraction of POC in algal group No 3 routed into G_3 class	0.095	none
KPDIAG(1)	reaction (decay) rates for G_1 class POP at 20°C	0.035	day^{-1}
KPDIAG(2)	reaction (decay) rates for G_2 class POP at 20°C	0.0018	day^{-1}
KPDIAG(3)	reaction (decay) rates for G_3 class POP at 20°C	0.0	day^{-1}
DPTHTA(1)	constant for T adjustment for G_1 class POP decay	1.10	none
DPTHTA(2)	constant for T adjustment for G_2 class POP decay	1.15	none
KNDIAG(1)	reaction (decay) rates for G_1 class PON at 20°C	0.035	day^{-1}
KNDIAG(2)	reaction (decay) rates for G_2 class PON at 20°C	0.0018	day^{-1}
KNDIAG(3)	reaction (decay) rates for G_3 class PON at 20°C	0.0	day^{-1}

Table 11 (con't)

DNTHTA(1)	constant for T adjustment for G_1 class PON decay	1.10	none
DNTHTA(2)	constant for T adjustment for G_2 class PON decay	1.15	none
KCDIAG(1)	reaction (decay) rates for G_1 class POC at 20°C	0.035	(day^{-1})
KCDIAG(2)	reaction (decay) rates for G_2 class POC at 20°C	0.0018	(day^{-1})
KCDIAG(3)	reaction (decay) rates for G_3 class POC at 20°C	0.0	(day^{-1})
DCTHTA(1)	constant for T adjustment for G_1 class POC decay	1.10	none
DCTHTA(2)	constant for T adjustment for G_2 class POC decay	1.15	none
KSI	1^{st}-order reaction (dissolution) rate of PSi at 20°C	0.5	day^{-1}
THTASI	constant for T adjustment for PSi dissolution	1.1	none
M1	solid concentrations in Layer 1	0.5	kg l^{-1}
M2	solid concentrations in Layer 2	0.5	kg l^{-1}
THTADP	constant for T adjustment for diffusion coefficient for particle mixing	1.117	none
THTADD	constant for T adjustment for diffusion coefficient for dissolved phase	1.08	none
KAPPNH4F	optimum reaction velocity for nitrification in Layer 1 for freshwater	0.20	m day^{-1}
KAPPNH4S	optimum reaction velocity for nitrification in Layer 1 for saltwater	0.14	m day^{-1}
THTANH4	constant for T adjustment for nitrification	1.08	none
KMNH4	half-saturation constant of NH_4 for nitrification	1500.0	mg N m^{-3}
KMNH4O2	half-saturation constant of DO for nitrification	1.0	g O_2 m^{-3}
PIENH4	partition coefficient for NH_4 in both layers	1.0	per kg l^{-1}
KAPPNO3F	reaction velocity for denitrification in Layer 1 at 20°C for freshwater	0.3	m day^{-1}
KAPPNO3S	reaction velocity for denitrification in Layer 1 at 20°C for saltwater	0.125	m day^{-1}

Table 11 (con't)

K2NO3	reaction velocity for denitrification in Layer 2 at 20°C	0.25	m day^{-1}
THTANO3	constant for T adjustment for denitrification	1.08	none
KAPPD1	reaction velocity for dissolved H_2S oxidation in Layer 1 at 20°C	0.2	m day^{-1}
KAPPP1	reaction velocity for particulate H_2S oxidation in Layer 1 at 20°C	0.4	m day^{-1}
PIE1S	partition coefficient for H_2S in Layer 1	100.0	per kg l^{-1}
PIE2S	partition coefficient for H_2S in Layer 2	100.0	per kg l^{-1}
THTAPD1	constant for T adjustment for both dissolved & particulate H2S oxidation	1.08	none
KMHSO2	constant to normalize H2S oxidation rate for oxygen	4.0	g O_2 m^{-3}
CSISAT	saturation concentration of Si in the pore water	40000.0	mg Si m^{-3}
DPIE1SI	incremental partition coefficient for Si in Layer 1	10.0	per kg l^{-1}
PIE2SI 2	partition coefficient for Si in Layer 2	100.0	per kg l^{-1}
O2CRITSI	critical DO concentration for Layer 1 incremental Si sorption	1.0	g O_2 m^{-3}
KMPSI	half-saturation constant of PSi for Si dissolution	5×10^7	mg Si m^{-3}
JSIDETR	detrital flux of PSi to account for PSi settling to the sediment that is not associated with algal flux of PSi	100.0	mg Si m^{-2} day^{-1}
DPIE1PO4F*	incremental partition coefficient for PO_4 in Layer 1 for freshwater	3000.0	per kg l^{-1}
DPIE1PO4S*	incremental partition coefficient for PO_4 in Layer 1 for saltwater	300.0	per kg l^{-1}
PIE2PO4*	partition coefficient for PO_4 in Layer 2	100.0	per kg l^{-1}
O2CRIT	critical DO concentration for Layer 1 incremental PO_4 sorption	2.0	g O_2 m^{-3}
KMO2DP	half-saturation constant of DO for particle mixing	4.0	g O_2 m^{-3}
TEMPBEN	temperature at which benthic stress accumulation is reset to zero	10.0	°C
KBENSTR	1^{st}-order decay rate for benthic stress	0.03	day^{-1}
KLBNTH	ratio of bio-irrigation to bioturbation	0.0	none
DPMIN	minimum diffusion coefficient for particle mixing	3×10^{-6}	m^2 day^{-1}
KAPPCH4	reaction velocity for dissolved CH_4 oxidation in Layer 1 at 20°C	0.2	m day^{-1}

Table 11 (con't)

THTACH4	constant for T adjustment for dissolved CH_4 oxidation	1.08	none
VSED	net burial (sedimentation) rate	0.25	cm yr^{-1}
VPMIX	diffusion coefficient for particle mixing	1.2×10^{-4}	m^2 day^{-1}
VDMIX	diffusion coefficient in pore water	0.001	m^2 day^{-1}
WSCNET	net settling velocity for algal group 1	0.1	m day^{-1}
WSDNET	net settling velocity for algal group 2	0.3	m day^{-1}
WSGNET	net settling velocity for algal group 3	0.1	m day^{-1}

DPIE1PO4F*: 1000.0 l / kg in sensitivity analysis in Back River.
DPIE1PO4S*: 100.0 l / kg in sensitivity analysis in Back River.
PIE2PO4*: 30.0 l / kg in sensitivity analysis in Back River.

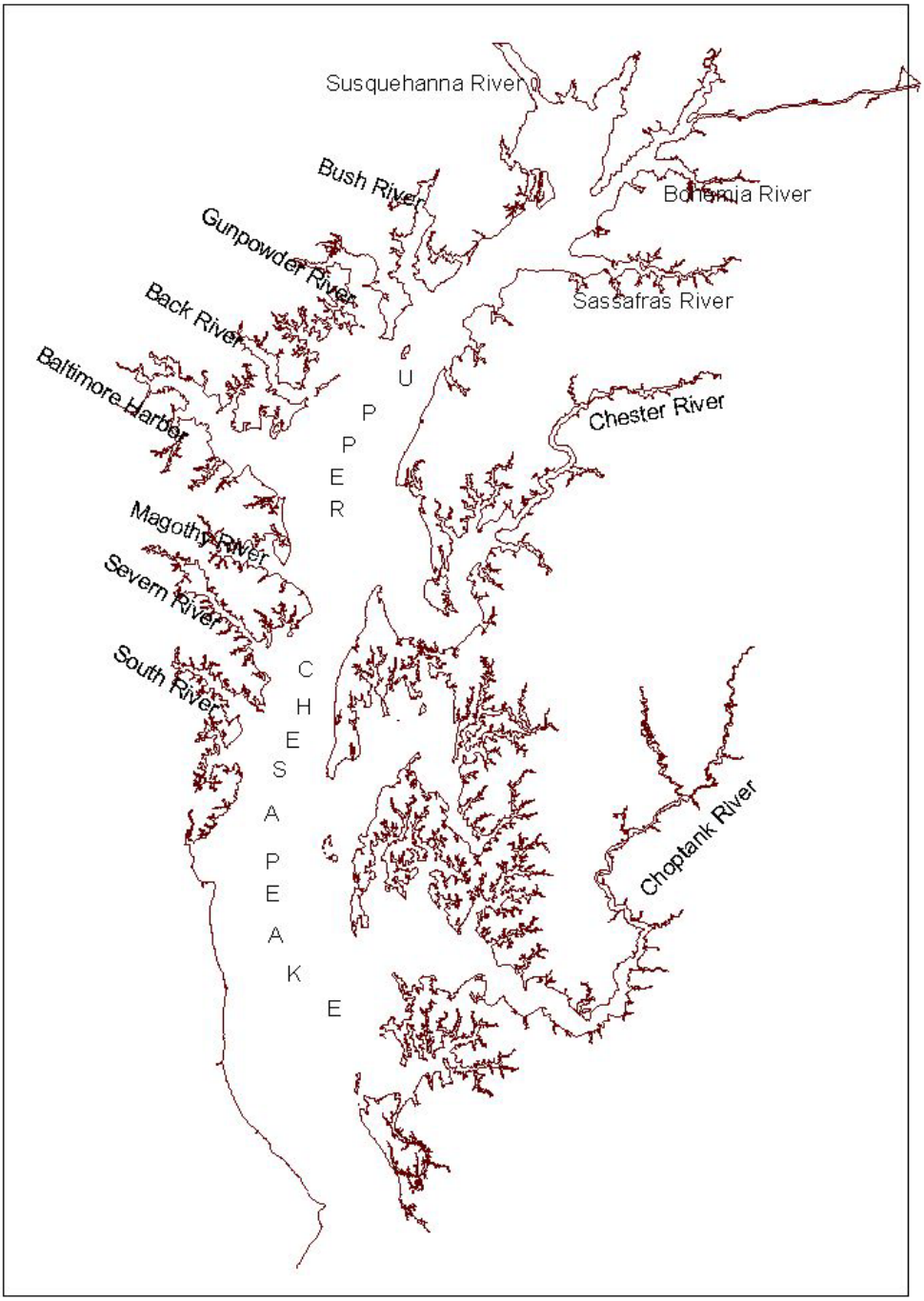

Fig. 1. The study domain for the hydrodynamic and water quality model

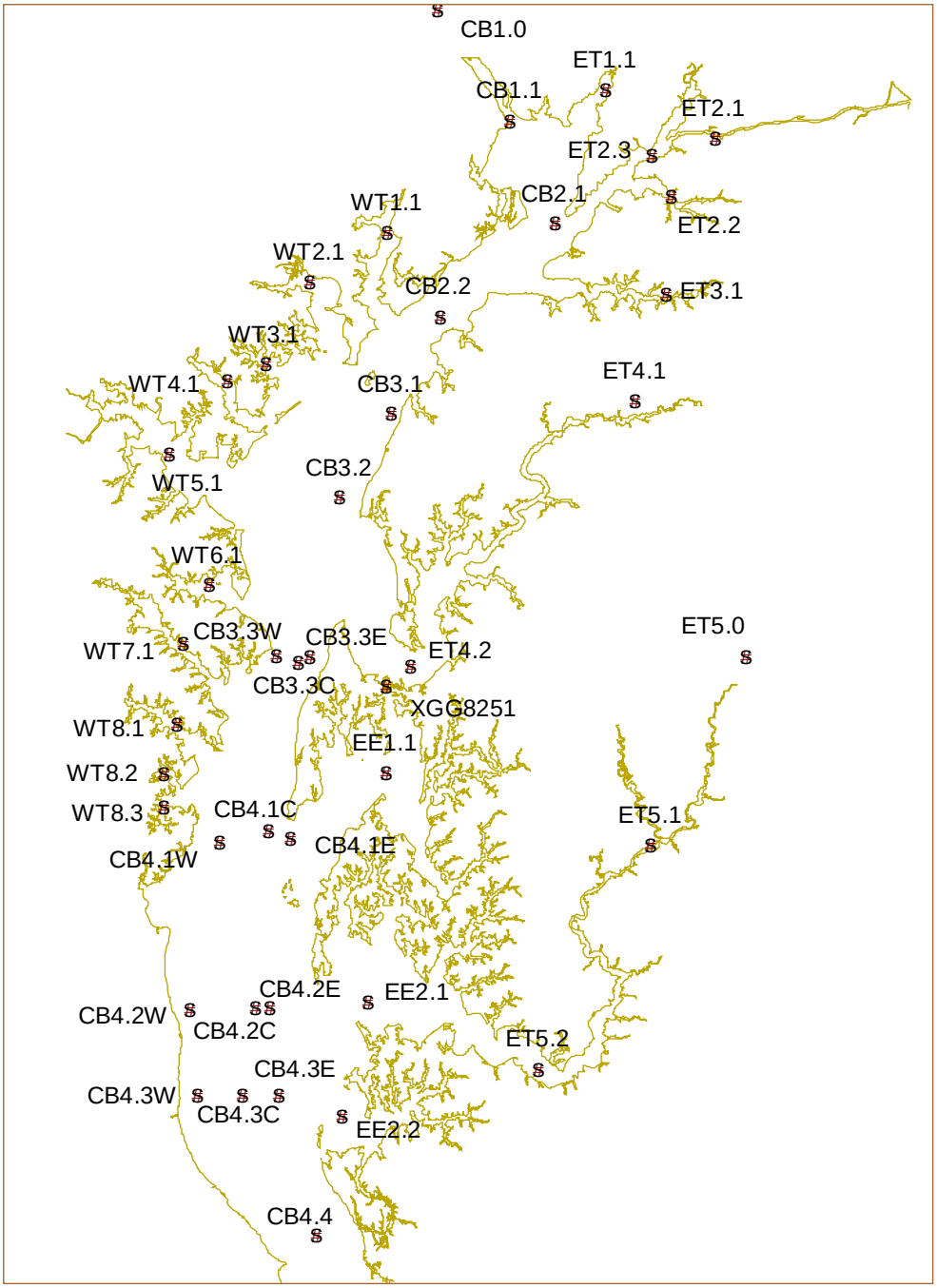

Fig. 2. Chesapeake Bay water quality monitoring stations

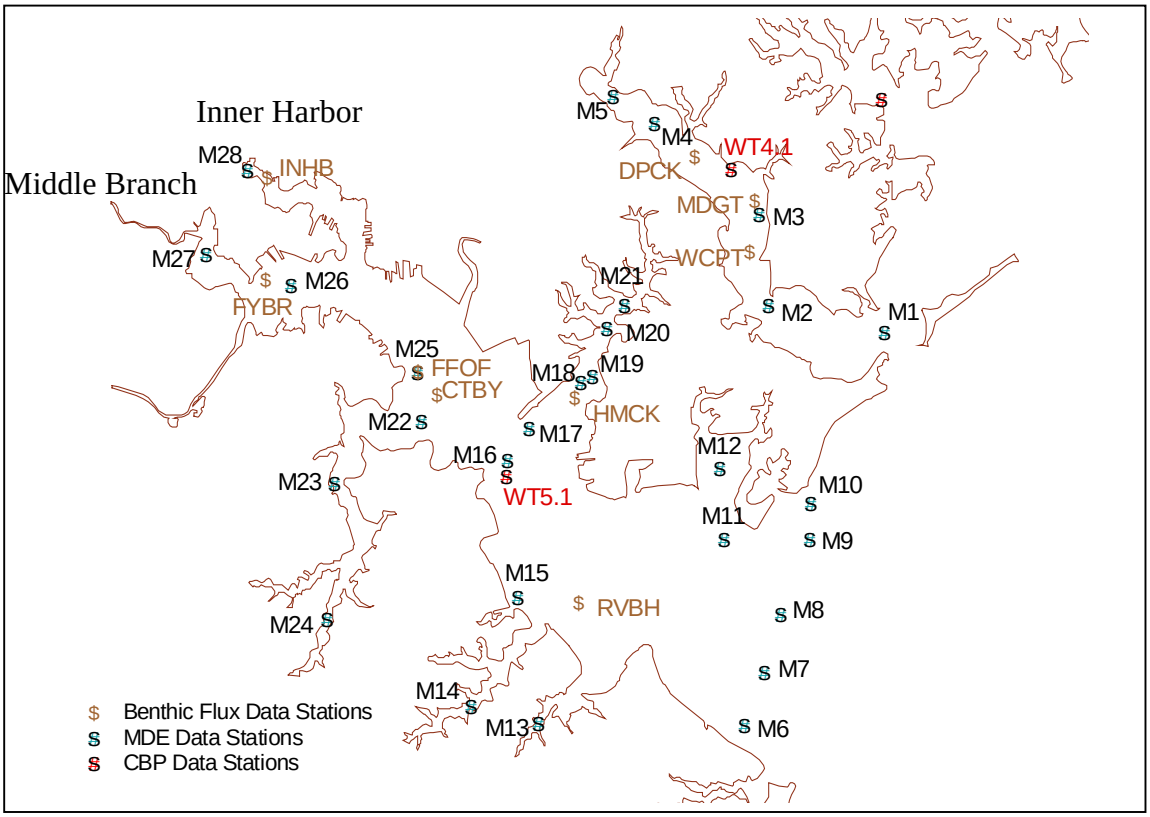

Fig. 3. Map of MDE water column monitoring stations and benthic flux stations

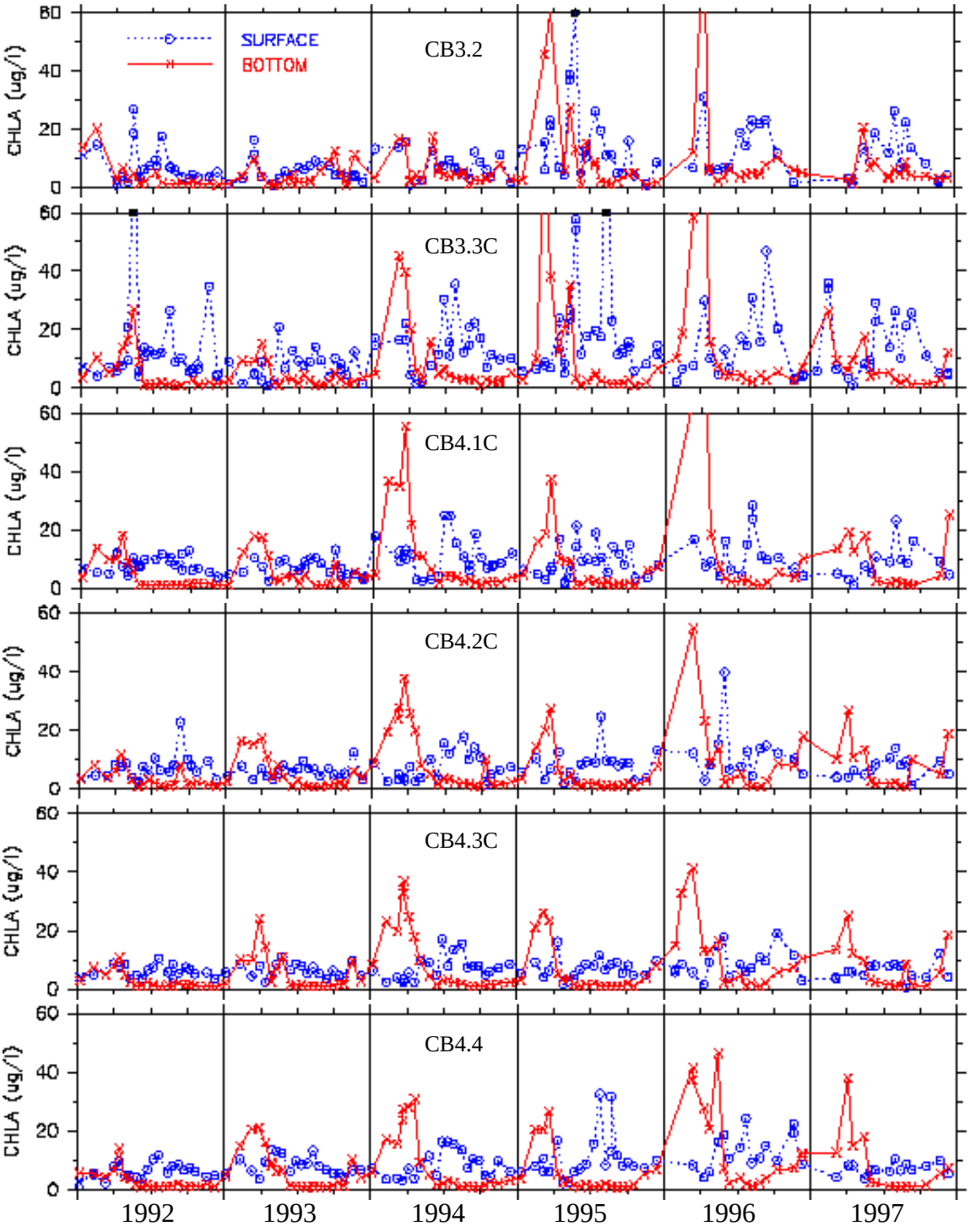

Fig. 4. Temporal distribution of chlorophyll a in the Upper Chesapeake Bay from CB4.4 upstream to CB3.2

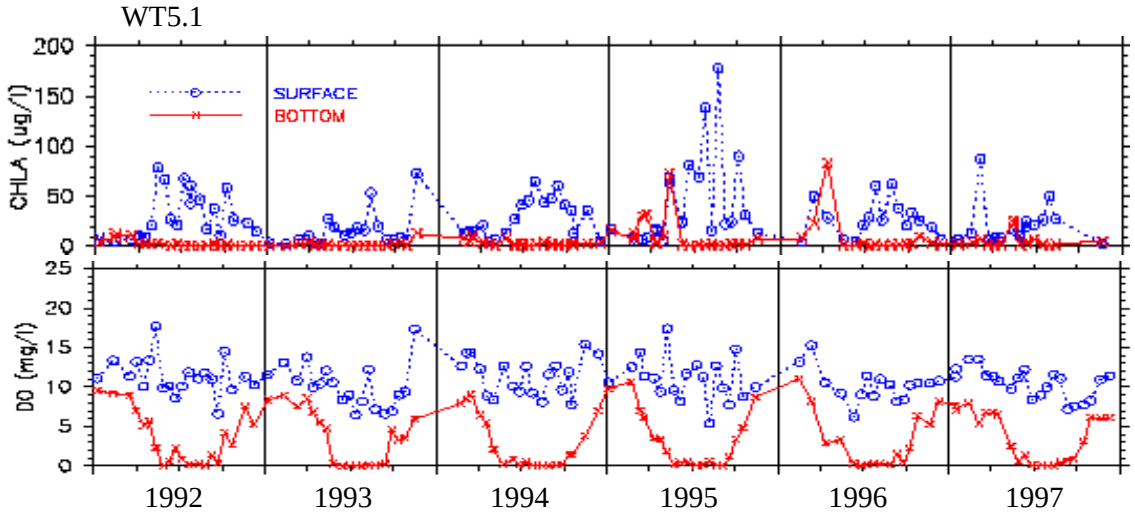

Fig. 5. Temporal distribution of chlorophyll a and DO in Baltimore Harbor at WT5.1

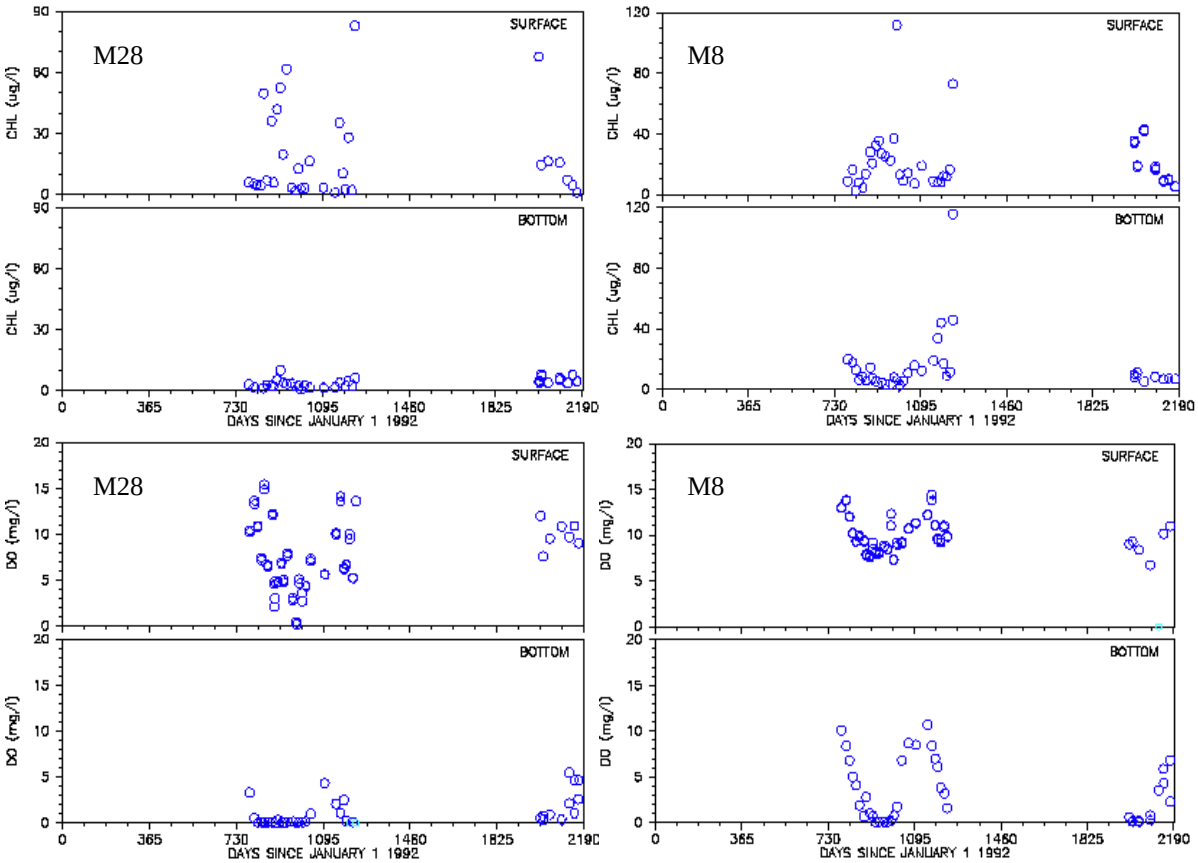

Fig. 6. Temporal distribution of chlorophyll a and DO at M28 (head) and M08 (mouth) of Baltimore Harbor, respectively

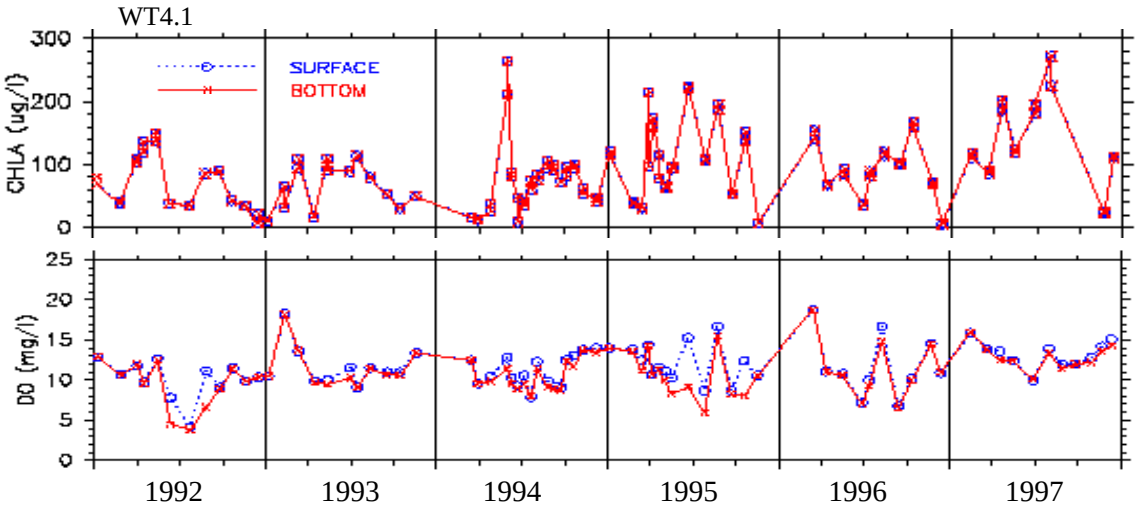

Fig. 7. Temporal distribution of chlorophyll a and DO in Back River at WT.4.1

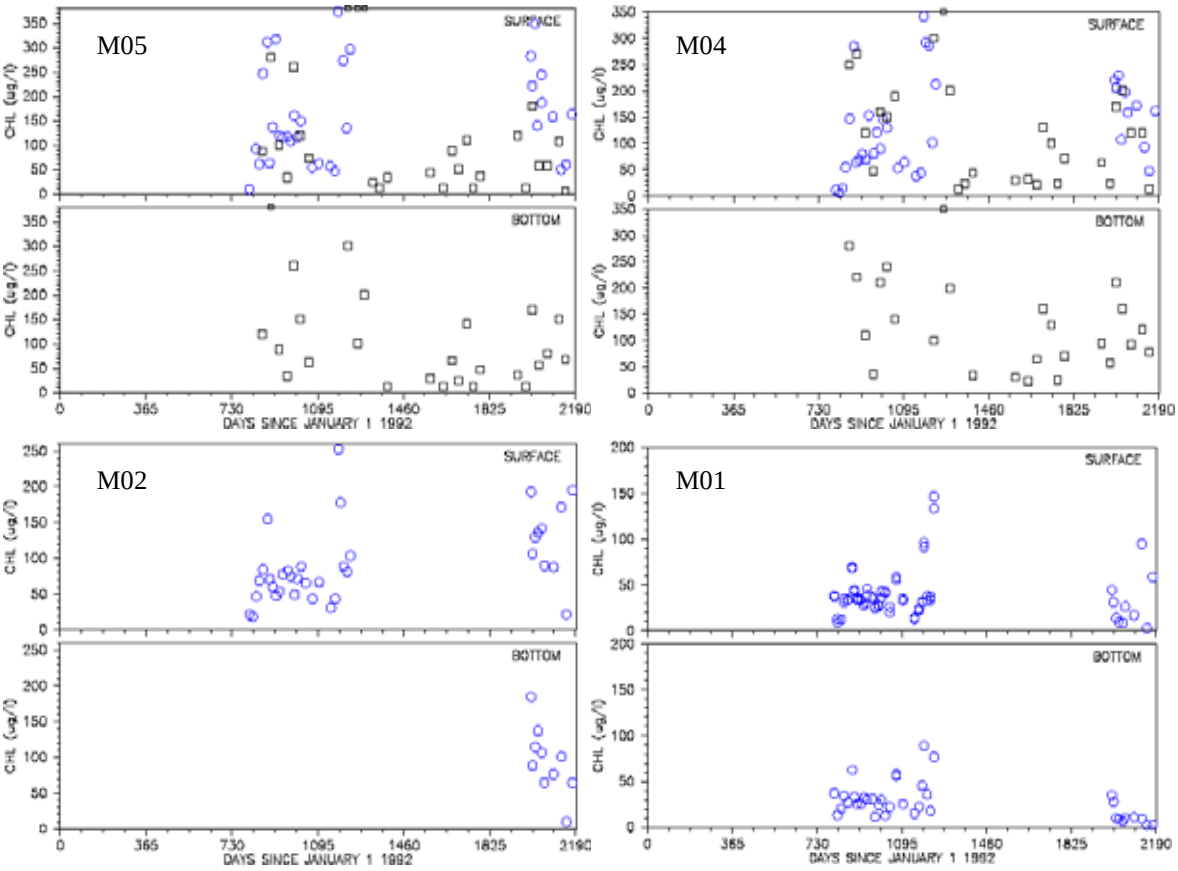

Fig. 8. Temporal distribution of chlorophyll a in Back River from M05 downstream to M01 (Circles are MDE data, Squares are additional Baltimore City data)

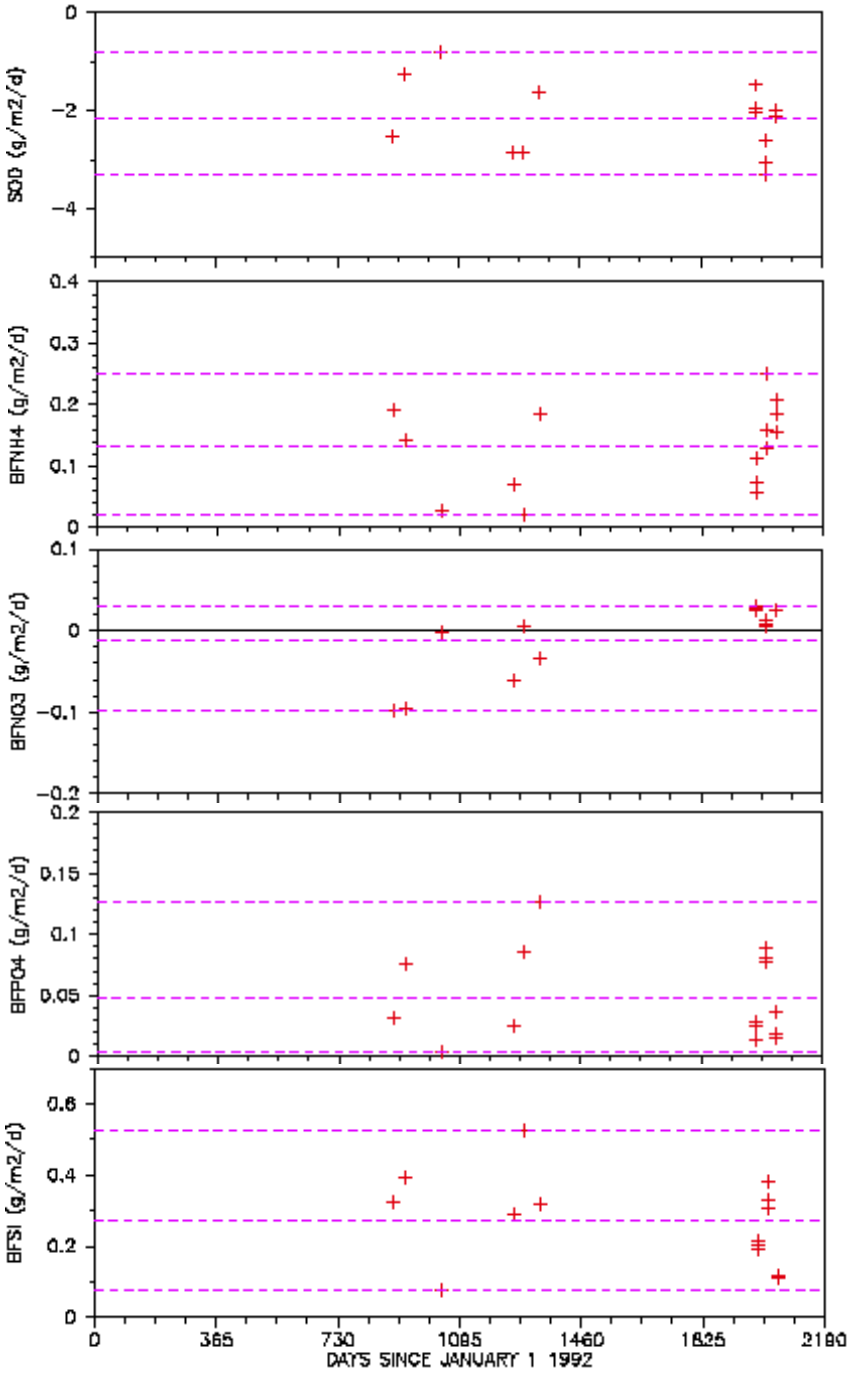

Fig. 9. Temporal distribution of benthic flux data a at WCPT of Back River (three dashed lines represent the maximum, mean, and minimum, from top to bottom, respectively)

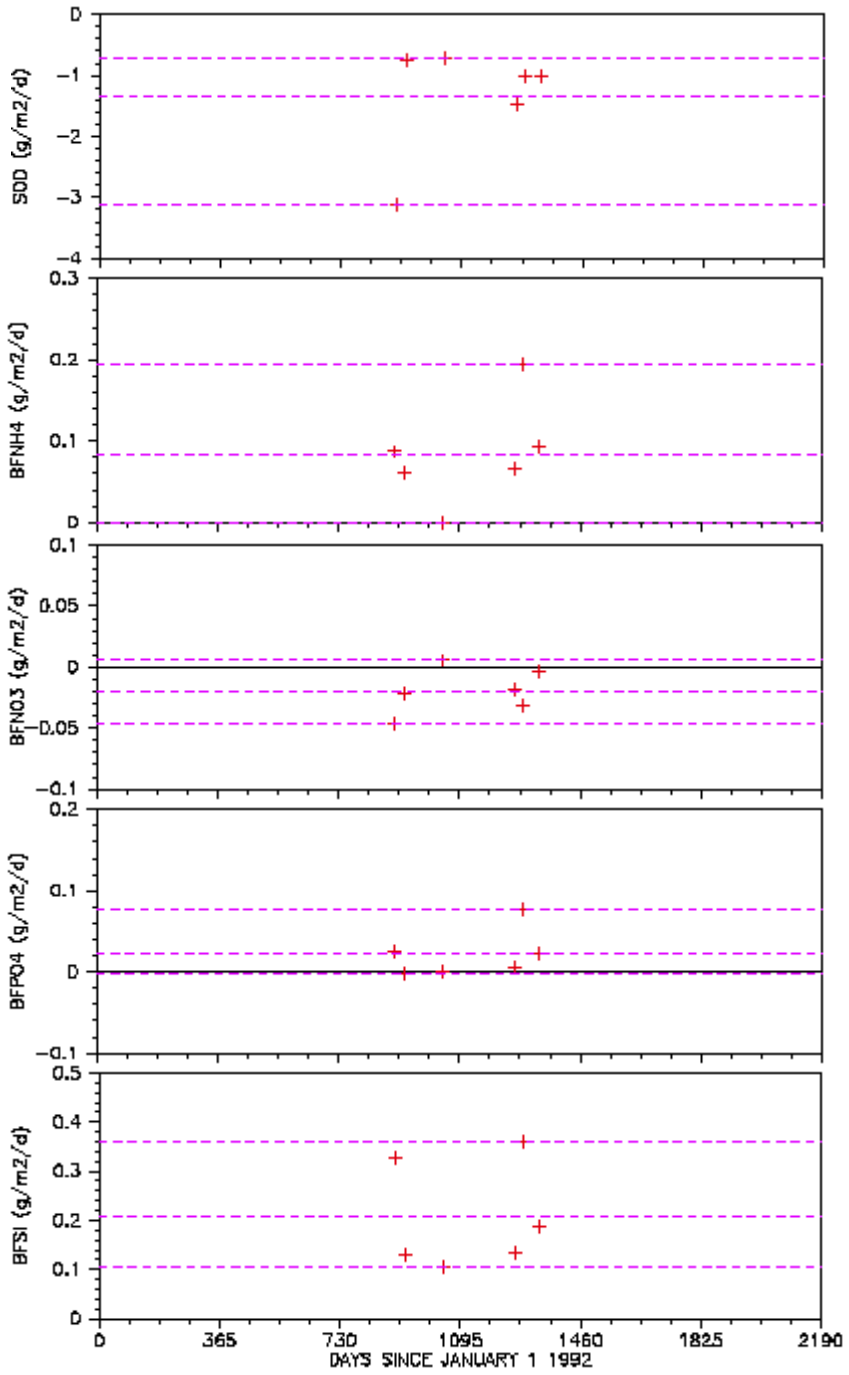

Fig. 10. Temporal distribution of benthic flux data at CTBY of Baltimore Harbor (three dashed lines represent maximum, minimum, and mean from top to bottom, respectively)

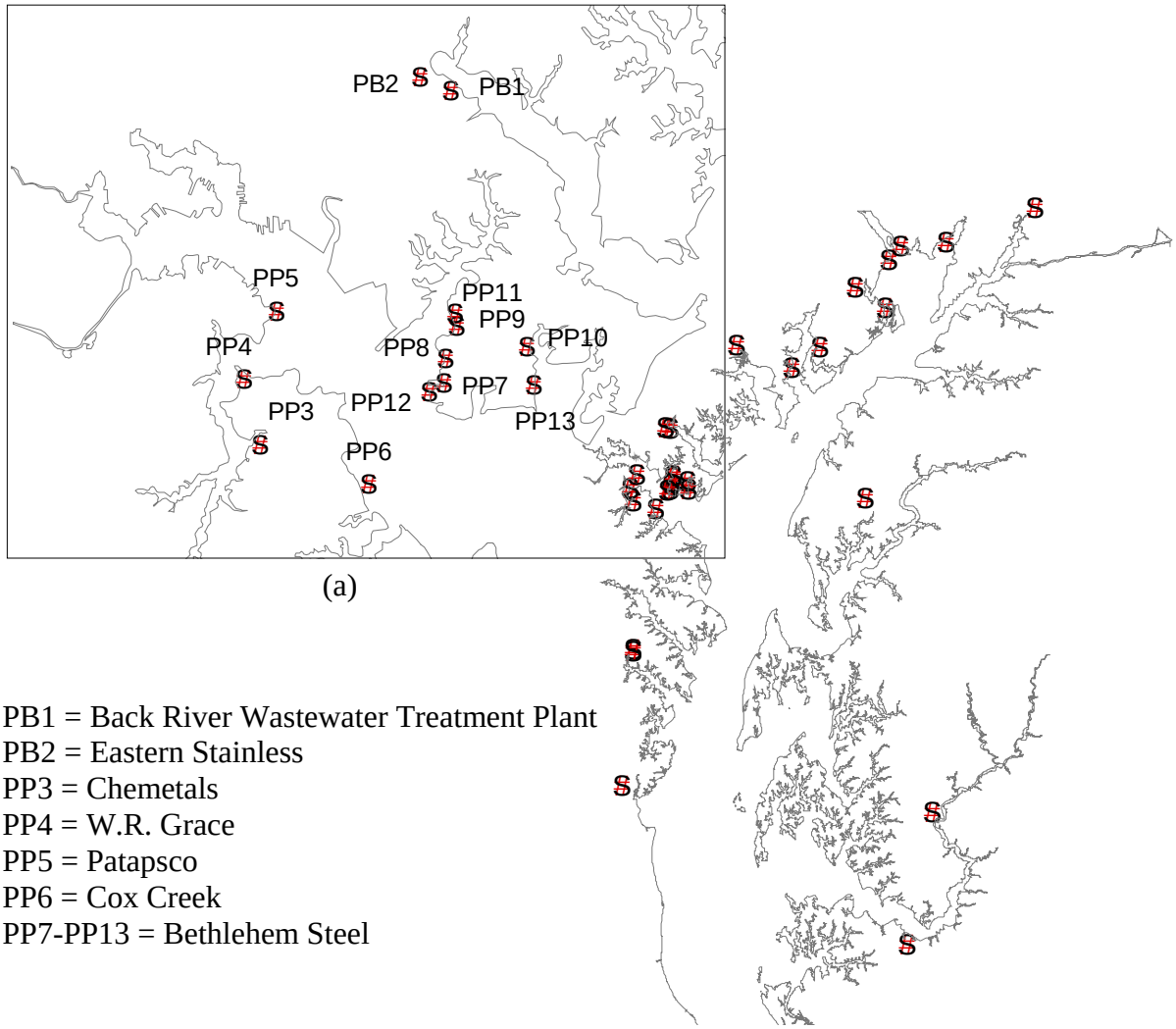

PB1 = Back River Wastewater Treatment Plant
PB2 = Eastern Stainless
PP3 = Chemetals
PP4 = W.R. Grace
PP5 = Patapsco
PP6 = Cox Creek
PP7-PP13 = Bethlehem Steel

Fig. 11. Point source outfall locations in Baltimore Harbor (a) and the Upper Chesapeake Bay (b)

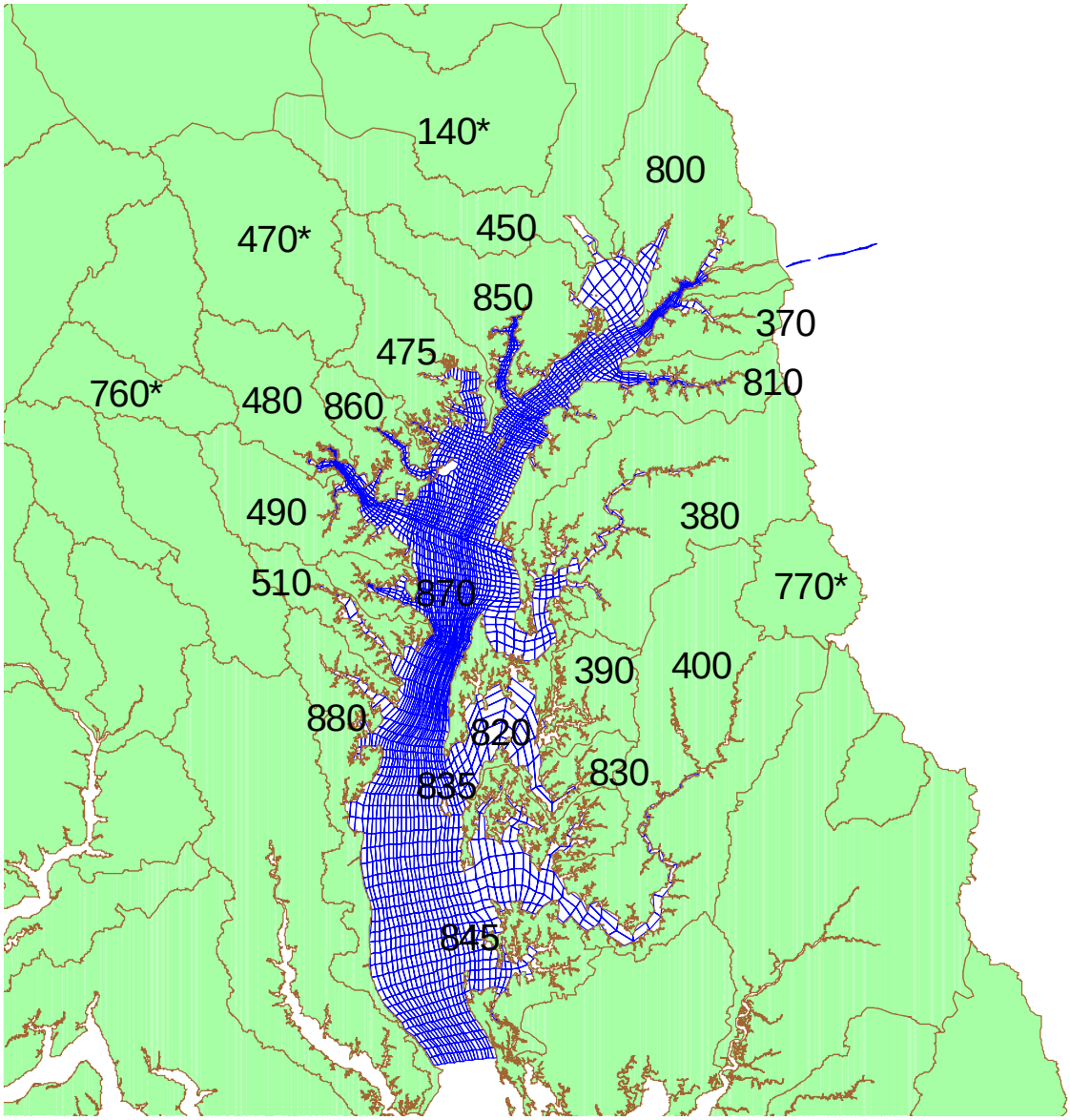

Fig. 12. Chesapeake Bay Program watershed model segments. There are 4 fall-line segments (those with *) and 19 below-fall-line segments coinciding with the hydrodynamic/water quality modeling domain

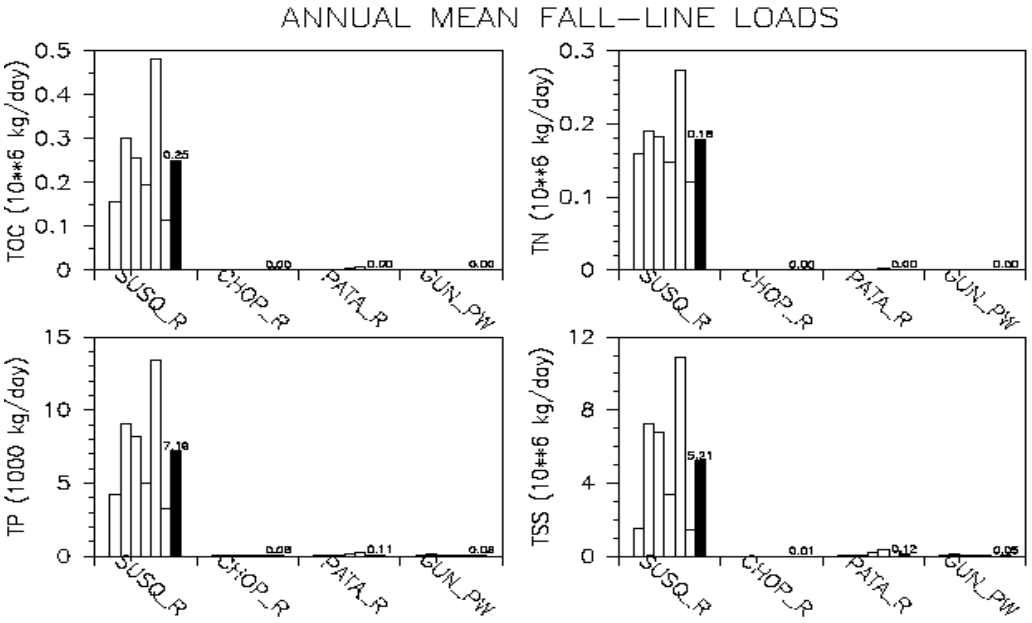

Fig. 13. External loads from Susquehanna, Choptank, Patapsco, and Gunpowder basins (six blank bars are from 1992 -1997, and dark bar is for 6-year mean)

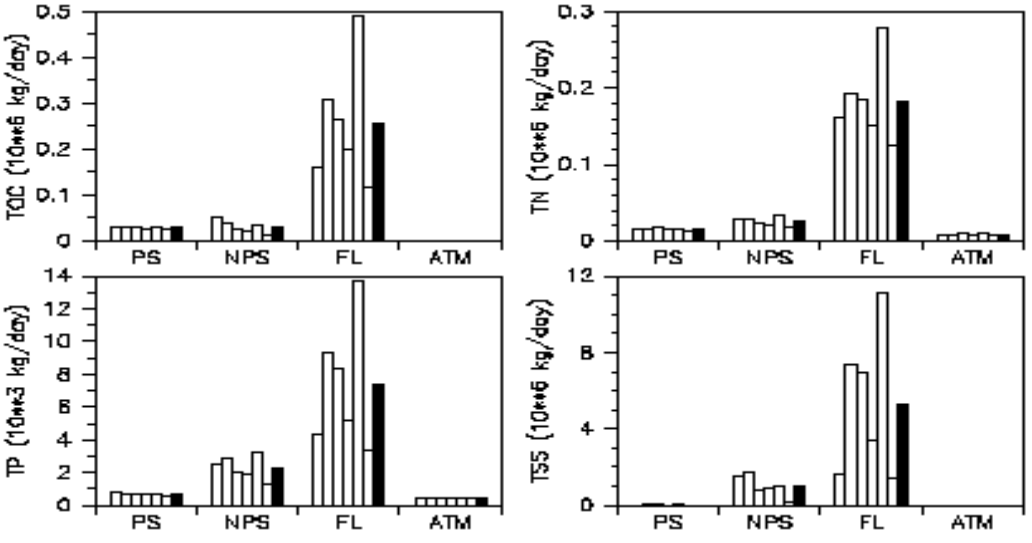

Fig. 14. External Loading from point source (PS), non-point source (NPS), fall-line (FL), and atmospheric loading (ATM) into the Upper Chesapeake Bay (six blank bars are from 1992-1997, and dark bar is for 6-year mean)

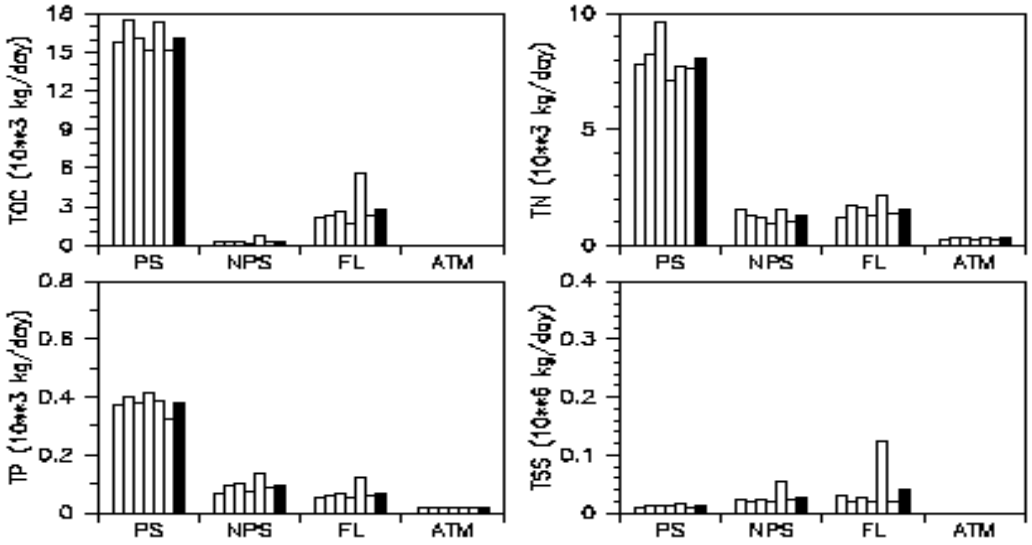

Fig. 15. External Loading from point source (PS), non-point source (NPS), fall-line (FL), and atmospheric loading (ATM) into Baltimore Harbor (six blank bars are from 1992-1997, and dark bar is for 6-year mean)

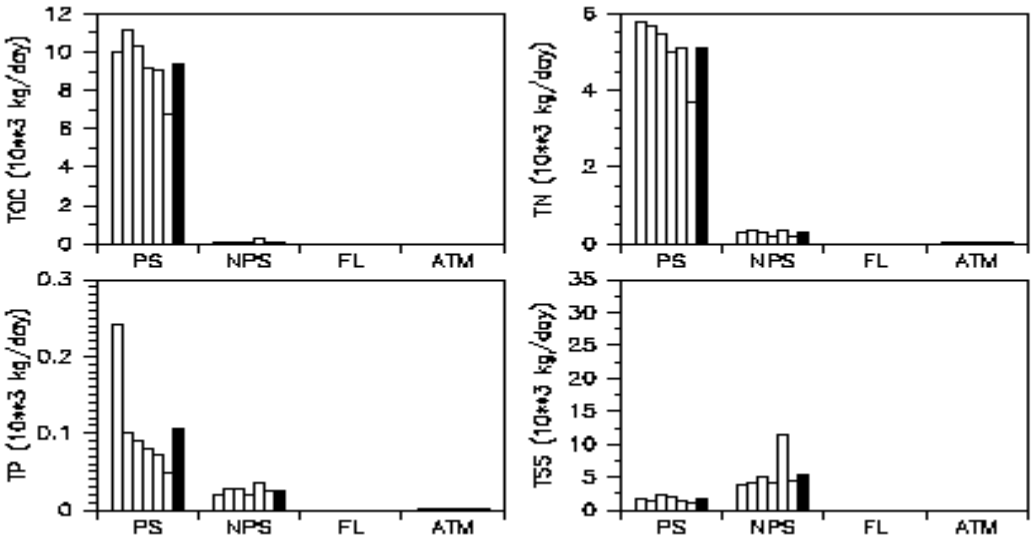

Fig. 16. External Loading from point source (PS), non-point source (NPS), fall-line (FL), and atmospheric loading (ATM) into Back River (six blank bars are from 1992-1997, and dark bar is for 6-year mean)

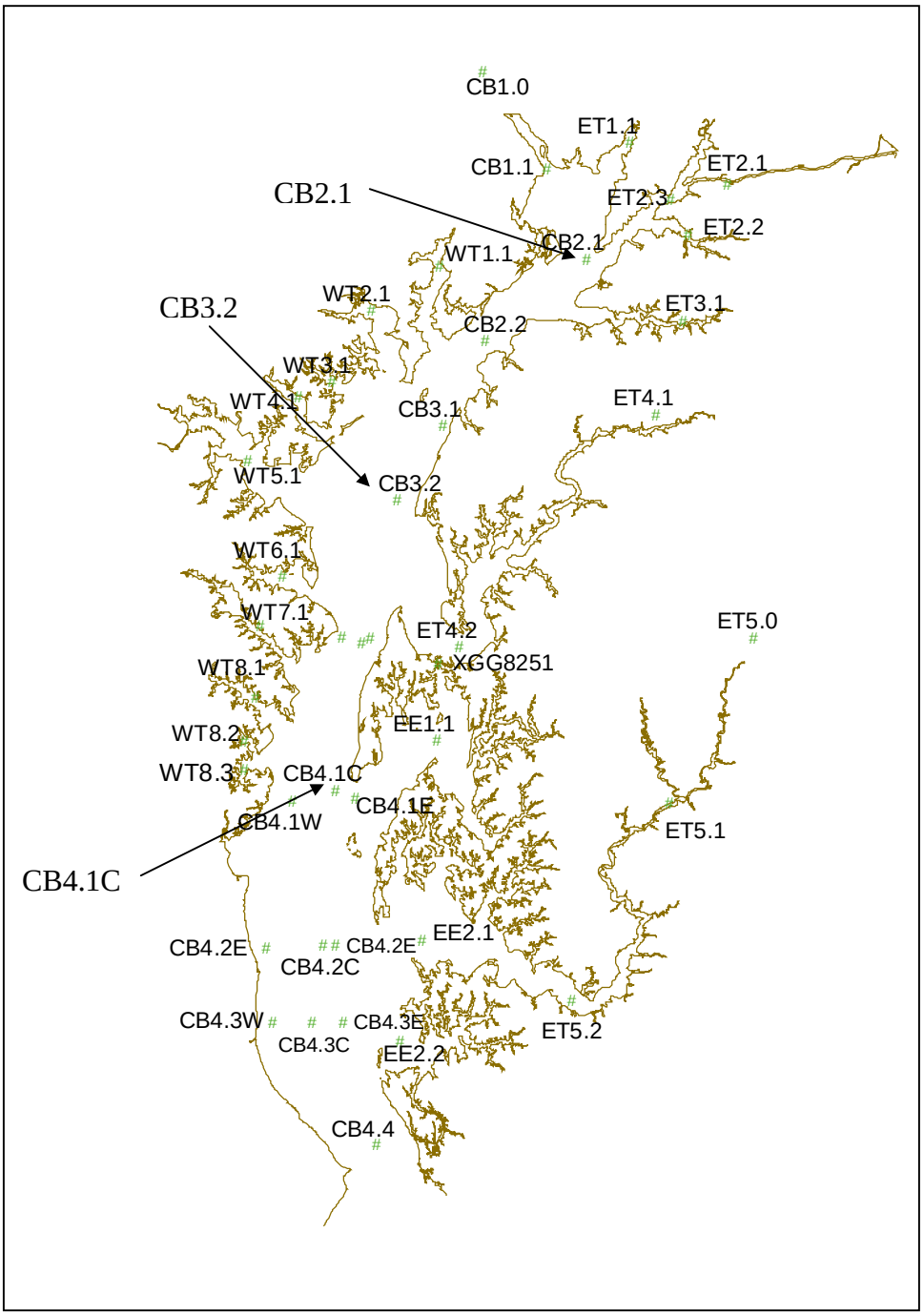

Fig. 17. CBP water quality monitoring stations

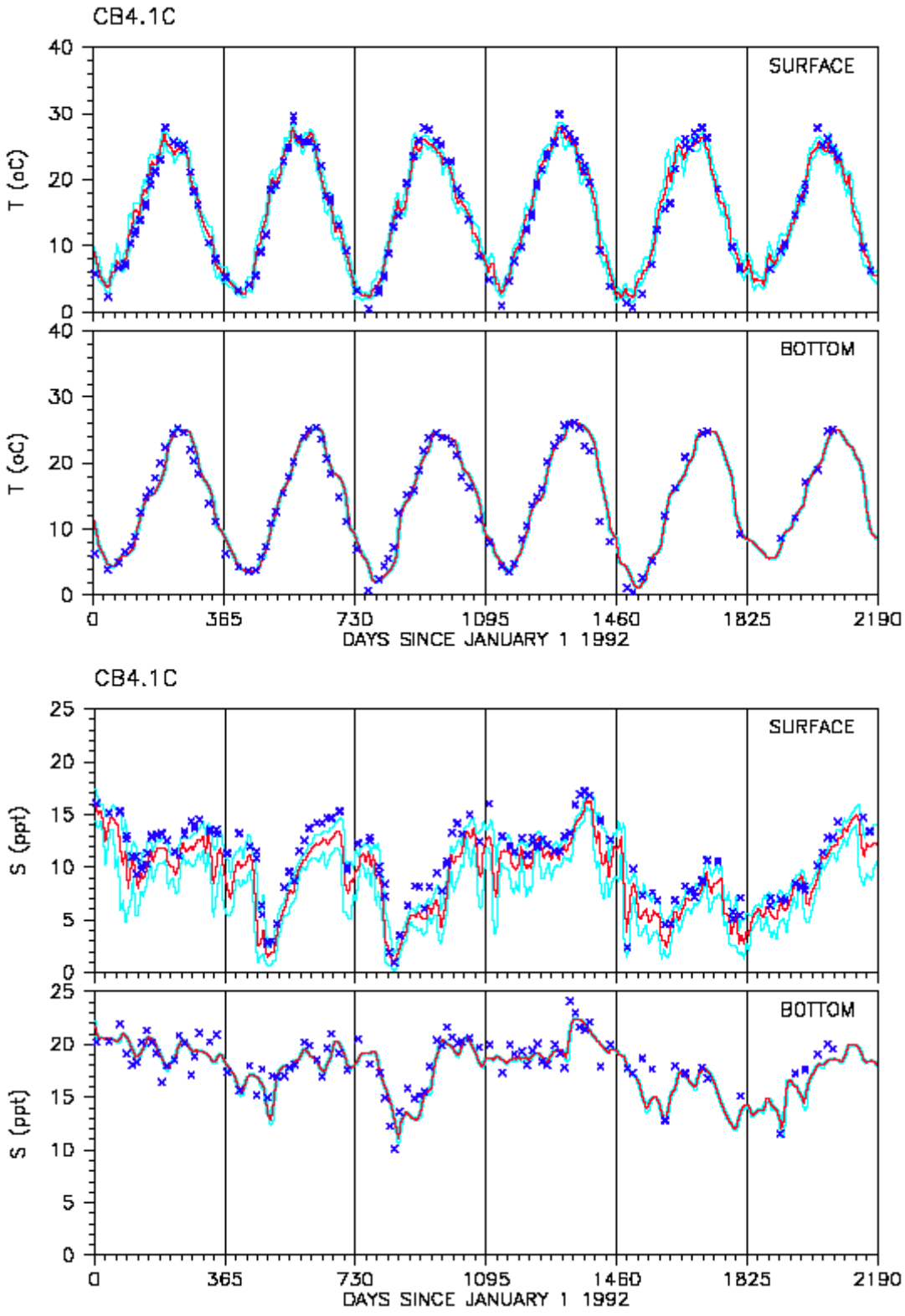

Fig. 18. Time series comparison of model calibration results and data for temperature and salinity in the Upper Chesapeake Bay (CB4.1C)

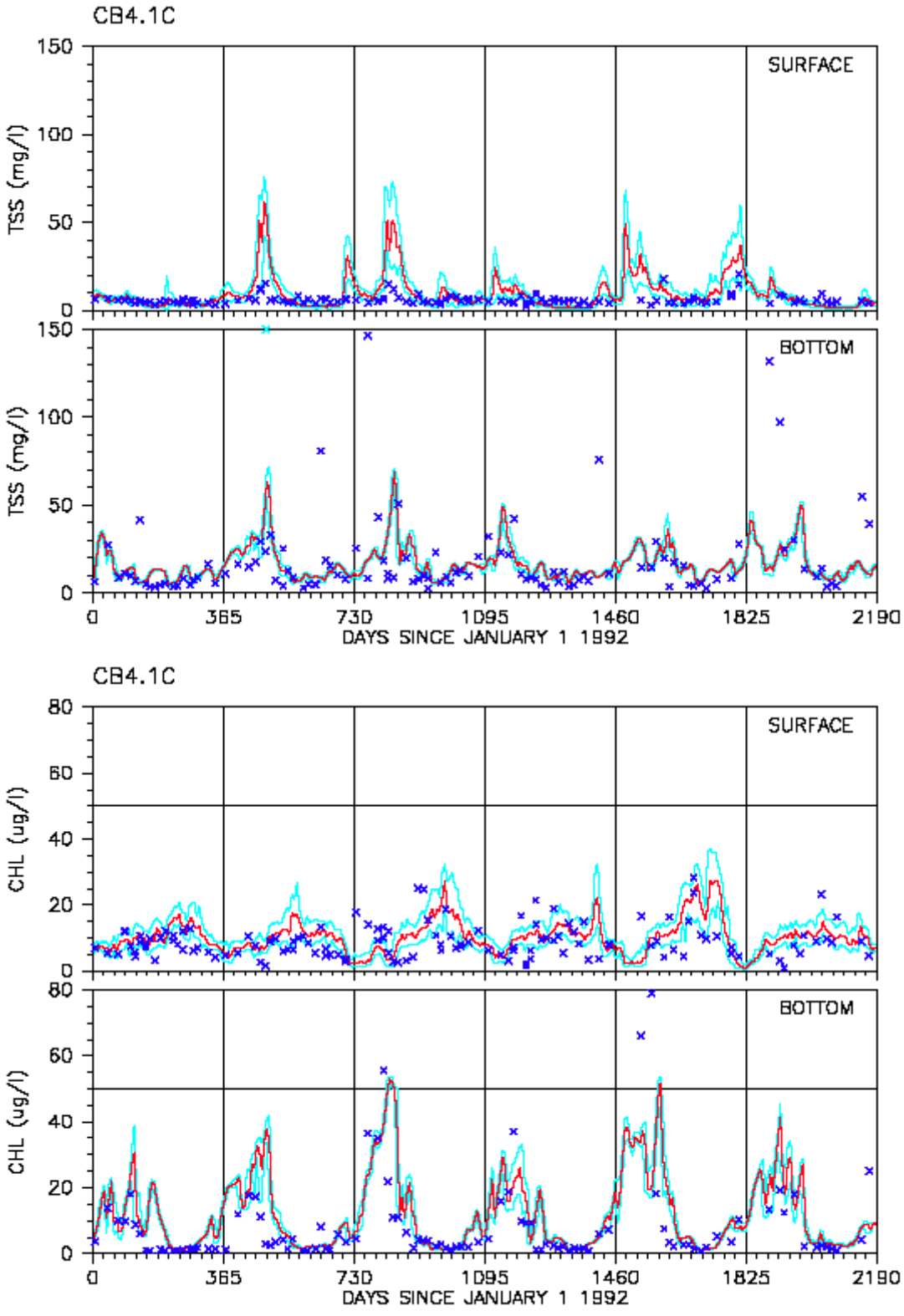

Fig. 19. Time series comparison of model calibration results and data for total suspended solids and chlorophyll a in the Upper Chesapeake Bay (CB4.1C)

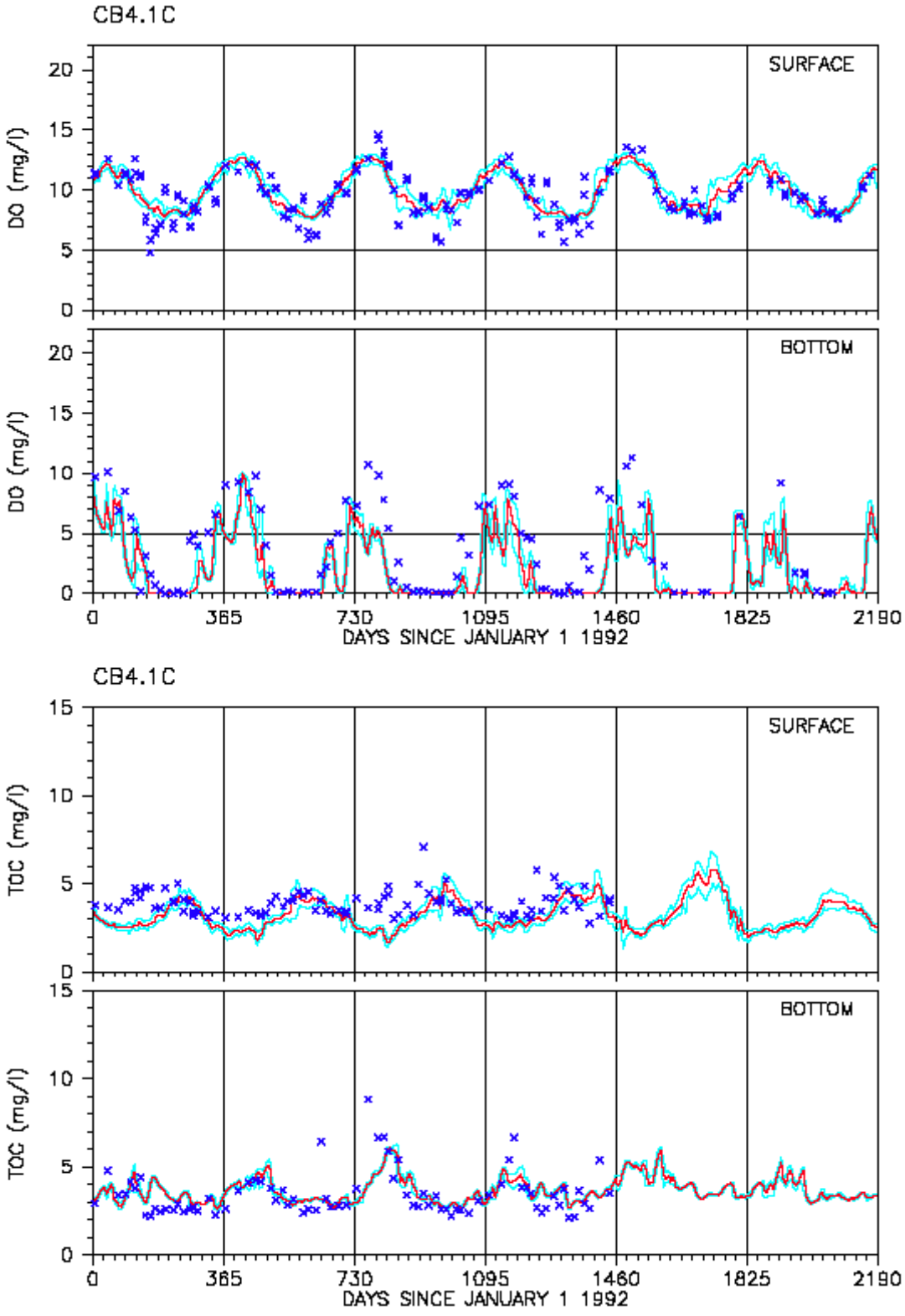

Fig. 20. Time series comparison of model calibration results and data for dissolved oxygen and total organic carbon in the Upper Chesapeake Bay (CB4.1C)

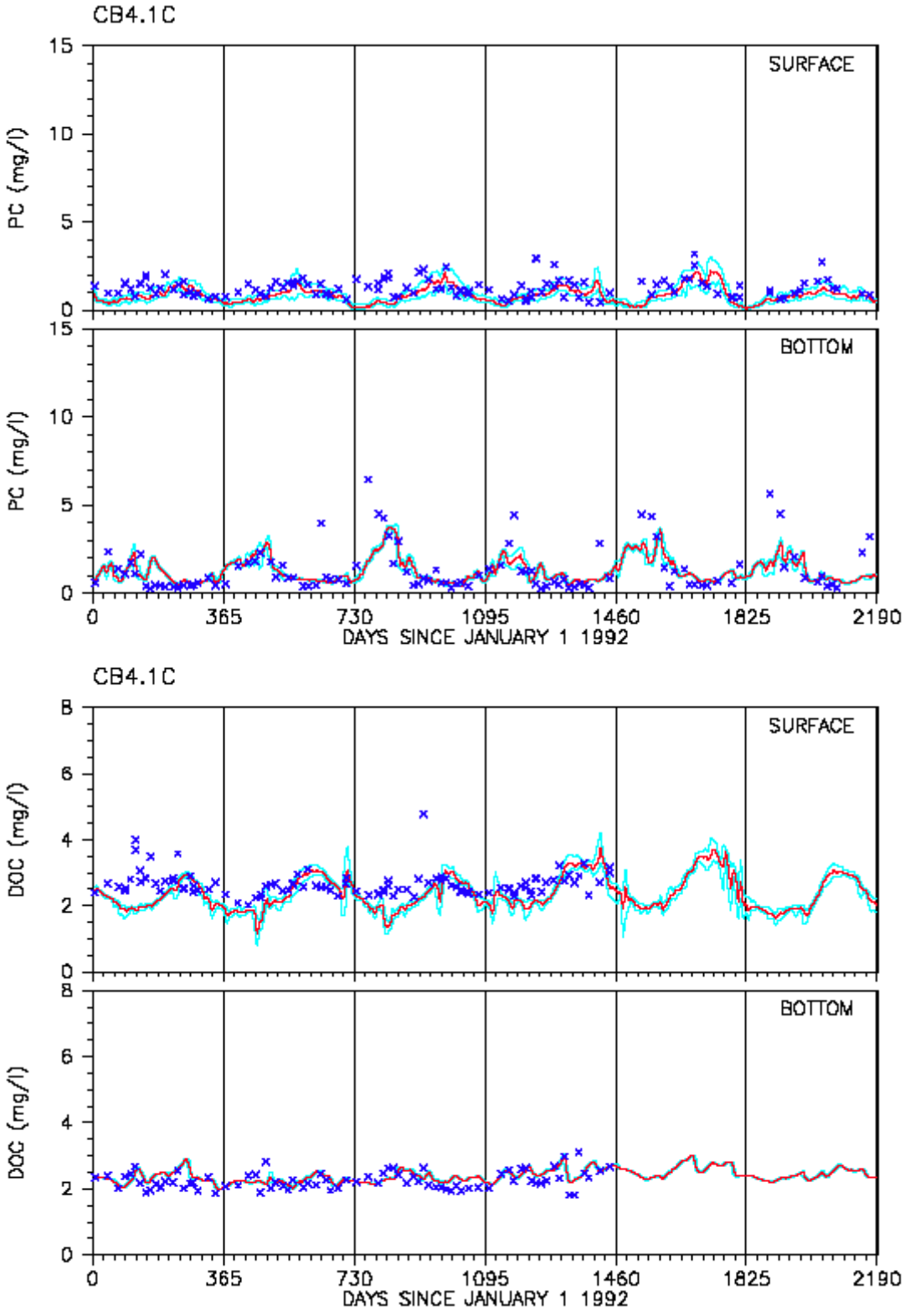

Fig. 21. Time series comparison of model calibration results and data for particulate organic carbon and dissolved organic carbon in the Upper Chesapeake Bay (CB4.1C)

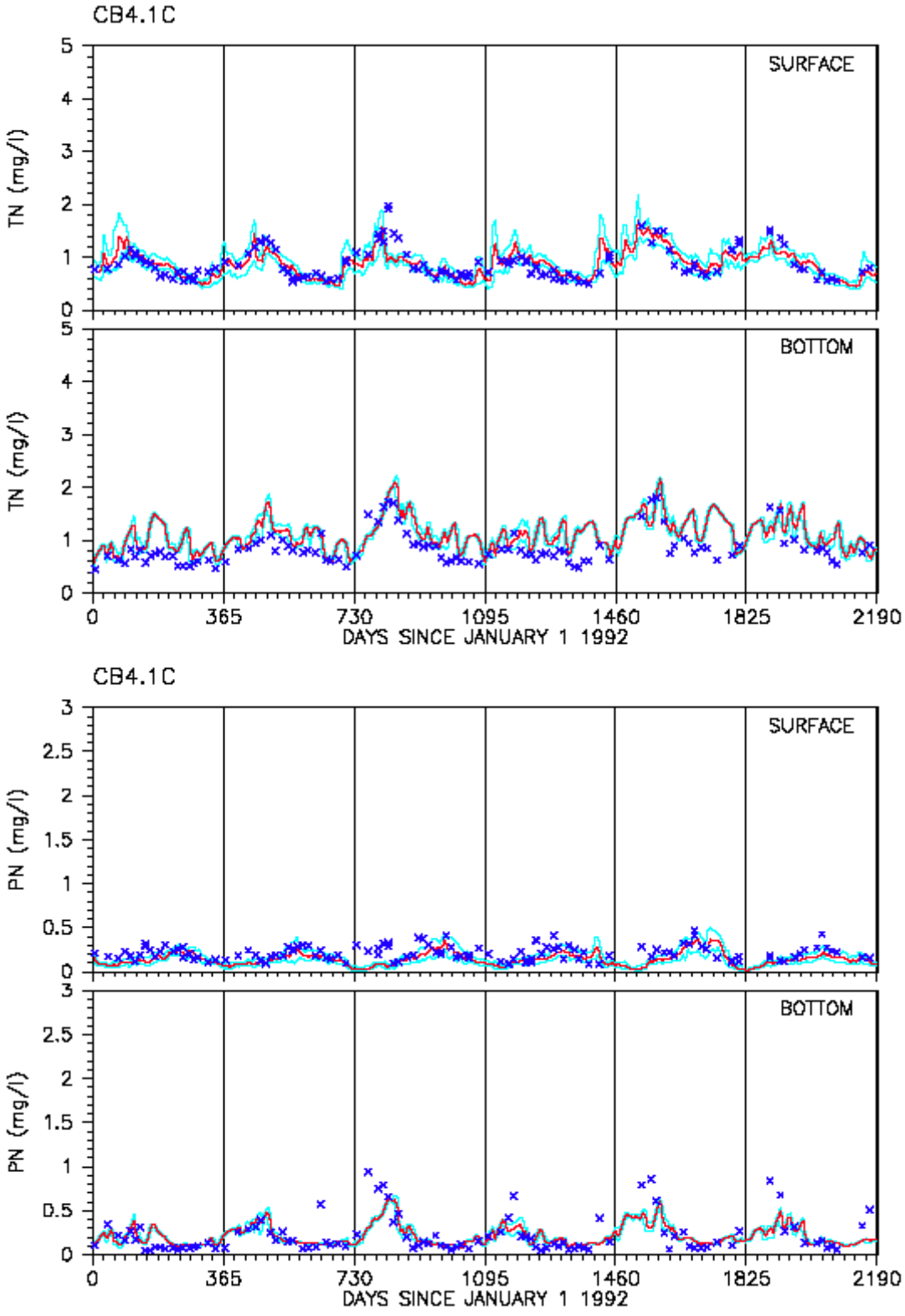

Fig. 22. Time series comparison of model calibration results and data for total nitrogen and particulate nitrogen in the Upper Chesapeake Bay (CB4.1C)

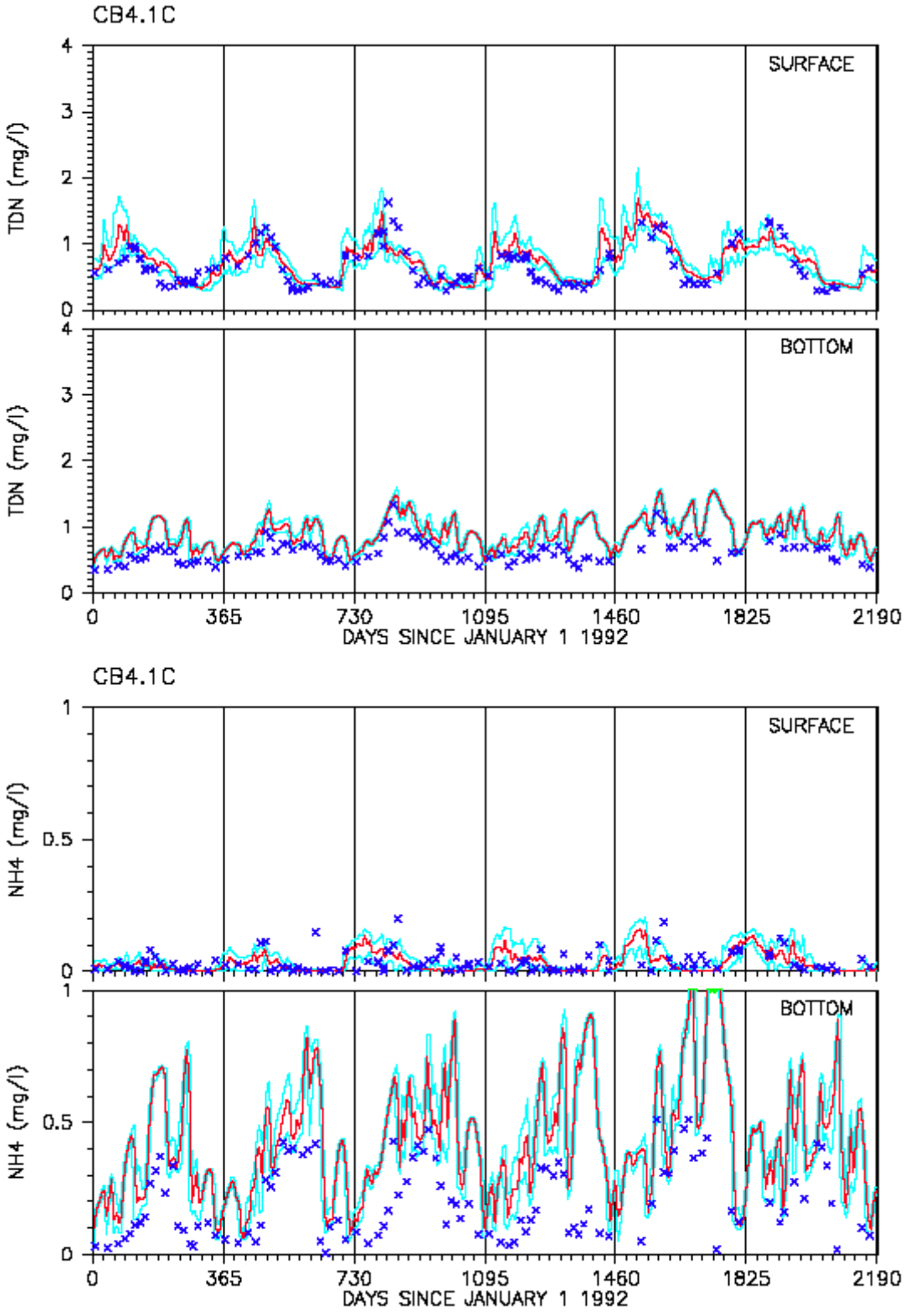

Fig. 23. Time series comparison of model calibration results and data for total dissolved nitrogen and ammomia in the Upper Chesapeake Bay (CB4.1C)

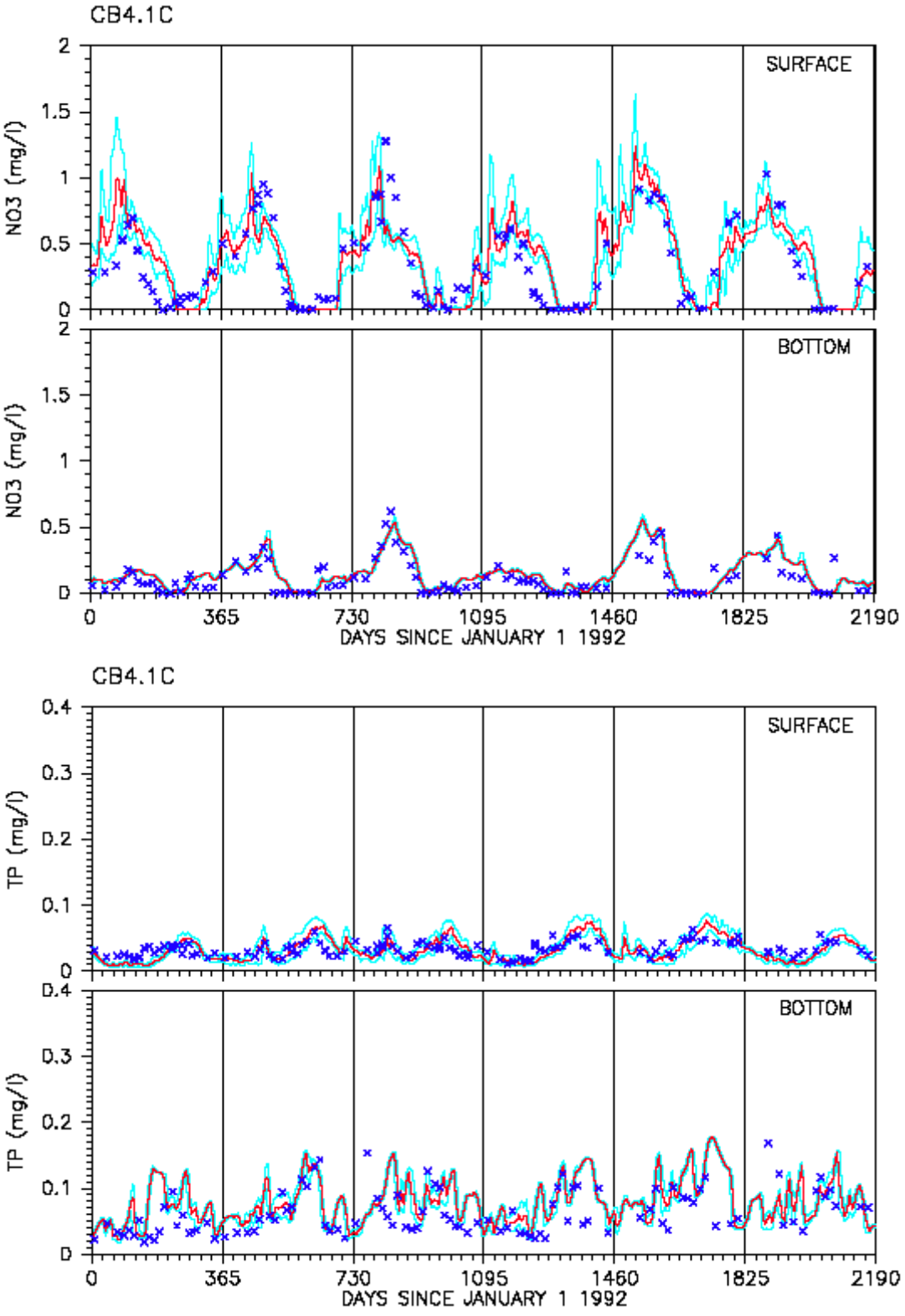

Fig. 24. Time series comparison of model calibration results and data for nitrate and total phosphorus in the Upper Chesapeake Bay (CB4.1C)

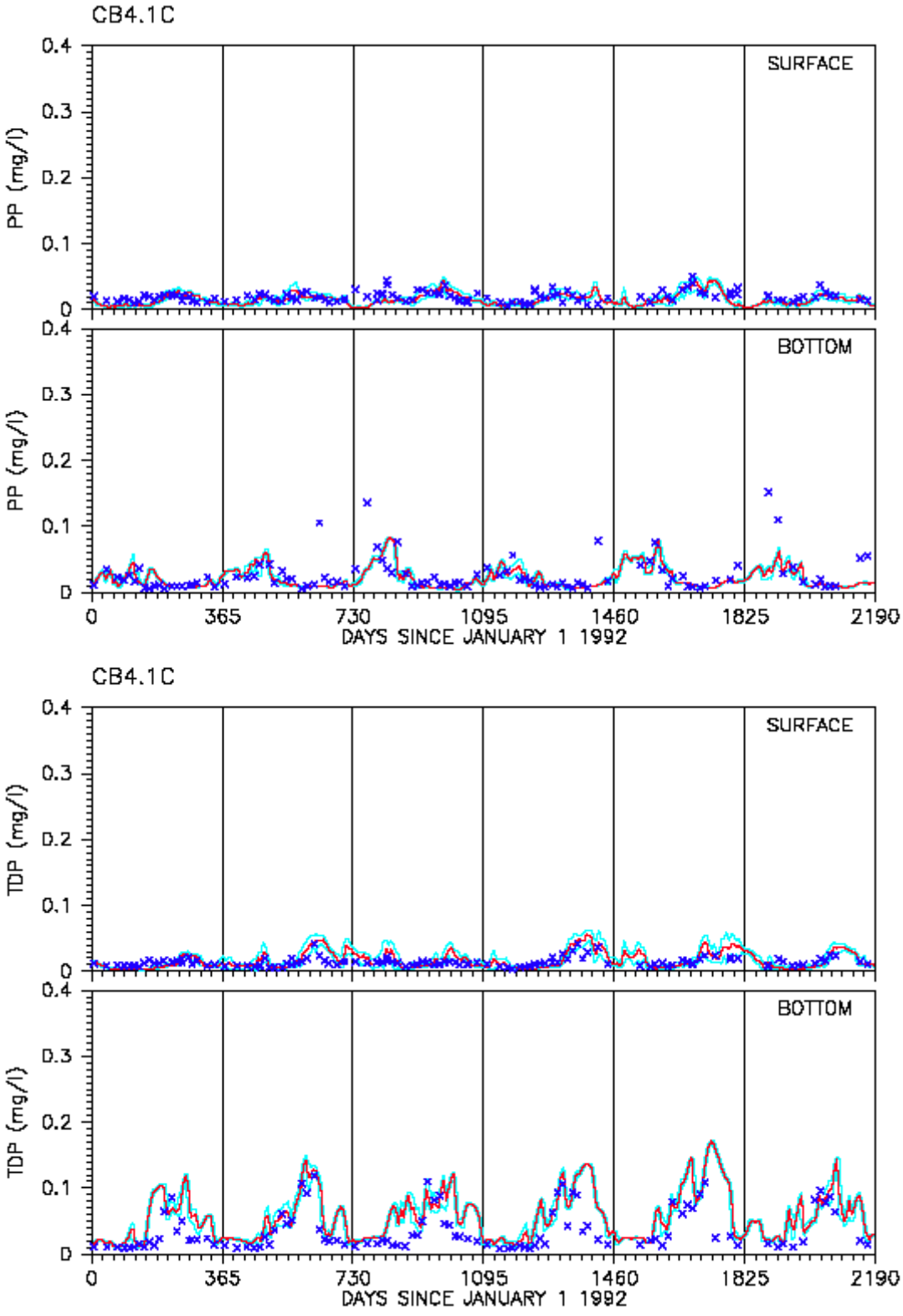

Fig. 25. Time series comparison of model calibration results and data for particulate phosphorus and total dissolved phosphorus in the Upper Chesapeake Bay (CB4.1C)

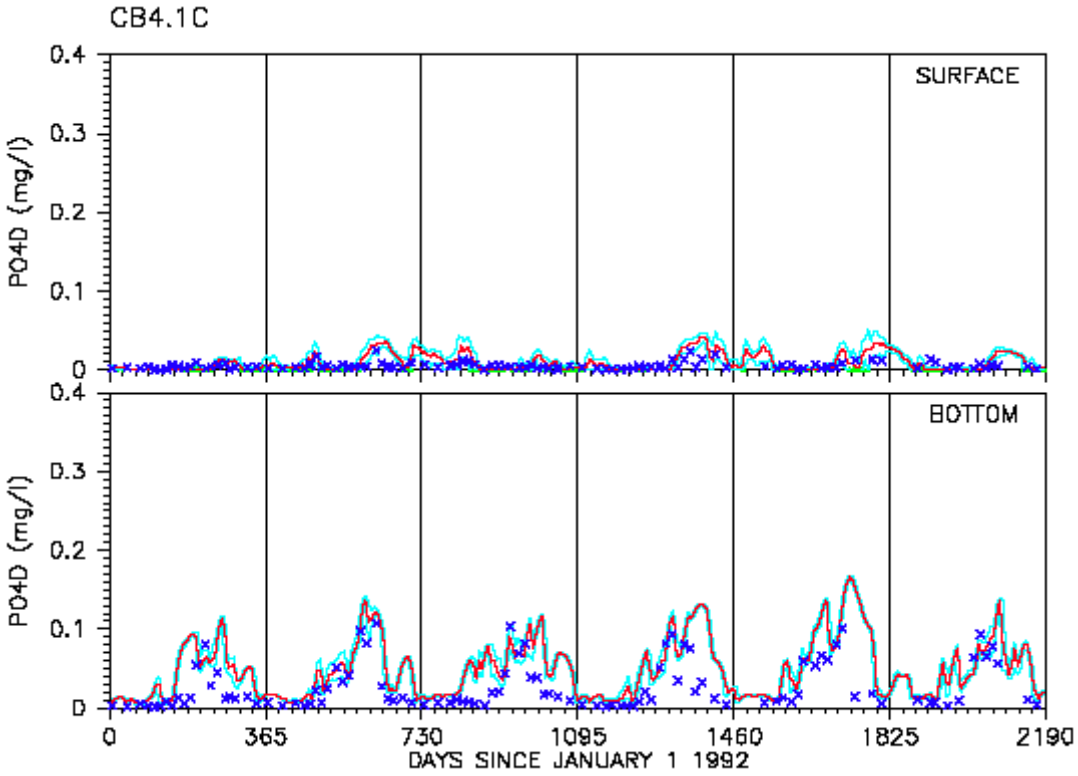

Fig. 26. Time series comparison of model calibration results and data for dissolved phosphate in the Upper Chesapeake Bay (CB4.1C)

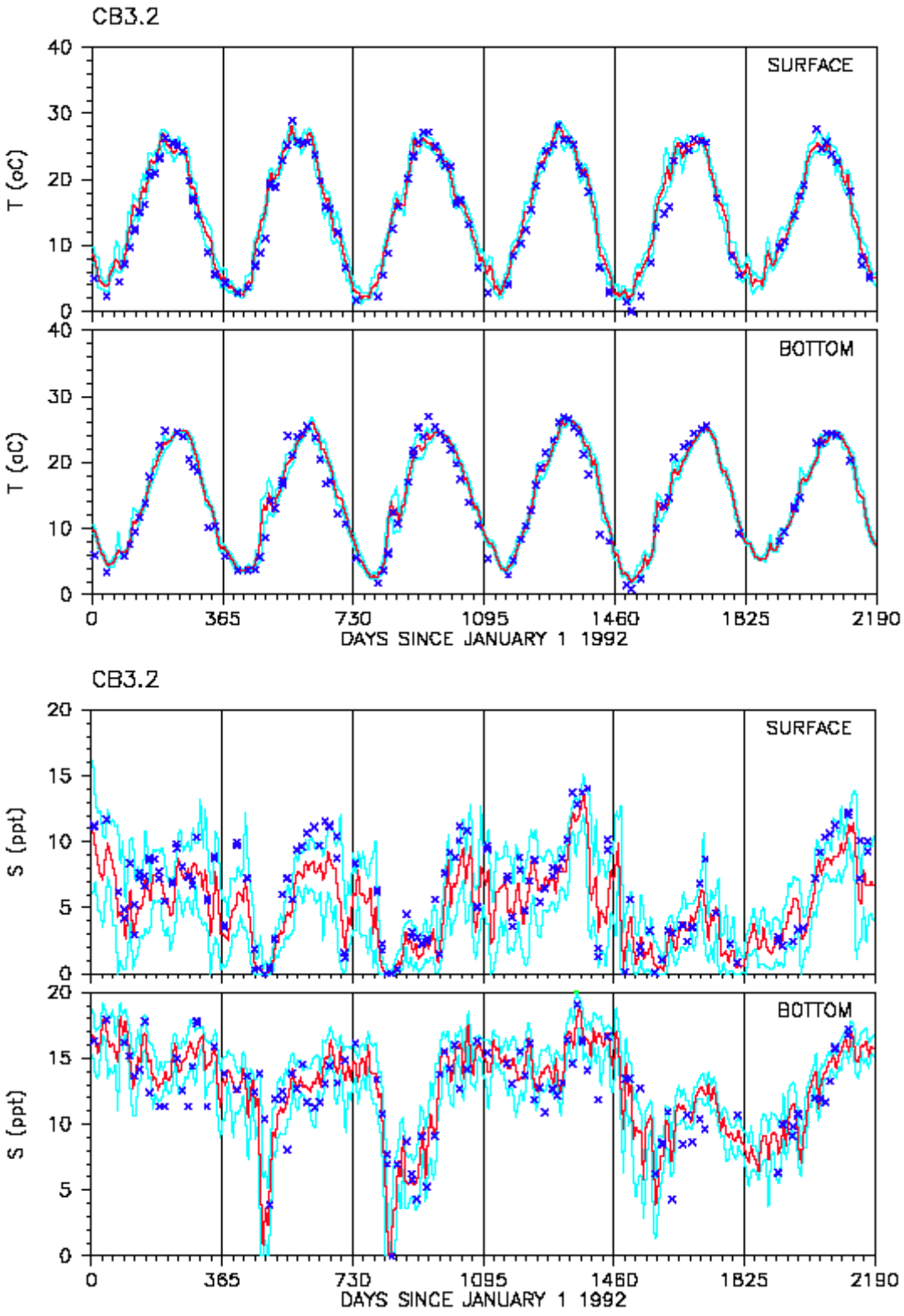

Fig. 27. Time series comparison of model calibration results and data for temperature and salinity in the Upper Chesapeake Bay (CB3.2)

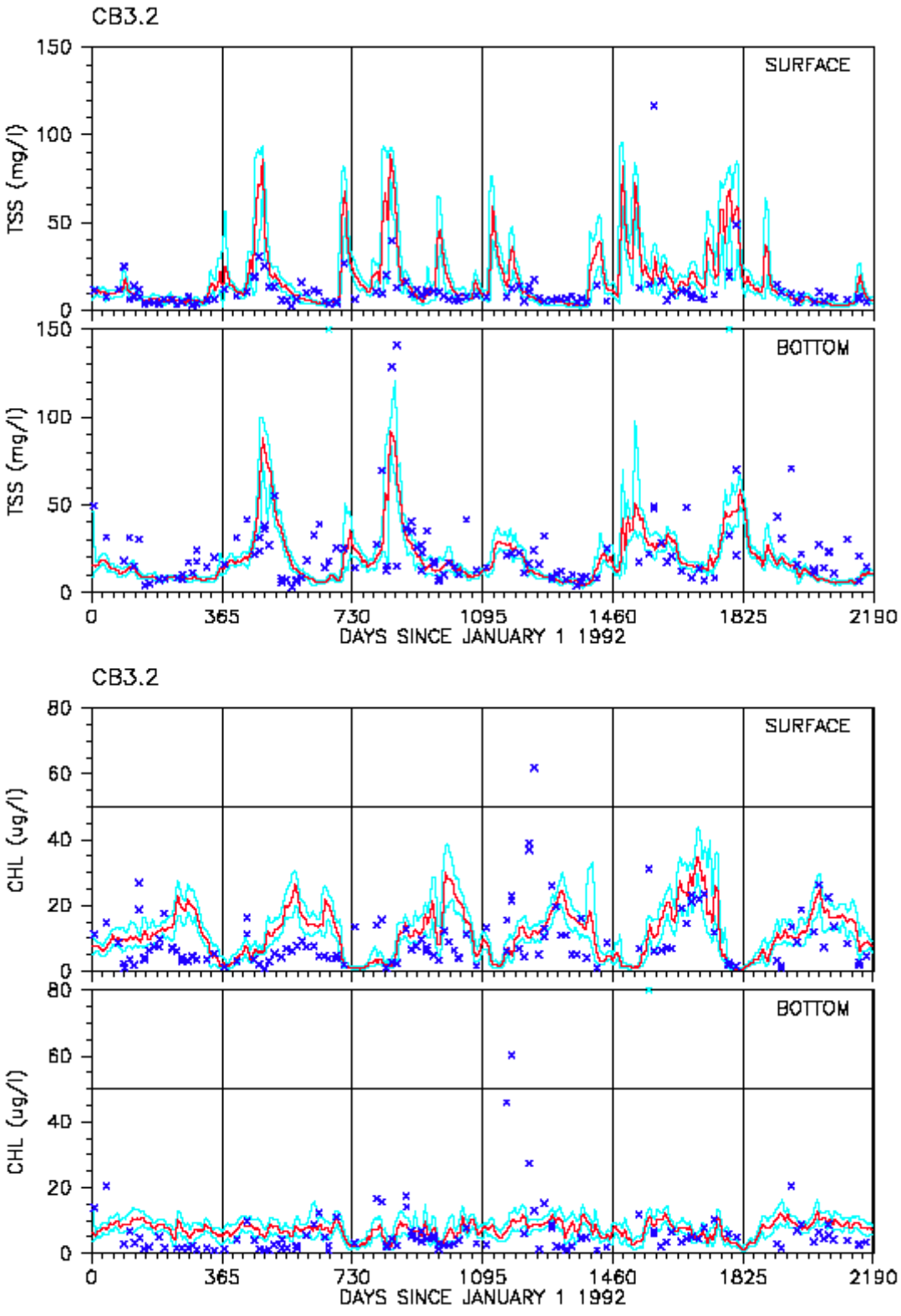

Fig. 28. Time series comparison of model calibration results and data for total suspended solids and chlorophyll a in the Upper Chesapeake Bay (CB3.2)

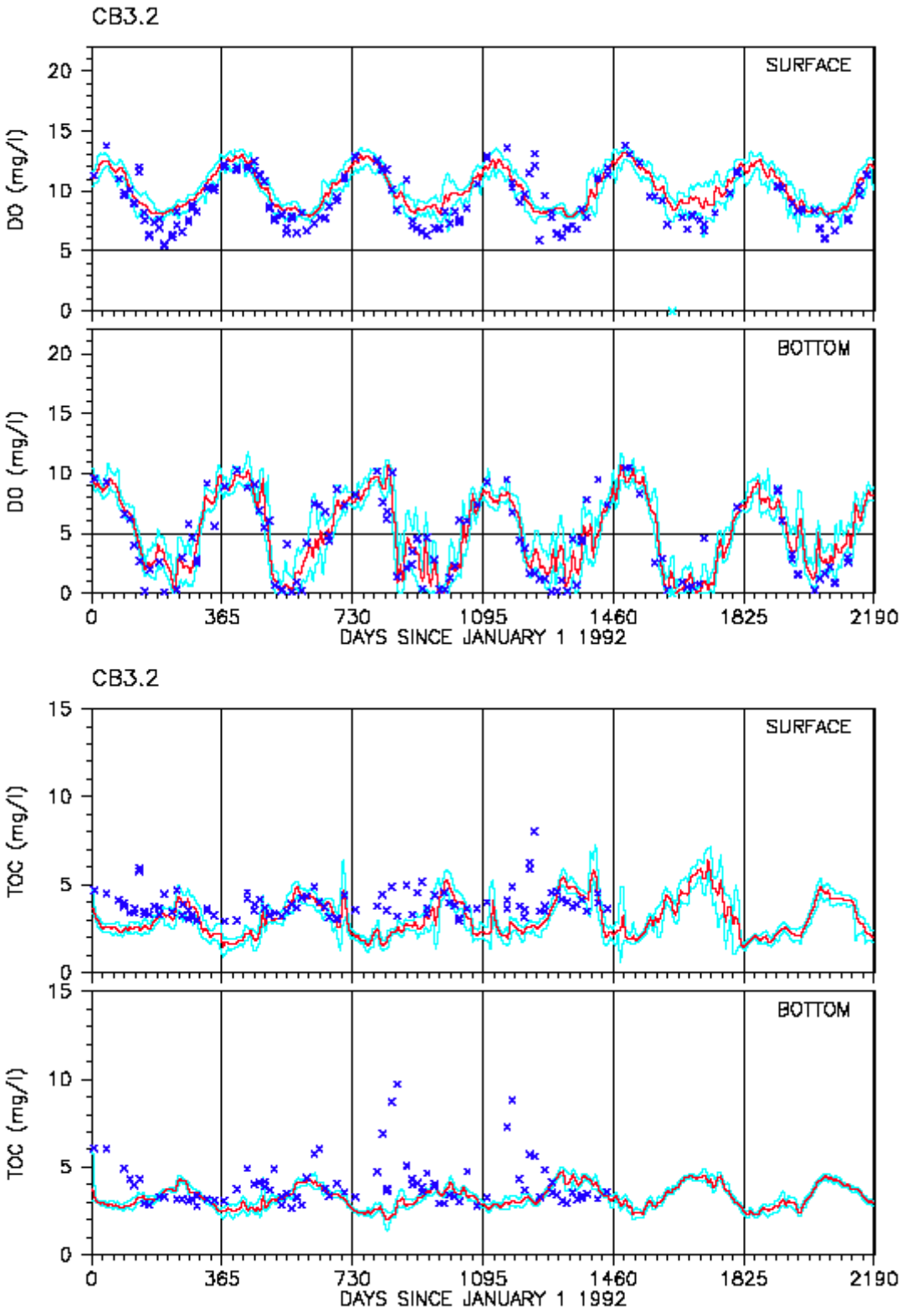

Fig. 29. Time series comparison of model calibration results and data for dissolved oxygen and total organic carbon in the Upper Chesapeake Bay (CB3.2)

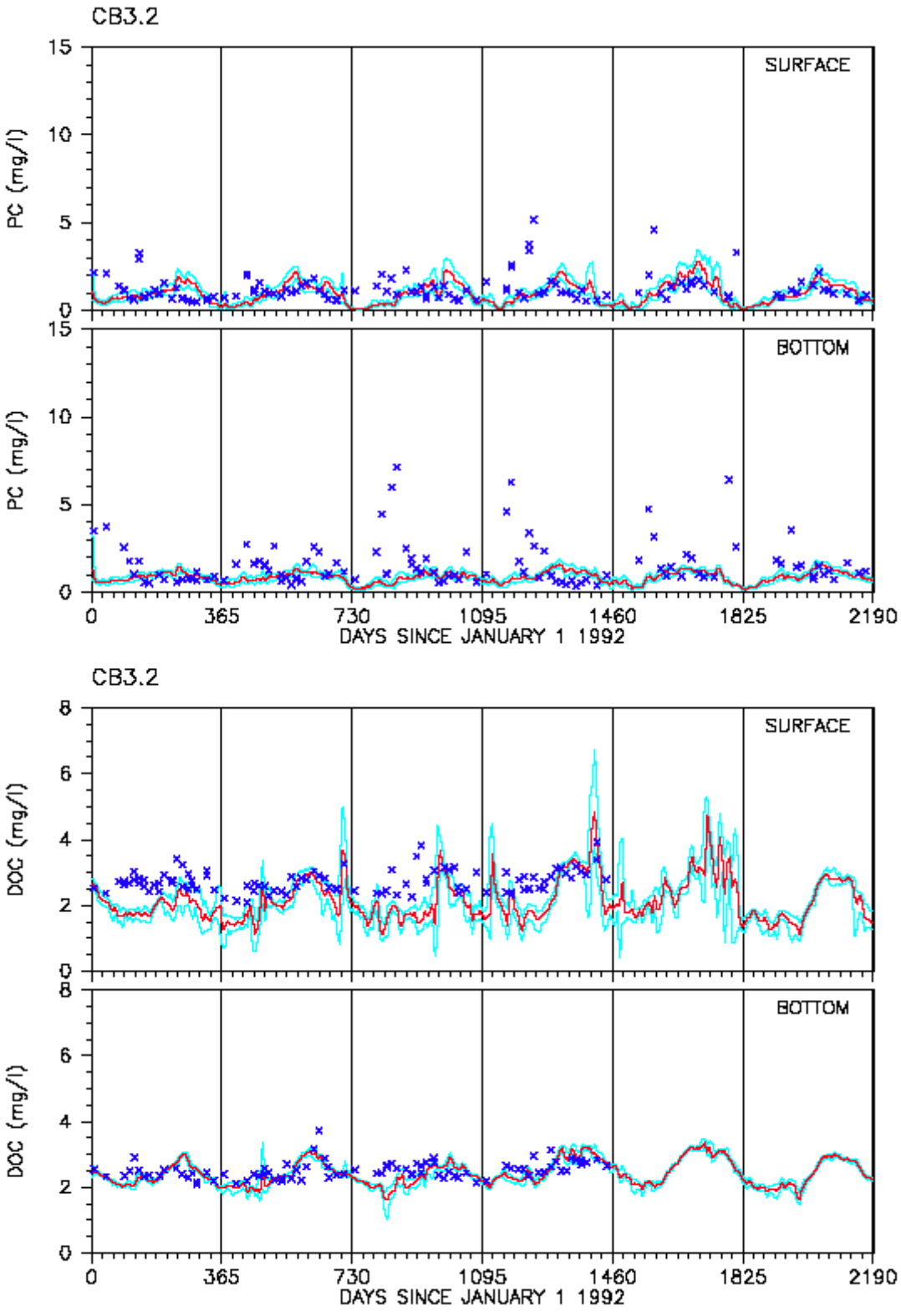

Fig. 30. Time series comparison of model calibration results and data for particulate organic carbon and dissolved organic carbon in the Upper Chesapeake Bay (CB3.2)

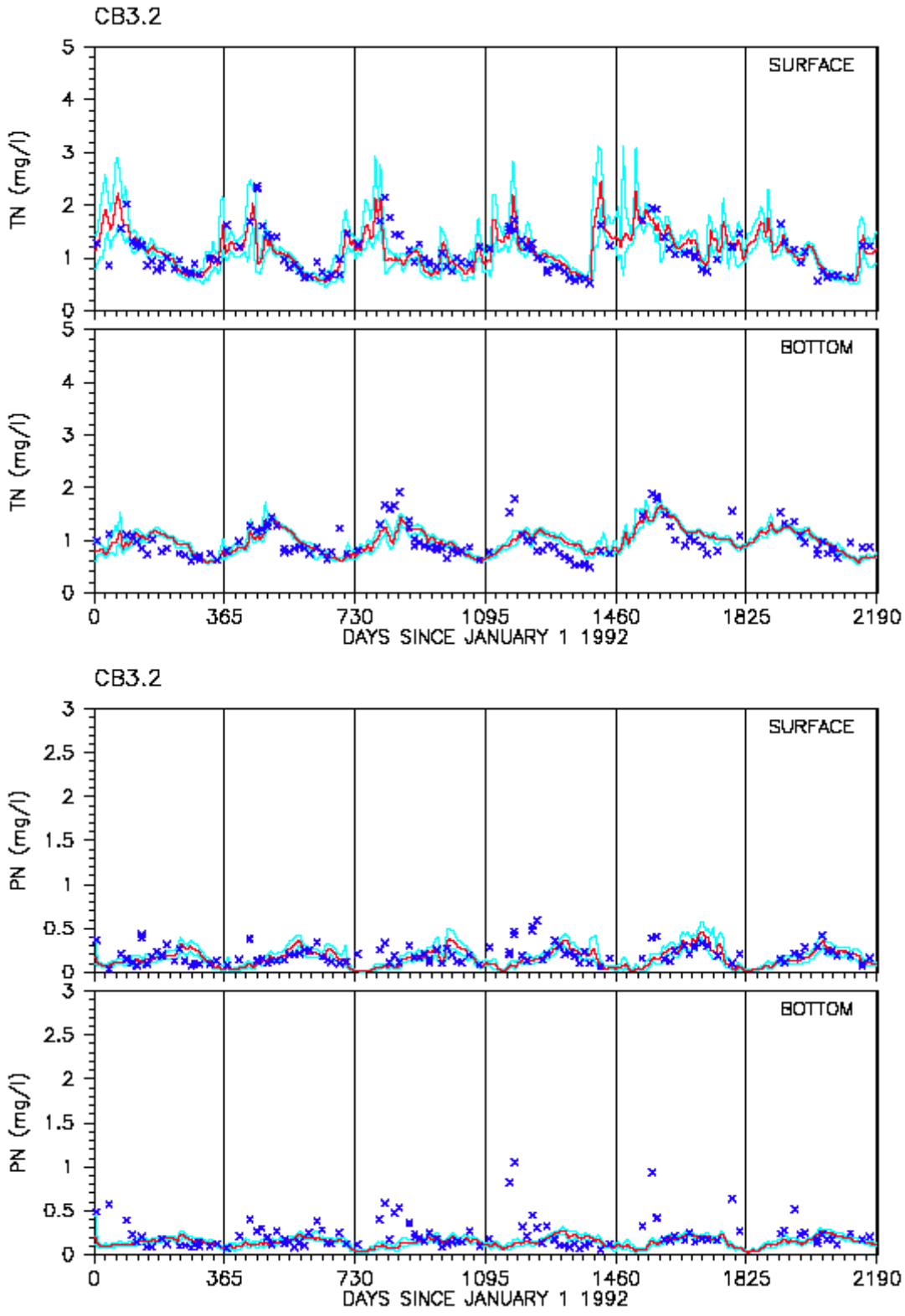

Fig. 31. Time series comparison of model calibration results and data for total nitrogen and particulate nitrogen in the Upper Chesapeake Bay (CB3.2)

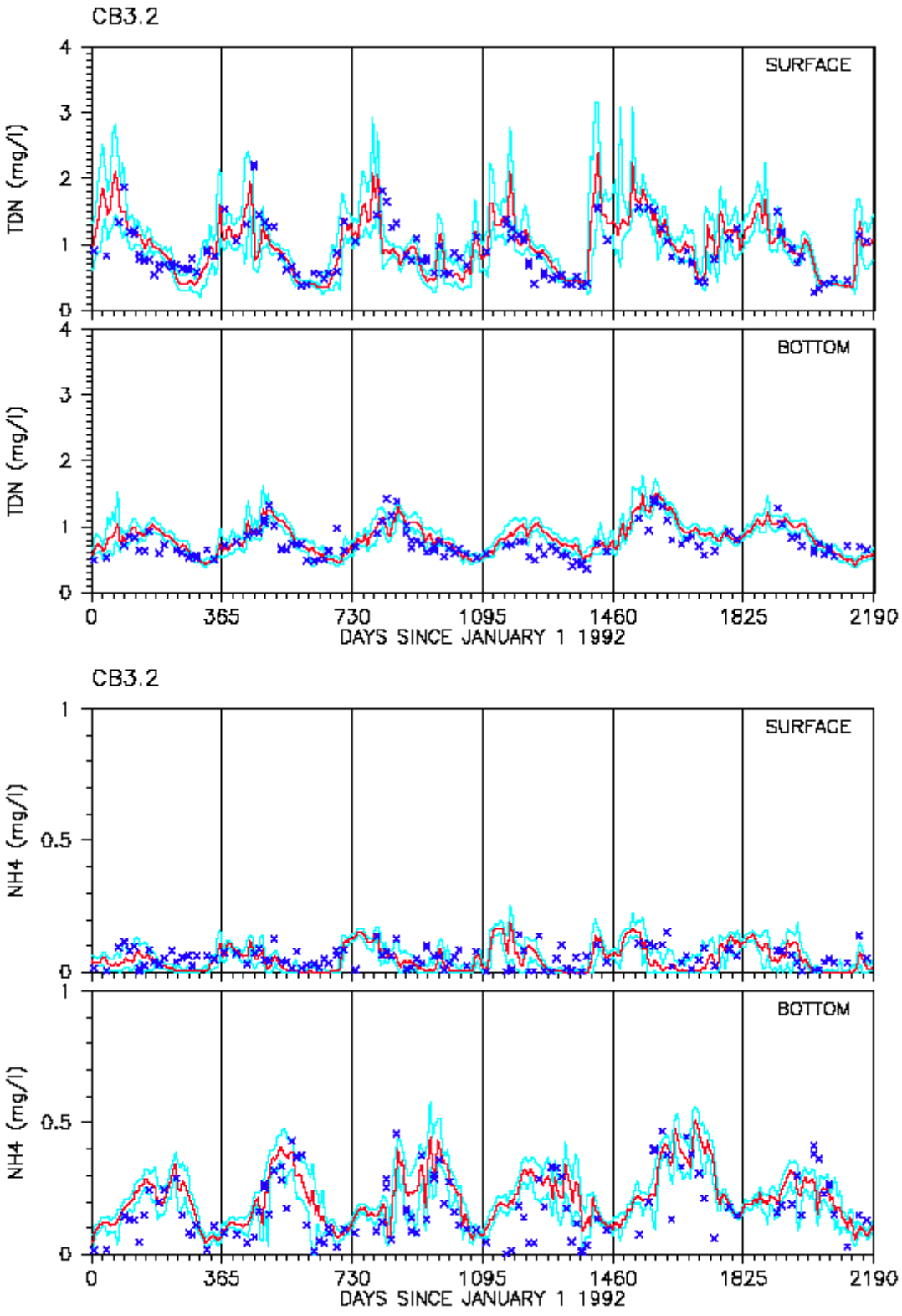

Fig. 32. Time series comparison of model calibration results and data for total dissolved nitrogen and ammonia in the Upper Chesapeake Bay (CB3.2)

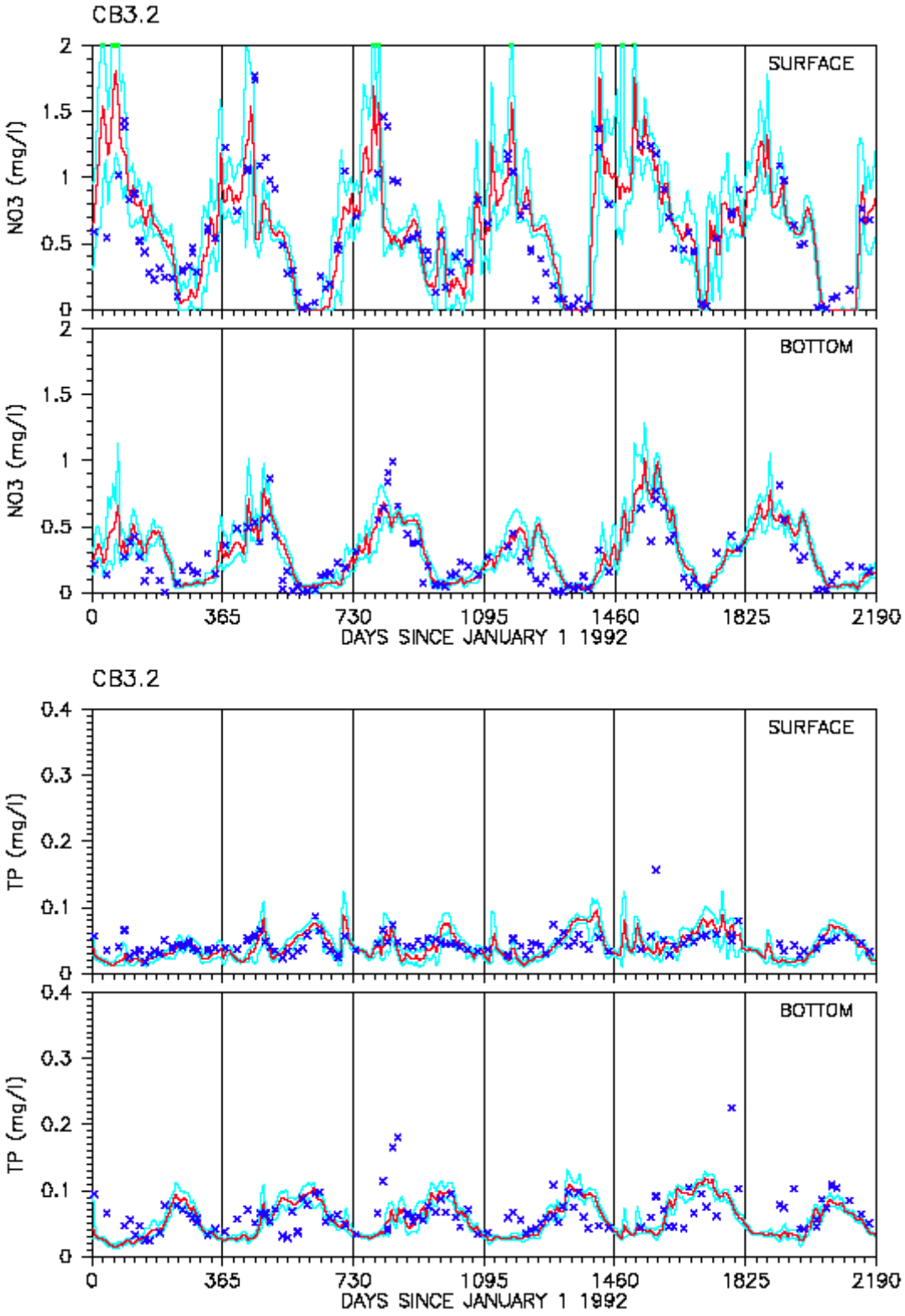

Fig. 33. Time series comparison of model calibration results and data for nitrate and total phosphorus in the Upper Chesapeake Bay (CB3.2)

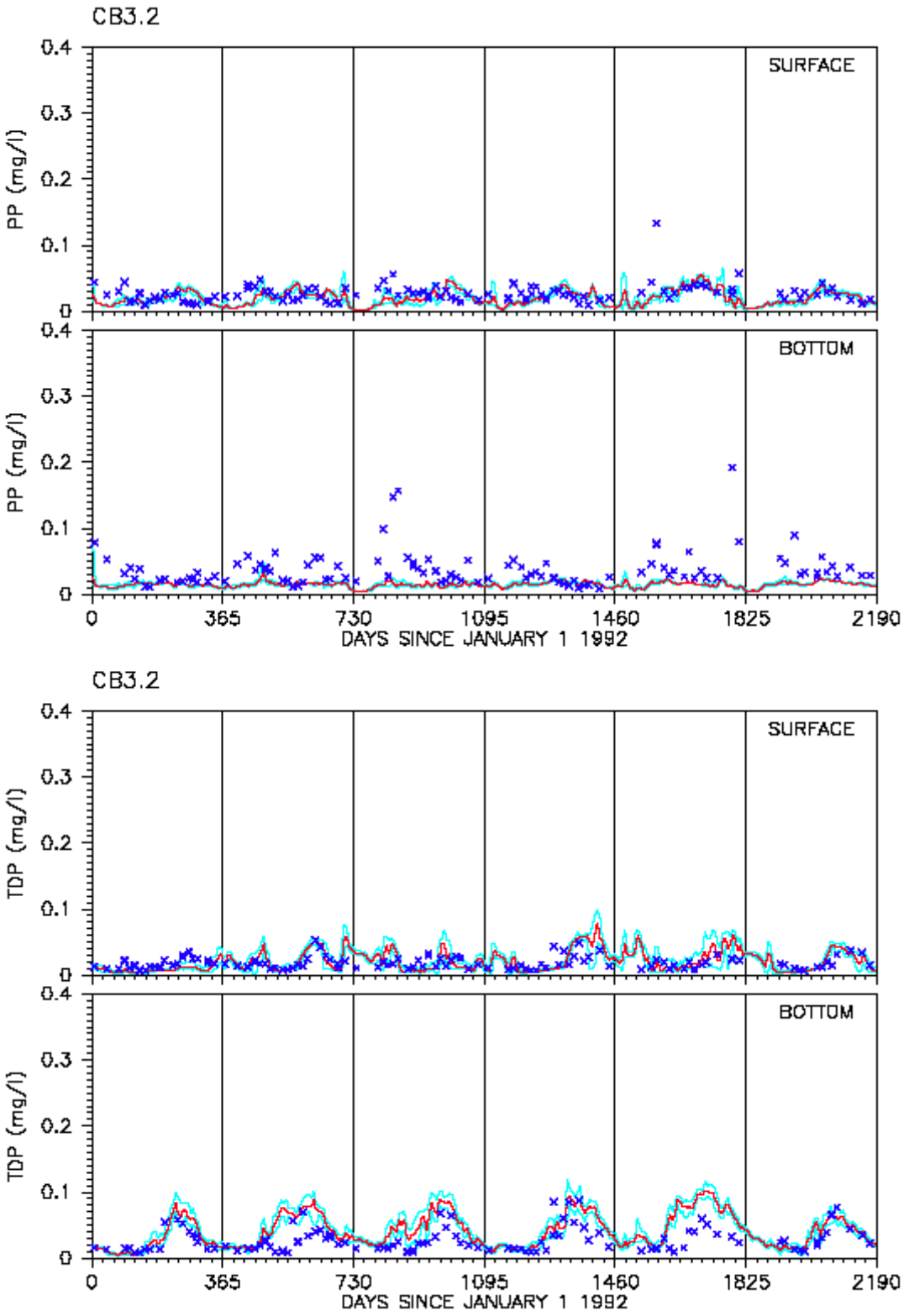

Fig. 34. Time series comparison of model calibration results and data for particulate phosphorus and total dissolved phosphorus in the Upper Chesapeake Bay (CB3.2)

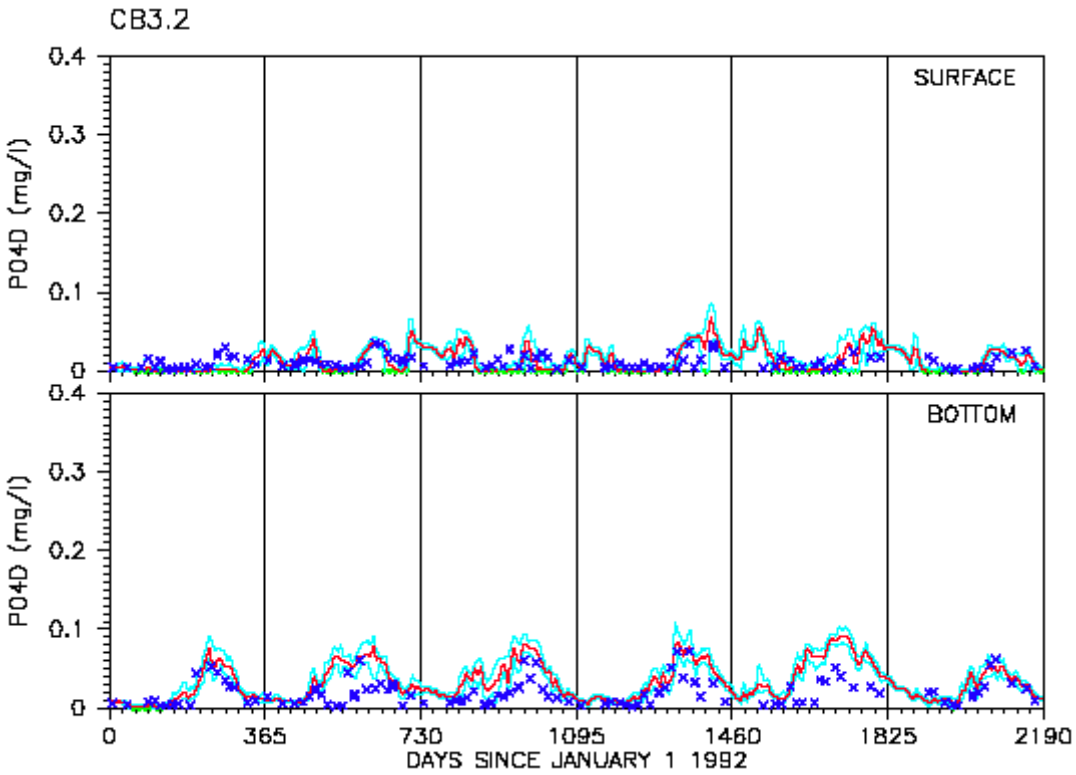

Fig. 35. Time series comparison of model calibration results and data for dissolved phosphate in the Upper Chesapeake Bay (CB3.2)

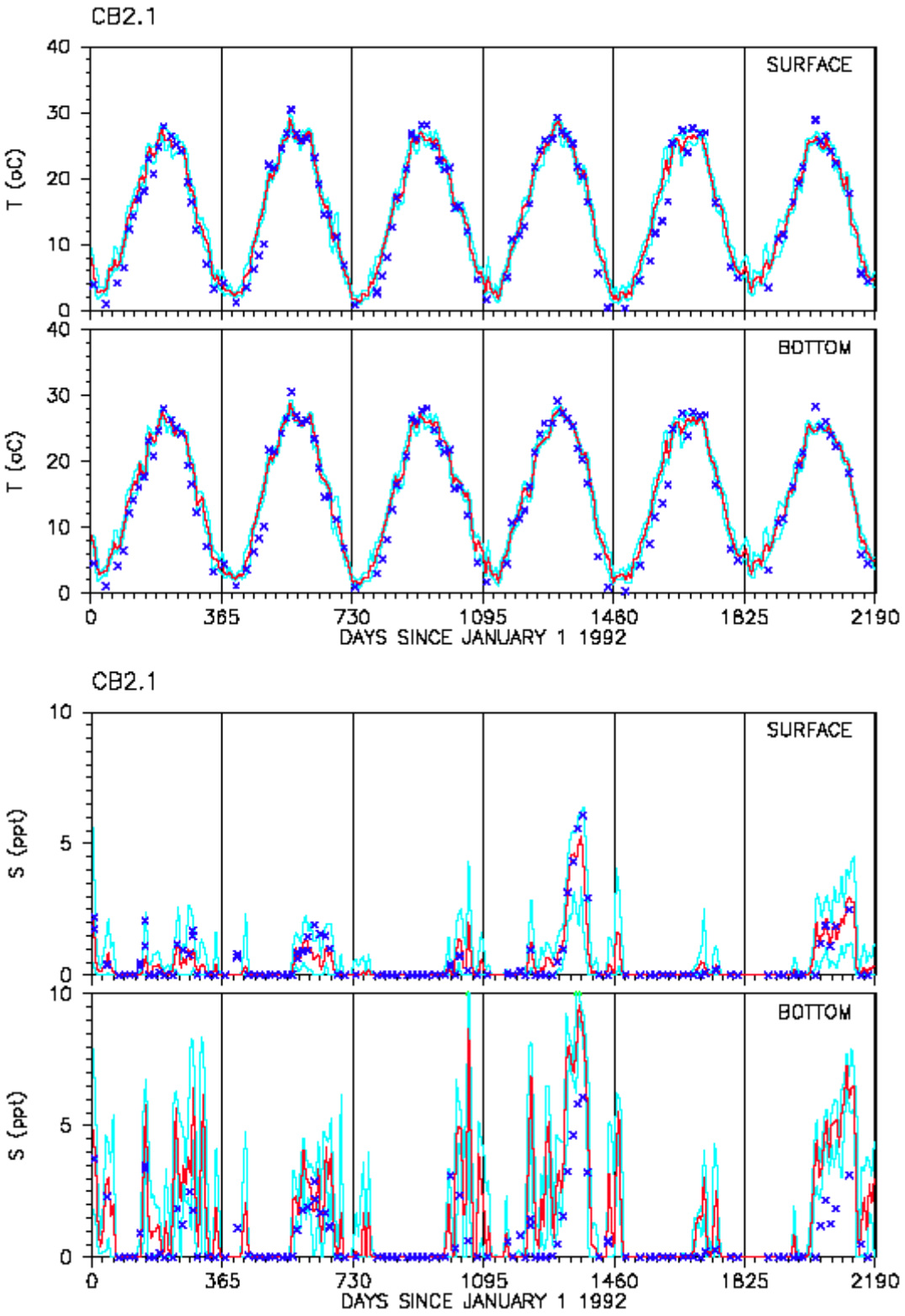

Fig. 36. Time series comparison of model calibration results and data for temperature and salinity in the Upper Chesapeake Bay (CB2.1)

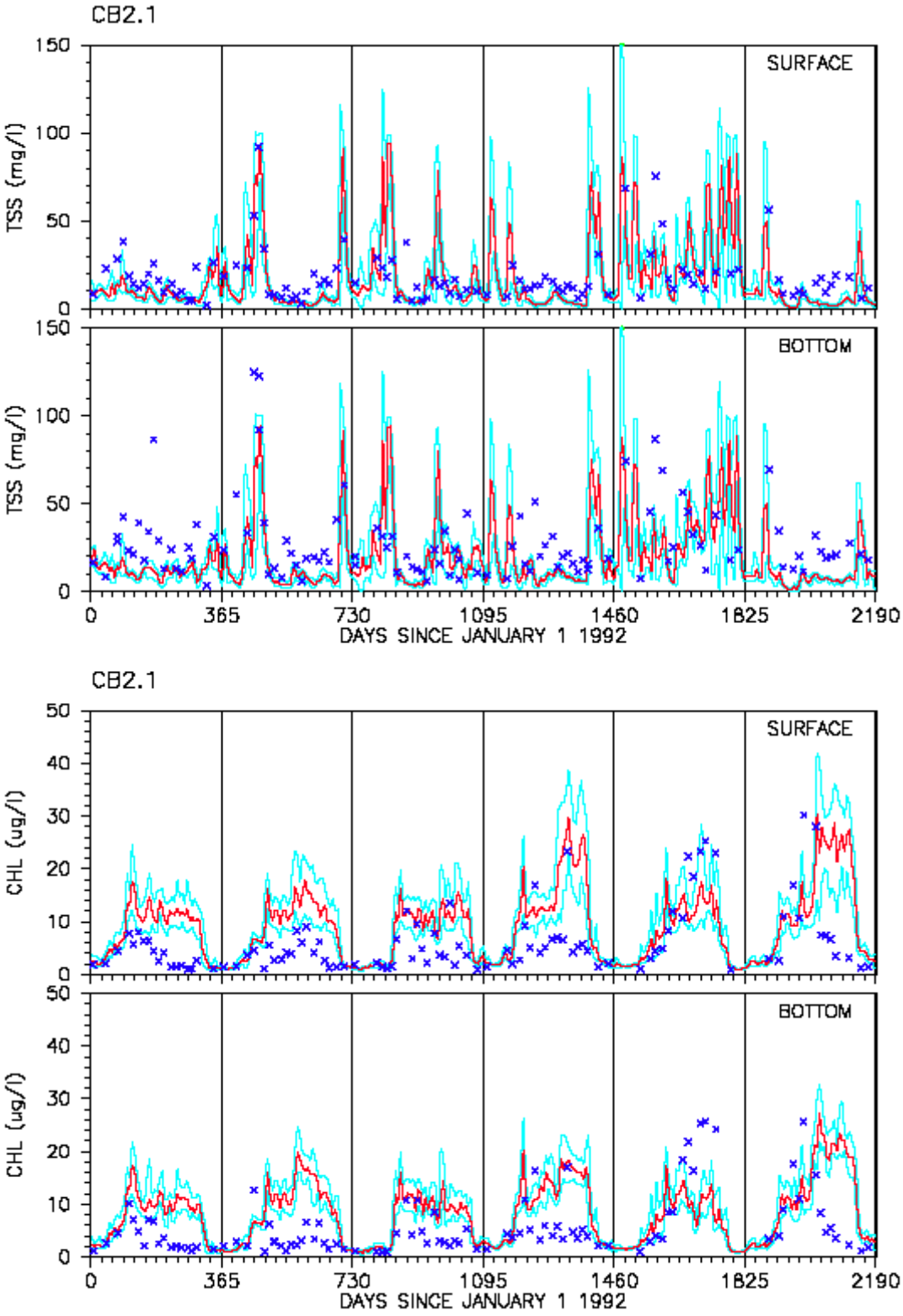

Fig. 37. Time series comparison of model calibration results and data for total suspended solids and chlorophyll a in the Upper Chesapeake Bay (CB2.1)

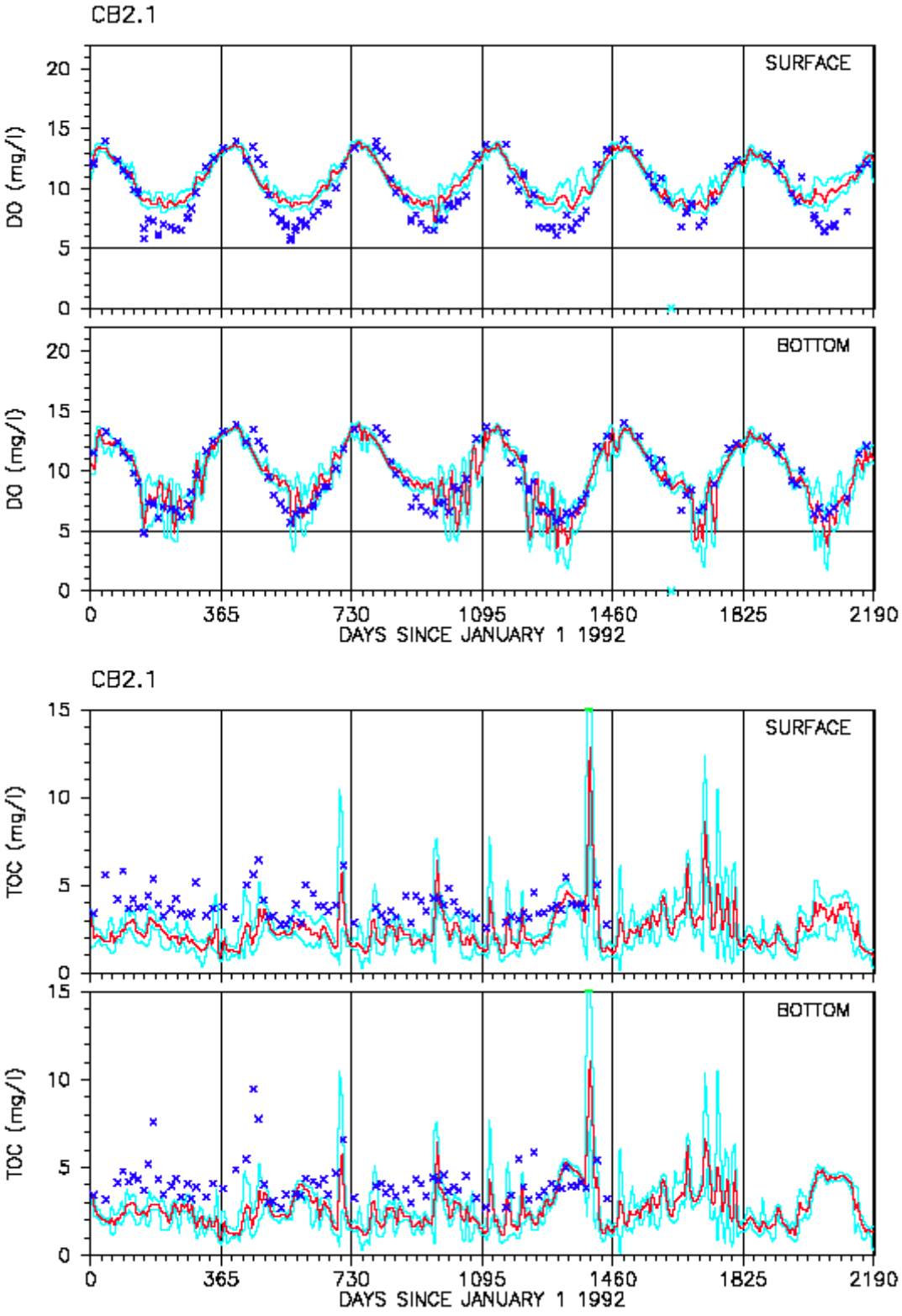

Fig. 38. Time series comparison of model calibration results and data for dissolved oxygen and total organic carbon in the Upper Chesapeake Bay (CB2.1)

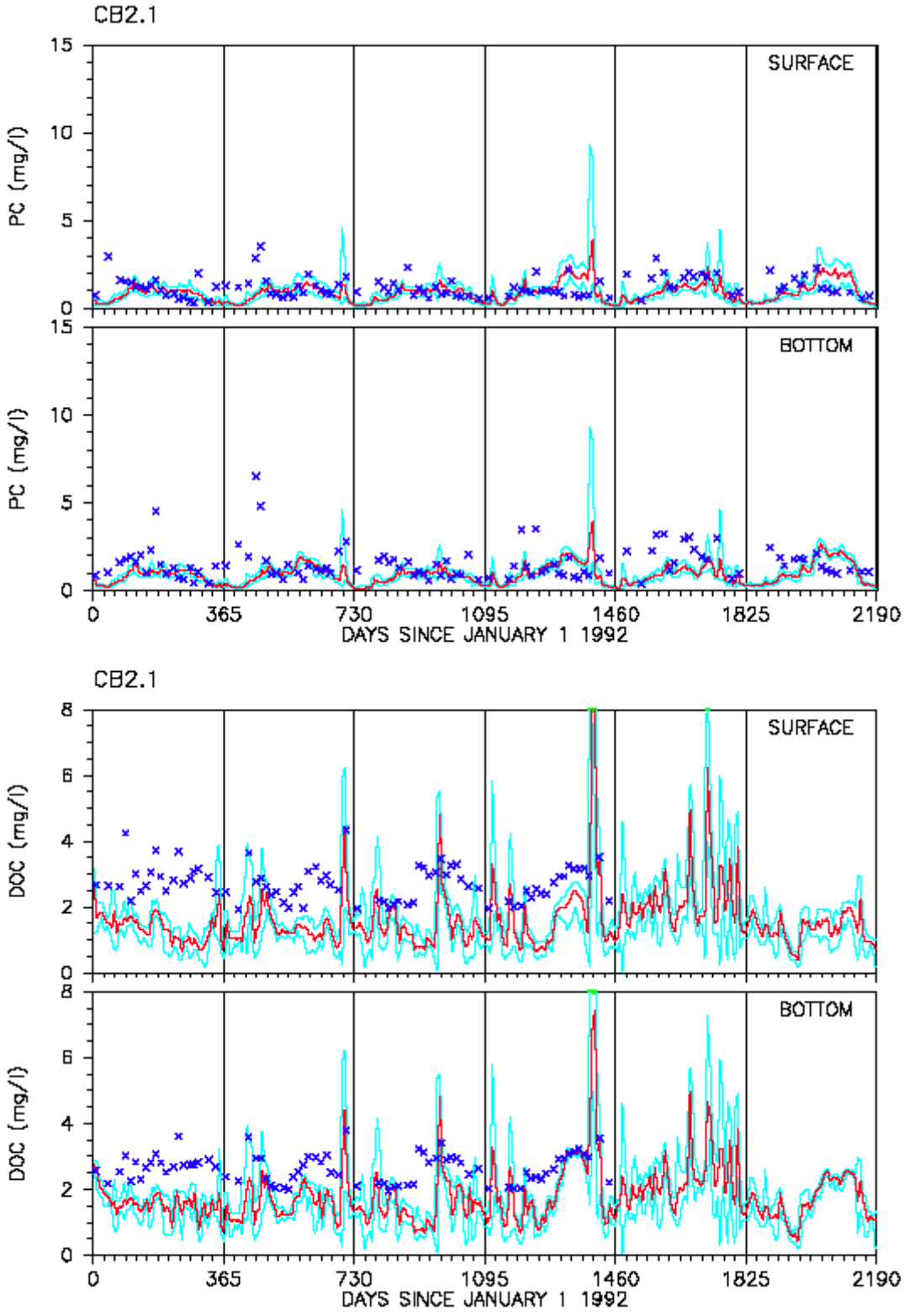

Fig. 39. Time series comparison of model calibration results and data for particulate organic carbon and dissolved organic carbon in the Upper Chesapeake Bay (CB2.1)

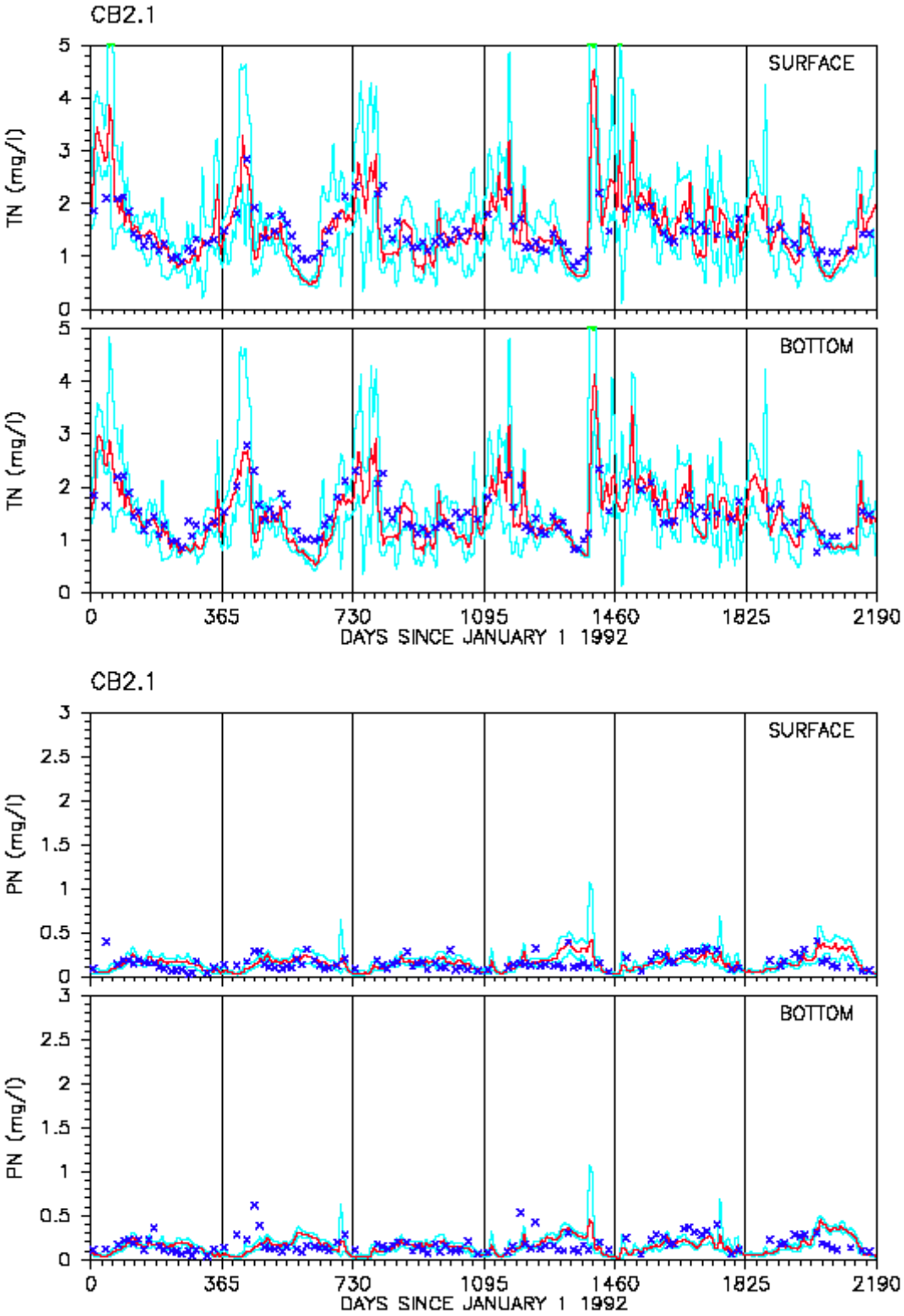

Fig. 40. Time series comparison of model calibration results and data for total nitrogen and particulate nitrogen in the Upper Chesapeake Bay (CB2.1)

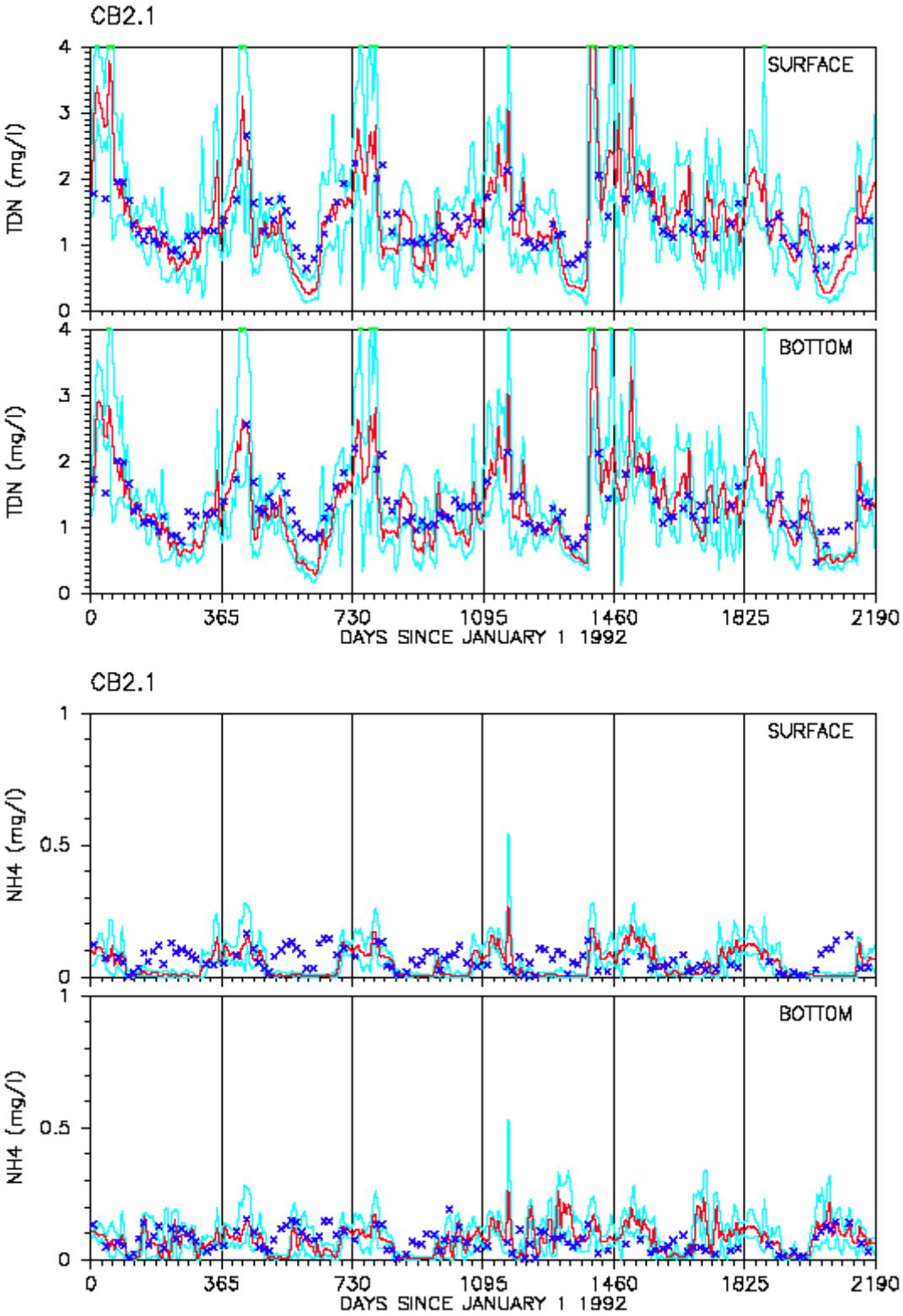

Fig. 41. Time series comparison of model calibration results and data for total dissolved nitrogen and ammonia in the Upper Chesapeake Bay (CB2.1)

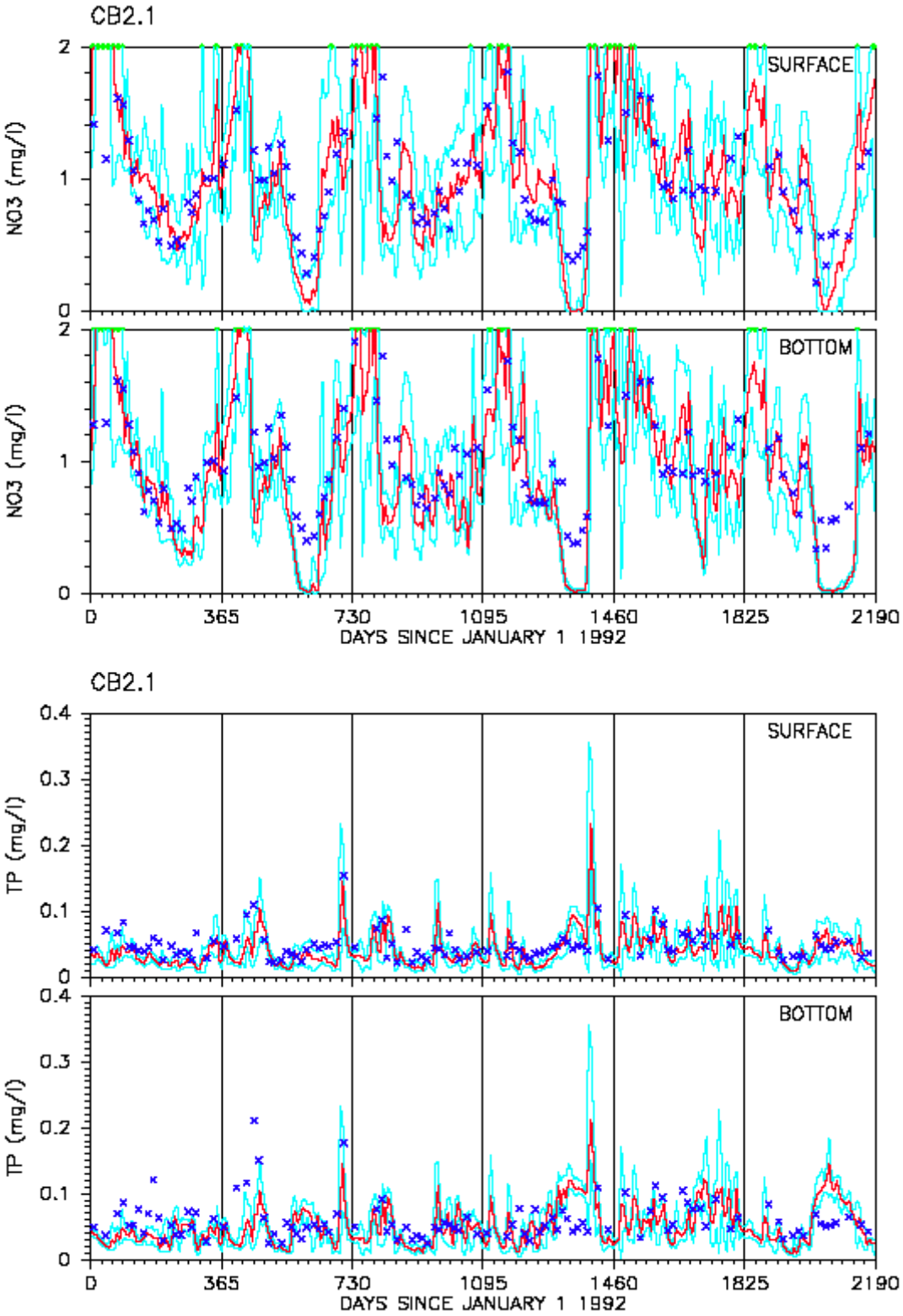

Fig. 42. Time series comparison of model calibration results and data for nitrate and total phosphorus in the Upper Chesapeake Bay (CB2.1)

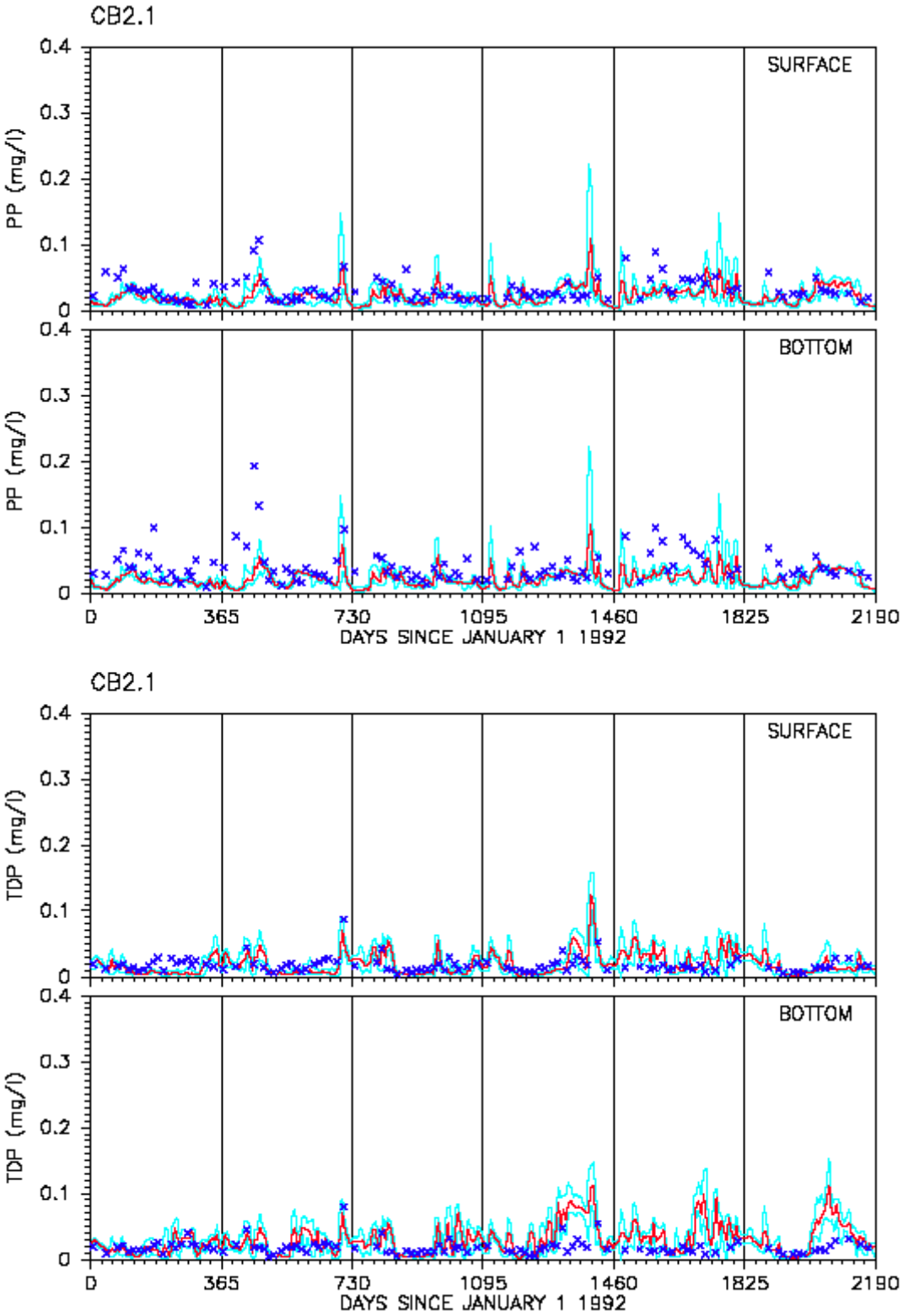

Fig. 43. Time series comparison of model calibration results and data for particulate phosphorus and total dissolved phosphorus in the Upper Chesapeake Bay (CB2.1)

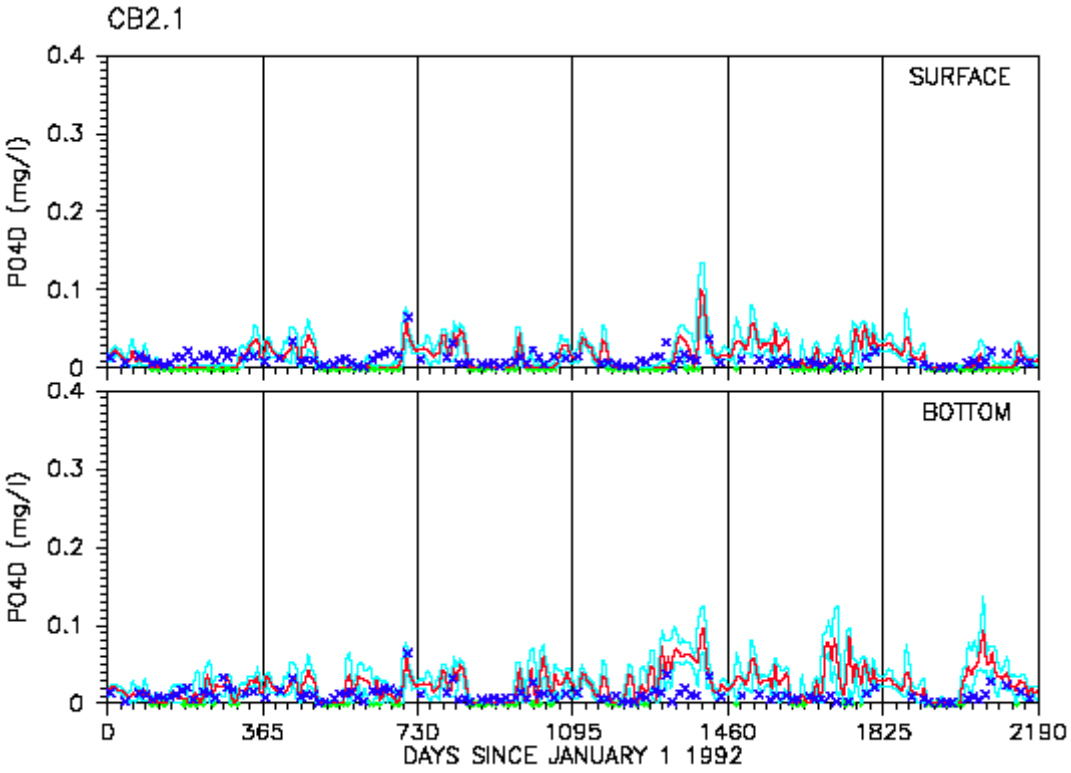

Fig. 44. Time series comparison of model calibration results and data for dissolved phosphate in the Upper Chesapeake Bay (CB2.1)

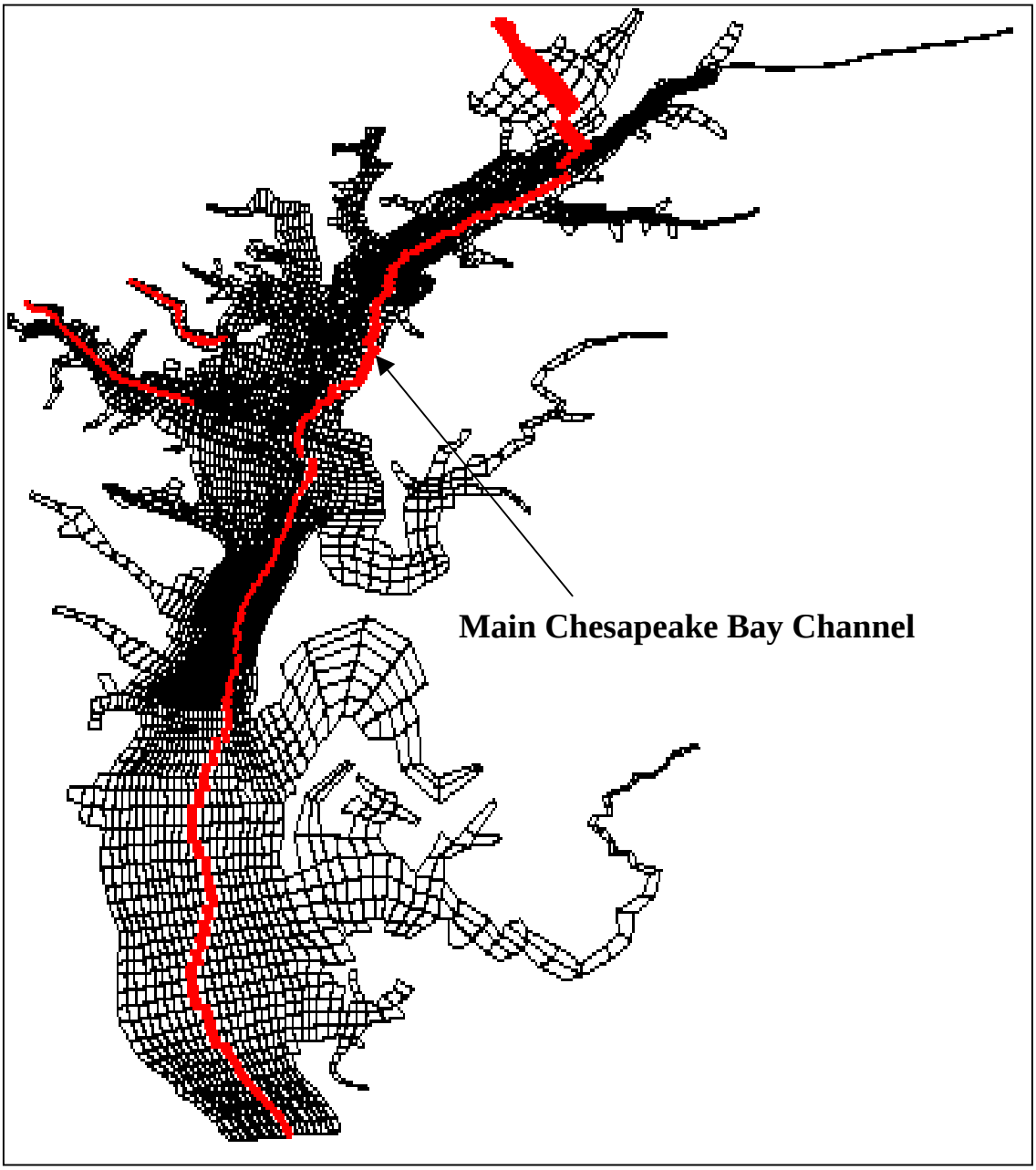

Fig. 45. Plan view of the model grid showing the transect of the Upper Chesapeake Bay

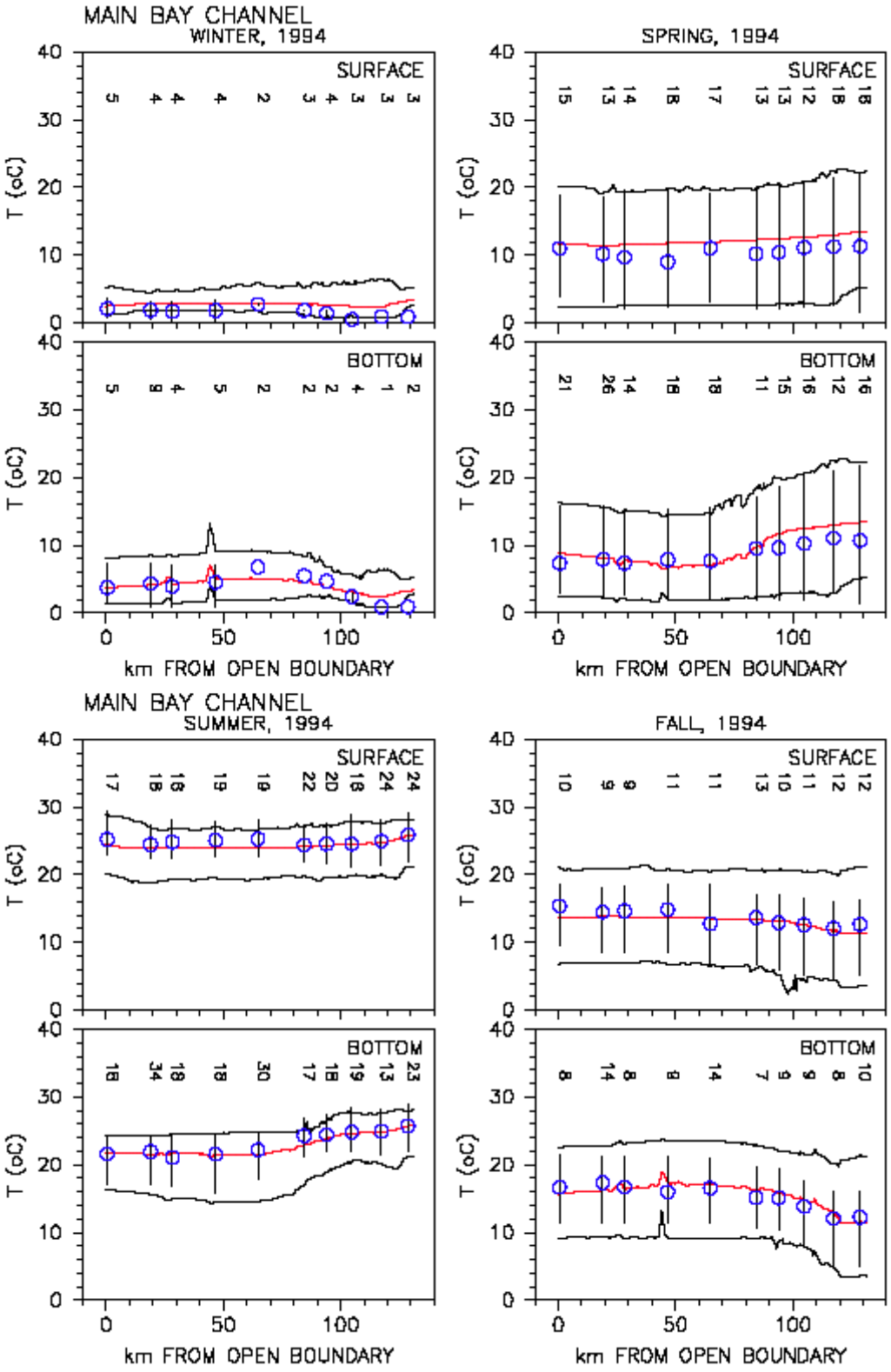

Fig. 46. Longitudinal comparison of model calibration results and data for temperature in the Upper Chesapeake Bay transect

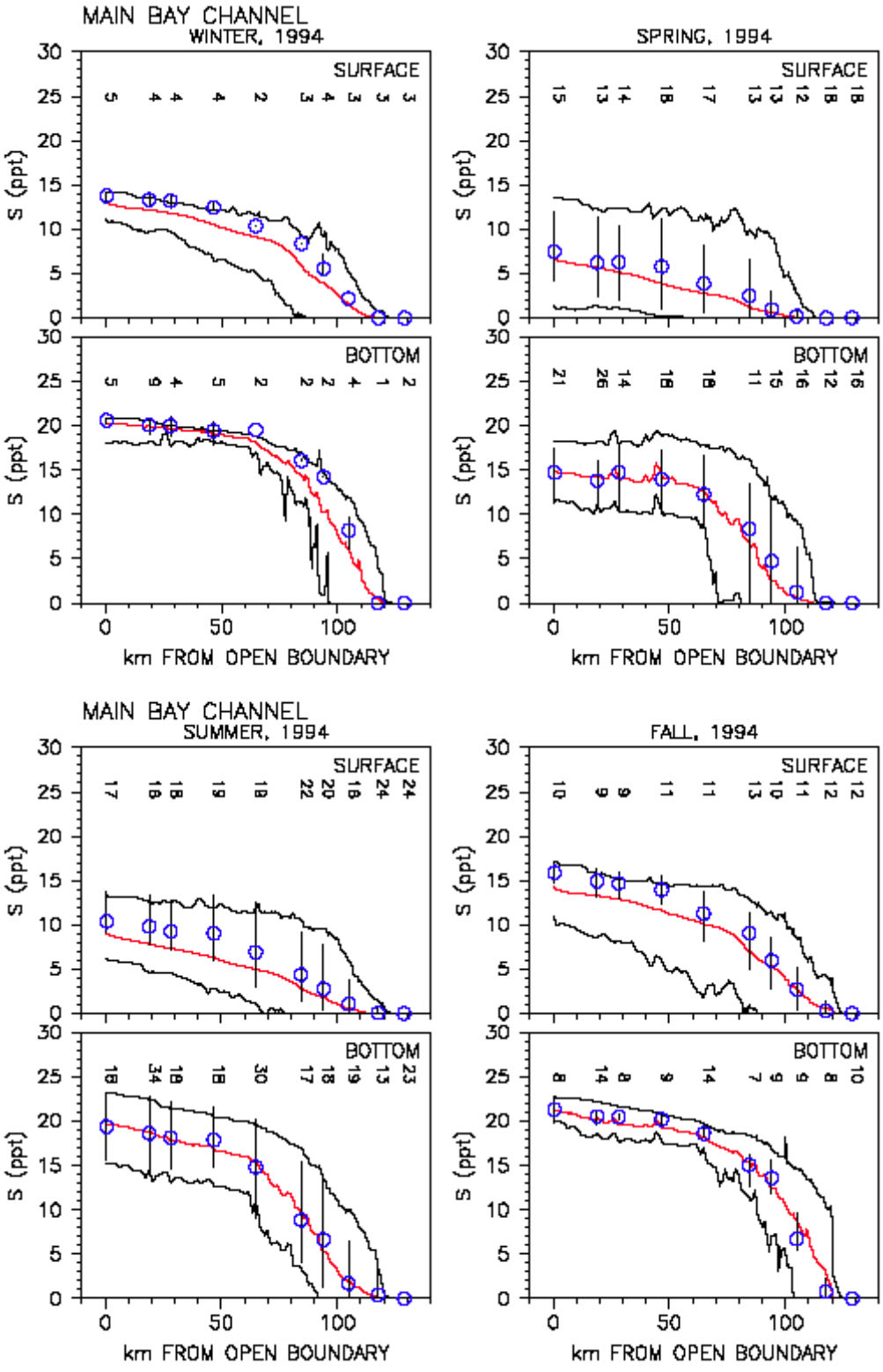

Fig. 47. Longitudinal comparison of model calibration results and data for salinity in the Upper Chesapeake Bay transect

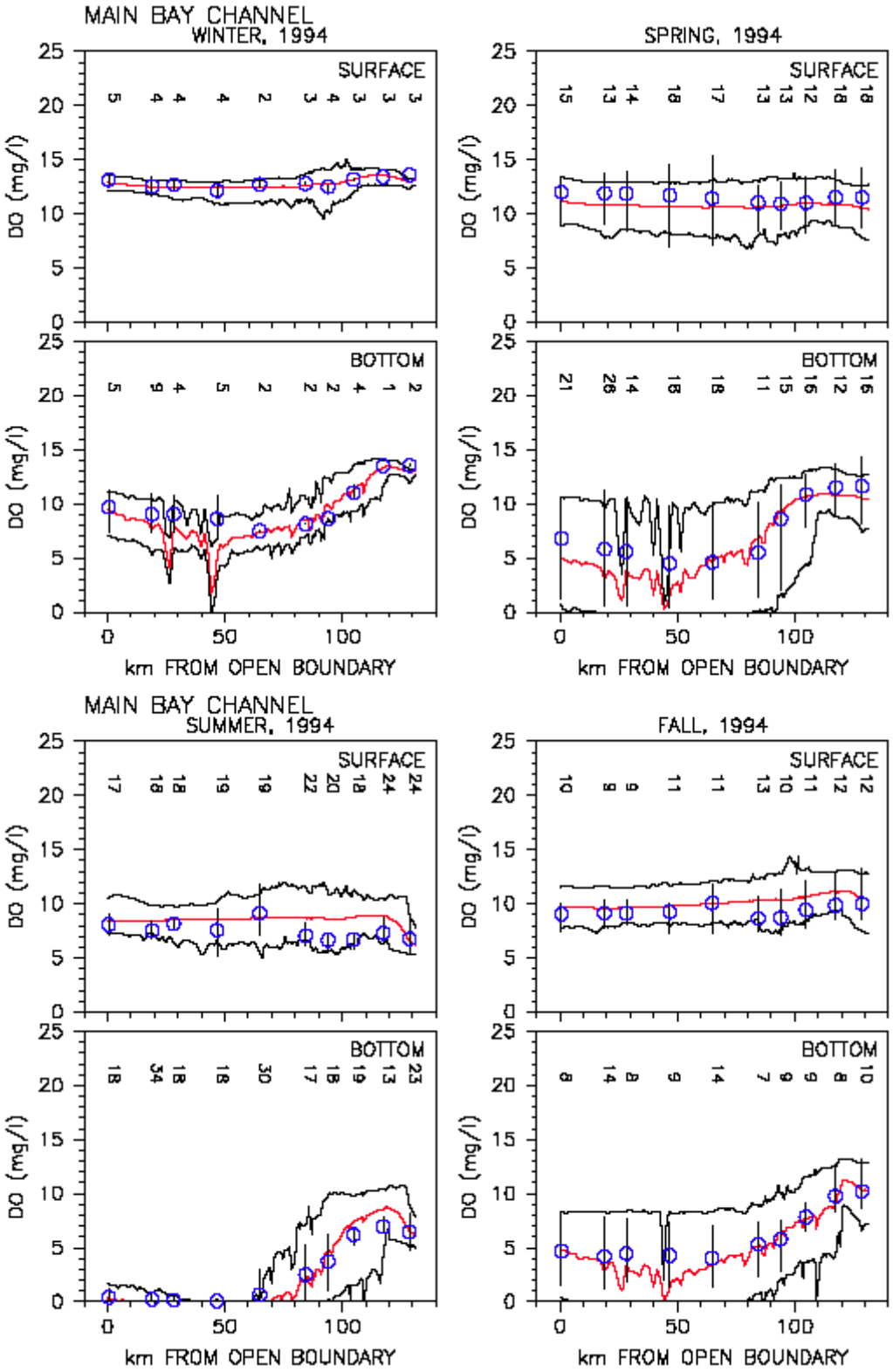

Fig. 48. Longitudinal comparison of model calibration results and data for dissolved oxygen in the Upper Chesapeake Bay transect

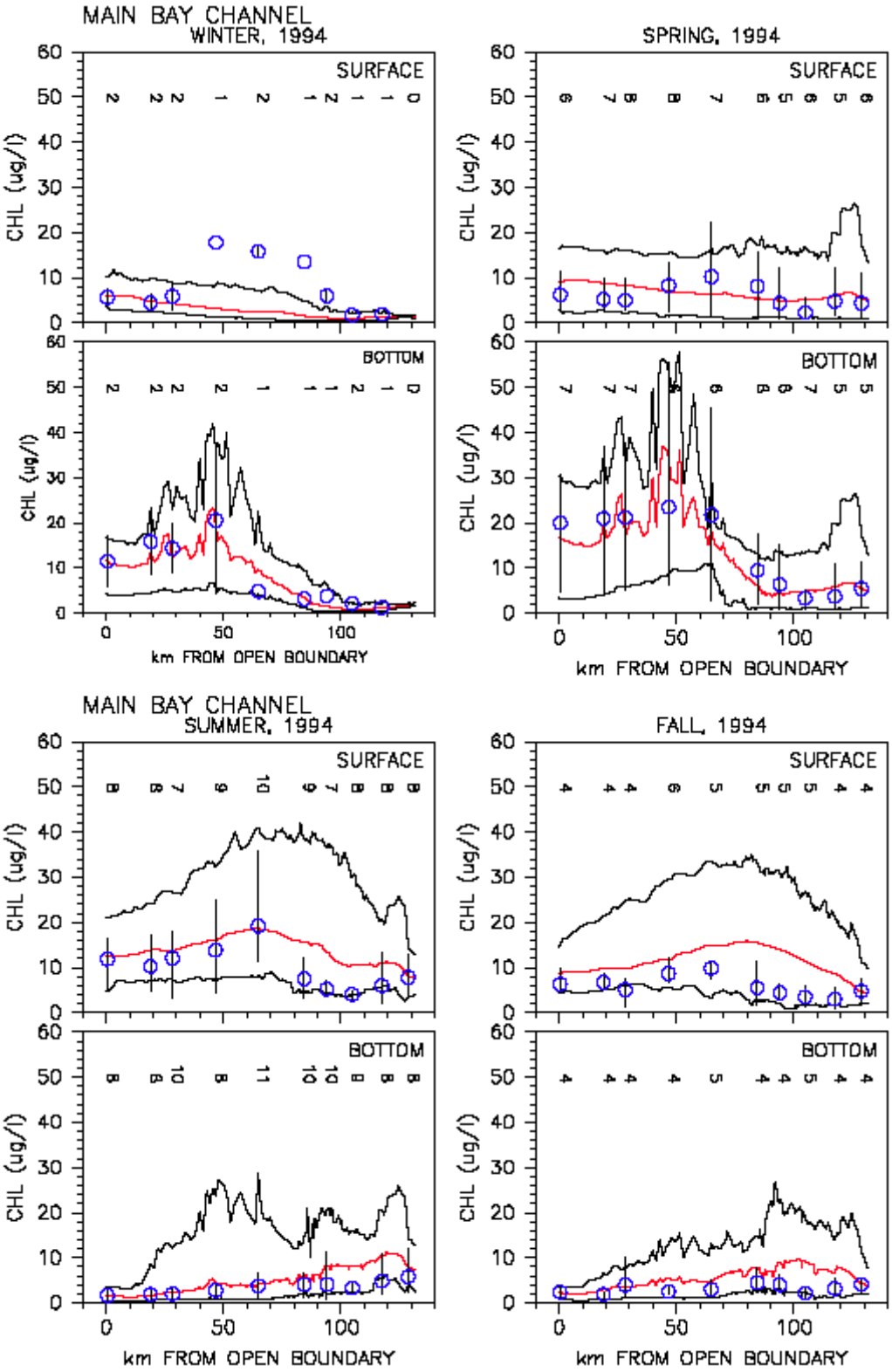

Fig. 49. Longitudinal comparison of model calibration results and data for chlorophyll a in the Upper Chesapeake Bay transect

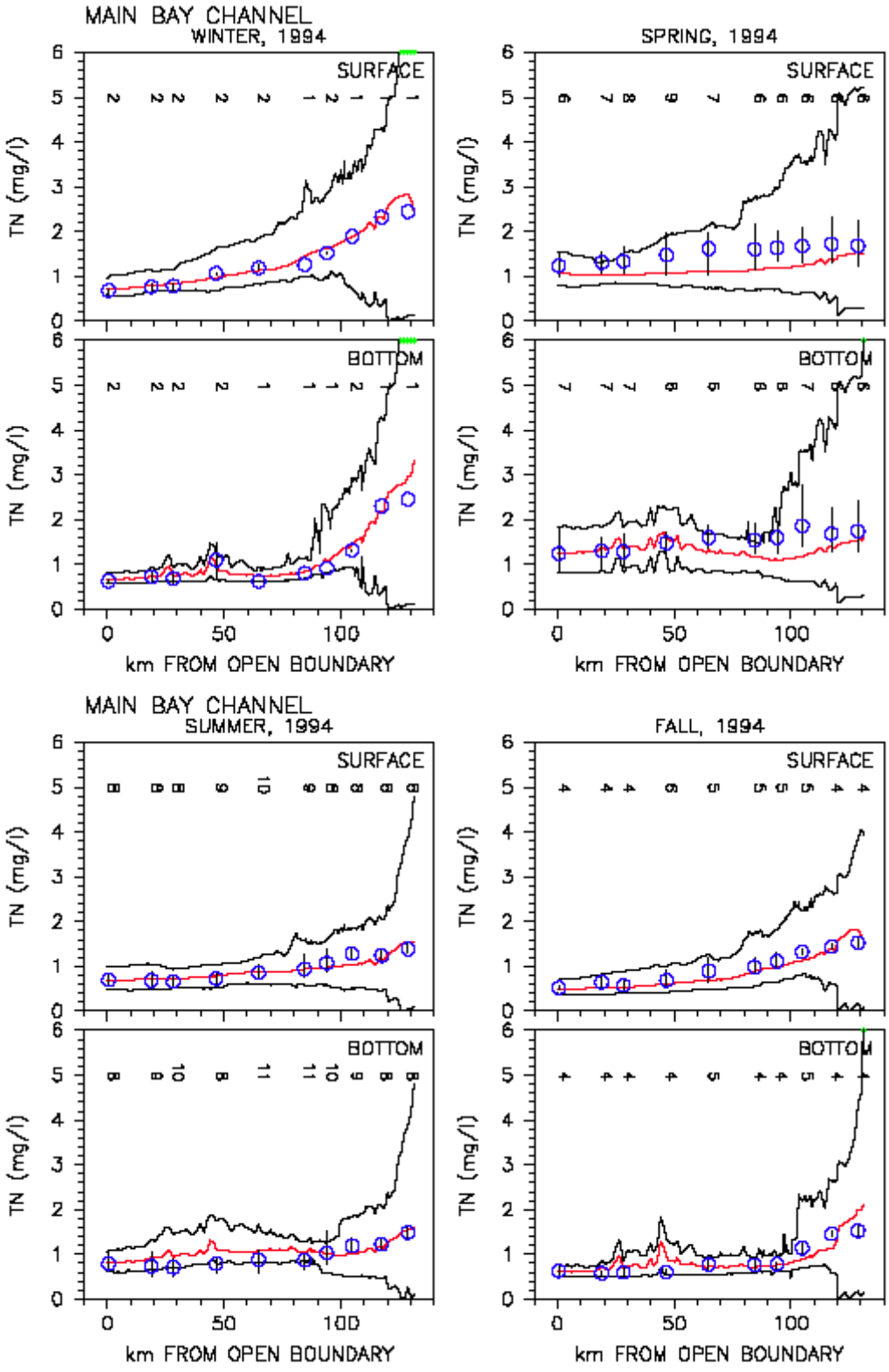

Fig. 50. Longitudinal comparison of model calibration results and data for total nitrogen in the Upper Chesapeake Bay transect

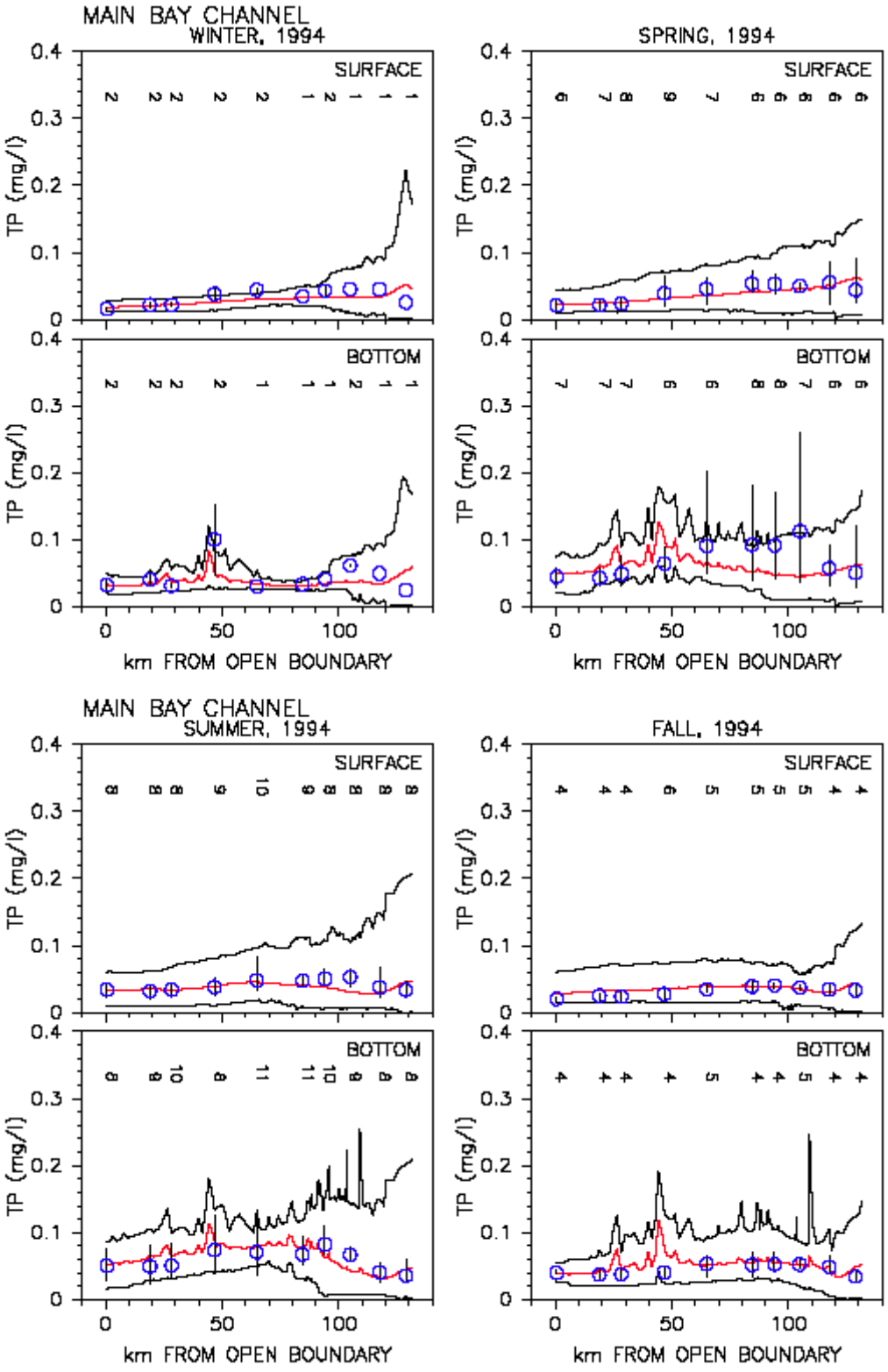

Fig. 51. Longitudinal comparison of model calibration results and data for total phosphorus in the Upper Chesapeake Bay transect

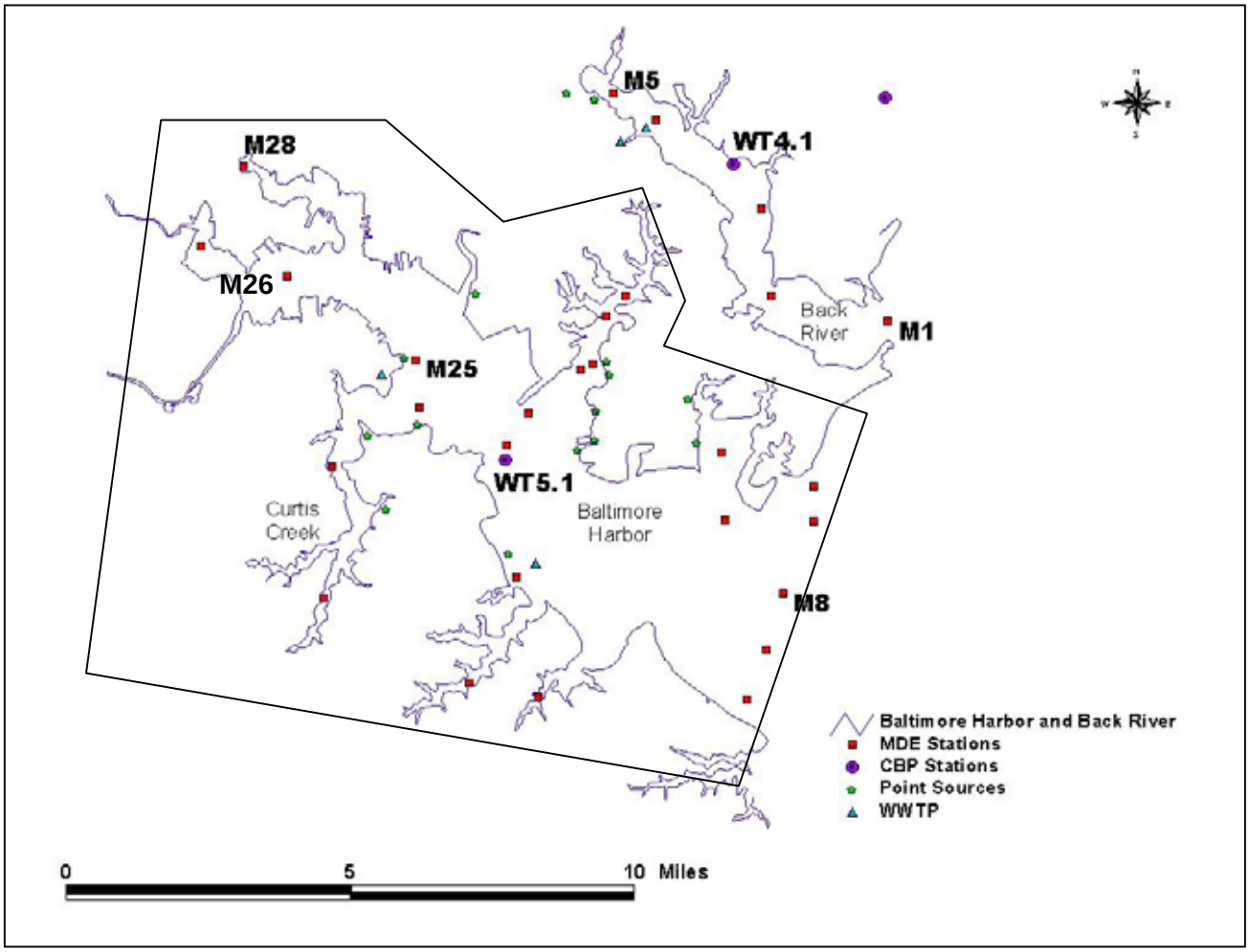

Fig. 52. Water quality monitoring station in Baltimore Harbor

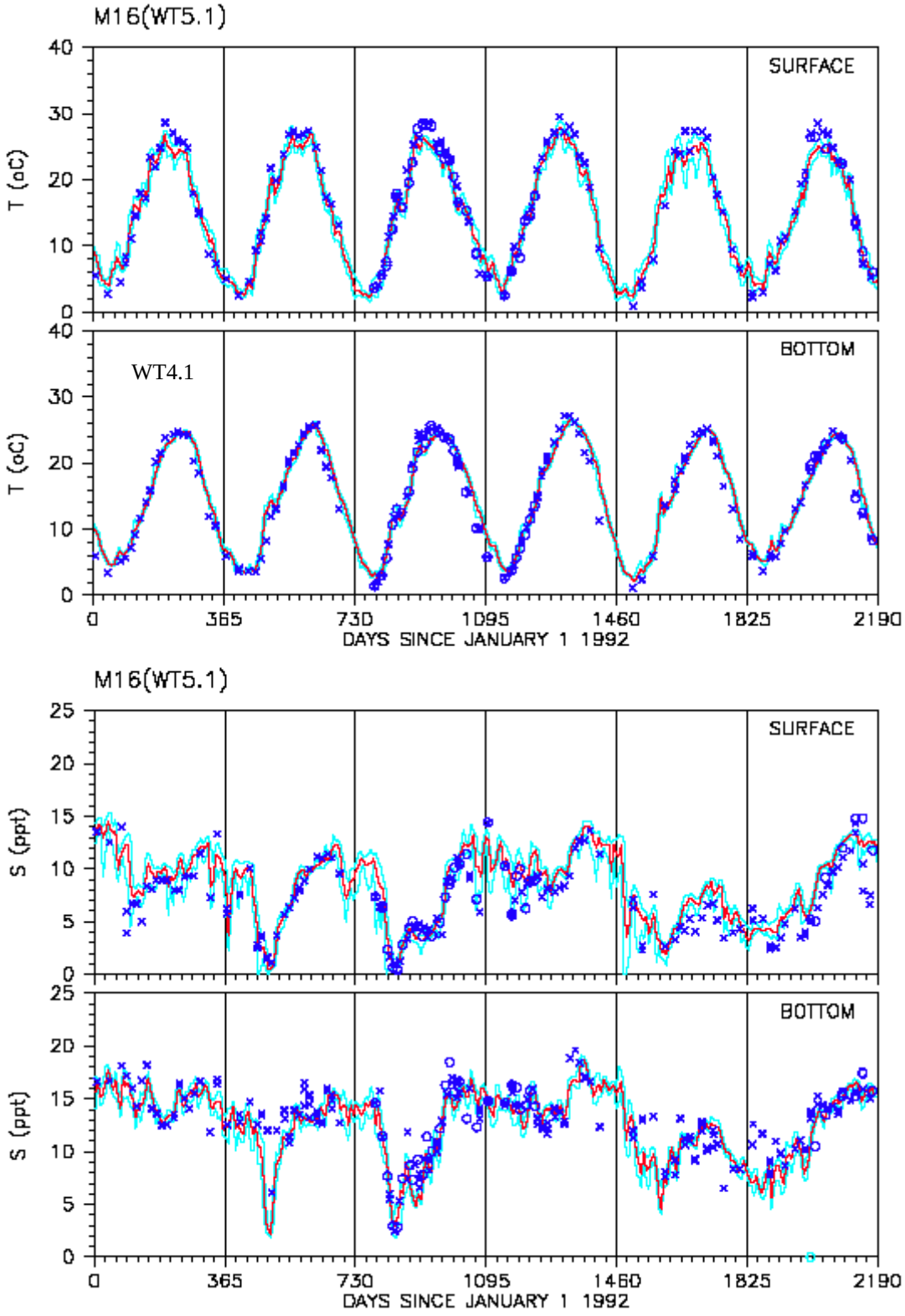

Fig 53. Time series comparison of model calibration results and data for temperature and salinity in Baltimore Harbor (WT5.1)

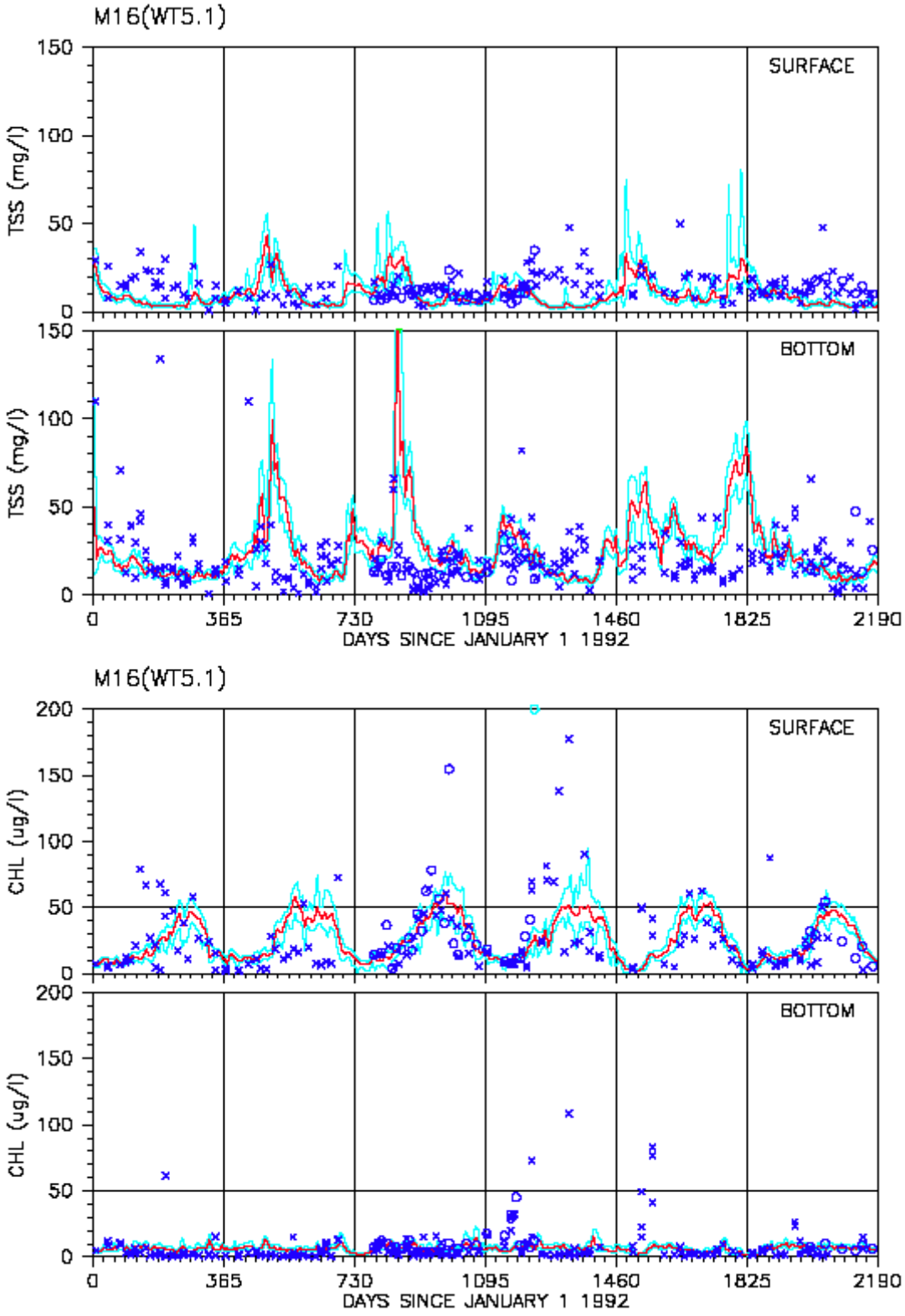

Fig 54. Time series comparison of model calibration results and data for total suspended solids and chlorophyll a in Baltimore Harbor (WT5.1)

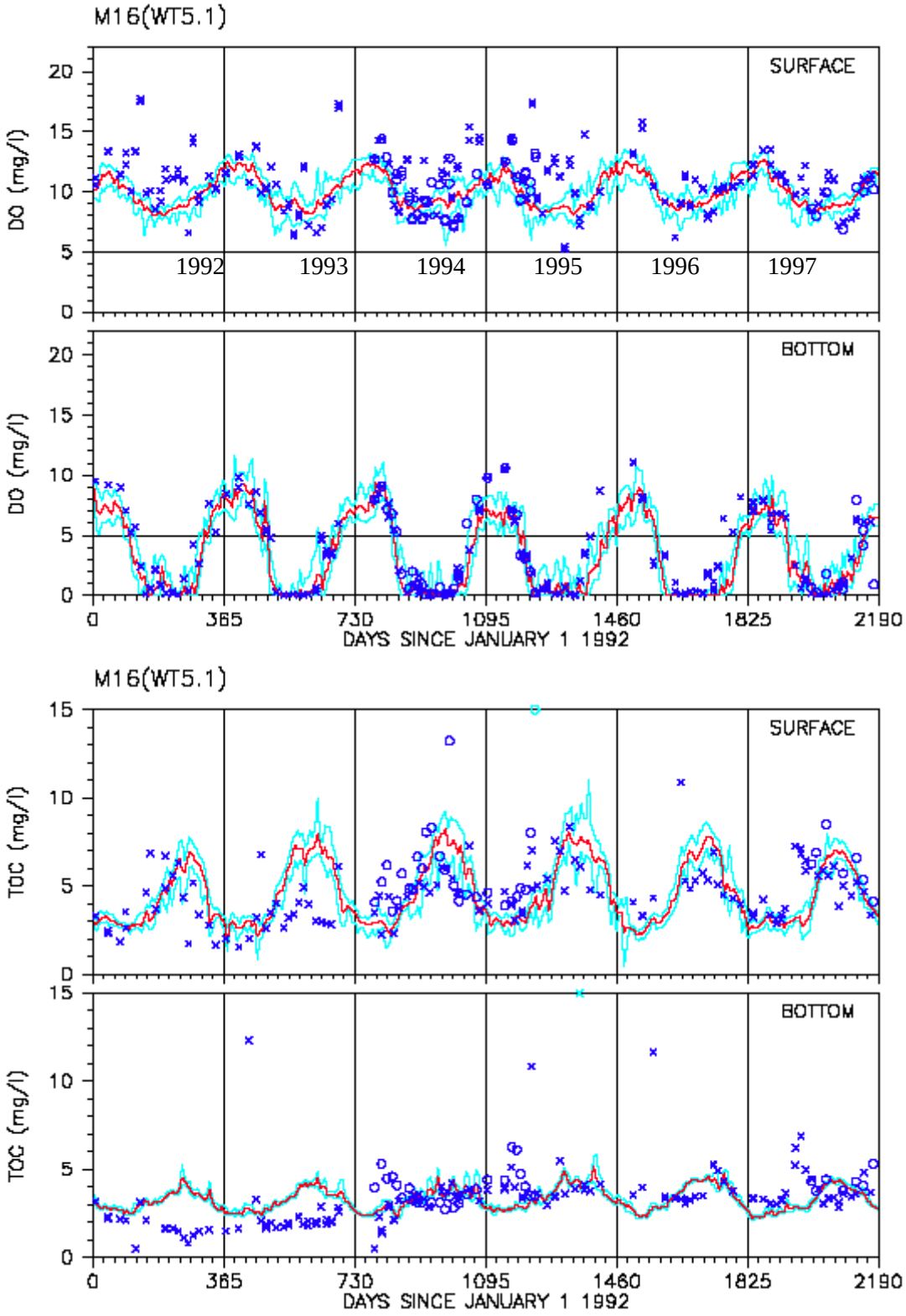

Fig. 55. Time series comparison of model calibration results and data for dissolved oxygen and total organic carbon in Baltimore Harbor (WT5.1)

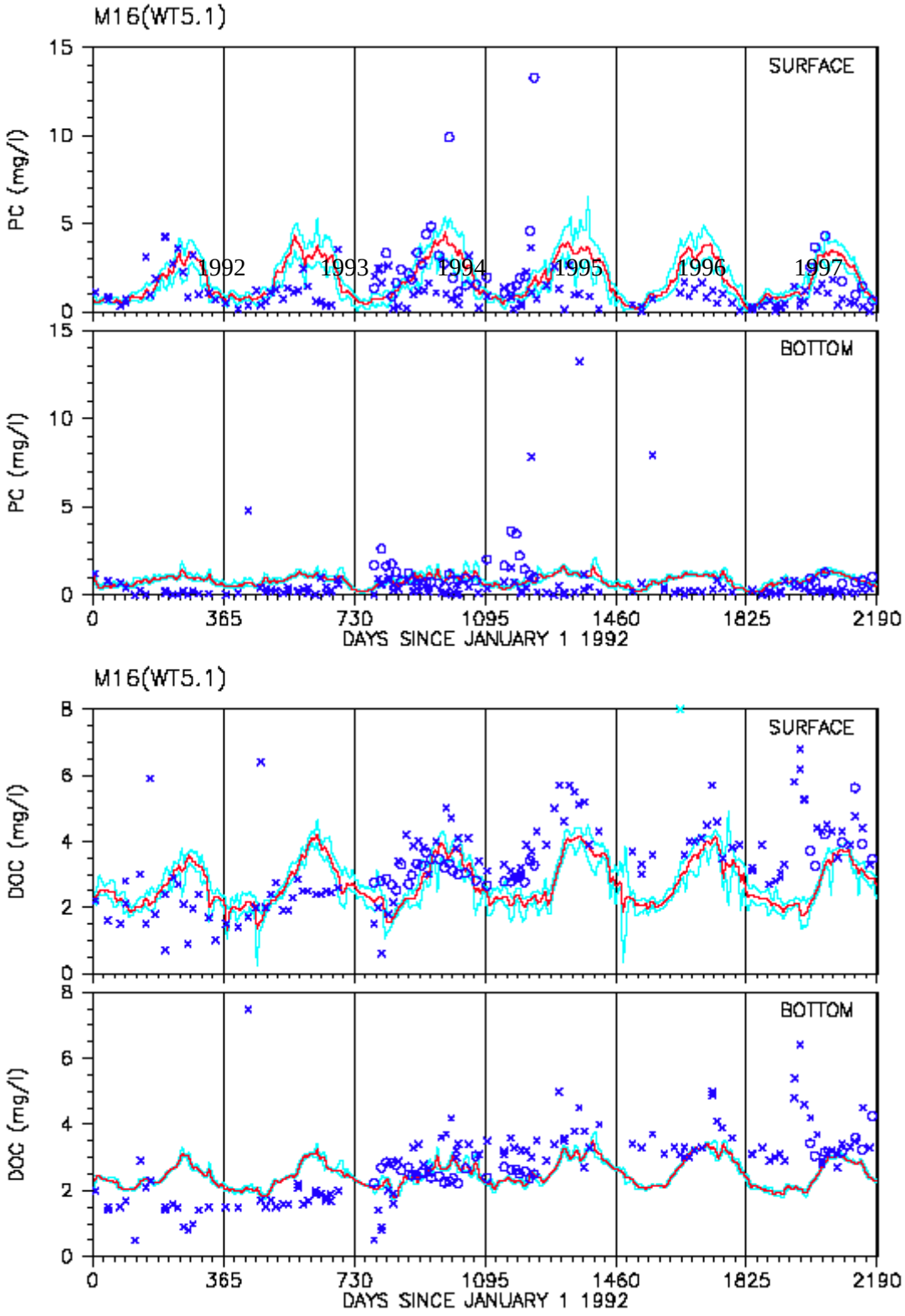

Fig. 56. Time series comparison of model calibration results and data for particulate carbon and dissolved organic carbon in Baltimore Harbor (WT5.1)

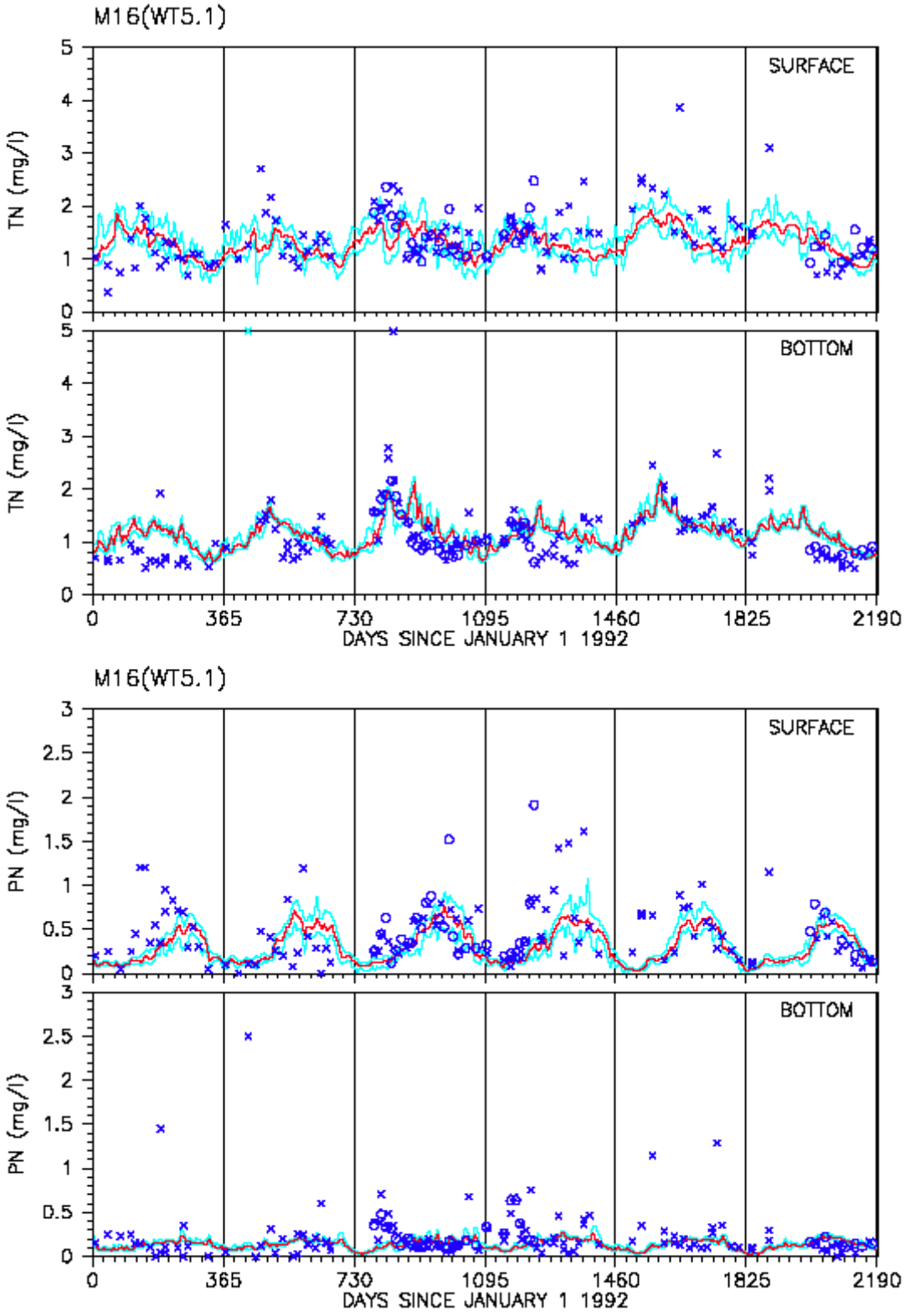

Fig. 57. Time series comparison of model calibration results and data for total nitrogen and particulate nitrogen in Baltimore Harbor (WT5.1)

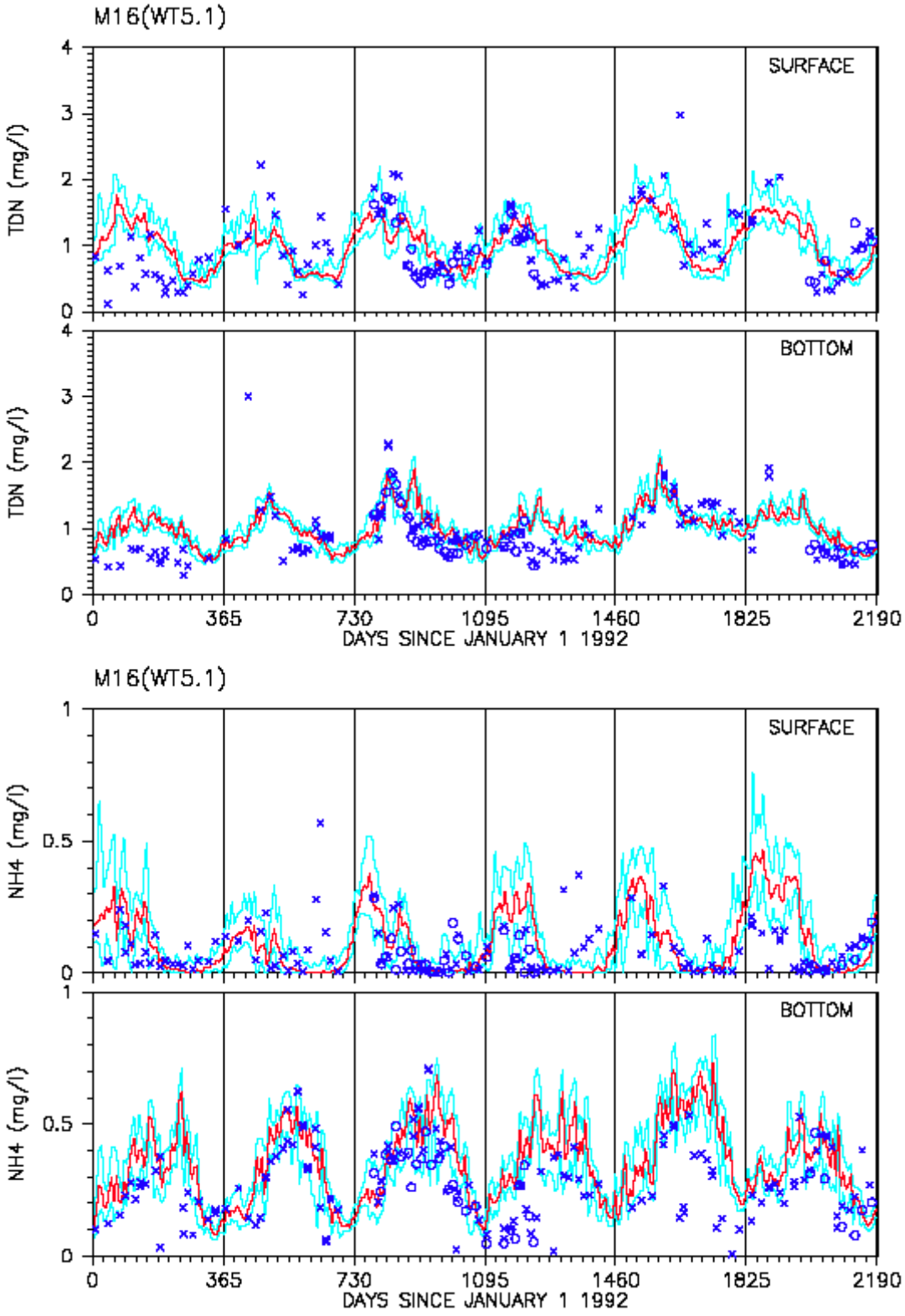

Fig. 58. Time series comparison of model calibration results and data for total dissolved nitrogen and ammonia in Baltimore Harbor (WT5.1)

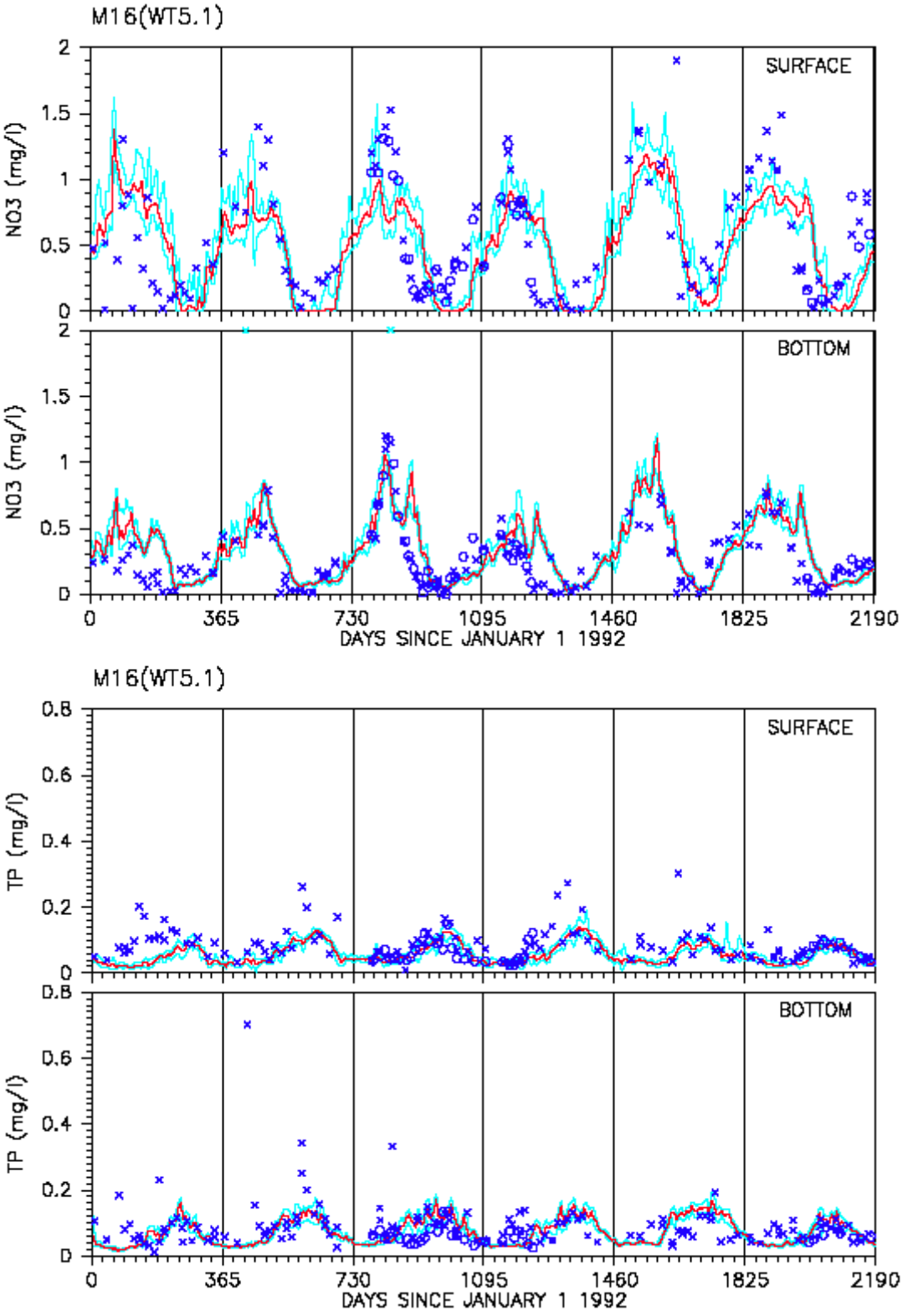

Fig. 59. Time series comparison of model calibration results and data for nitrate and total phosphorus in Baltimore Harbor (WT5.1)

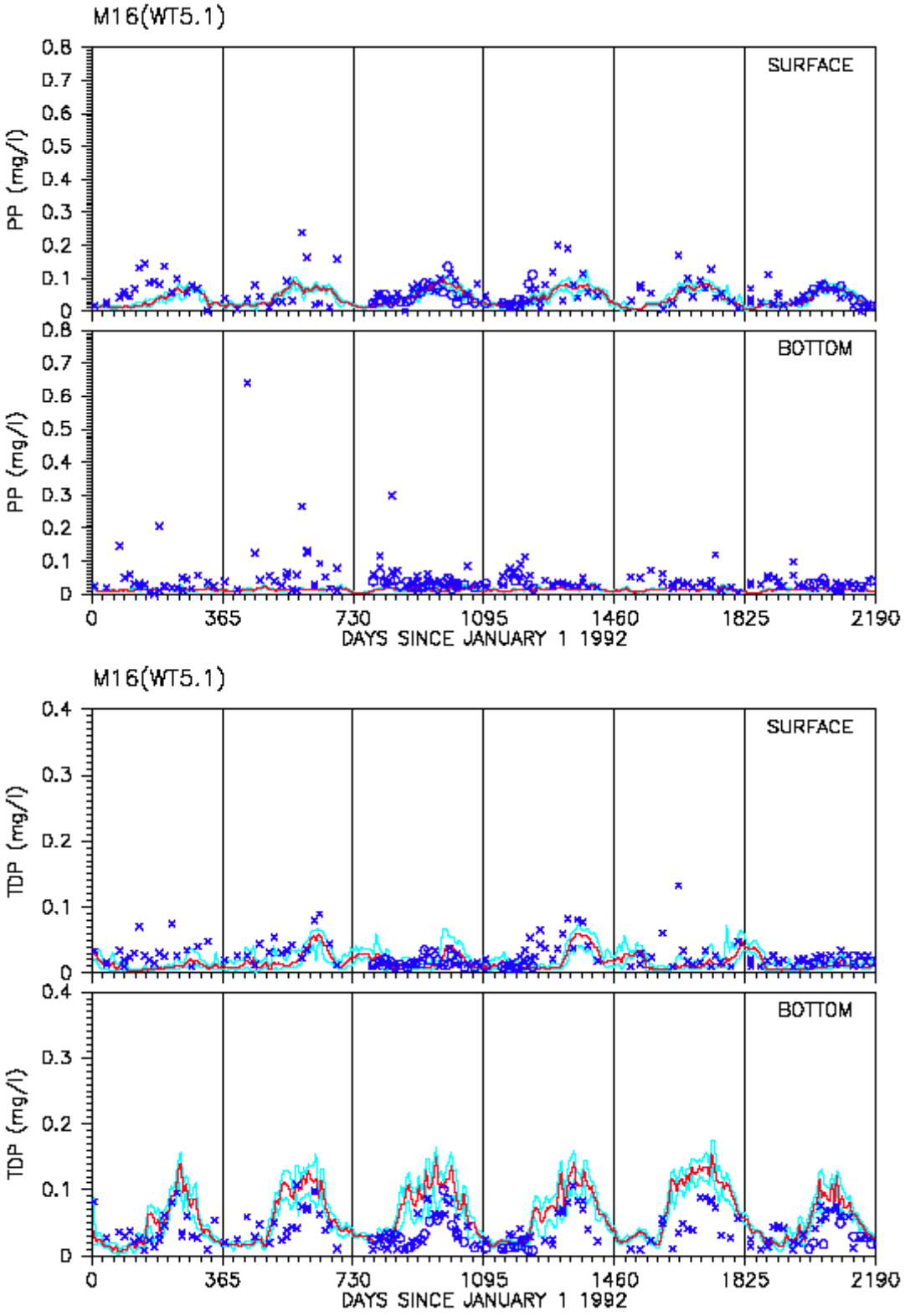

Fig. 60. Time series comparison of model calibration results and data for particulate phosphorus and total dissolved phosphorus in Baltimore Harbor (WT5.1)

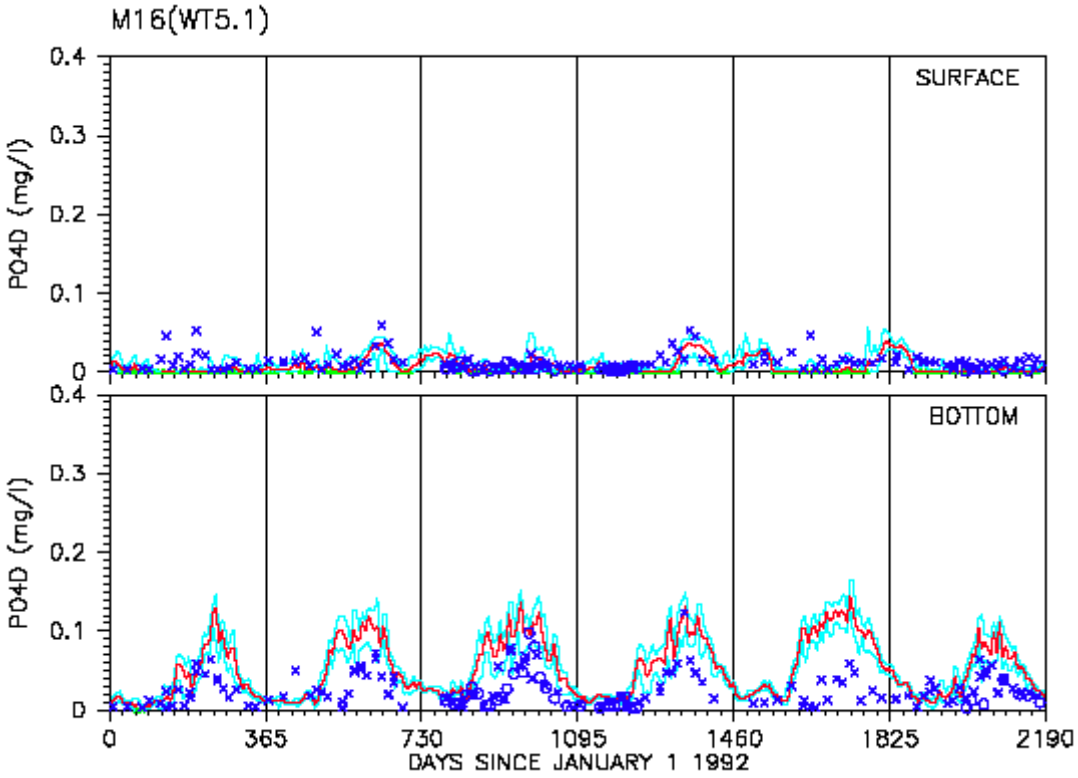

Fig. 61. Time series comparison of model calibration results and data for phosphate in Baltimore Harbor (WT5.1)

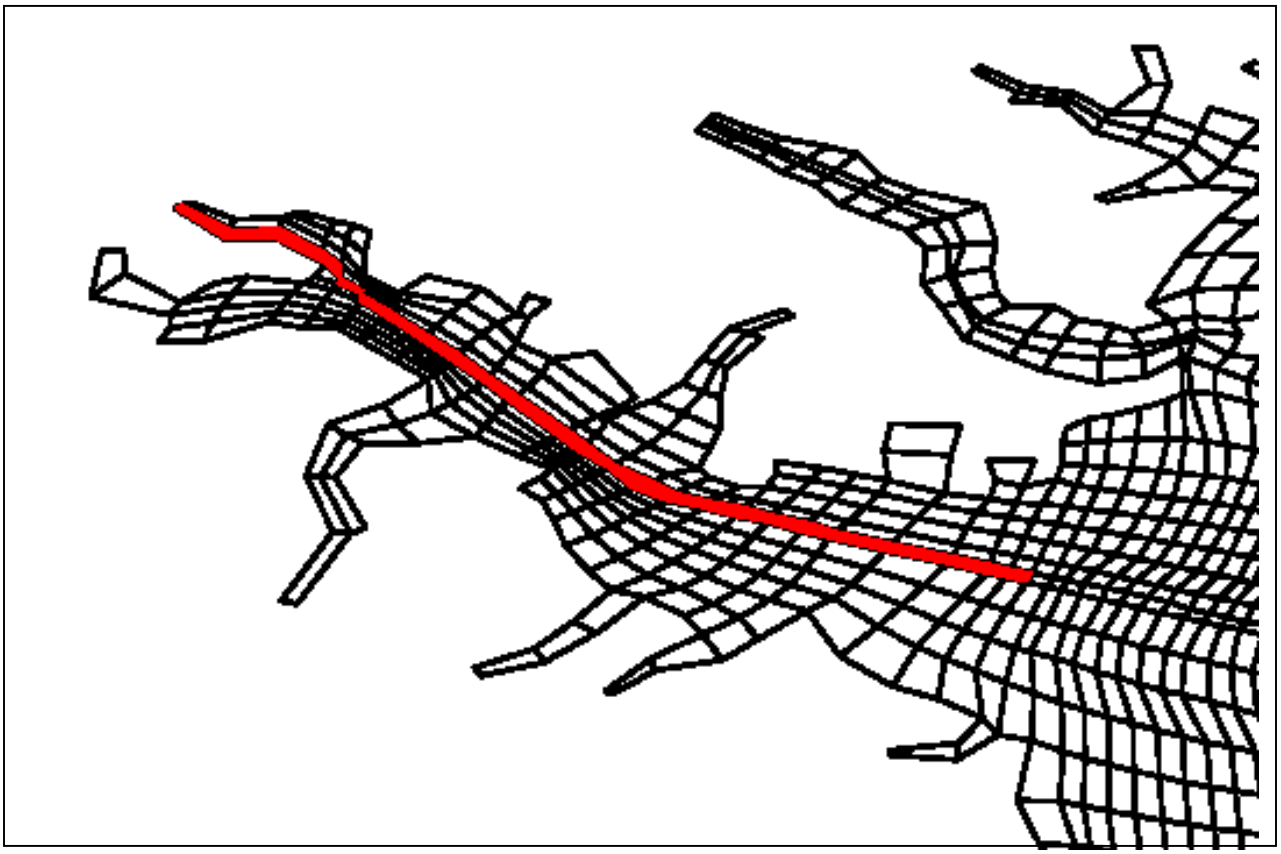

Fig. 62. Plan view of the model grid showing the transect of Baltimore Harbor from the mouth into inner harbor

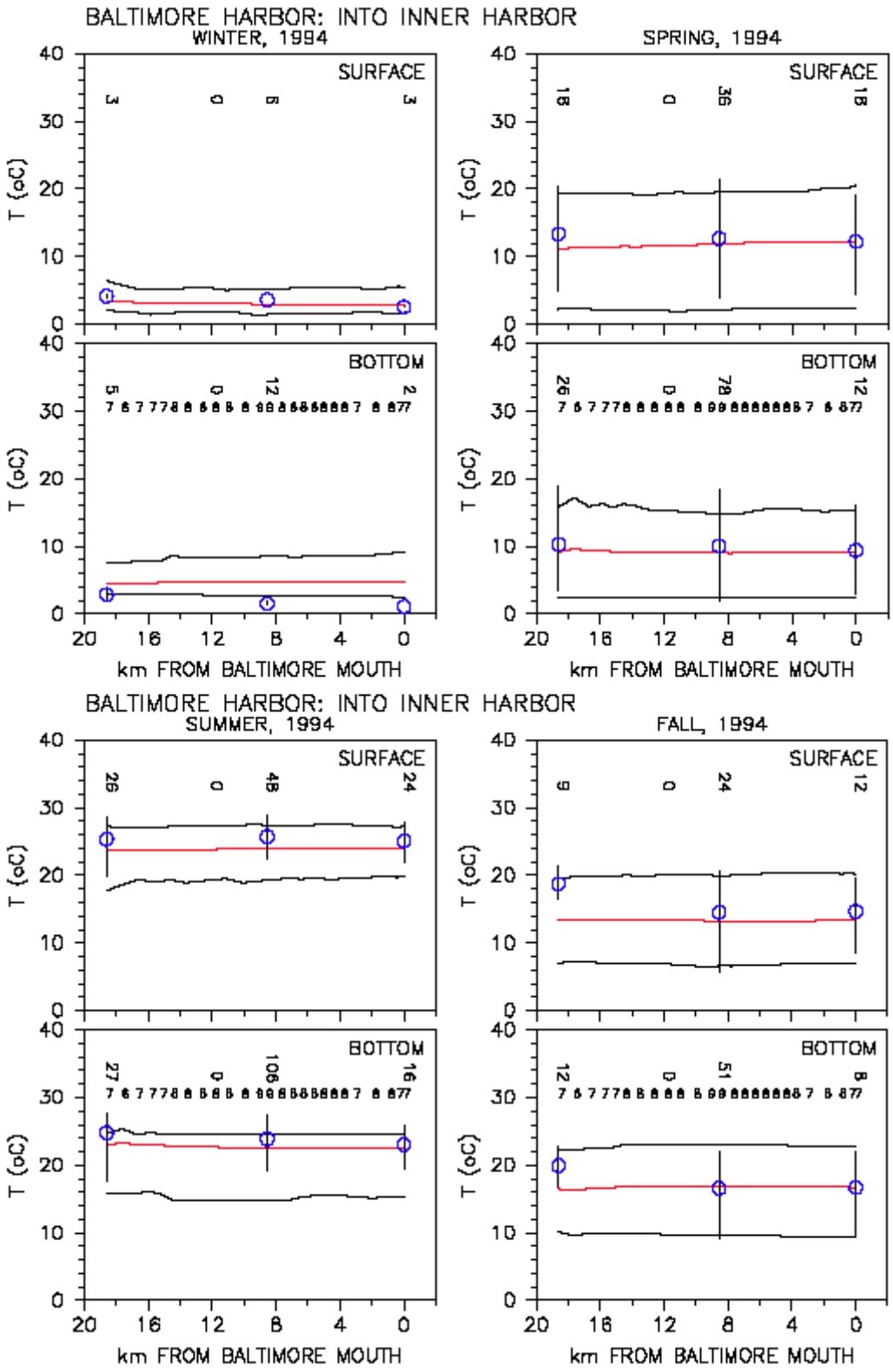

Fig. 63. Longitudinal comparison of model calibration results and data for temperature in Baltimore Harbor transect

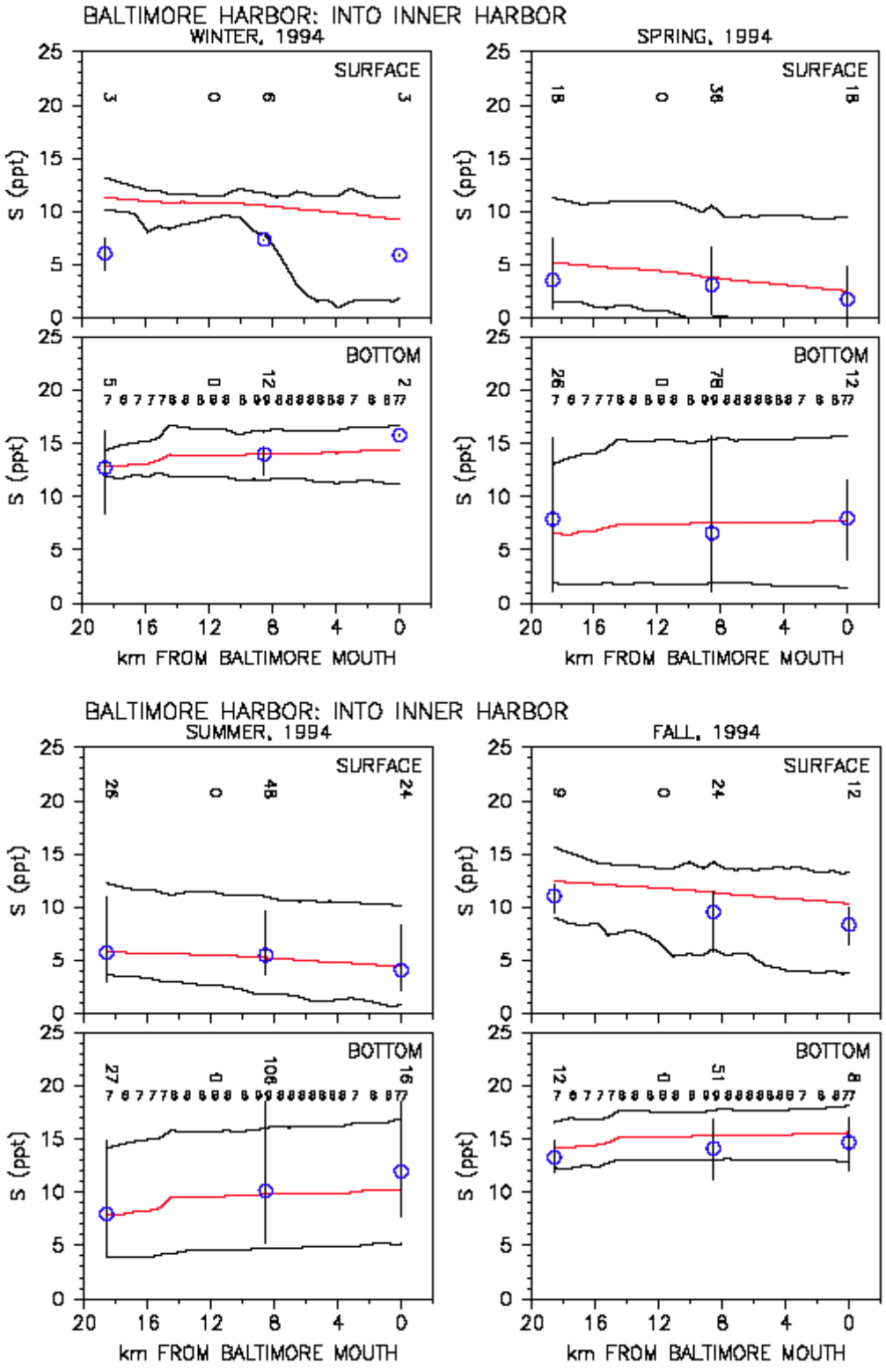

Fig. 64. Longitudinal comparison of model calibration results and data for salinity in Baltimore Harbor transect

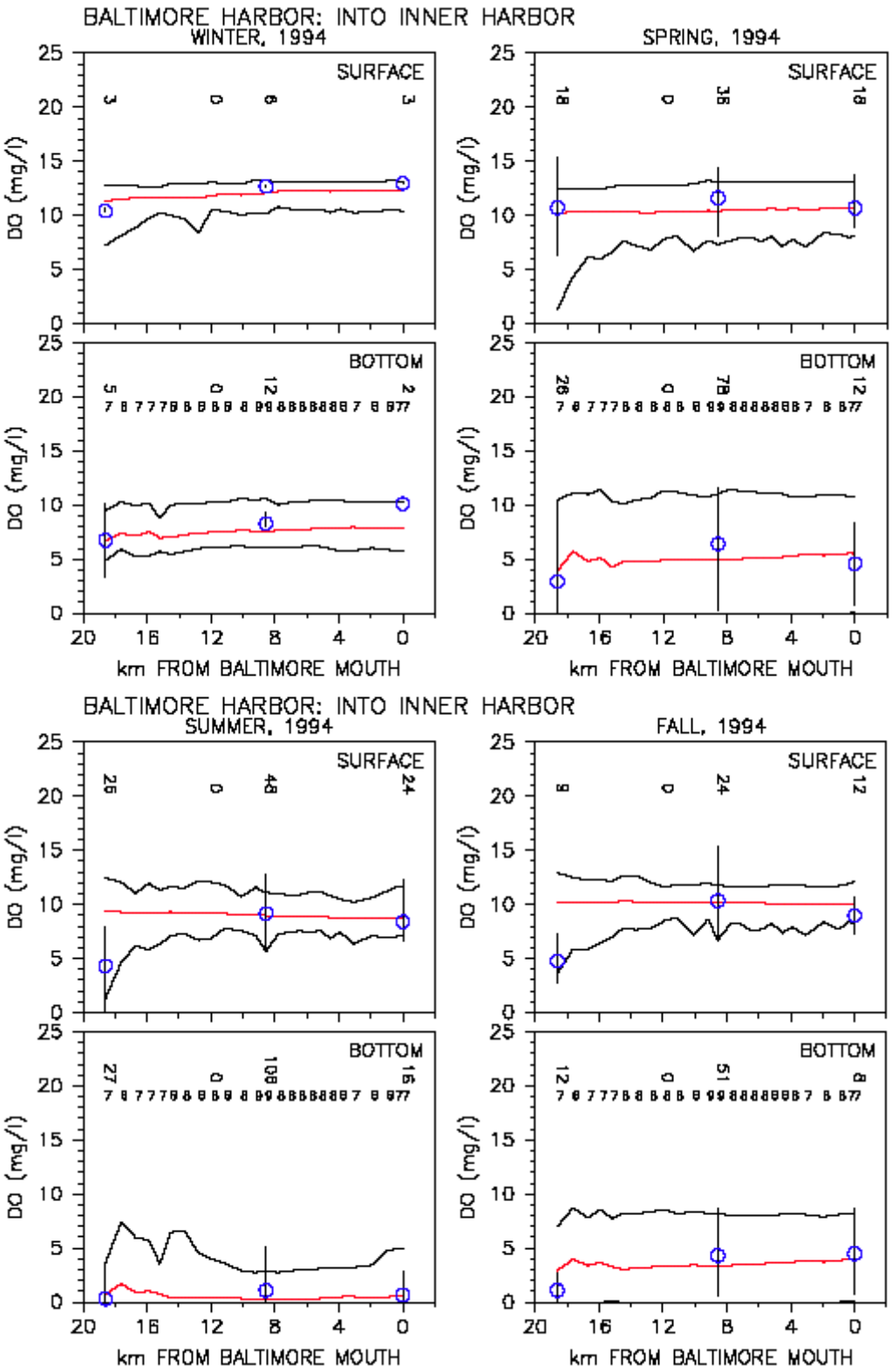

Fig. 65. Longitudinal comparison of model calibration results and data for dissolved oxygen in Baltimore Harbor transect

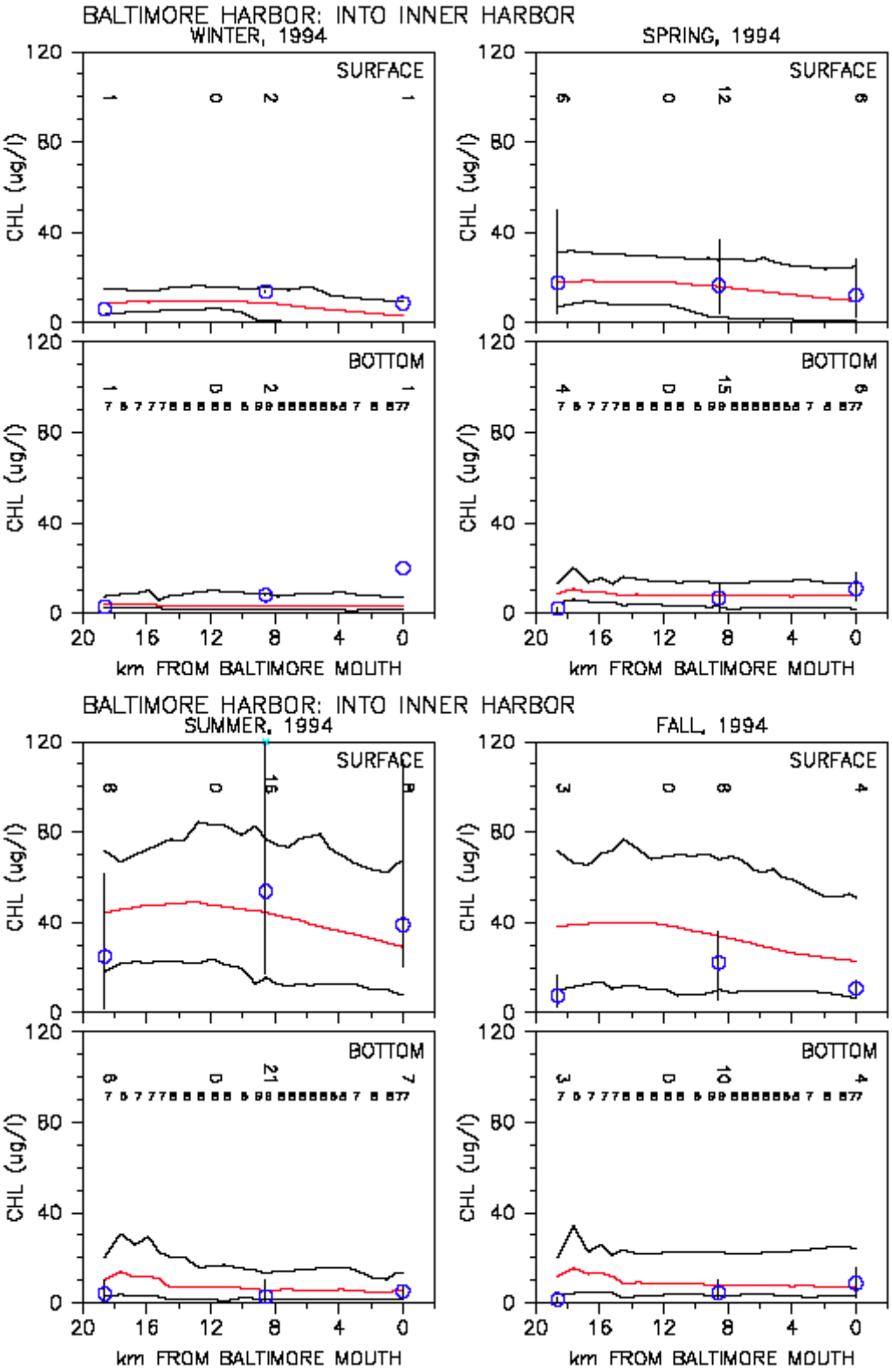

Fig. 66. Longitudinal comparison of model calibration results and data for chlorophyll a in Baltimore Harbor transect

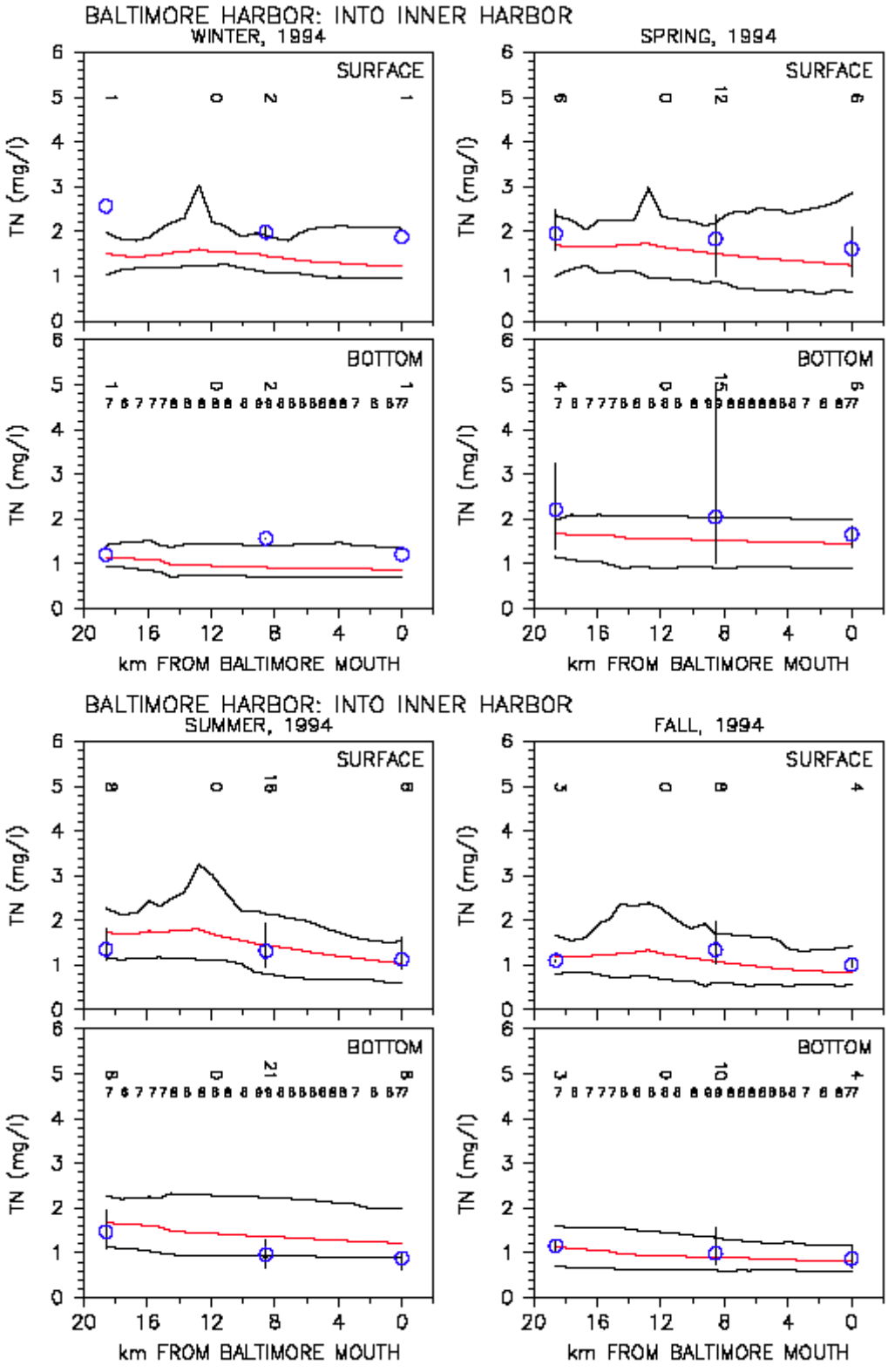

Fig. 67. Longitudinal comparison of model calibration results and data for total nitrogen in Baltimore Harbor transect

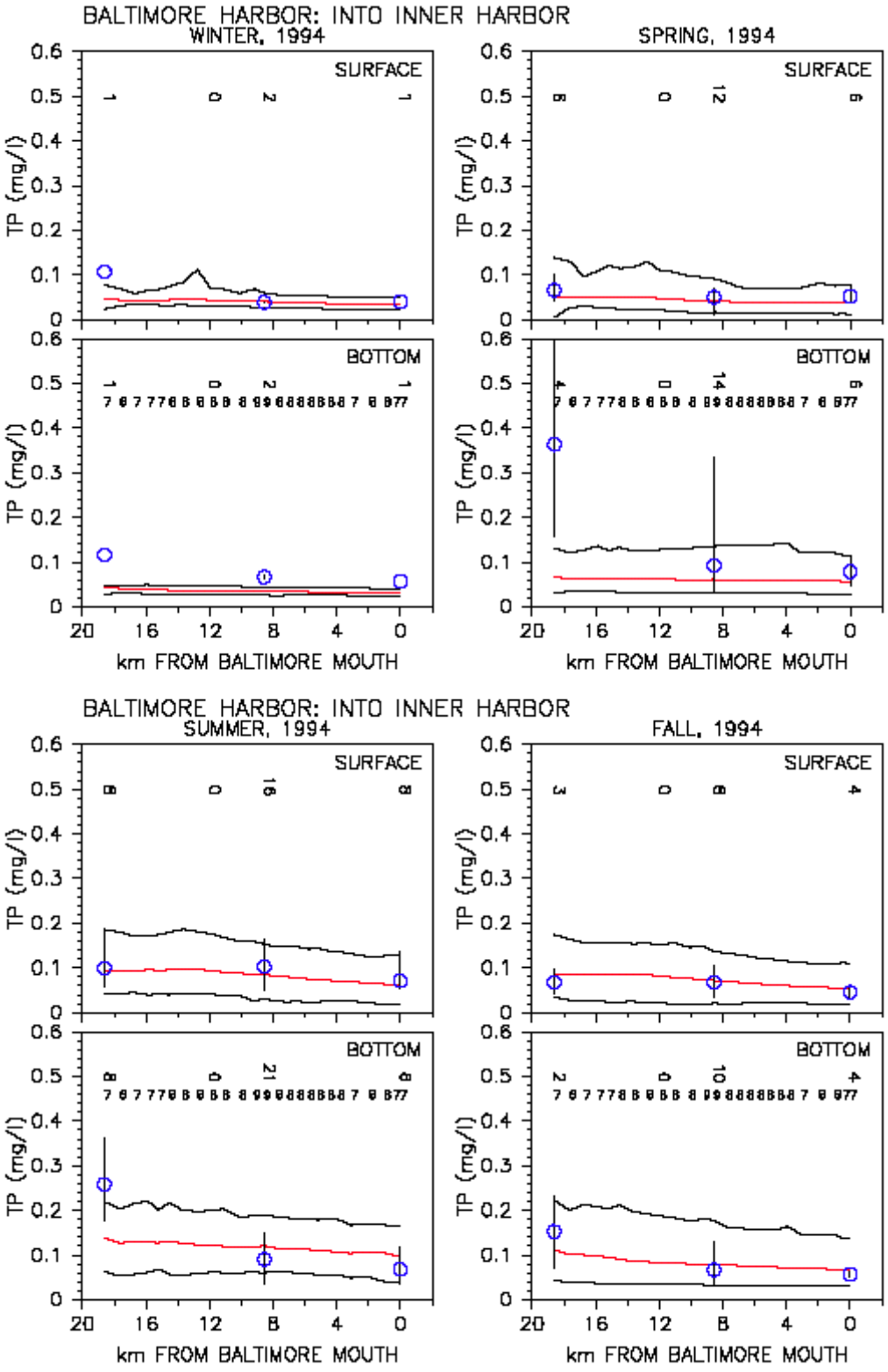

Fig. 68. Longitudinal comparison of model calibration results and data for total phosphorus in Baltimore Harbor transect

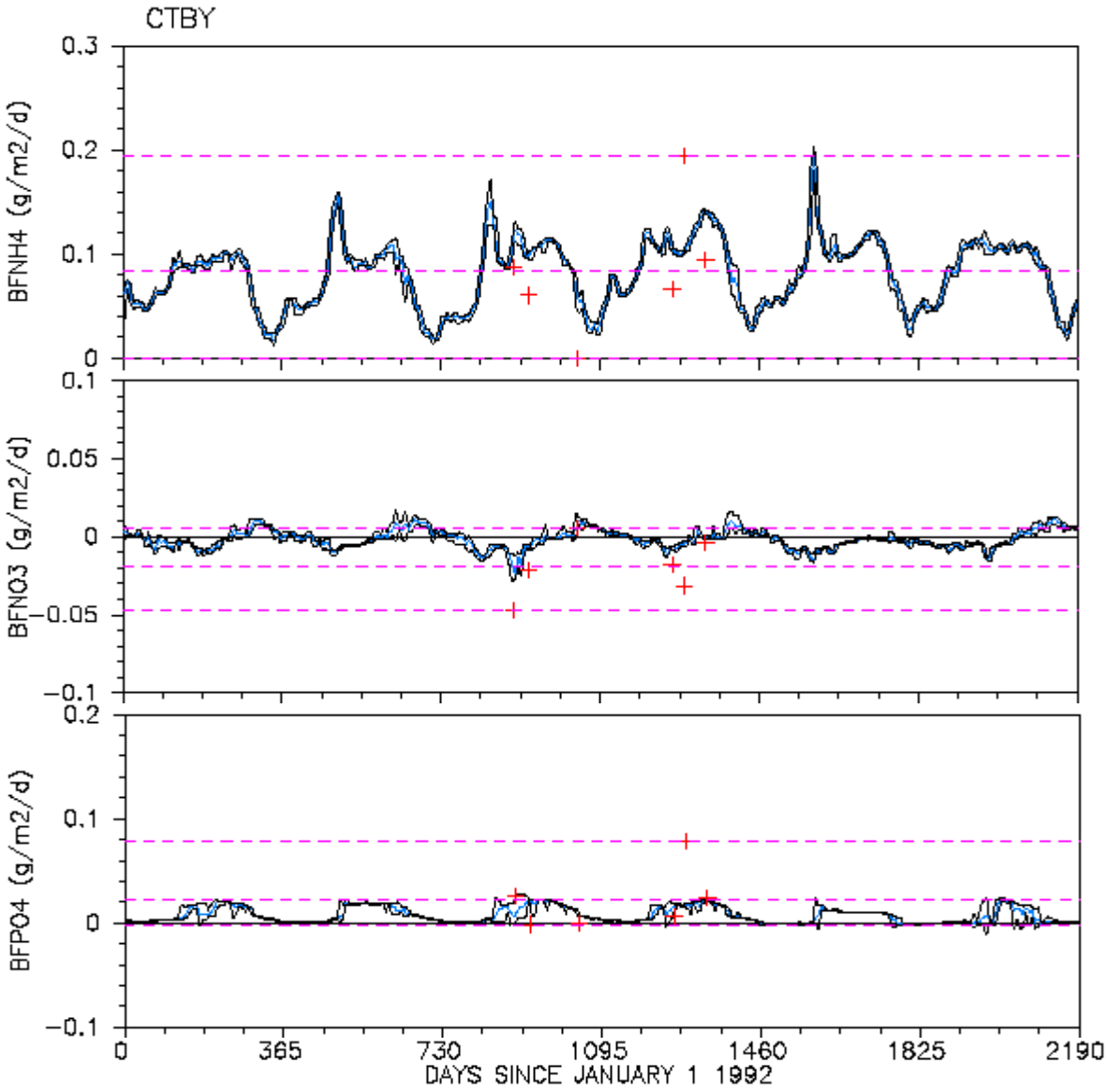

Fig. 69. Time series comparison of model simulated sediment fluxes and data in Baltimore Harbor (CTBY)

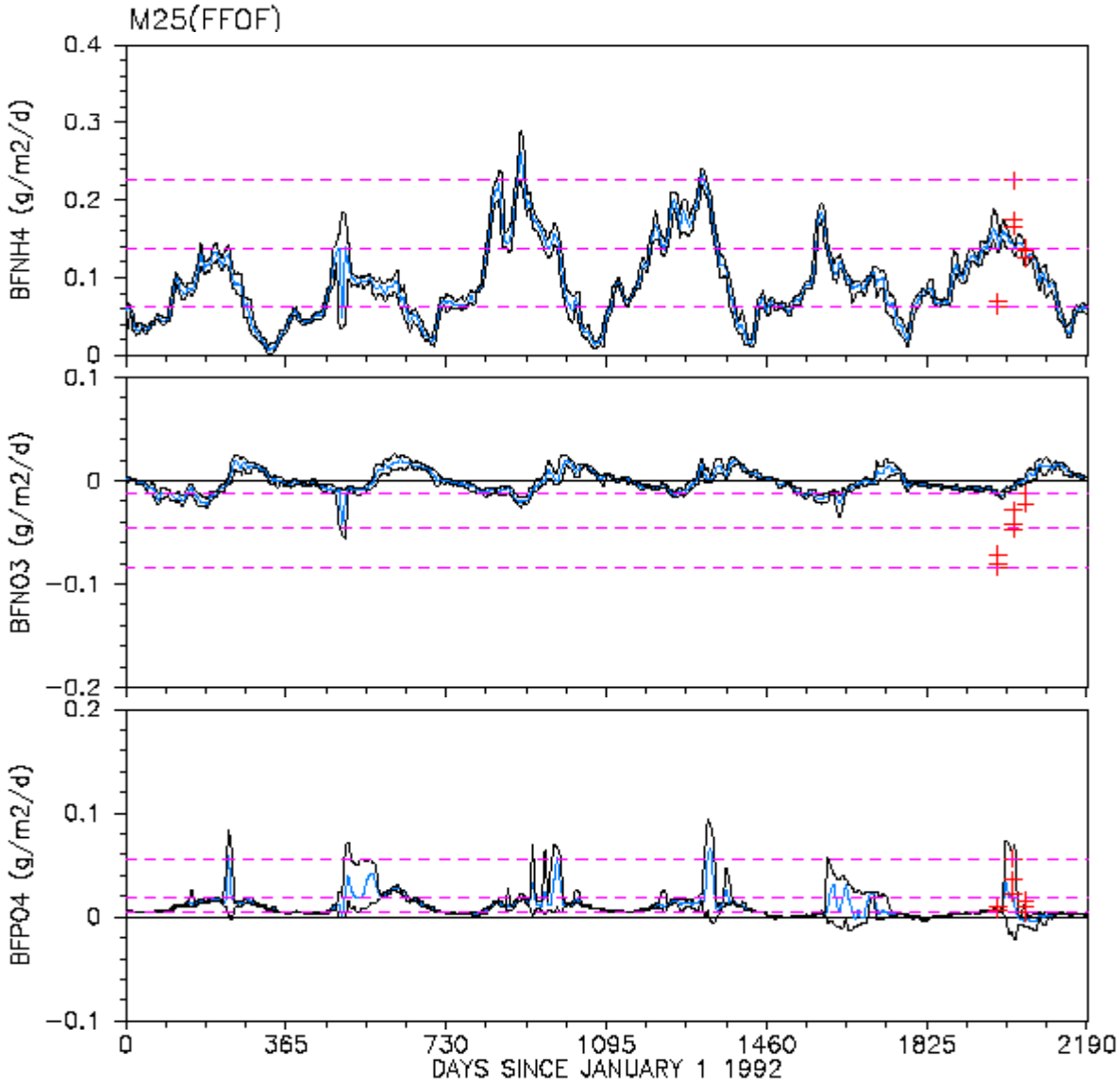

Fig. 70. Time series comparison of model simulated sediment fluxes and data in Baltimore Harbor (FFOF)

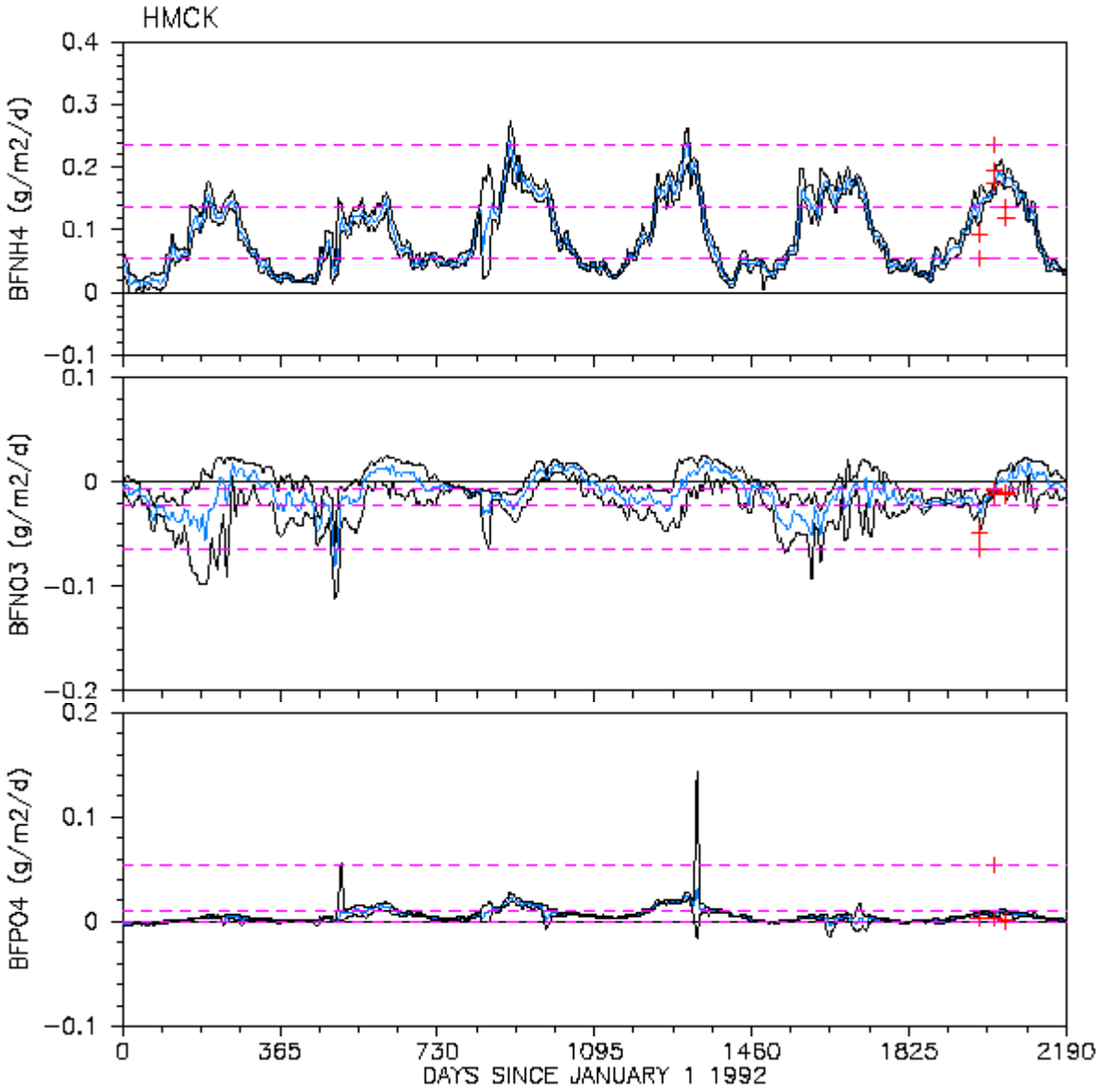

Fig. 71. Time series comparison of model simulated sediment fluxes and data in Baltimore Harbor (HMCK)

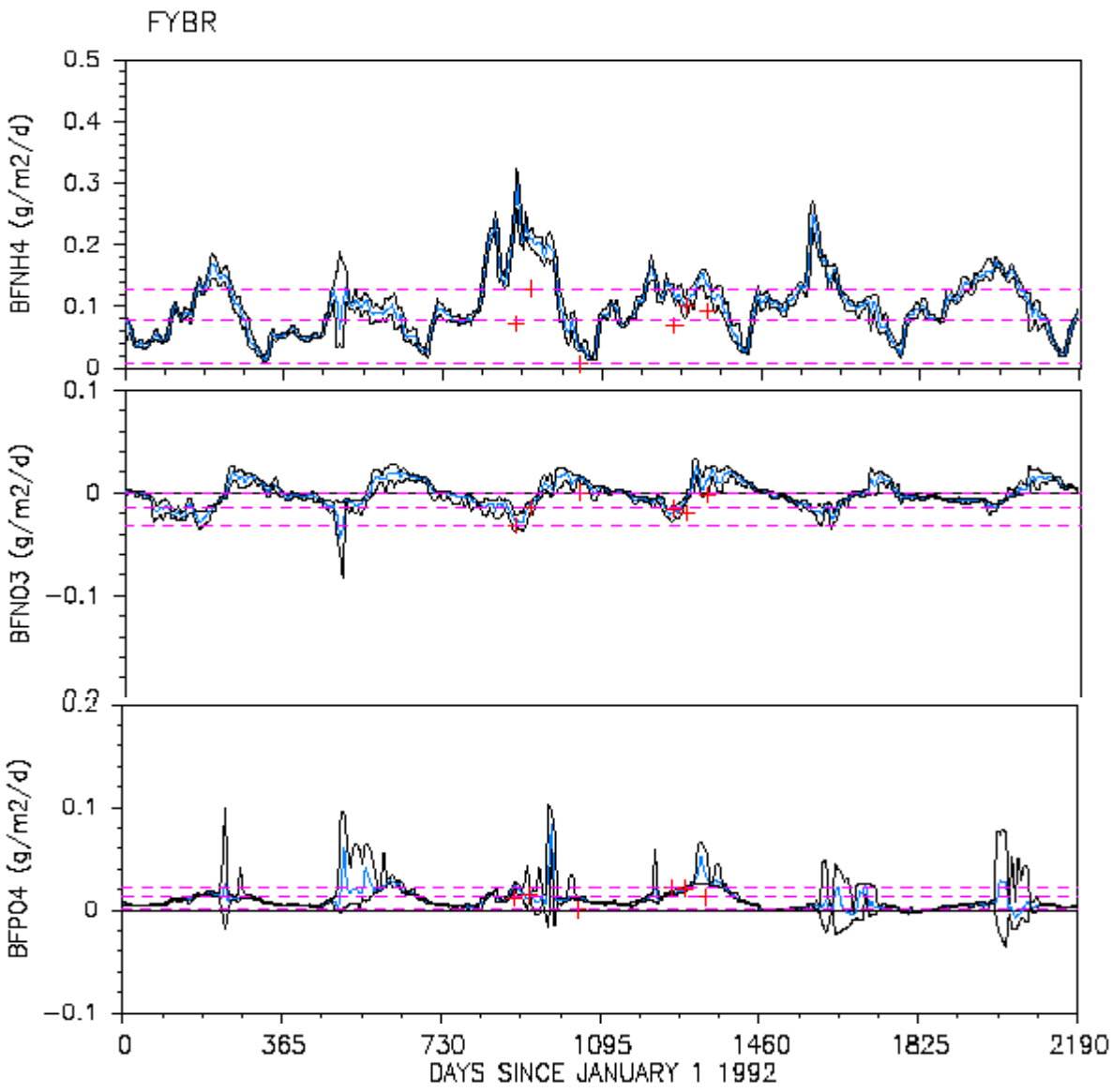

Fig. 72. Time series comparison of model simulated sediment fluxes and data in Baltimore Harbor (FYBR)

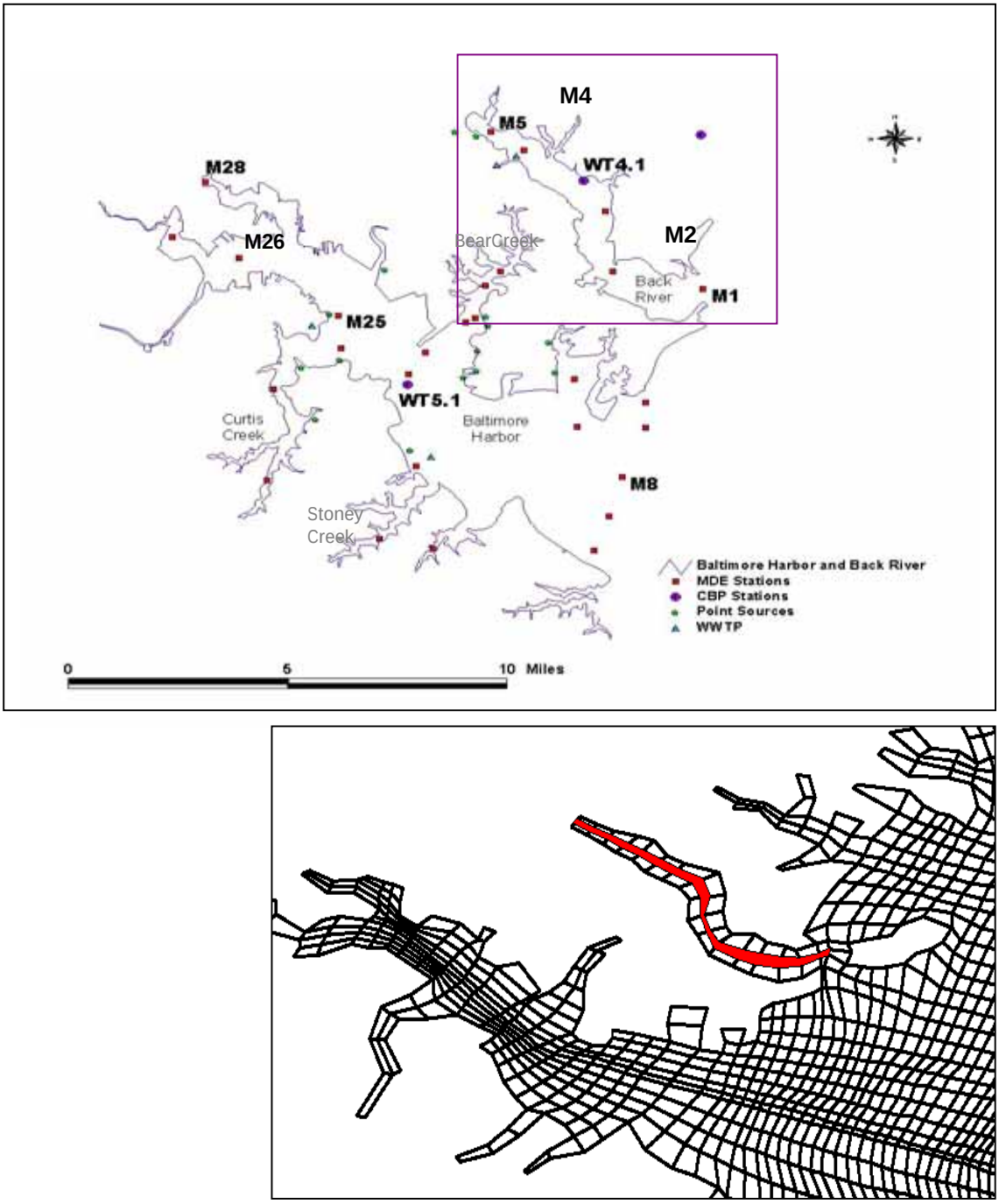

Fig. 73. Water Quality monitoring stations and plan view of the model grid showing the transect of Back River

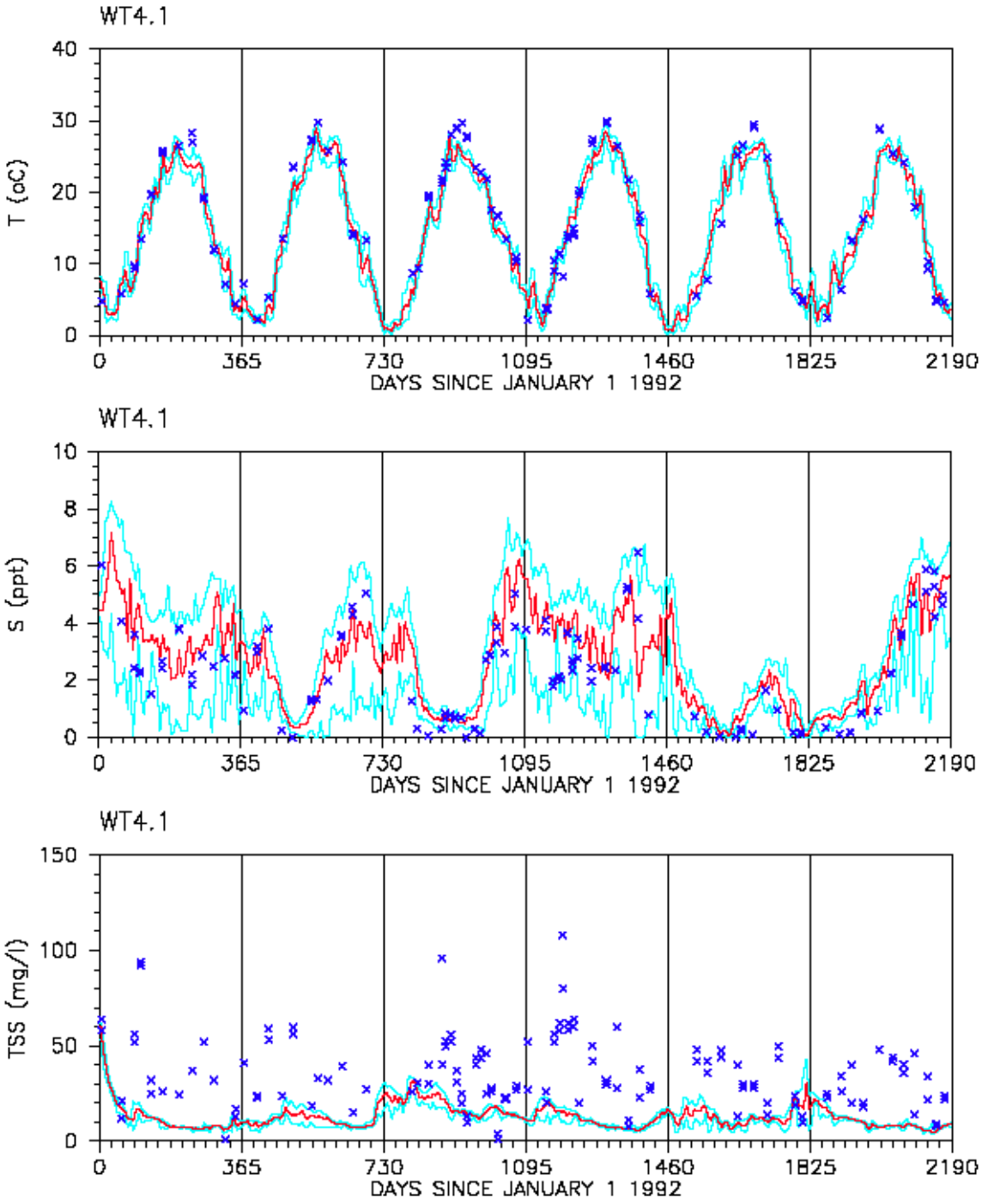

Fig. 74. Time series comparison of model calibration results and data for temperature, salinity, and total suspended solids in Back River (WT4.1)

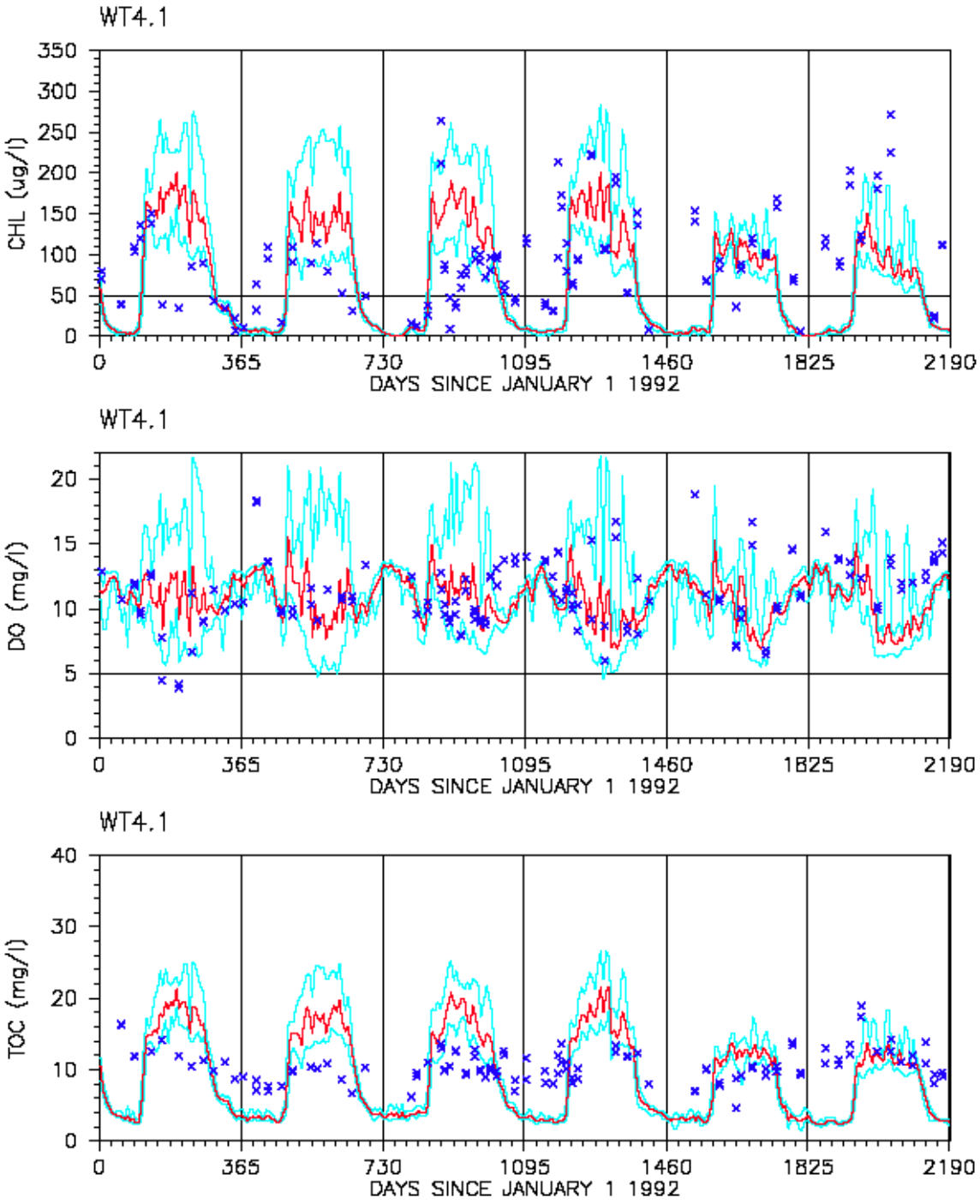

Fig. 75. Time series comparison of model calibration results and data for chlorophyll a, dissolved oxygen, and total organic carbon in Back River (WT4.1)

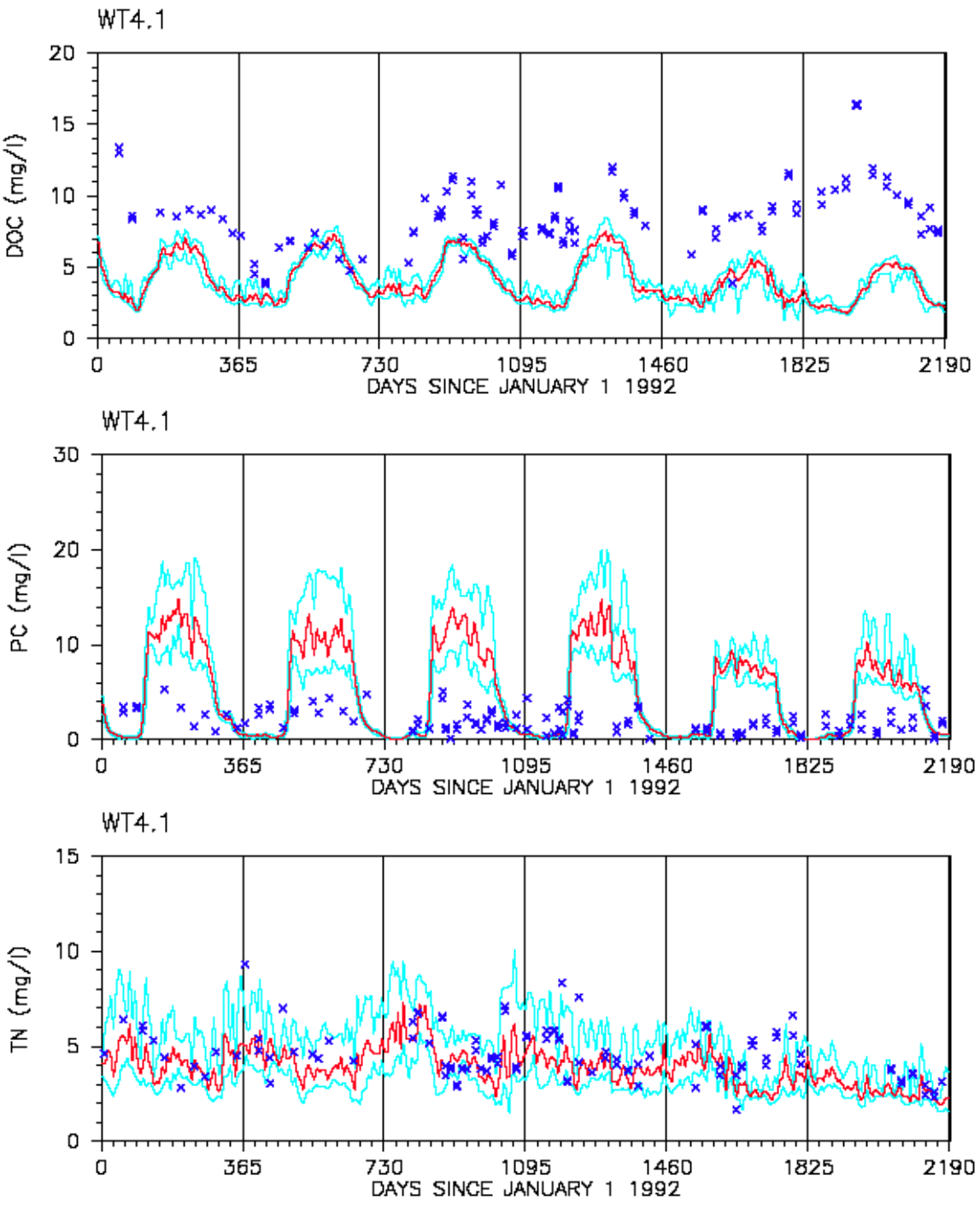

Fig. 76. Time series comparison of model calibration results and data for dissolved organic carbon, particulate organic carbon, and total nitrogen in Back River (WT4.1)

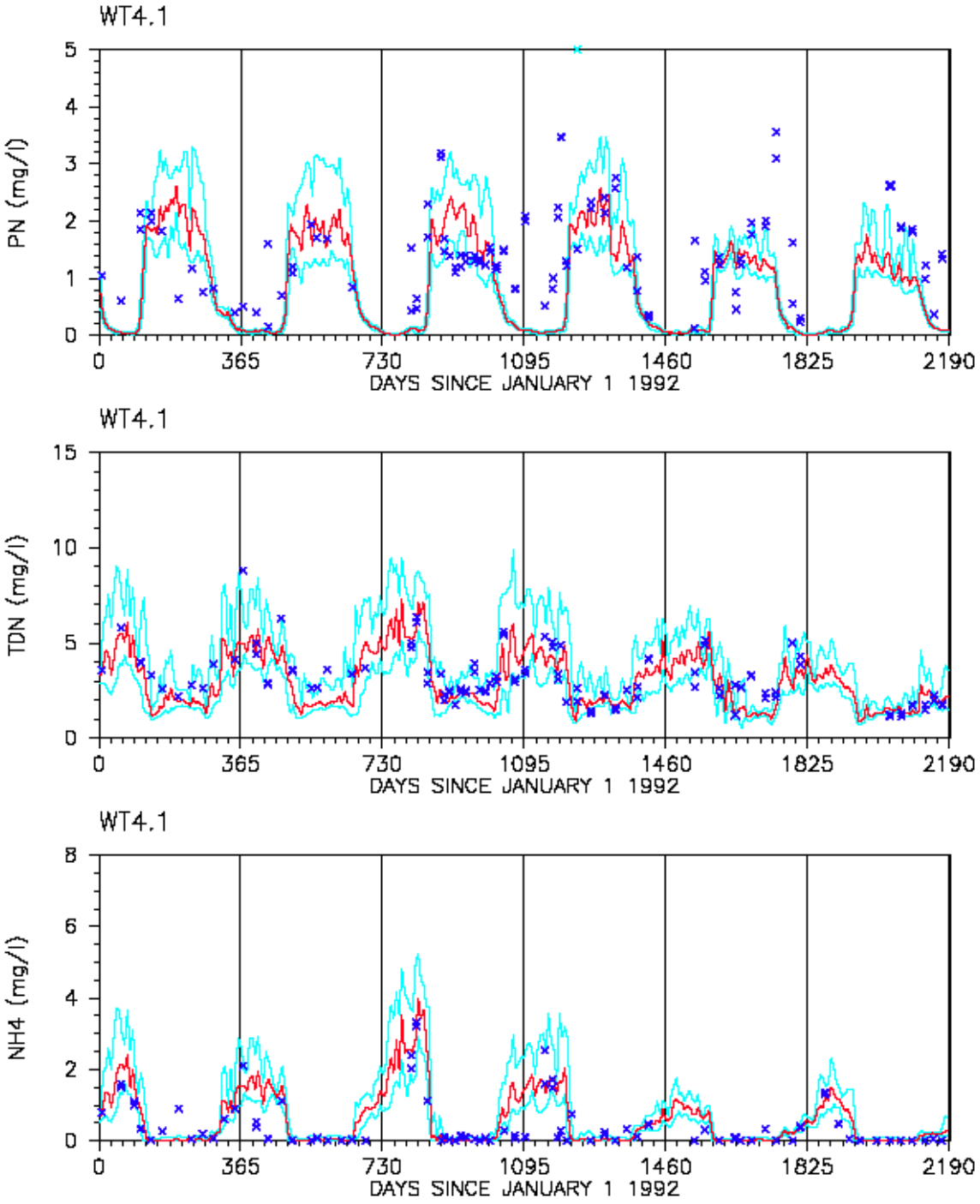

Fig. 77. Time series comparison of model calibration results and data for particulate nitrogen, total dissolved nitrogen, and ammonia in Back River (WT4.1)

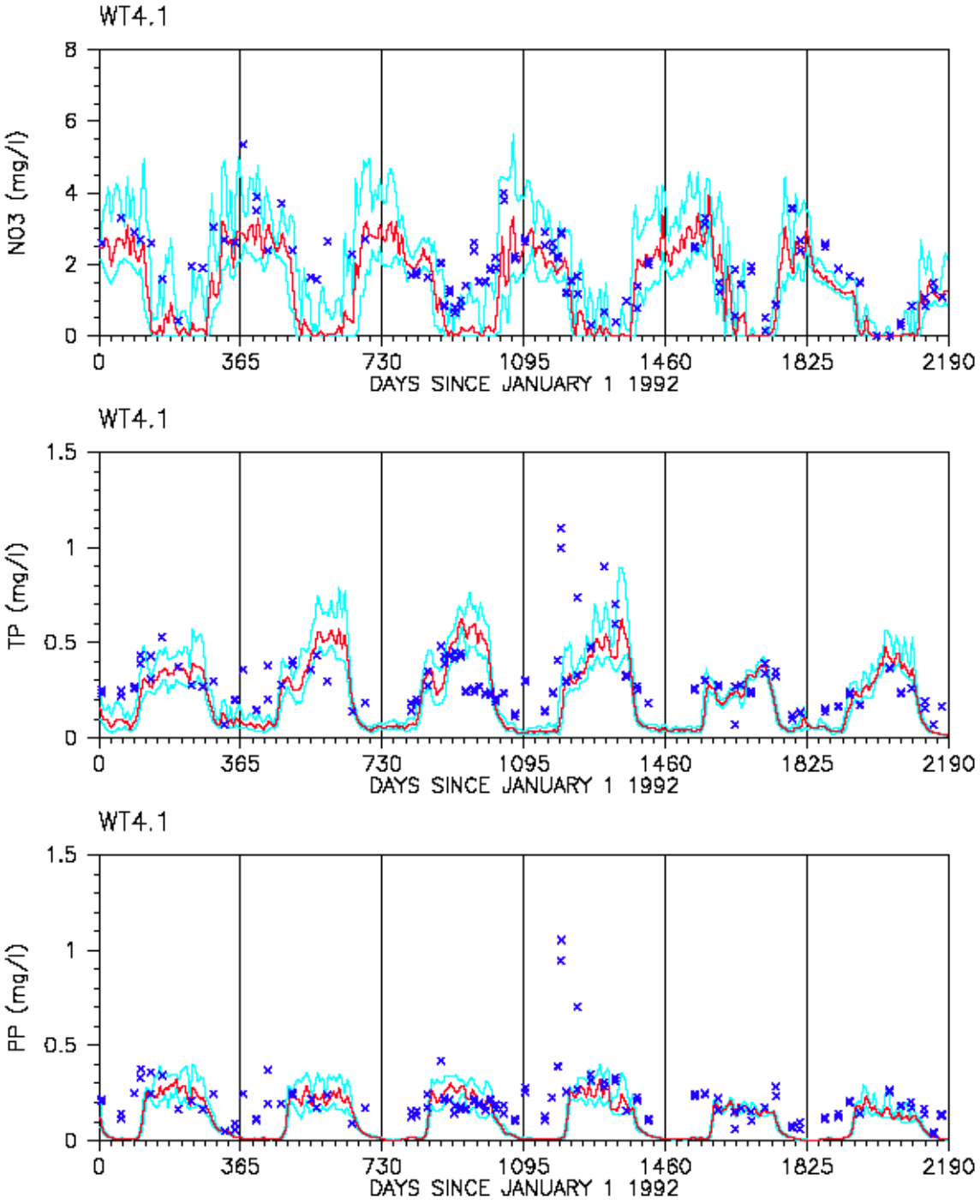

Fig. 78. Time series comparison of model calibration results and data for nitrate, total phosphorus, and particulate phosphorus in Back River (WT4.1)

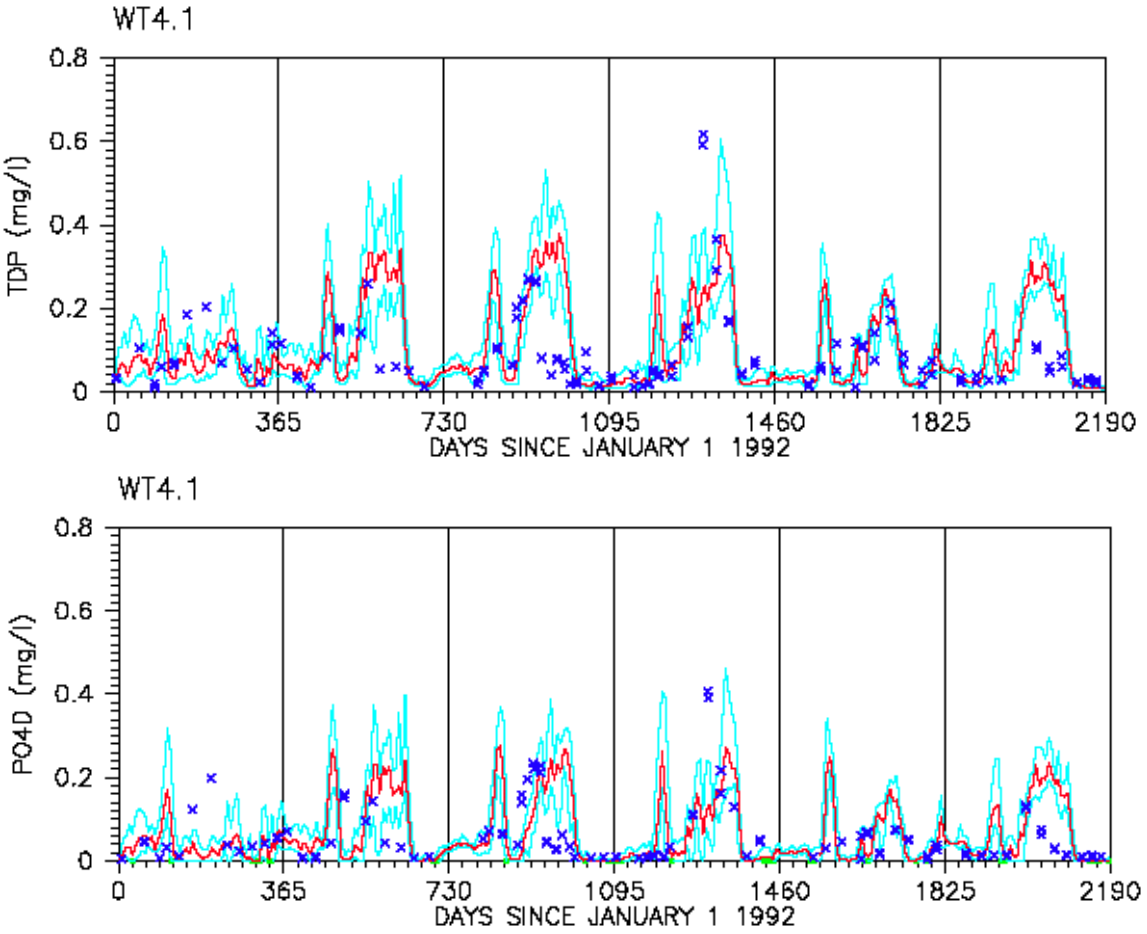

Fig. 79. Time series comparison of model calibration results and data for total dissolved phosphorus and dissolved phosphate in Back River (WT4.1)

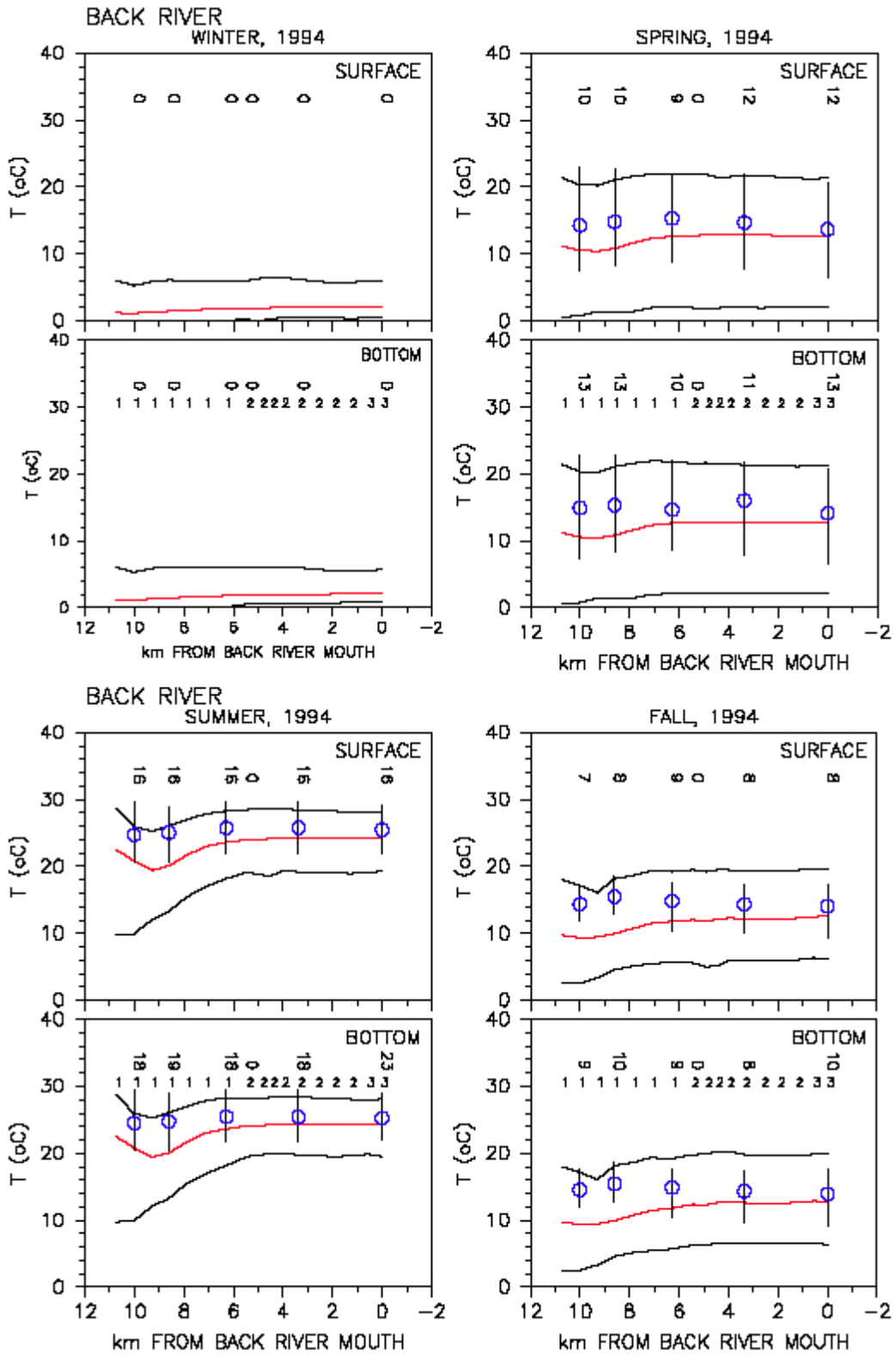

Fig. 80. Longitudinal comparison of model calibration results and data for temperature in Back River transect

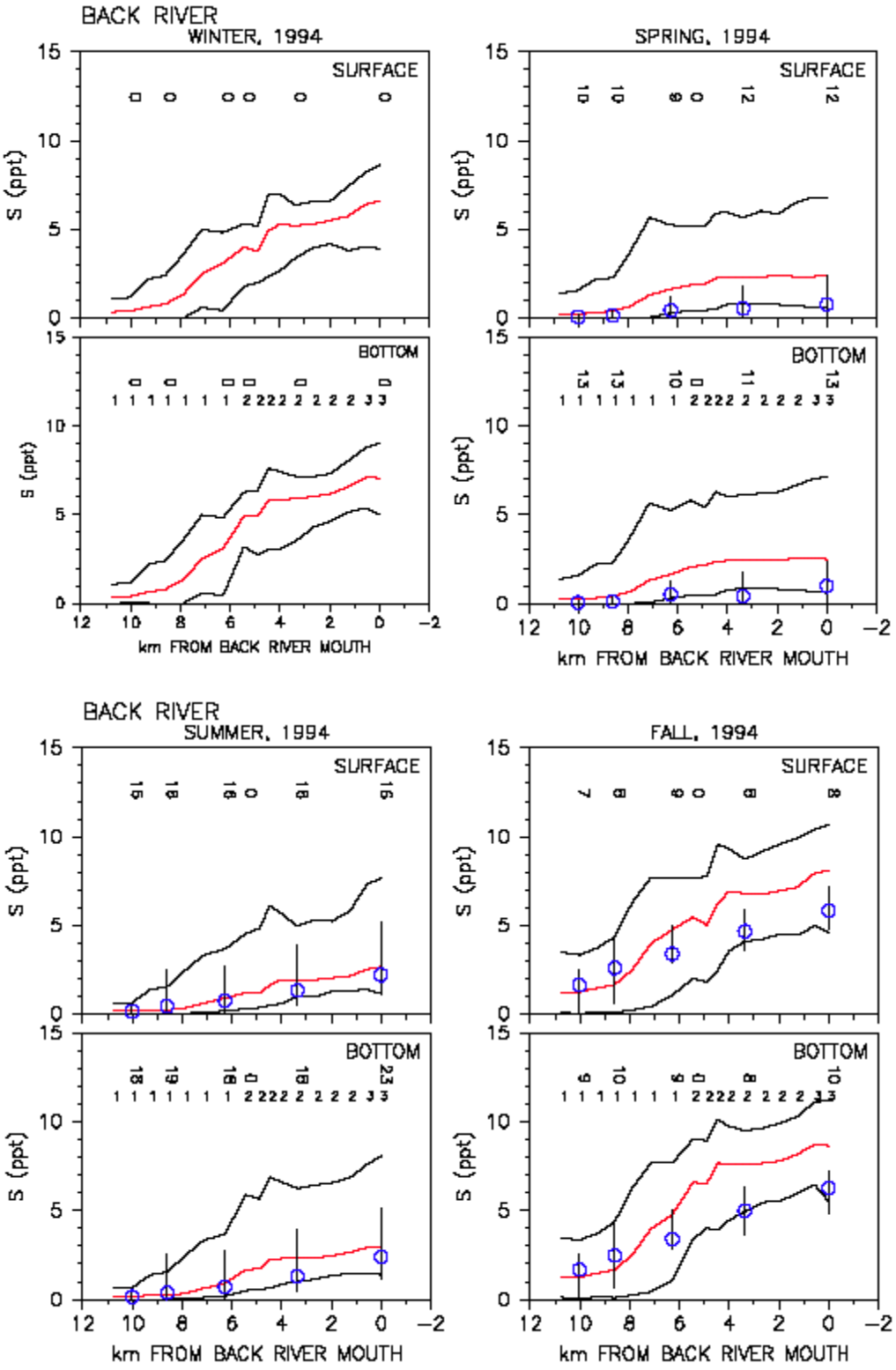

Fig. 81. Longitudinal comparison of model calibration results and data for salinity in Back River transect

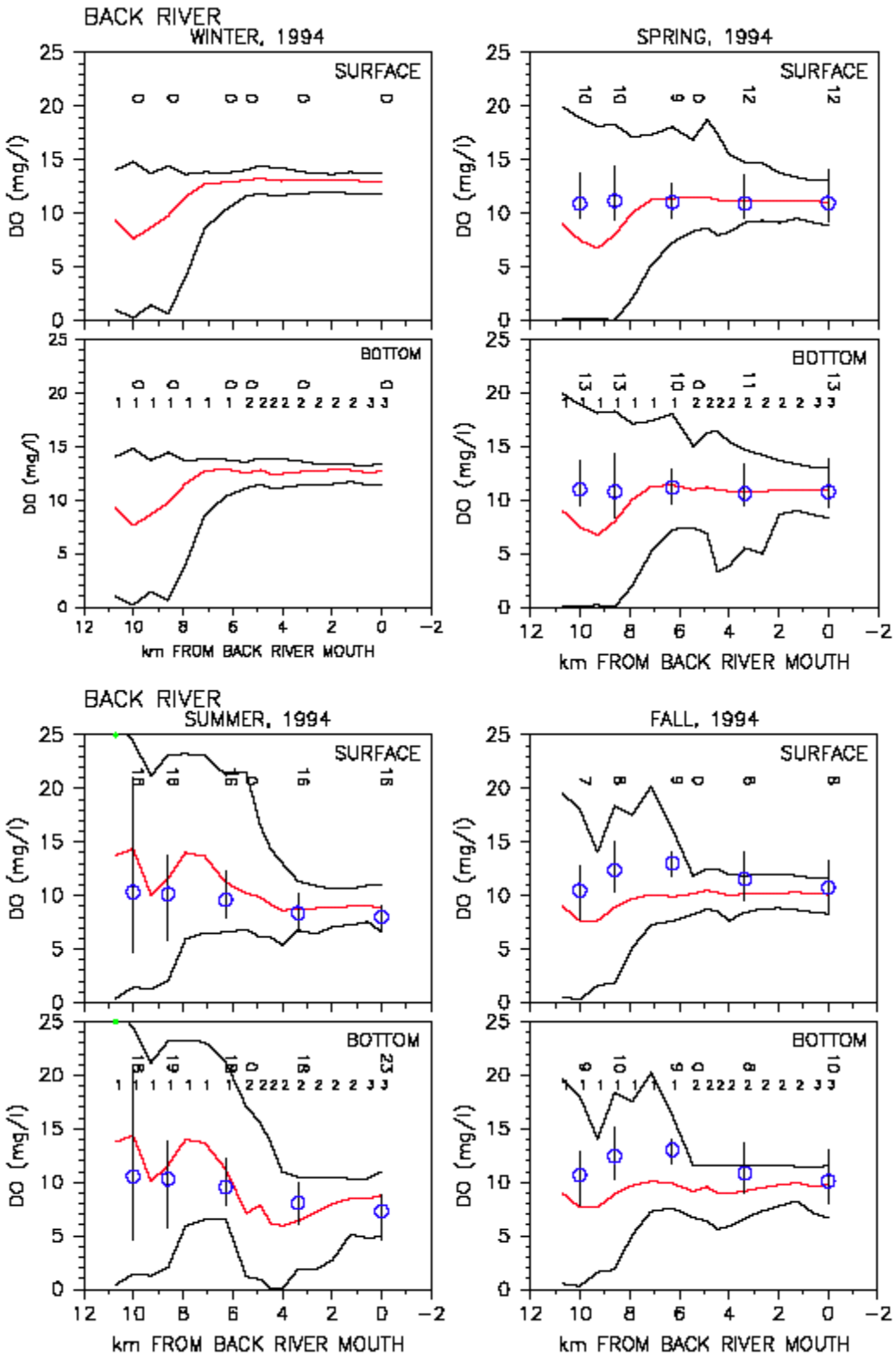

Fig. 82. Longitudinal comparison of model calibration results and data for dissolved oxygen in Back River transect

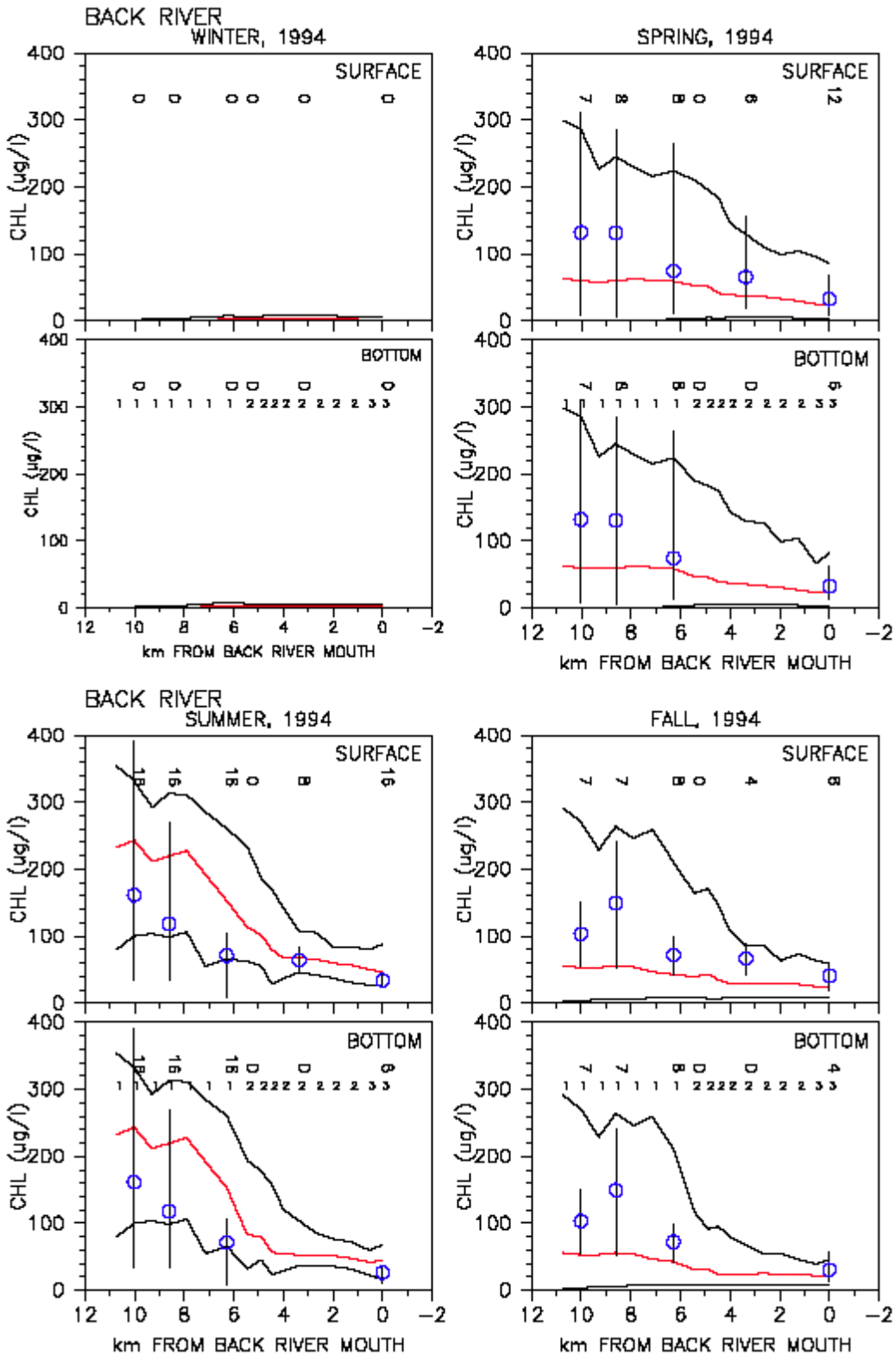

Fig. 83. Longitudinal comparison of model calibration results and data for chlorophyll a in Back River transect

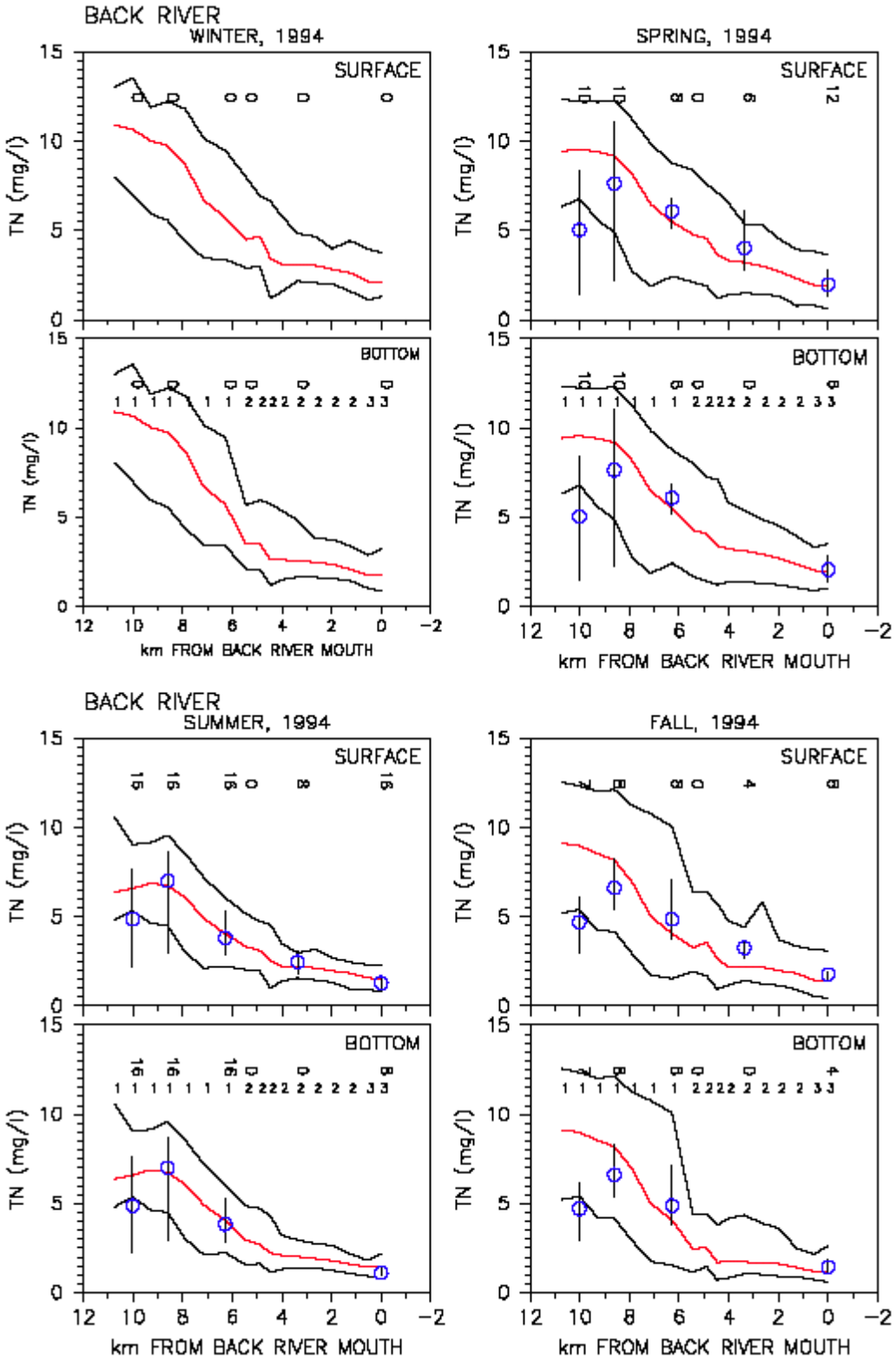

Fig. 84. Longitudinal comparison of model calibration results and data for total nitrogen in Back River transect

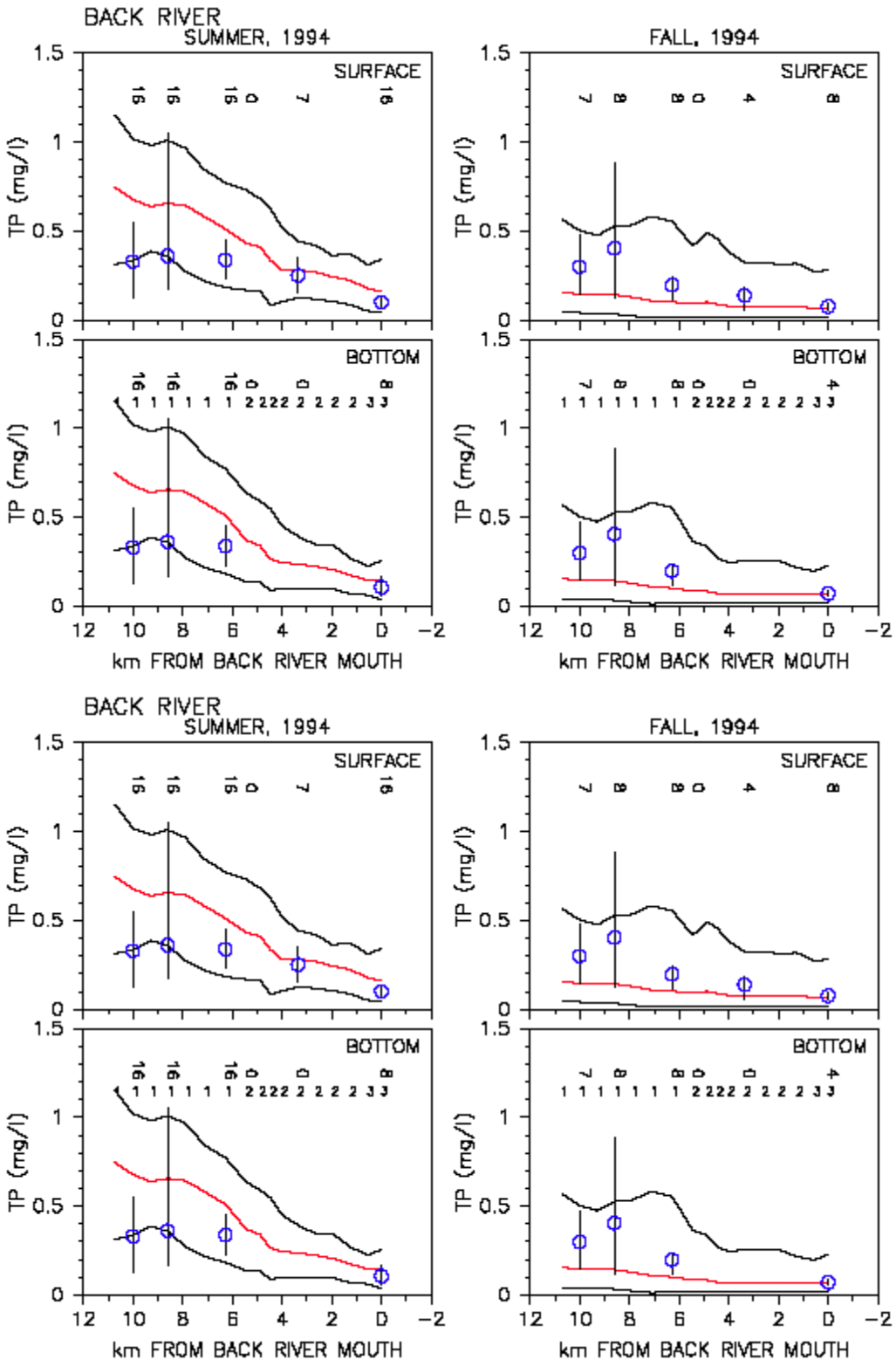

Fig. 85. Longitudinal comparison of model calibration results and data for total phosphorus in Back River transect

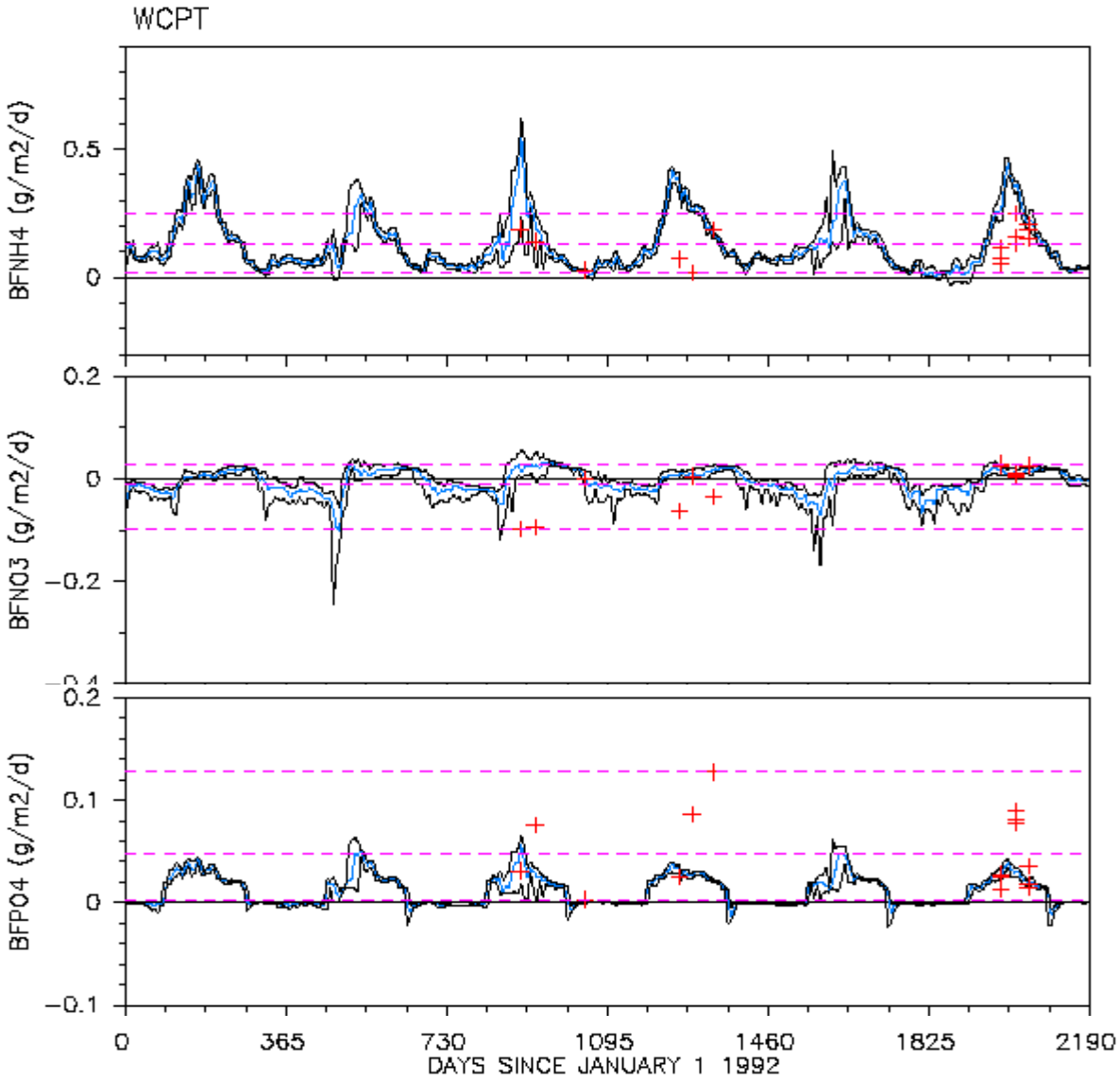

Fig. 86. Time series comparison of model simulated sediment fluxes and data in Back River (WCPT)

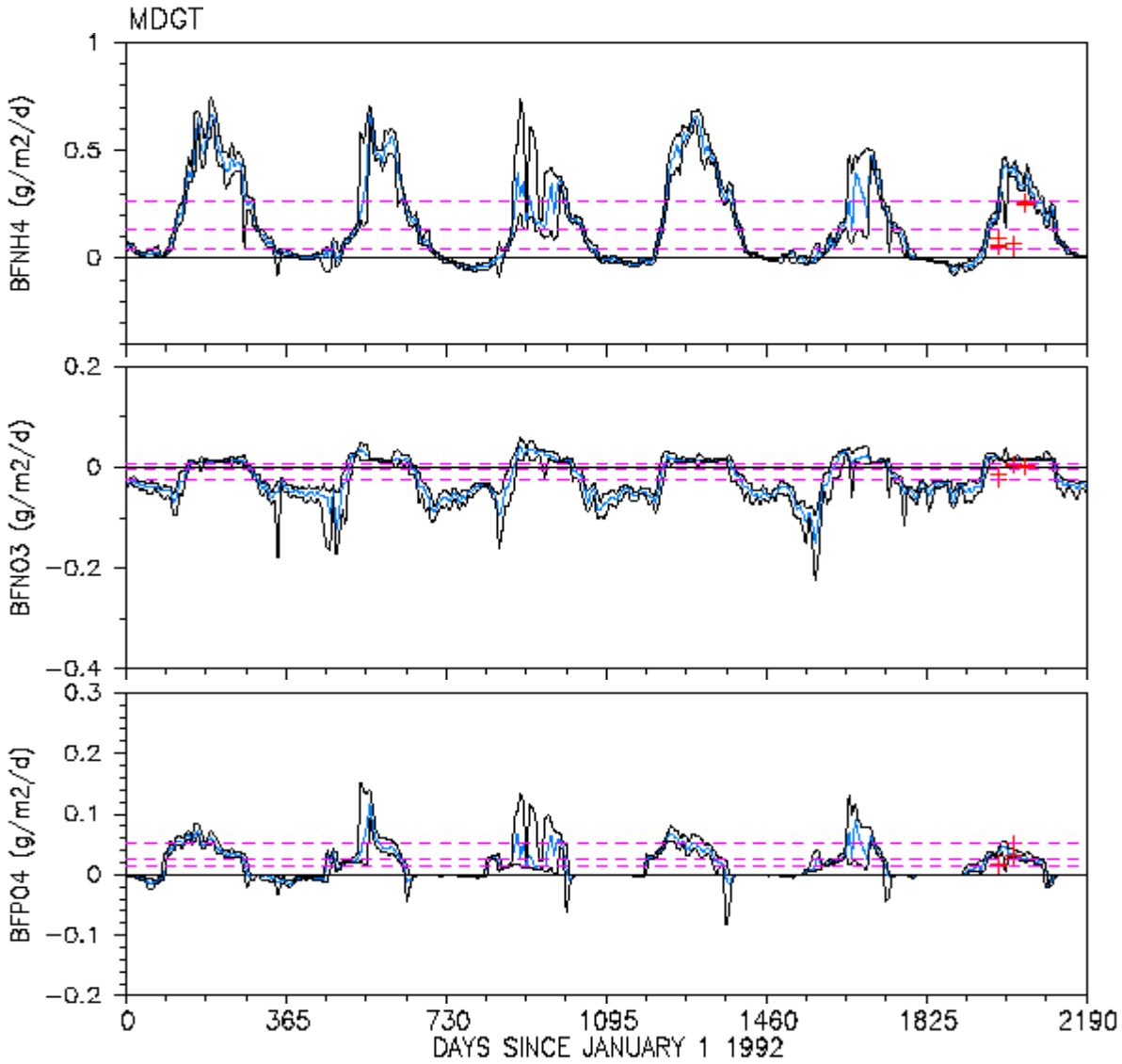

Fig. 87. Time series comparison of model simulated sediment fluxes and data in Back River (MDGT)

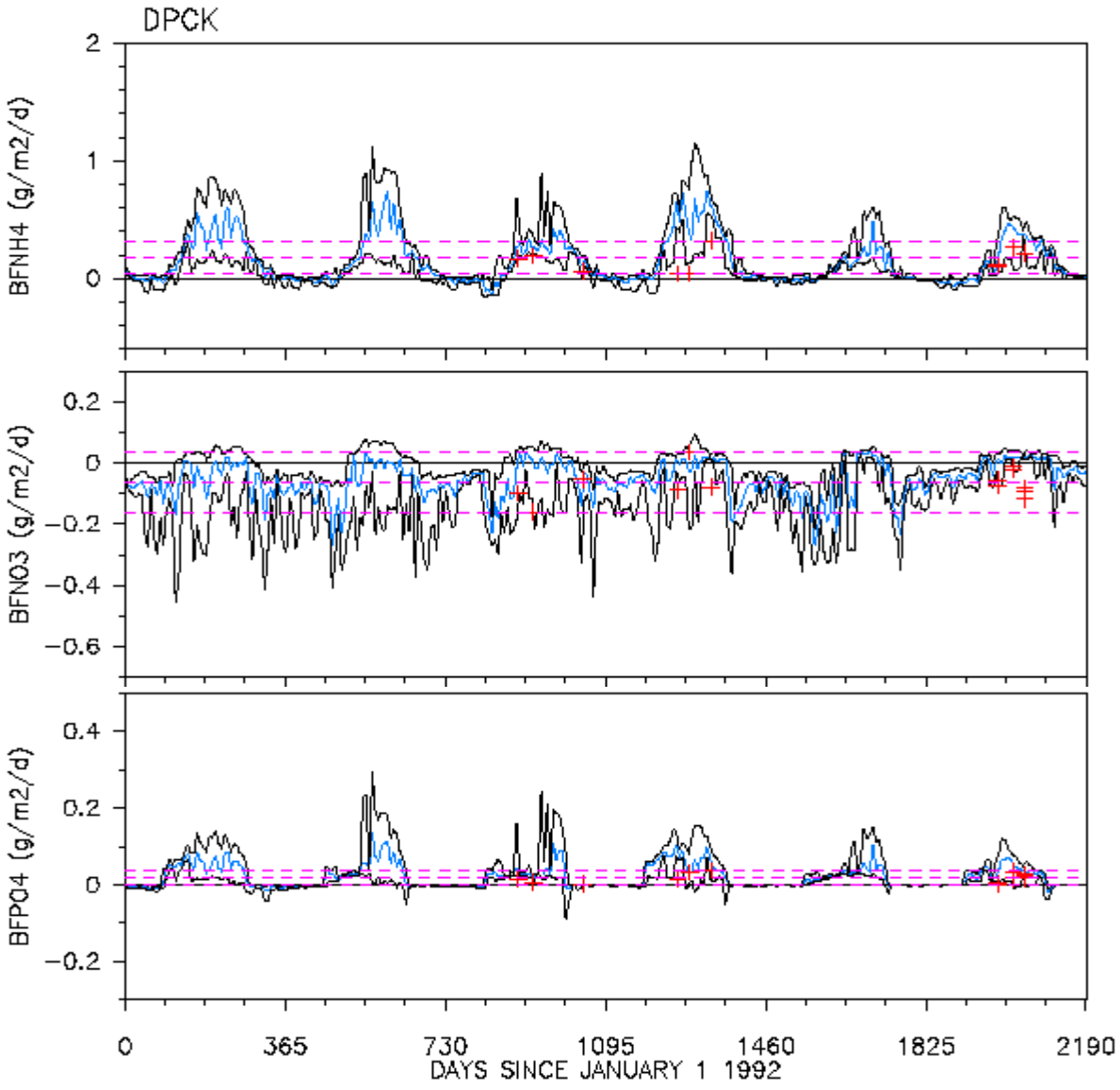

Fig. 88. Time series comparison of model simulated sediment fluxes and data in Back River (DPCK)

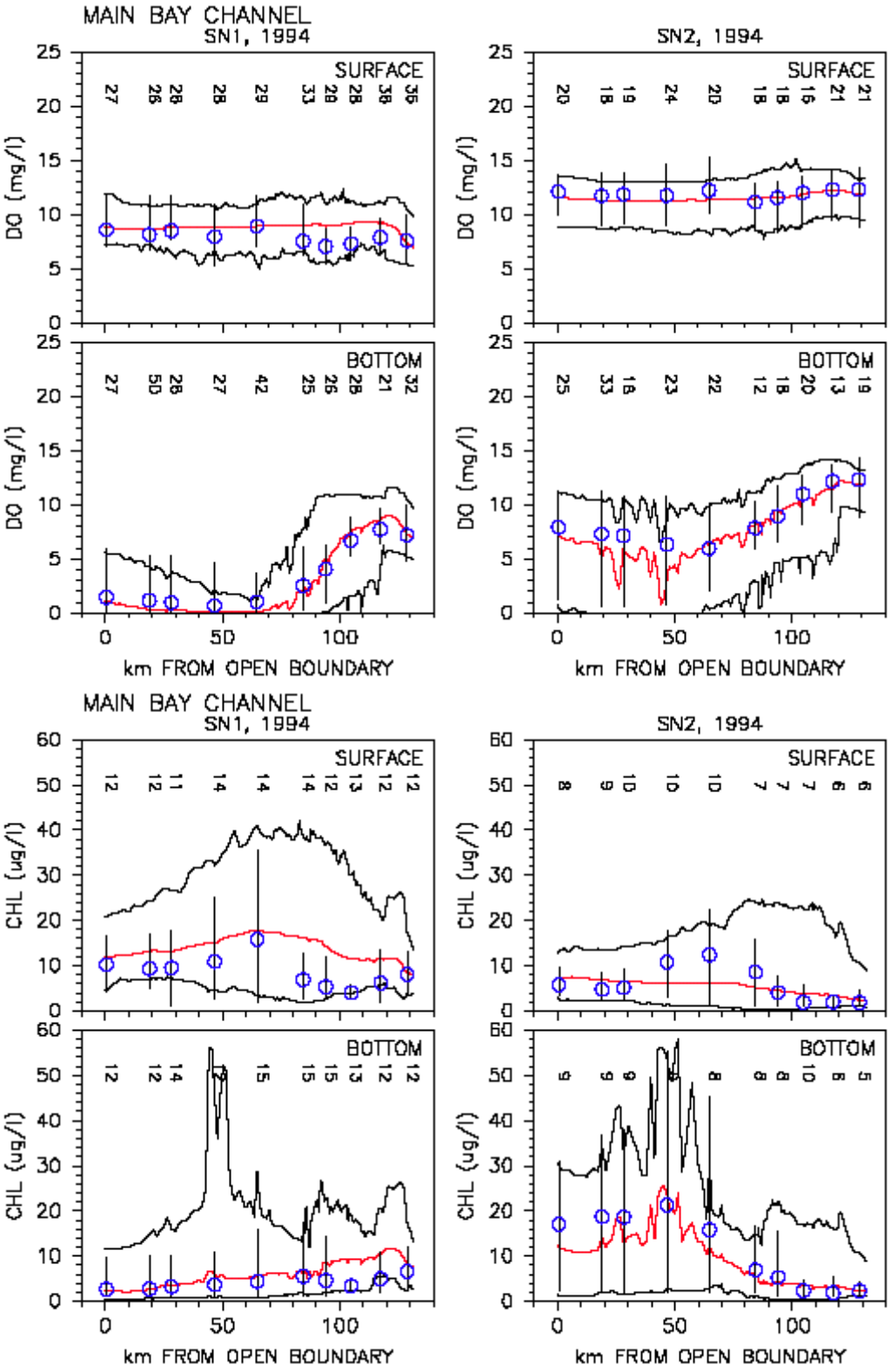

Fig. 89. Longitudinal comparison of model calibration results and data for dissolved oxygen and chlorophyll a in the Upper Chesapeake Bay transect

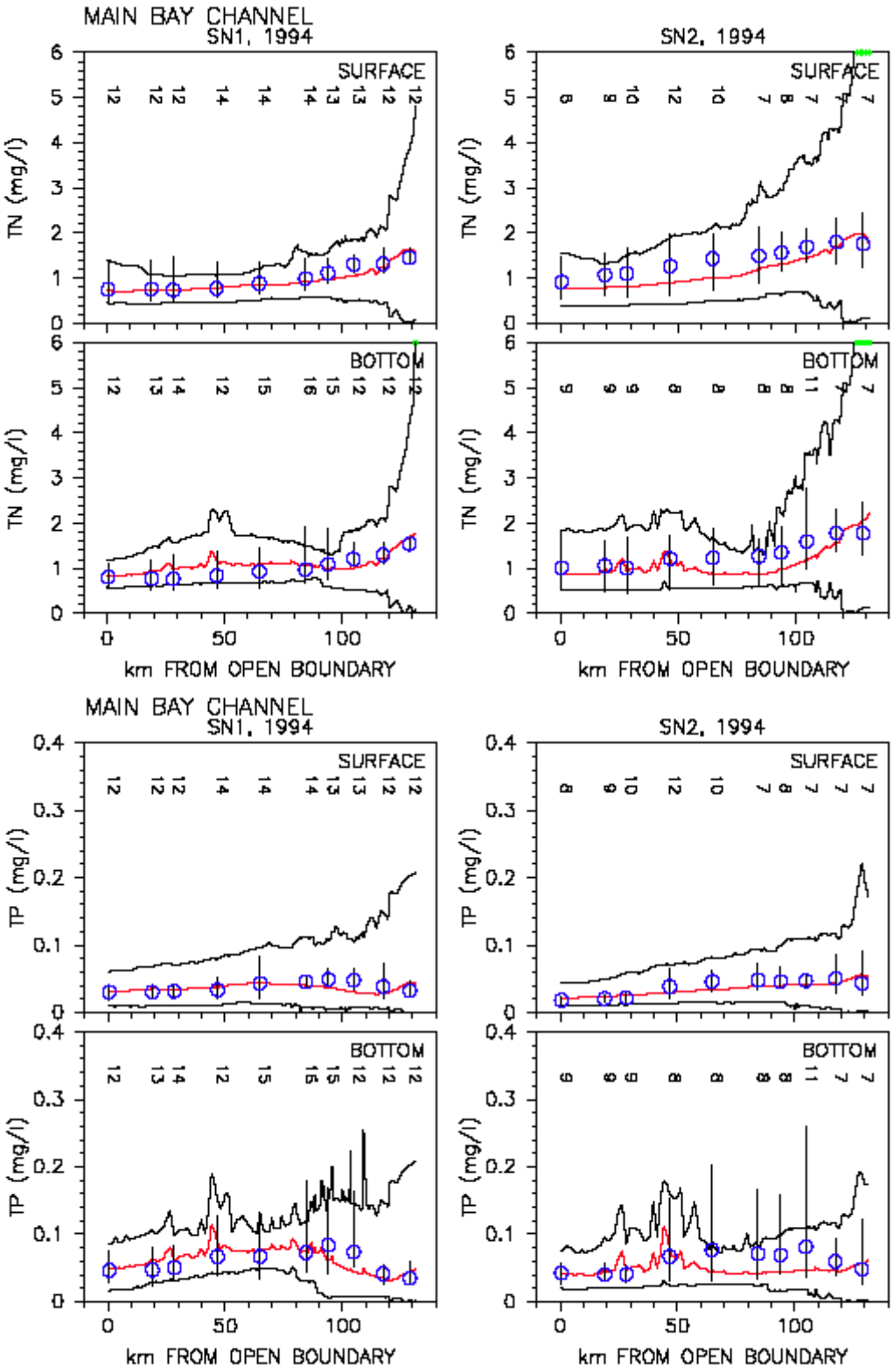

Fig. 90. Longitudinal comparison of model calibration results and data for total nitrogen and total phosphorus in the Upper Chesapeake Bay transect

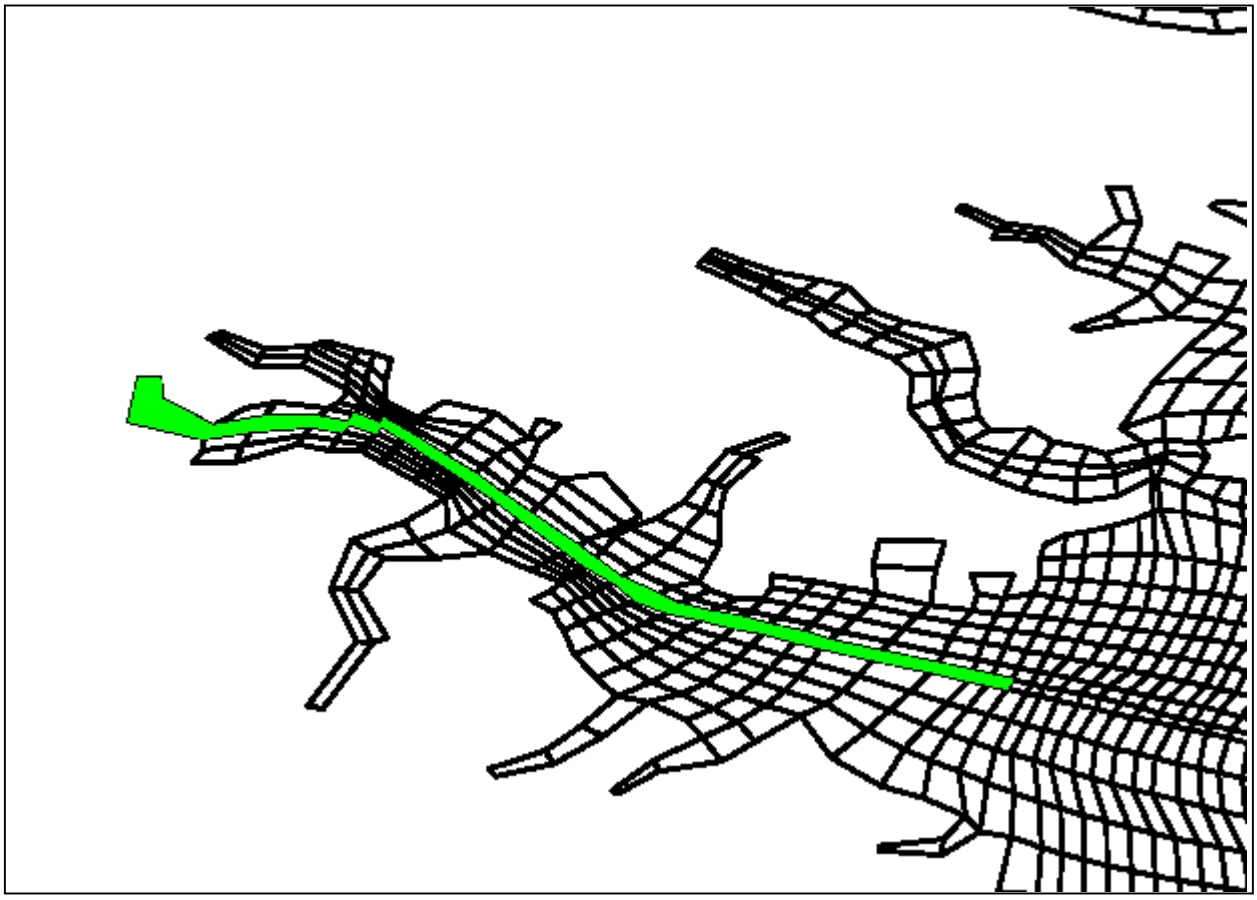

Fig. 91. Plan view of the model grid showing the transect of Baltimore Harbor into Middle Branch

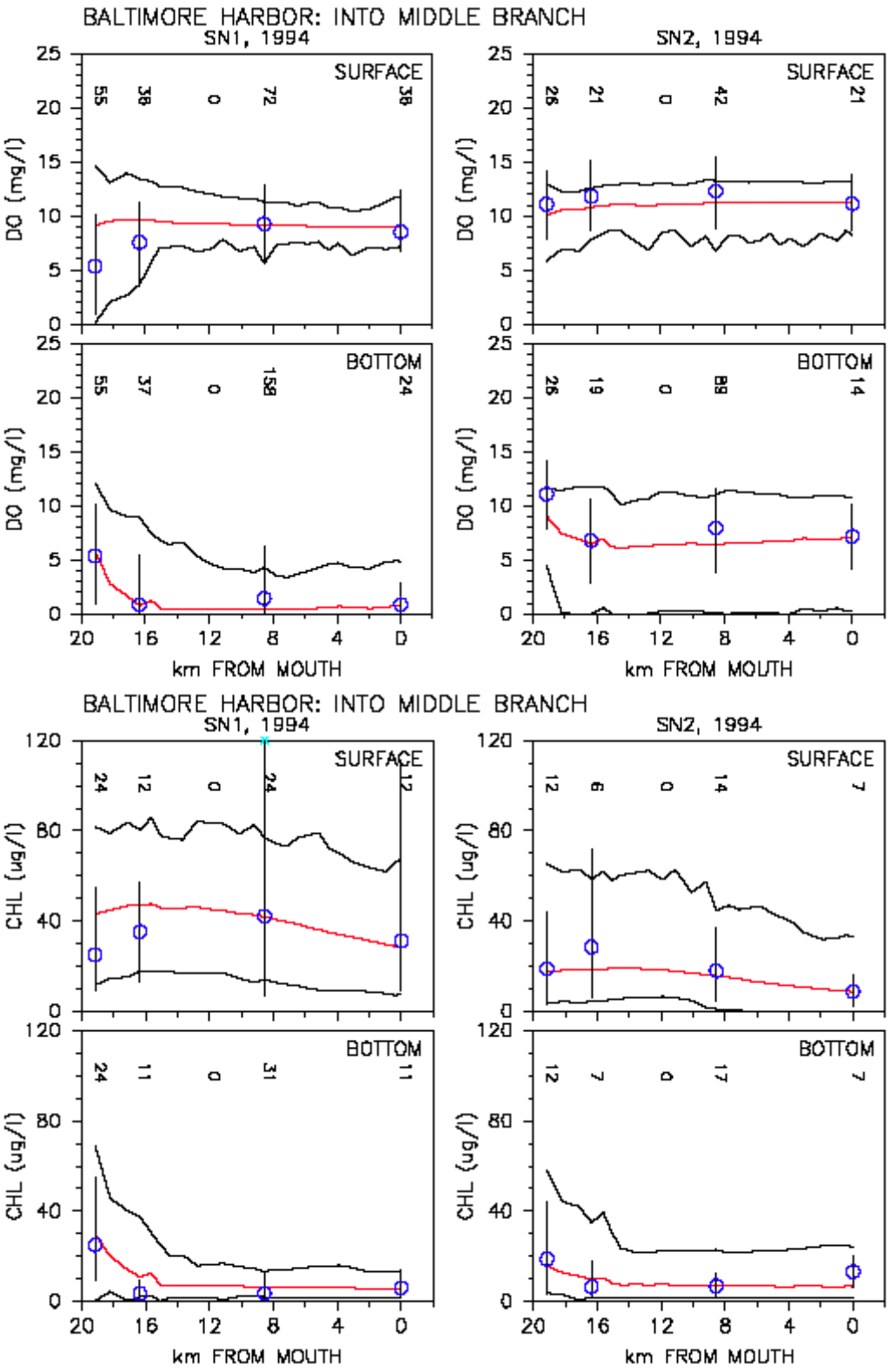

Fig. 92. Longitudinal comparison of model calibration results and data for dissolved oxygen and chlorophyll a in Baltimore Harbor into Middle Branch

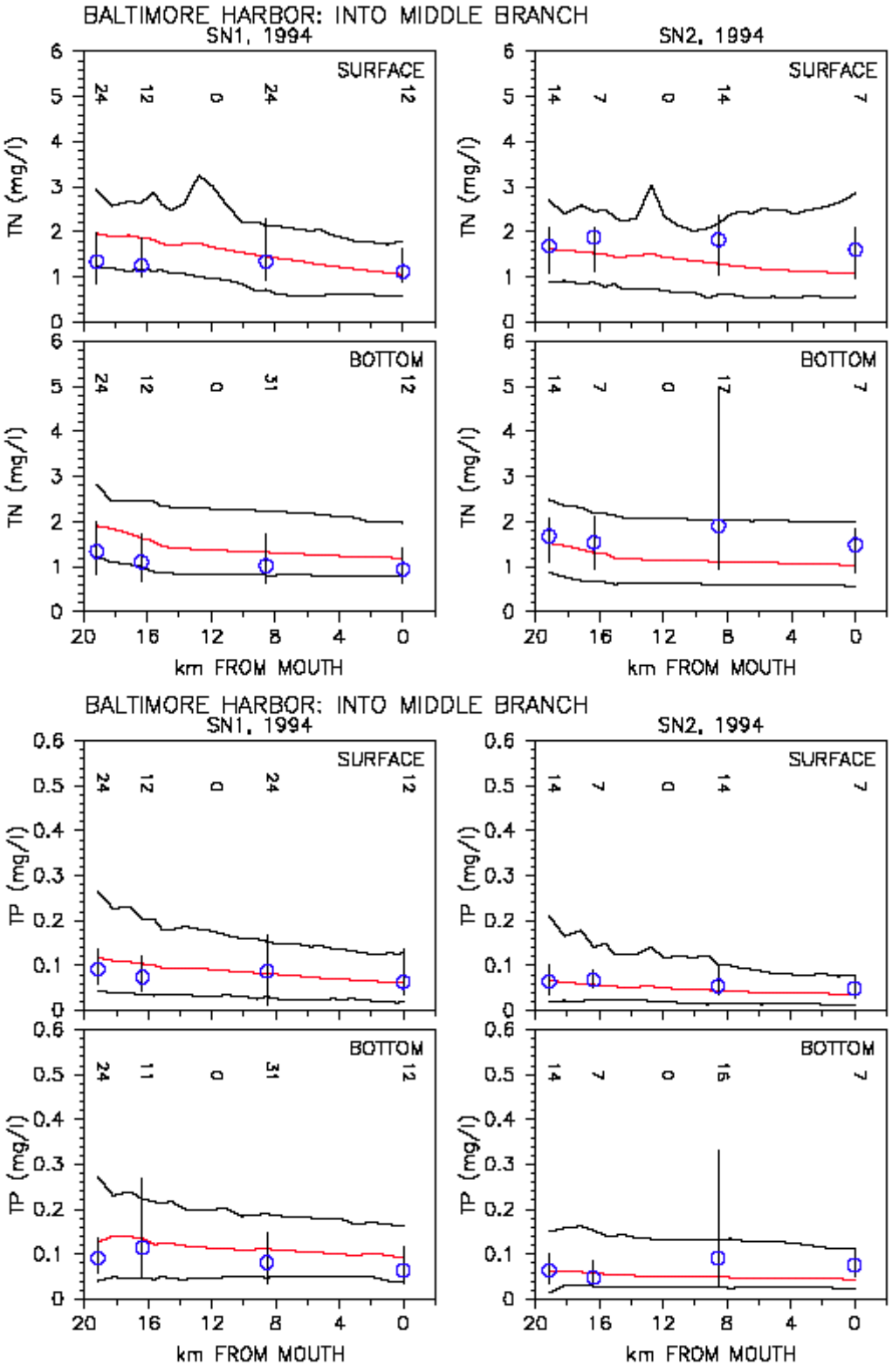

Fig. 93. Longitudinal comparison of model calibration results and data for total nitrogen and total phosphorus in Baltimore Harbor into Middle Branch

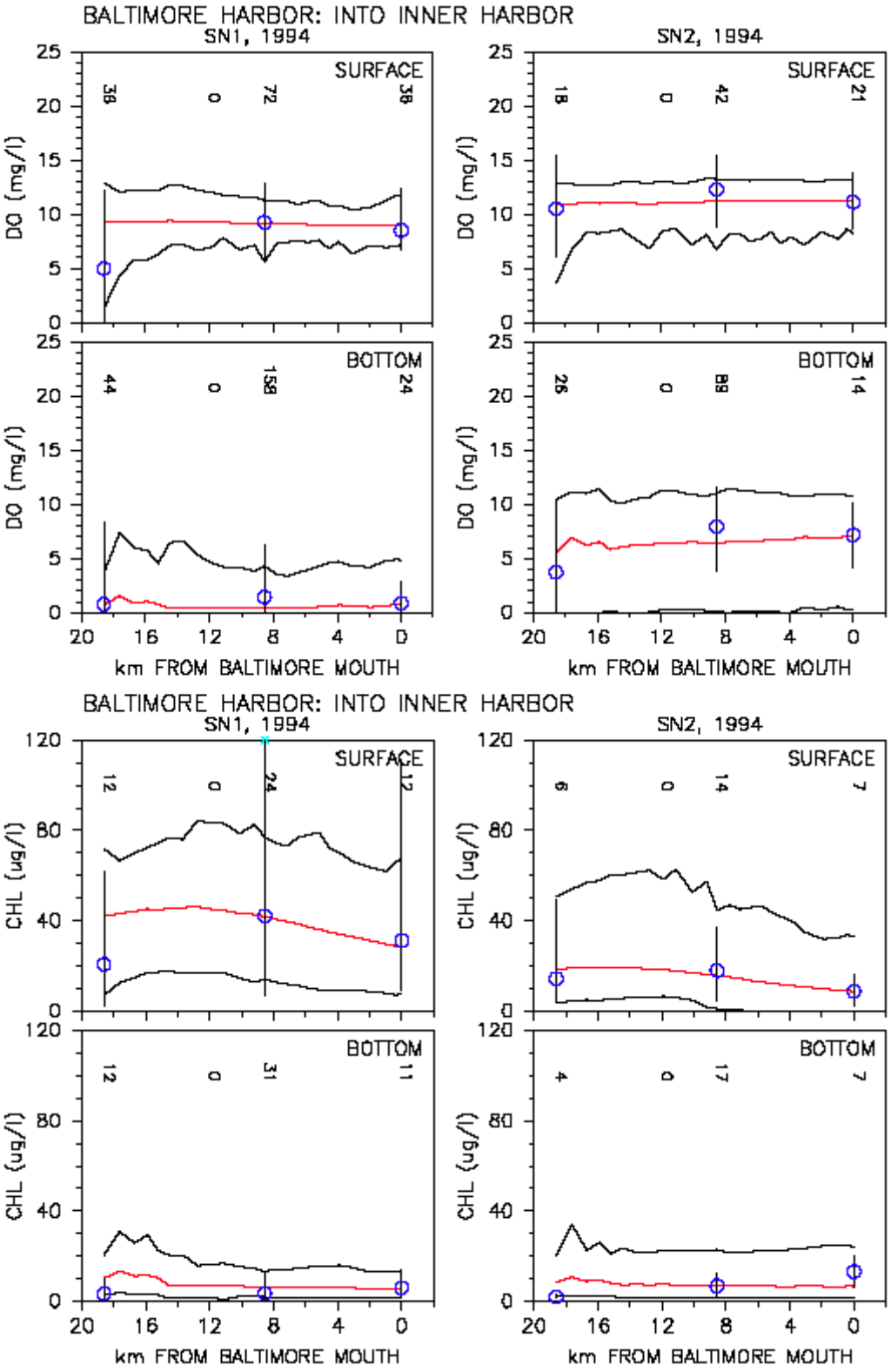

Fig. 94. Longitudinal comparison of model calibration results and data for dissolved oxygen and chlorophyll a in Baltimore Harbor into Inner Harbor

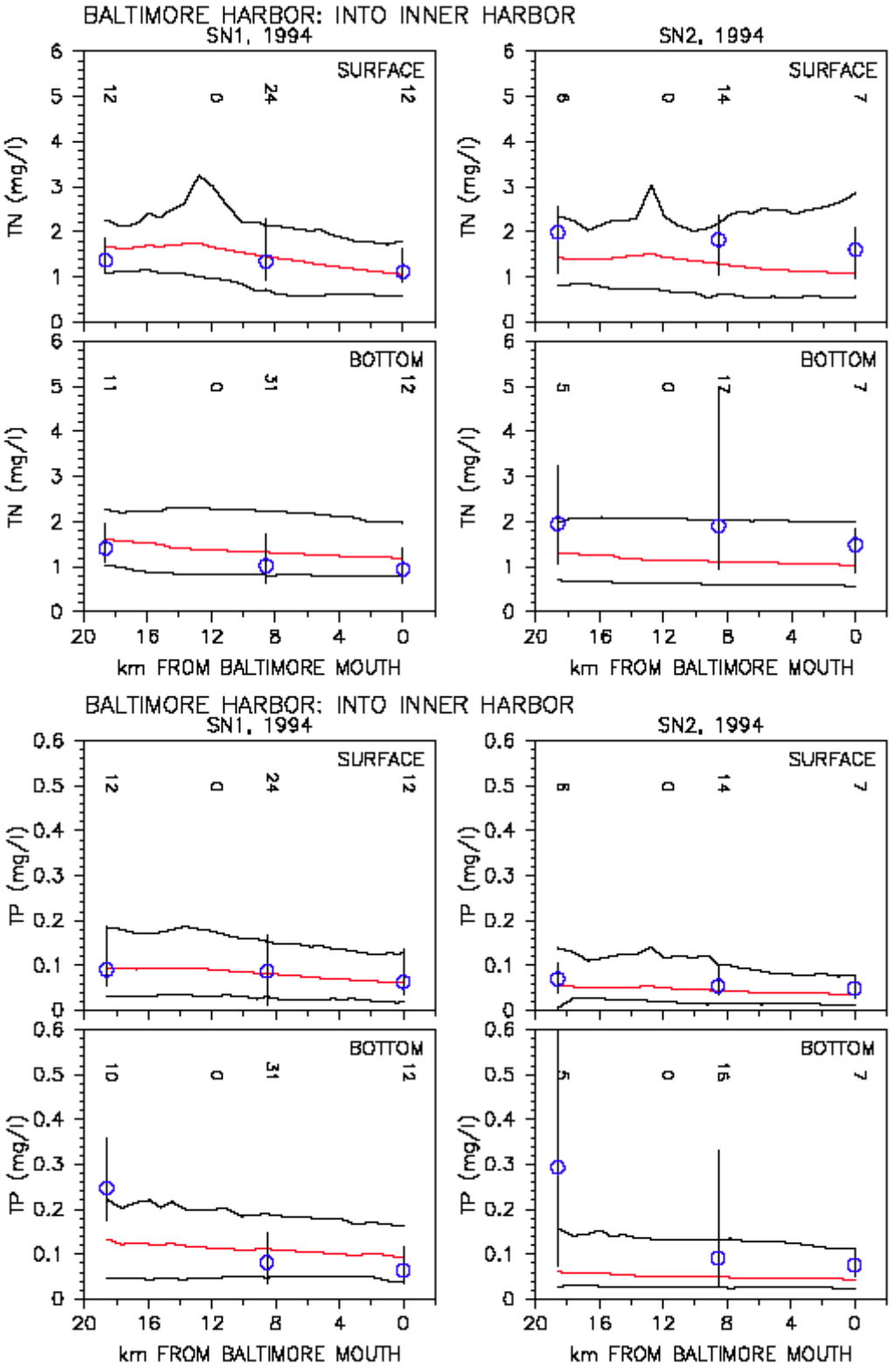

Fig. 95. Longitudinal comparison of model calibration results and data for total nitrogen and total phosphorus in Baltimore Harbor into Inner Harbor

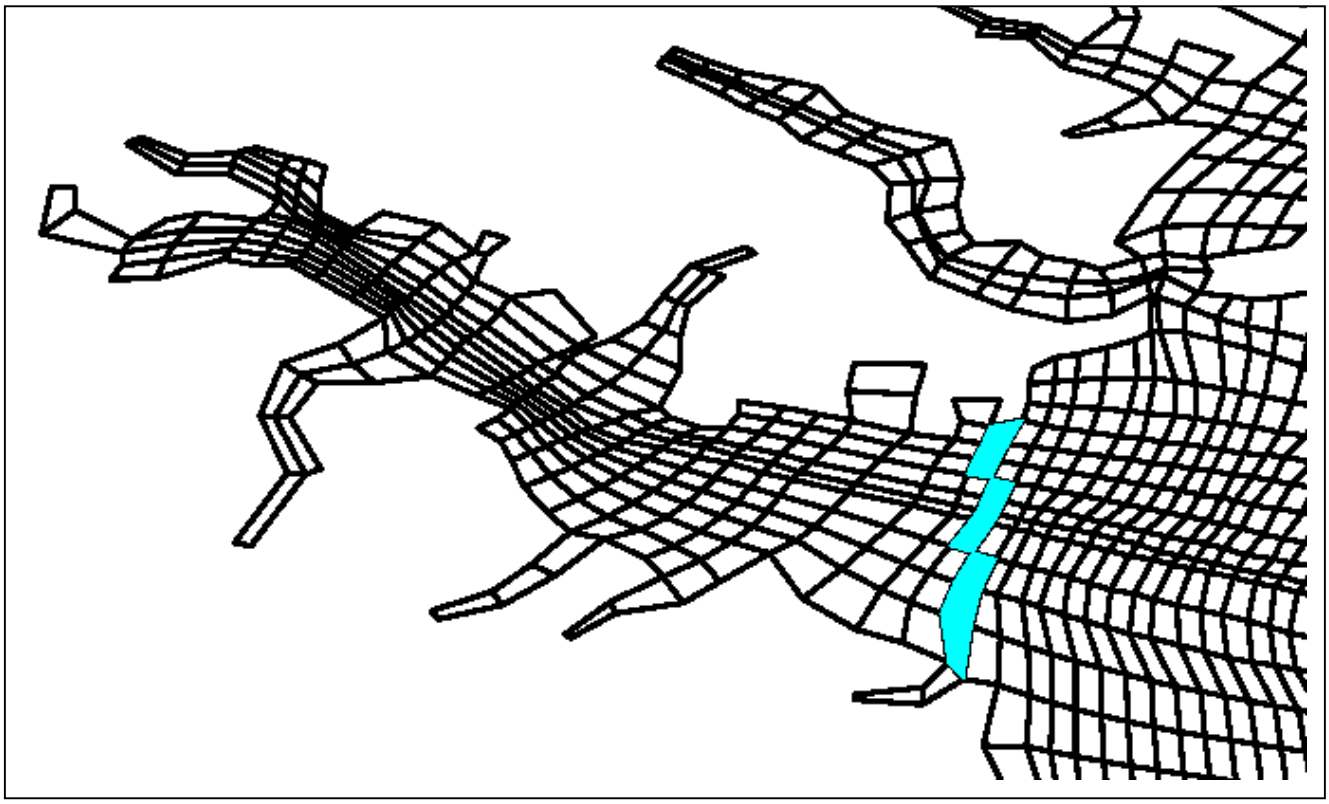

Fig. 96. Plan view of the model grid showing the transect of Baltimore Harbor Mouth

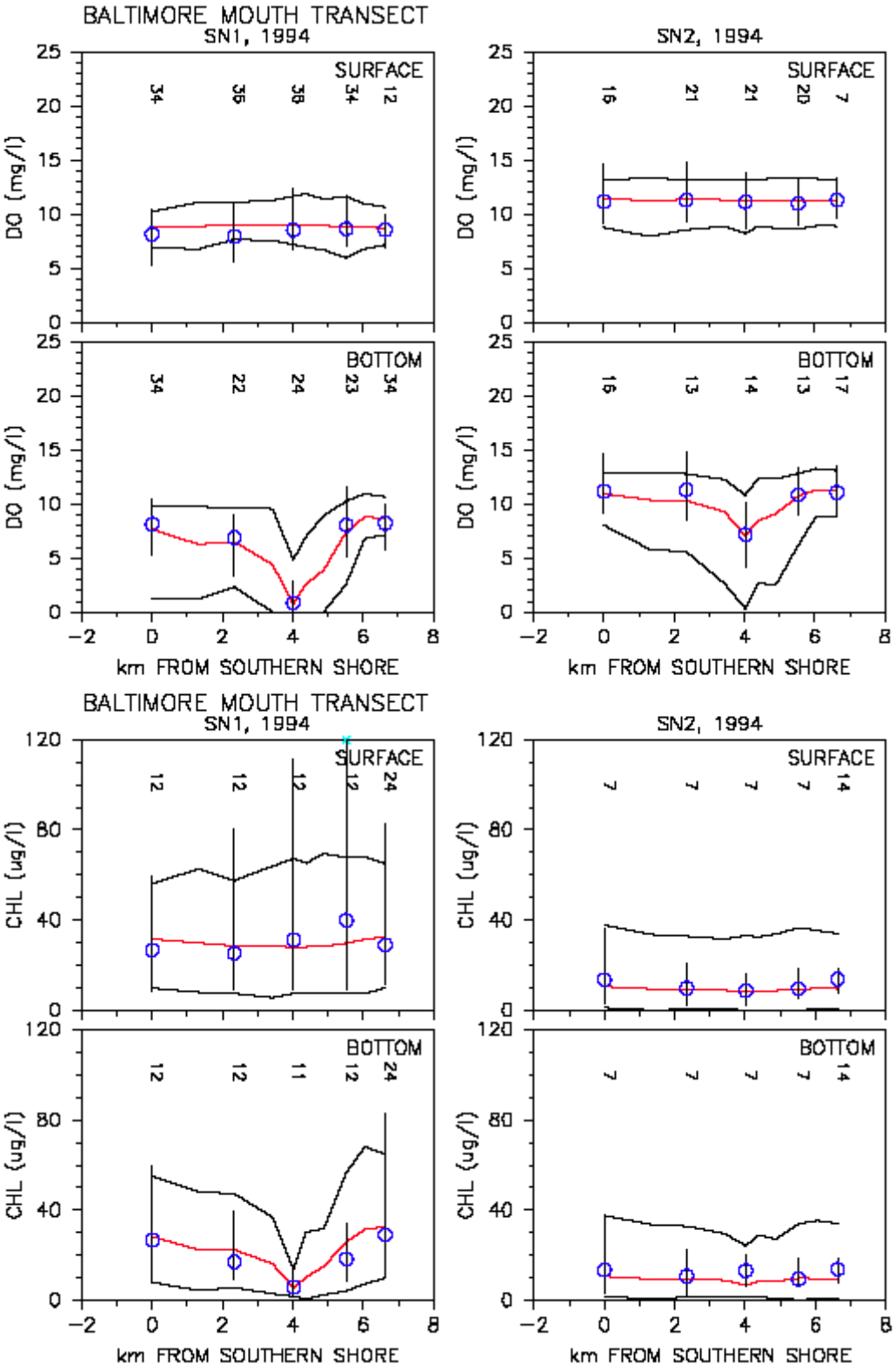

Fig. 97. Longitudinal comparison of model calibration results and data for dissolved oxygen and chlorophyll a in Baltimore Harbor mouth

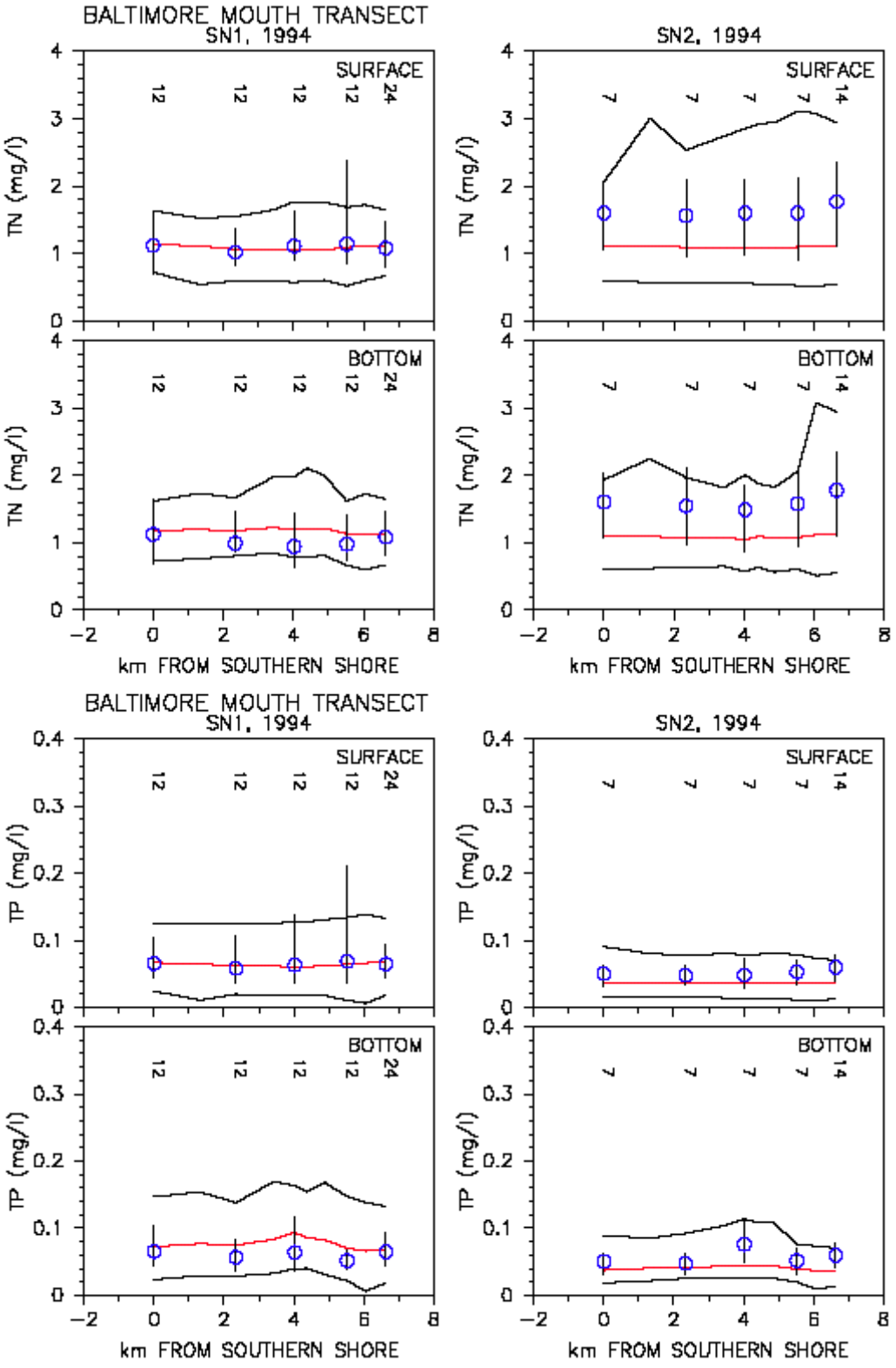

Fig. 98. Longitudinal comparison of model calibration results and data for total nitrogen and total phosphorus in Baltimore Harbor mouth

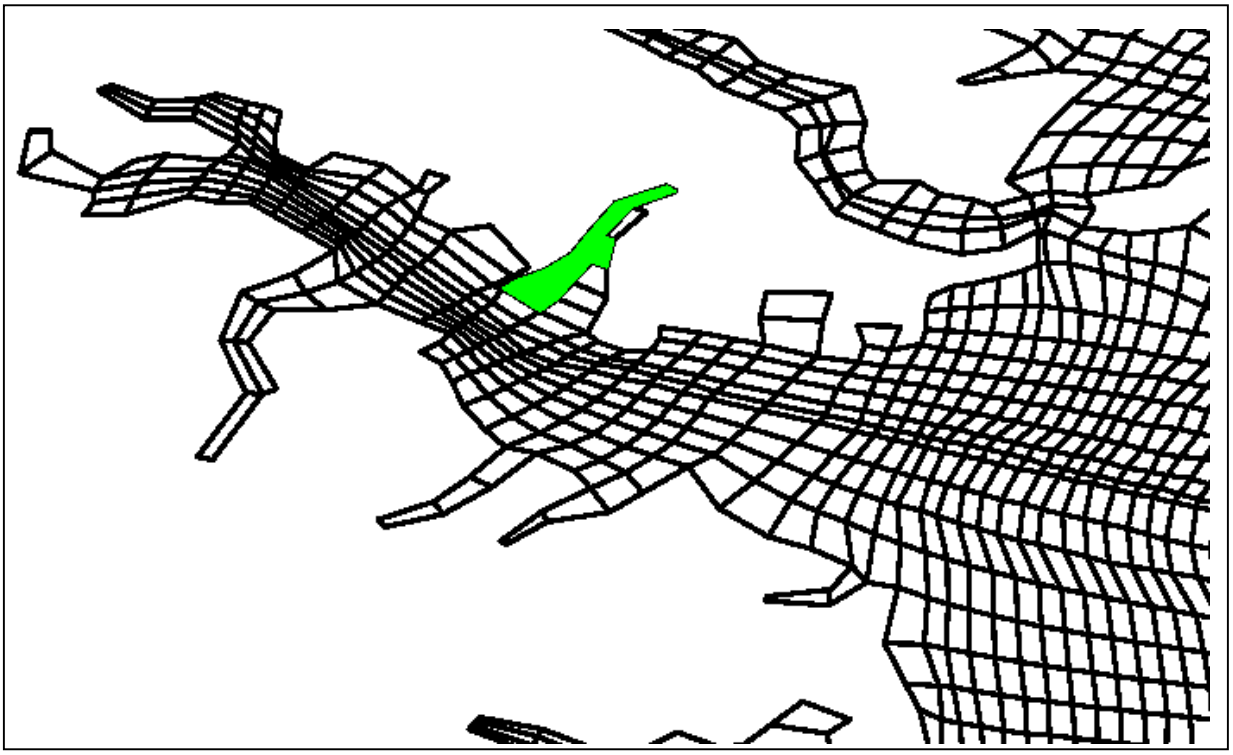

Fig. 99. Plan view of the model grid showing the transect of Bear Creek

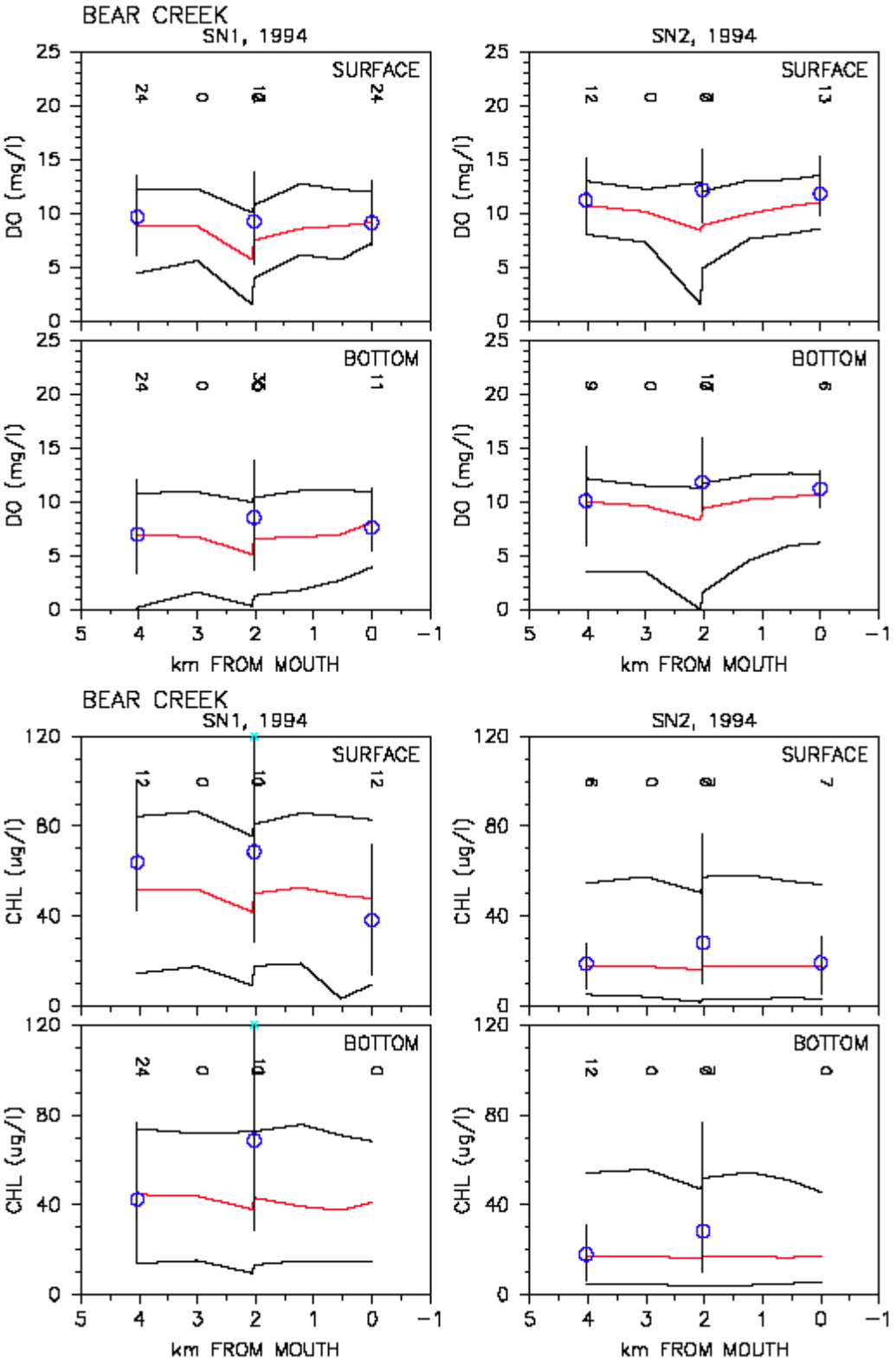

Fig. 100. Longitudinal comparison of model calibration results and data for dissolved oxygen and chlorophyll a in Bear Creek

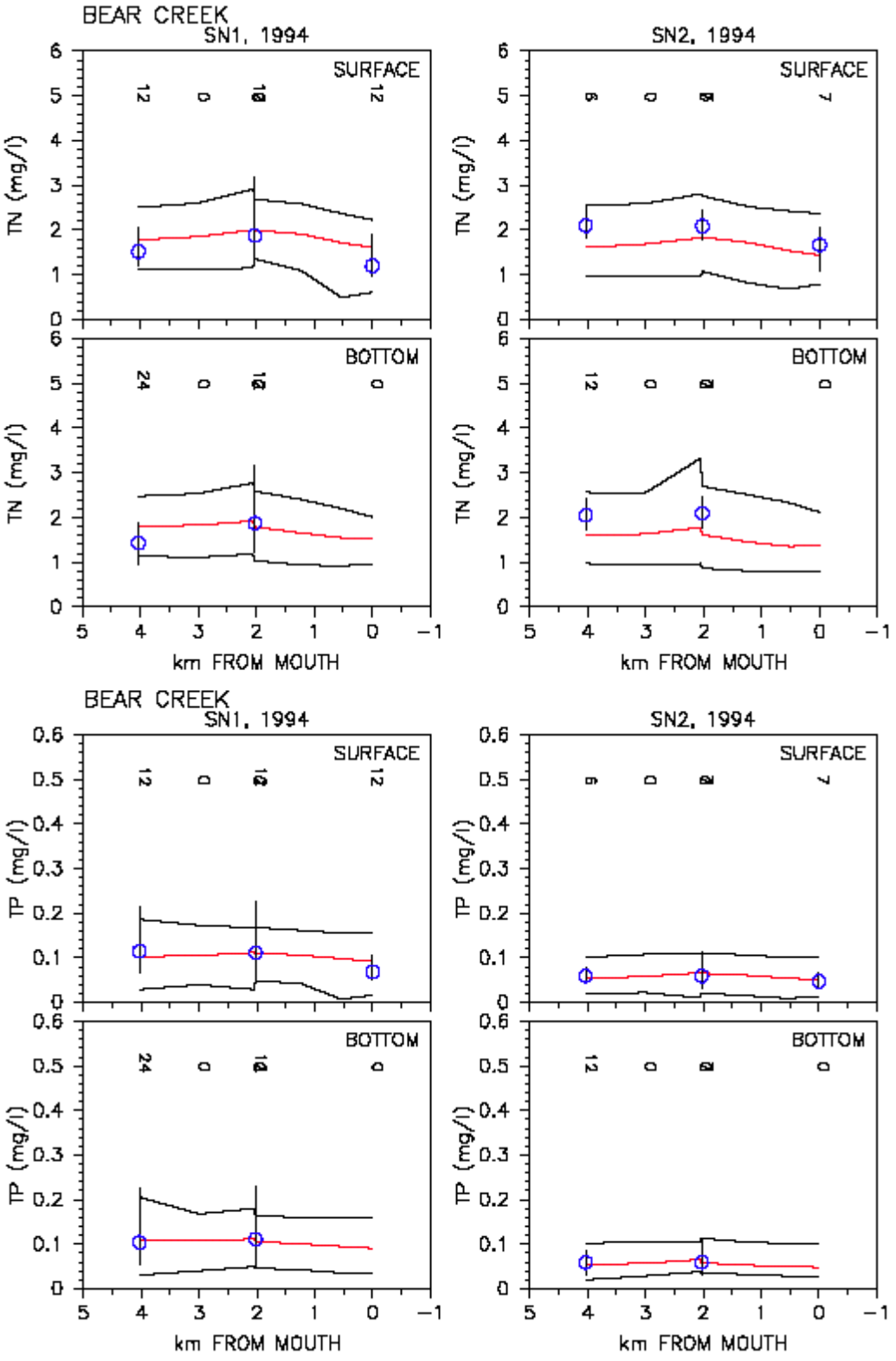

Fig. 101. Longitudinal comparison of model calibration results and data for total nitrogen and total phosphorus in Bear Creek

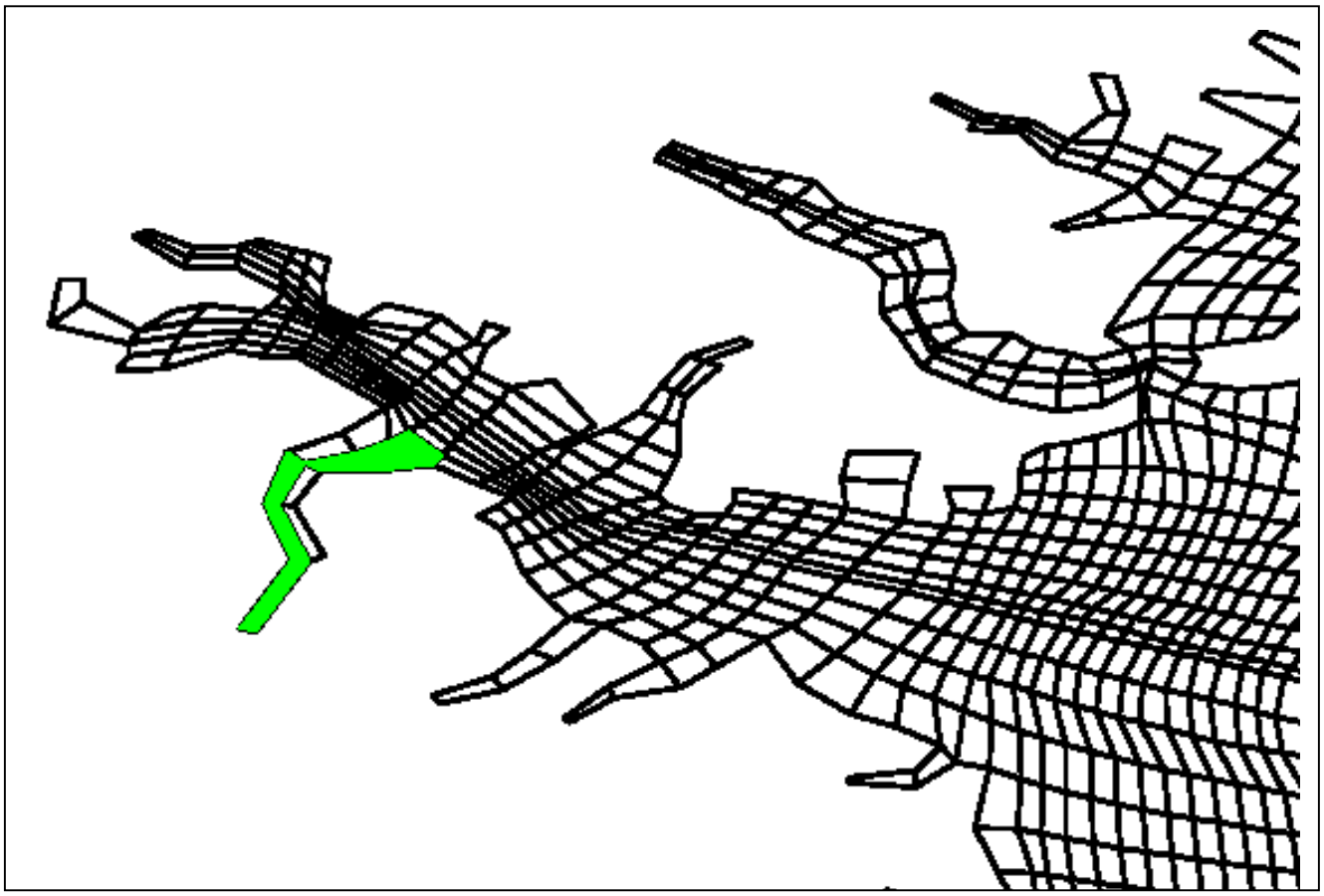

Fig. 102. Plan view of the model grid showing the transect of Curtis Creek

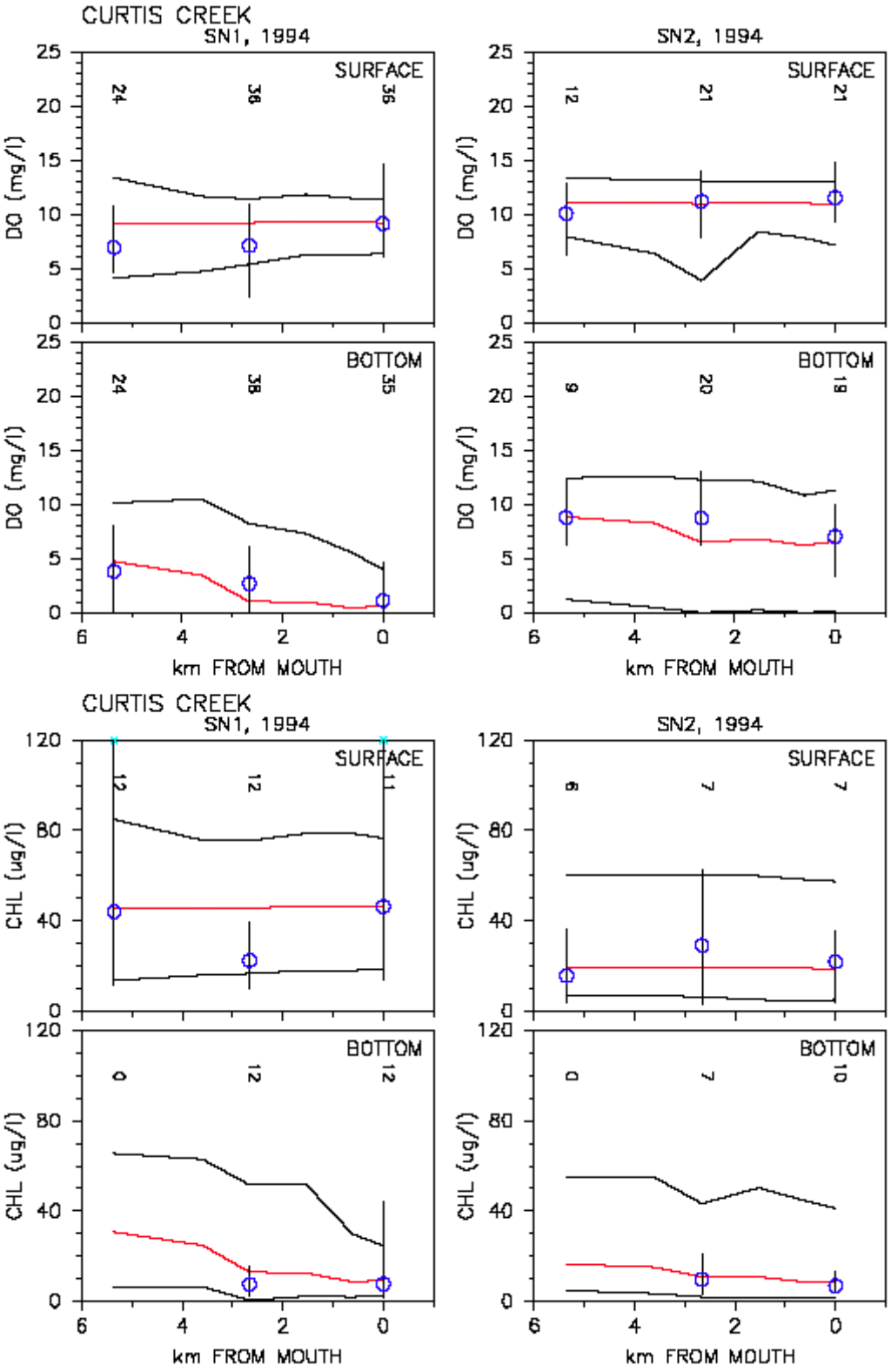

Fig. 103. Longitudinal comparison of model calibration results and data for dissolved oxygen and chlorophyll a in Curtis Creek

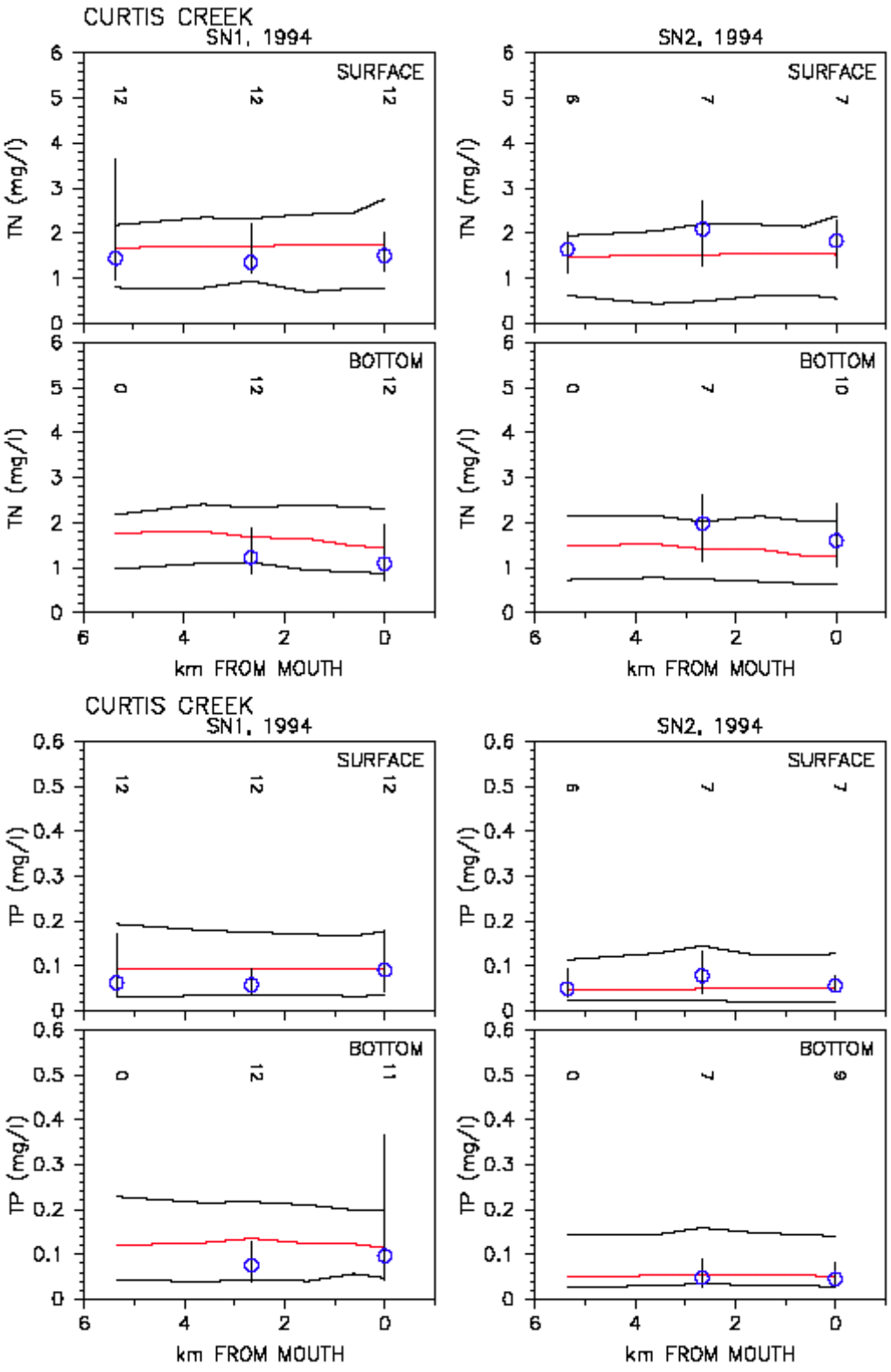

Fig. 104. Longitudinal comparison of model calibration results and data for total nitrogen and total phosphorus in Curtis Creek

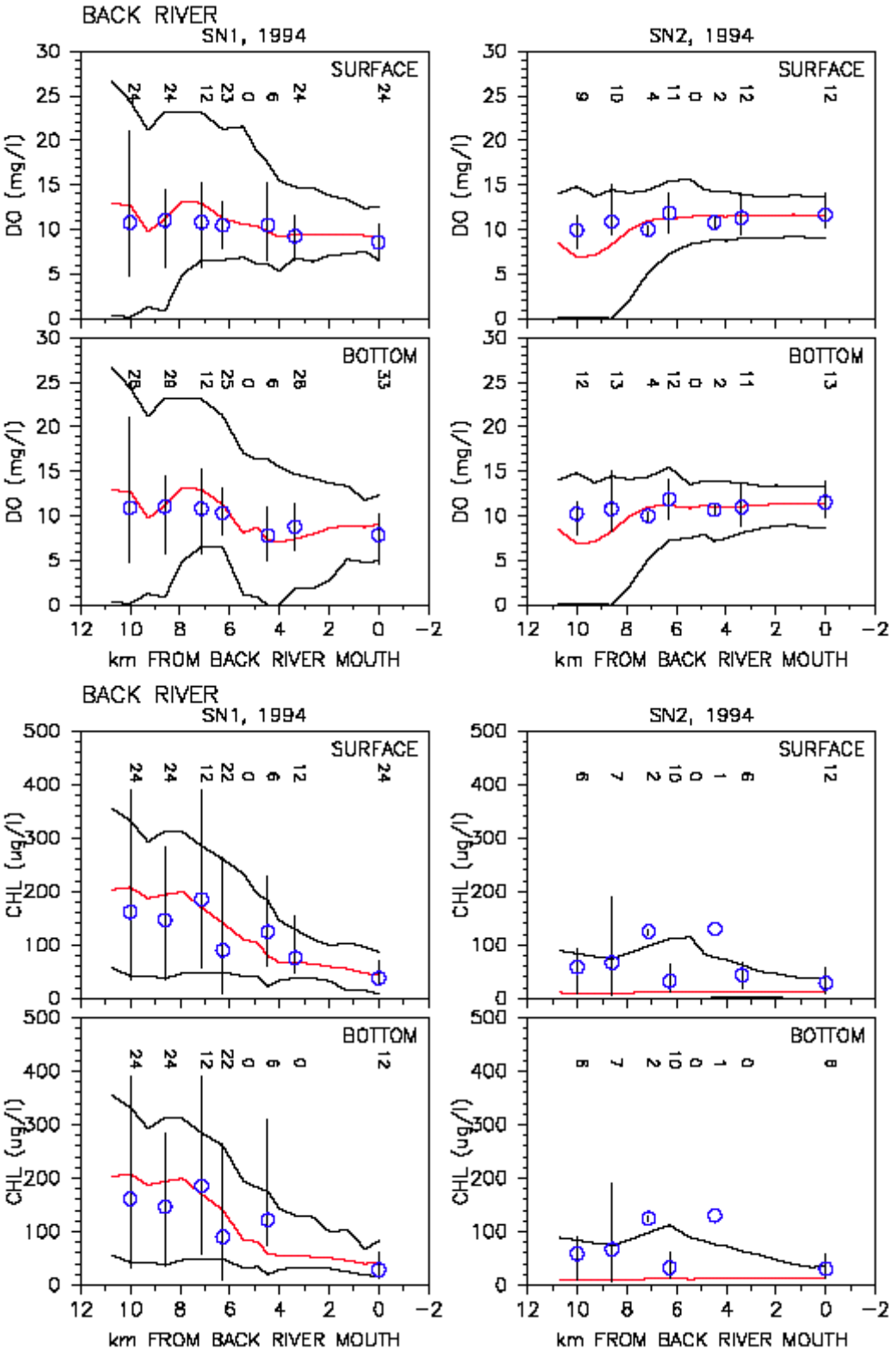

Fig. 105. Longitudinal comparison of model calibration results and data for dissolved oxygen and chlorophyll a in Back River

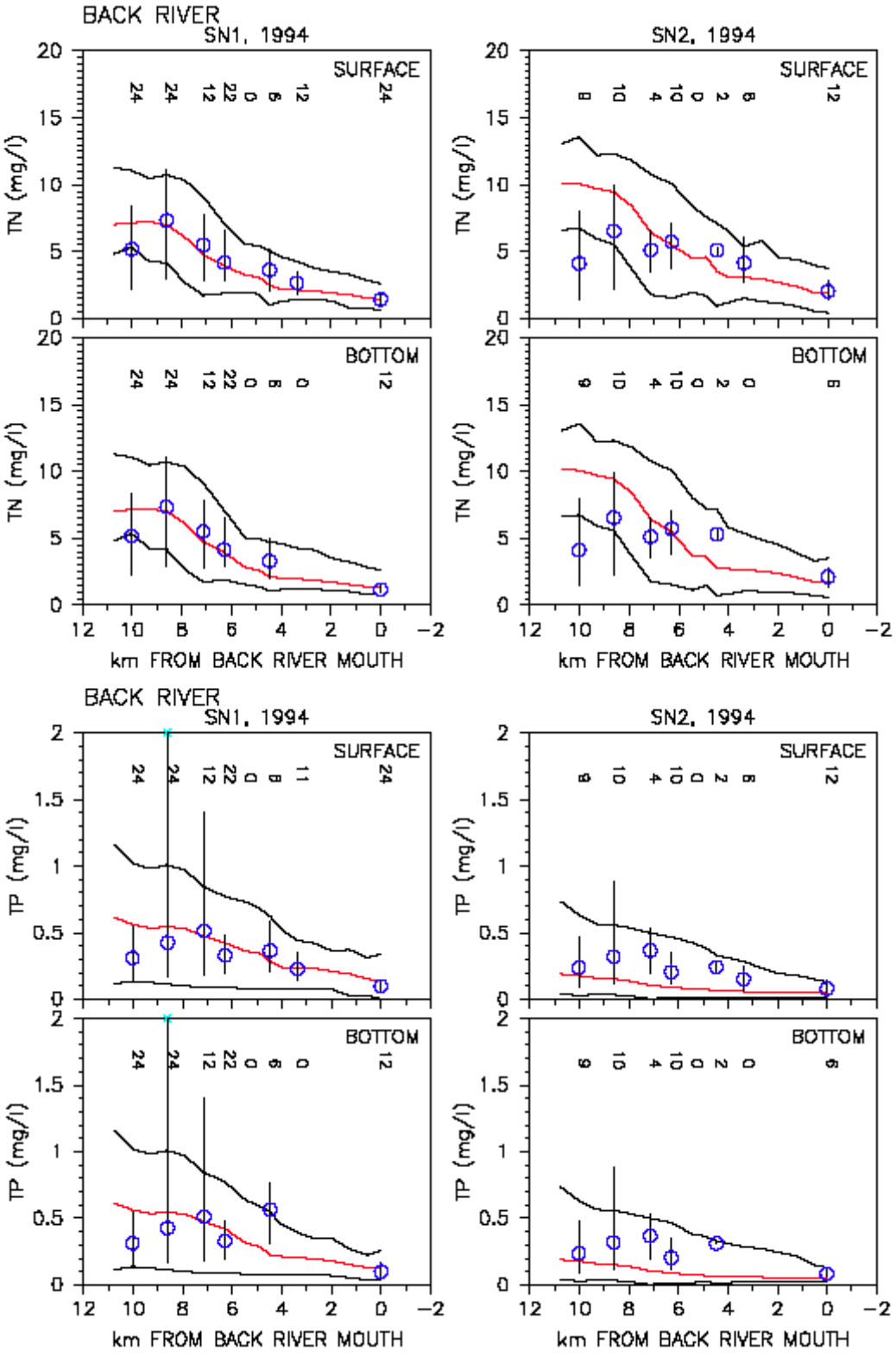

Fig. 106. Longitudinal comparison of model calibration results and data for total nitrogen and total phosphorus in Back River

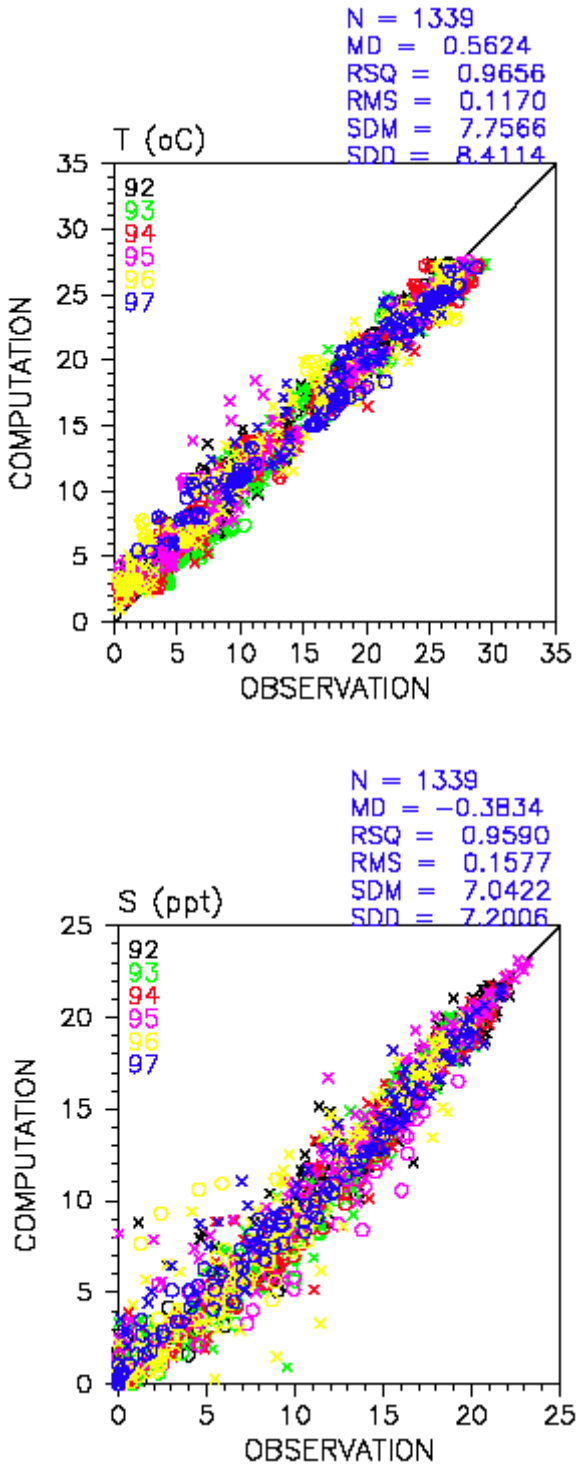

Fig. 107. Scatter plots for temperature and salinity in the Upper Chesapeake Bay

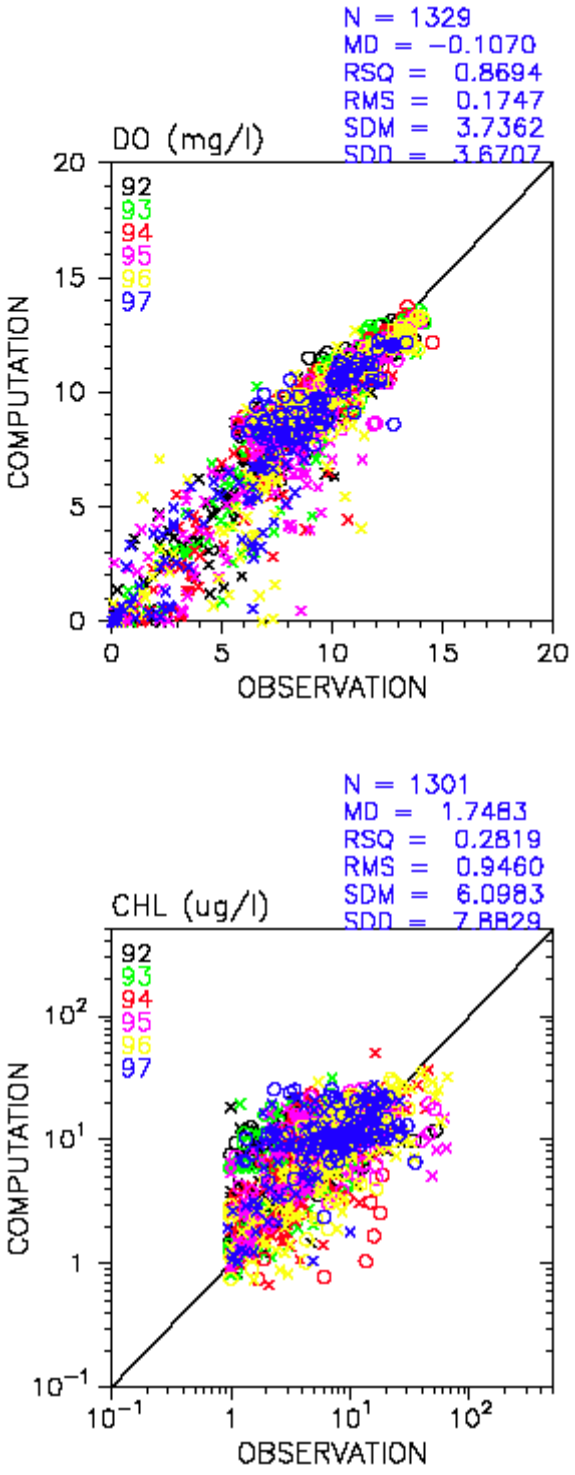

Fig. 108. Scatter plots for dissolved oxygen and chlorophyll a in the Upper Chesapeake Bay

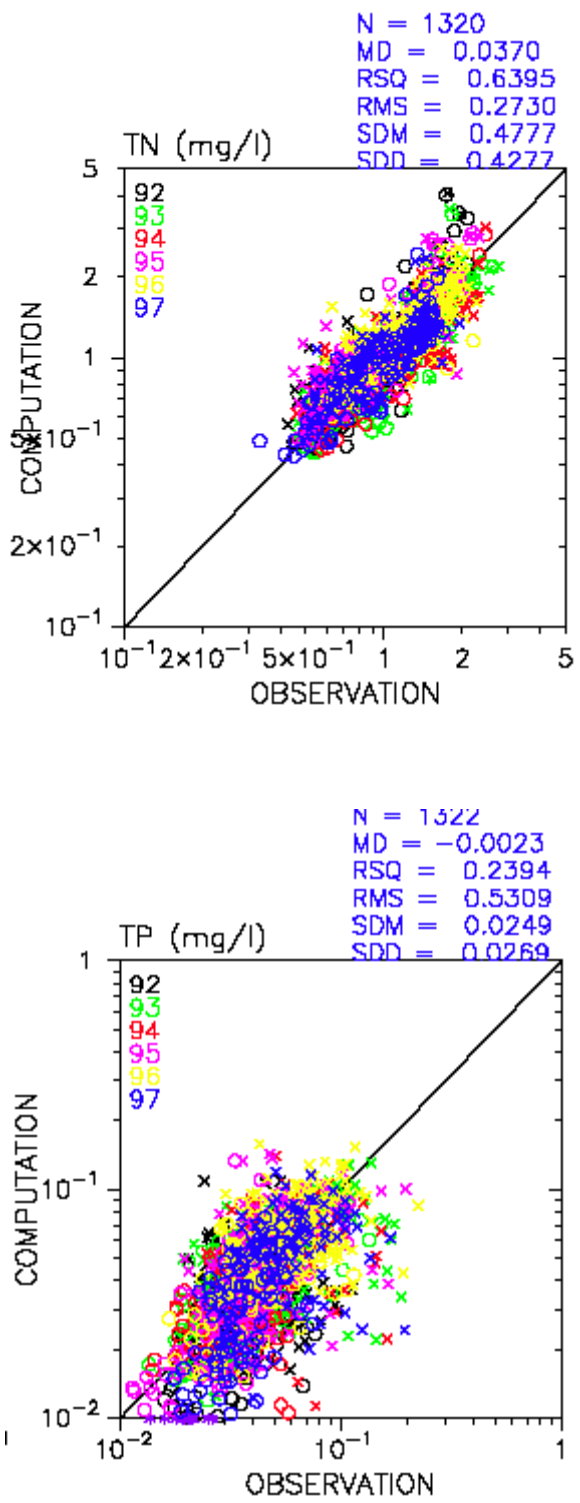

Fig. 109. Scatter plots for total nitrogen and total phosphorus in the Upper Chesapeake Bay

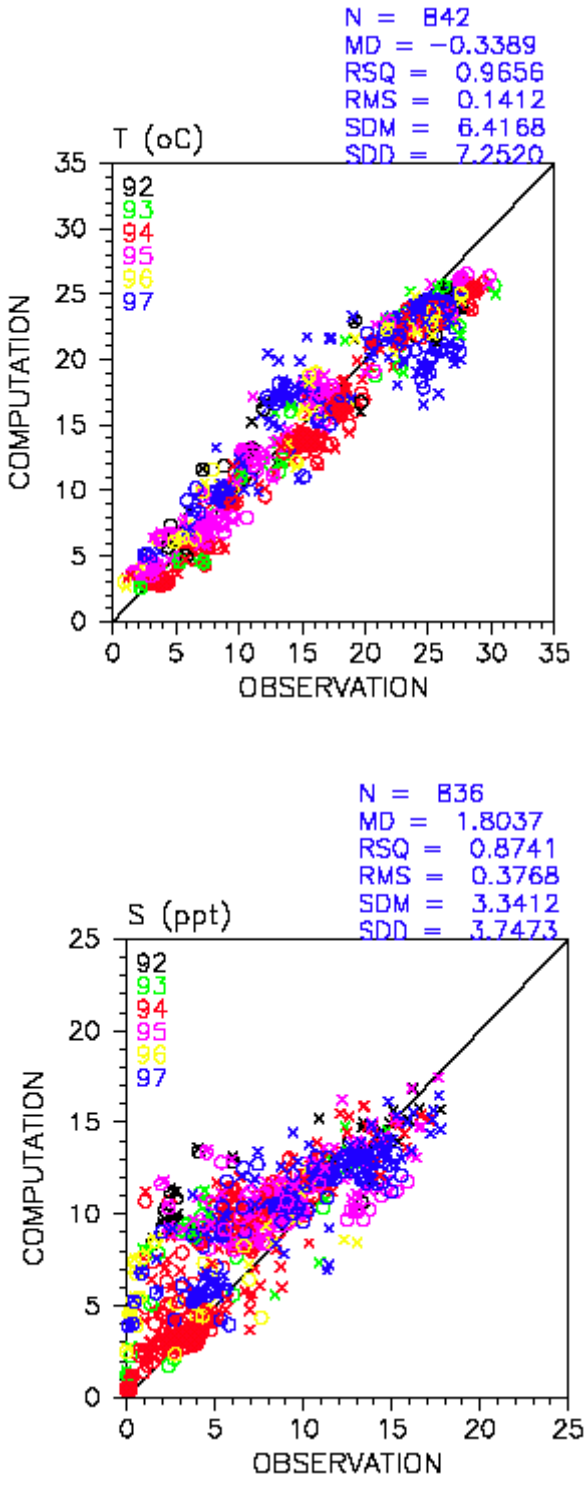

Fig. 110. Scatter plots for temperature and salinity in Baltimore Harbor

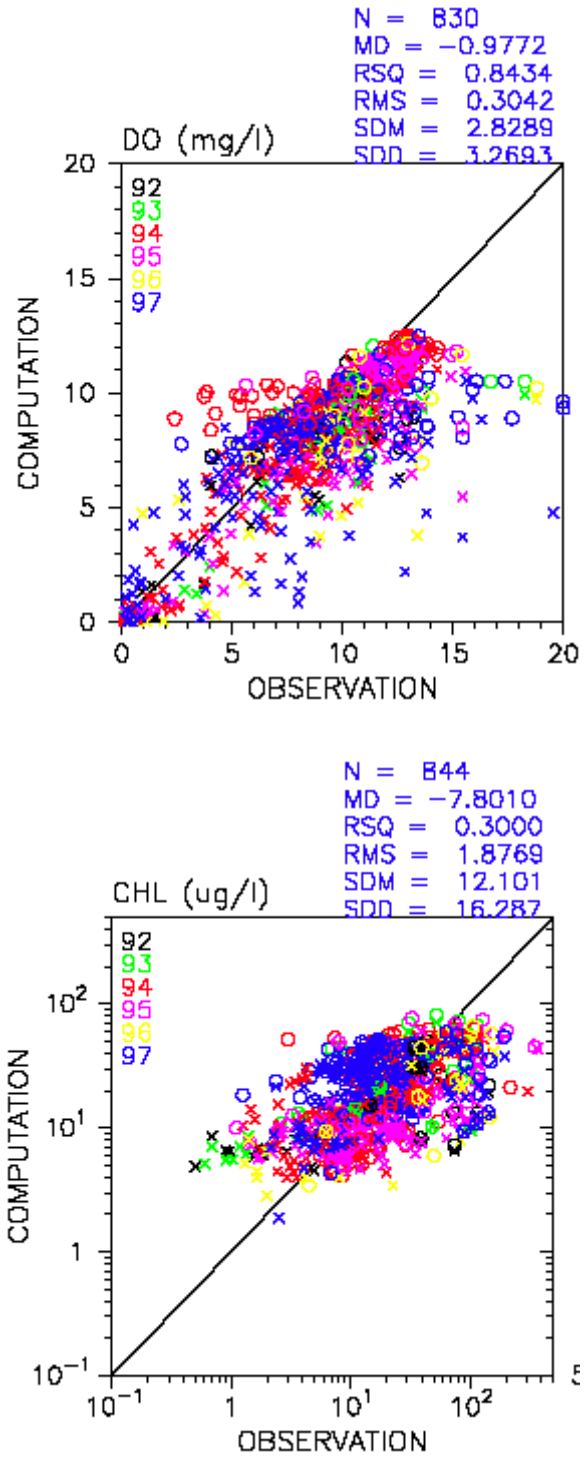

Fig. 111. Scatter plots for dissolved oxygen and chlorophyll a in Baltimore Harbor

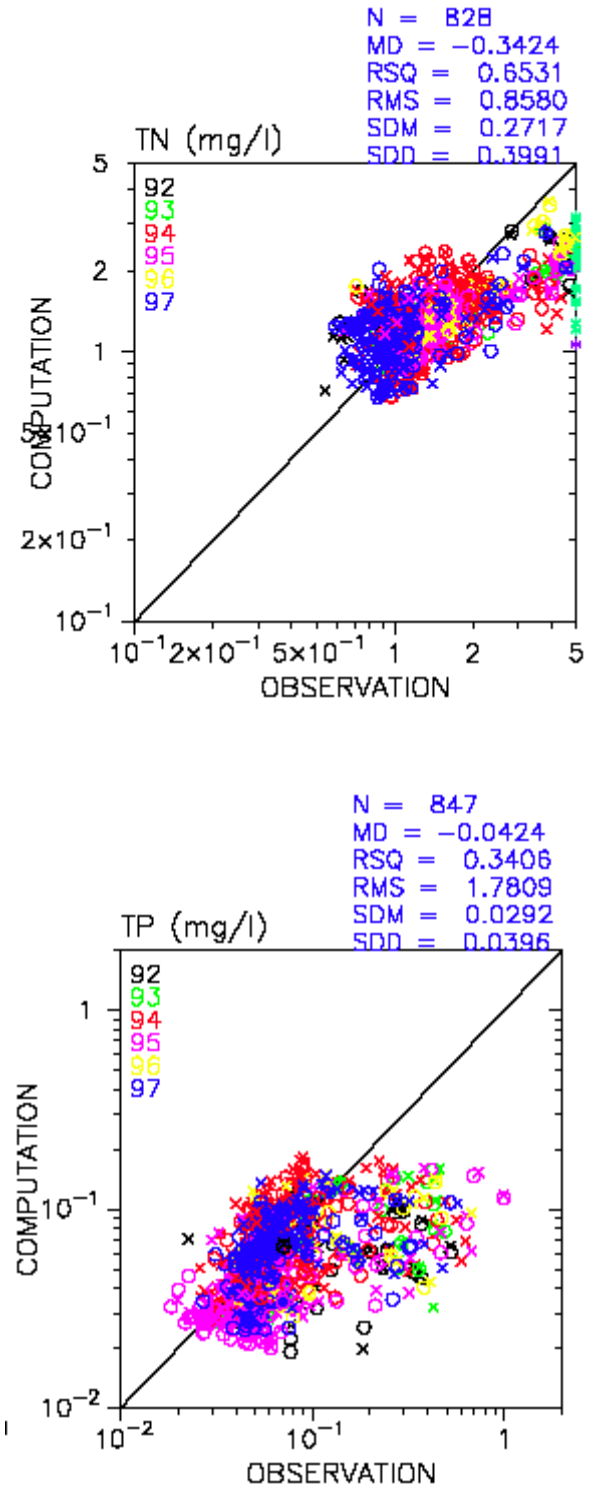

Fig. 112. Scatter plots for total nitrogen and total phosphorus in Baltimore Harbor

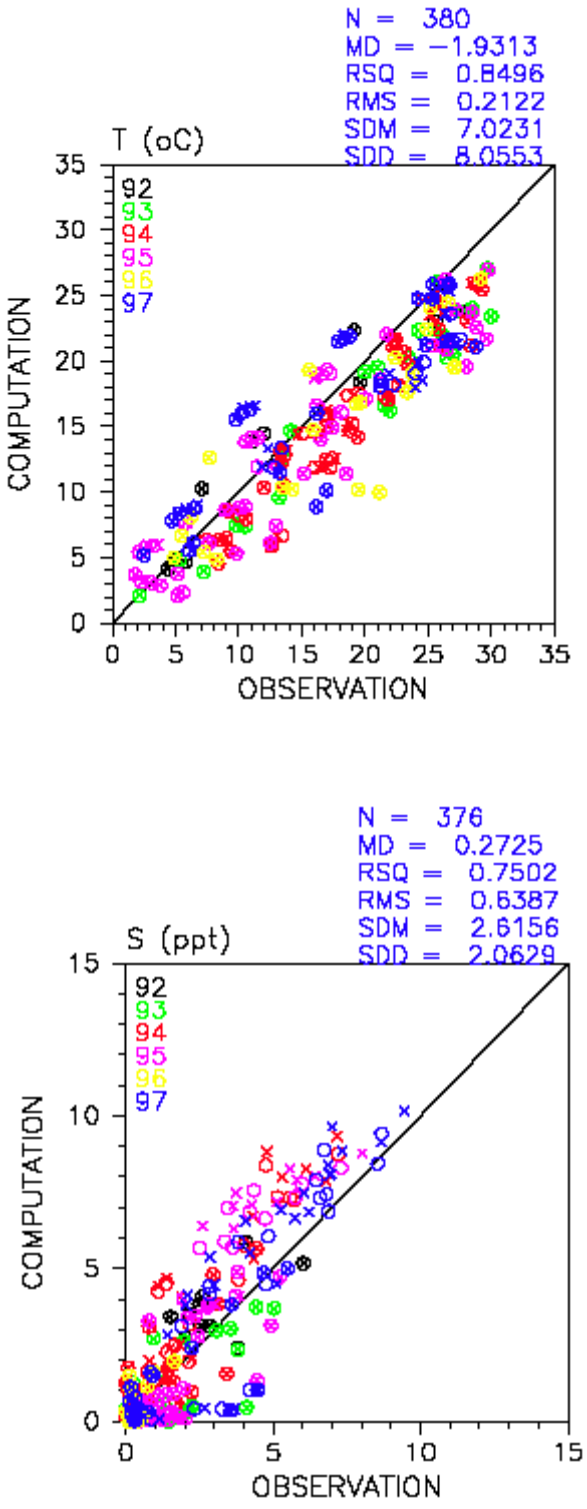

Fig. 113. Scatter plots for temperature and salinity in Back River

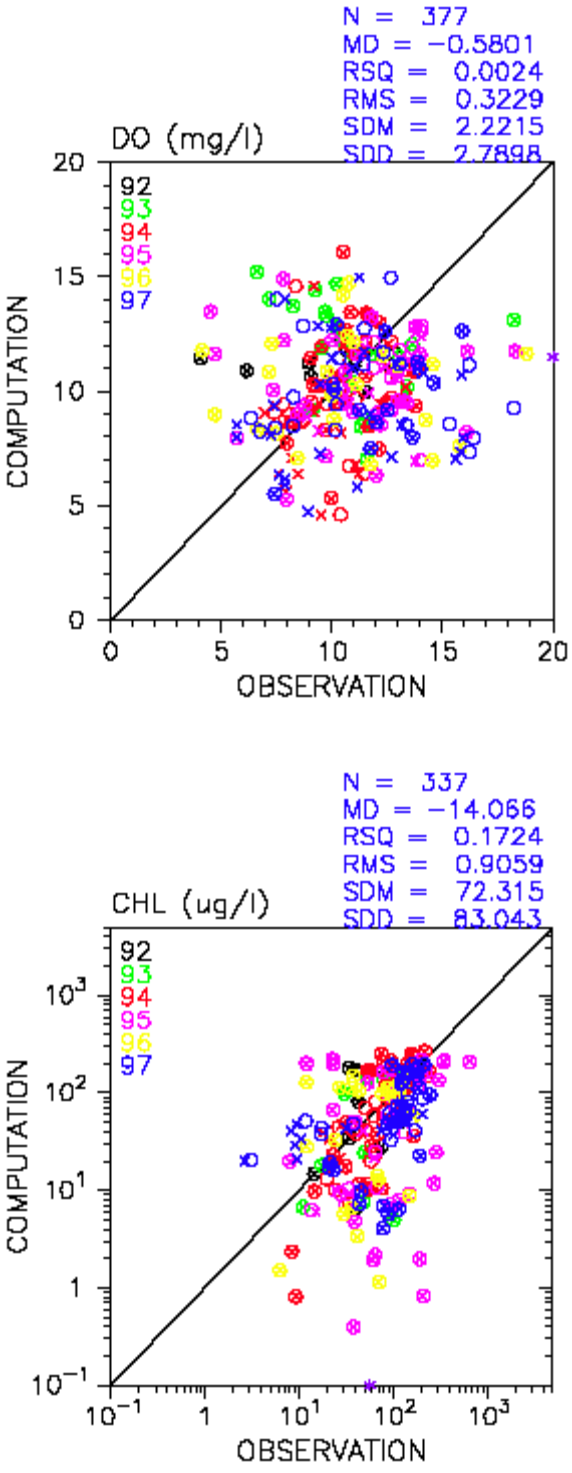

Fig. 114. Scatter plots for dissolved oxygen and chlorophyll a in Back River

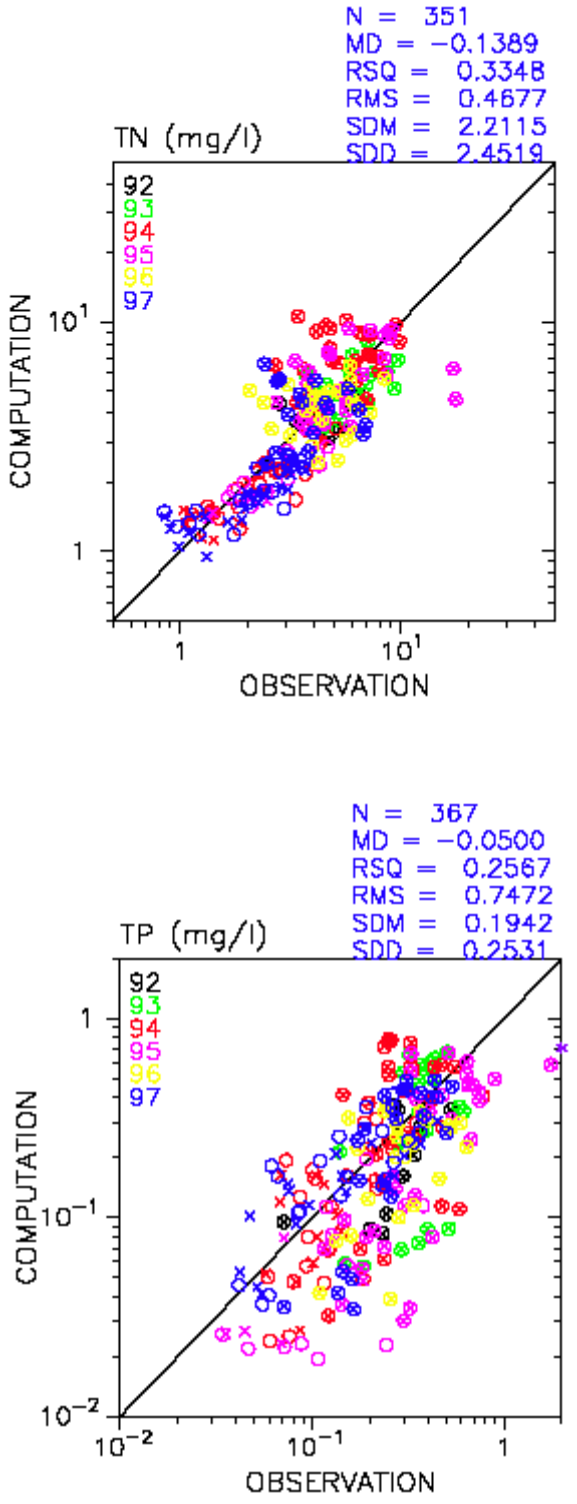

Fig. 115. Scatter plots for total nitrogen and total phosphorus in Back River

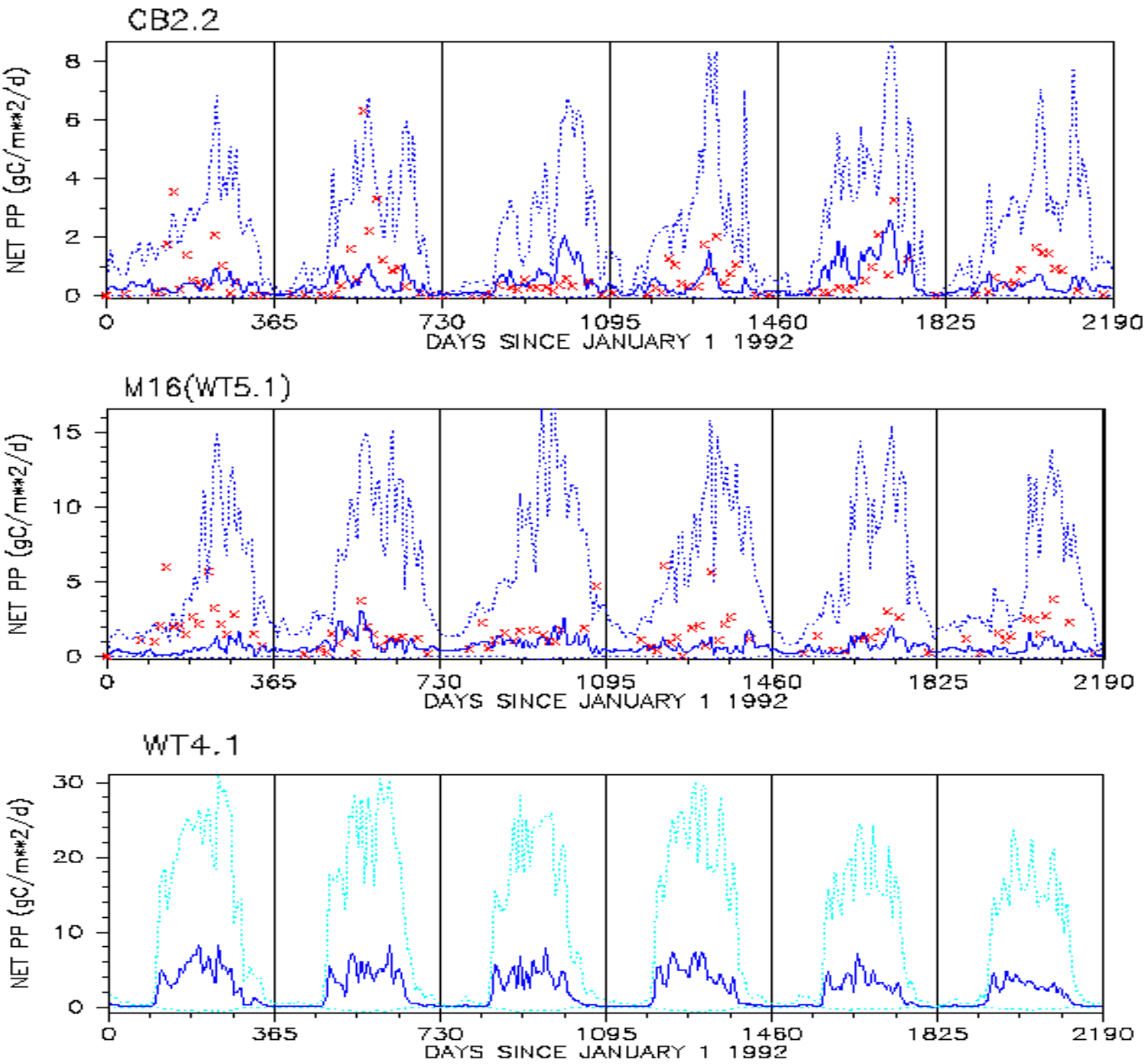

Fig. 116. Time series comparison of modeled primary production and data for the Upper Chesapeake Bay (CB2.2) and Baltimore Harbor

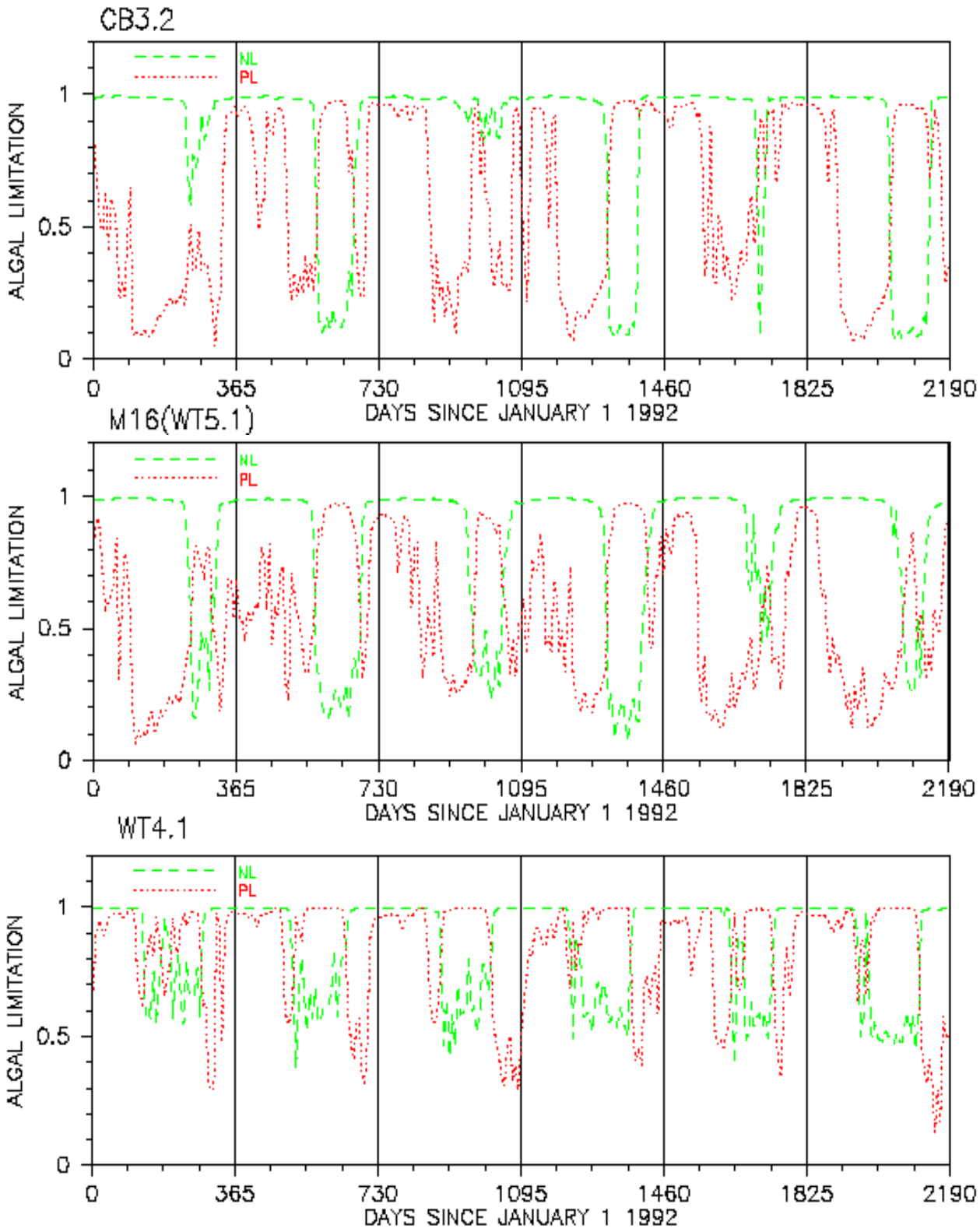

Fig. 117. Time series plots of modeled nutrient limitation in the Upper Chesapeake Bay (CB3.2), Baltimore Harbor (WT5.1), and Back River (WT4.1)

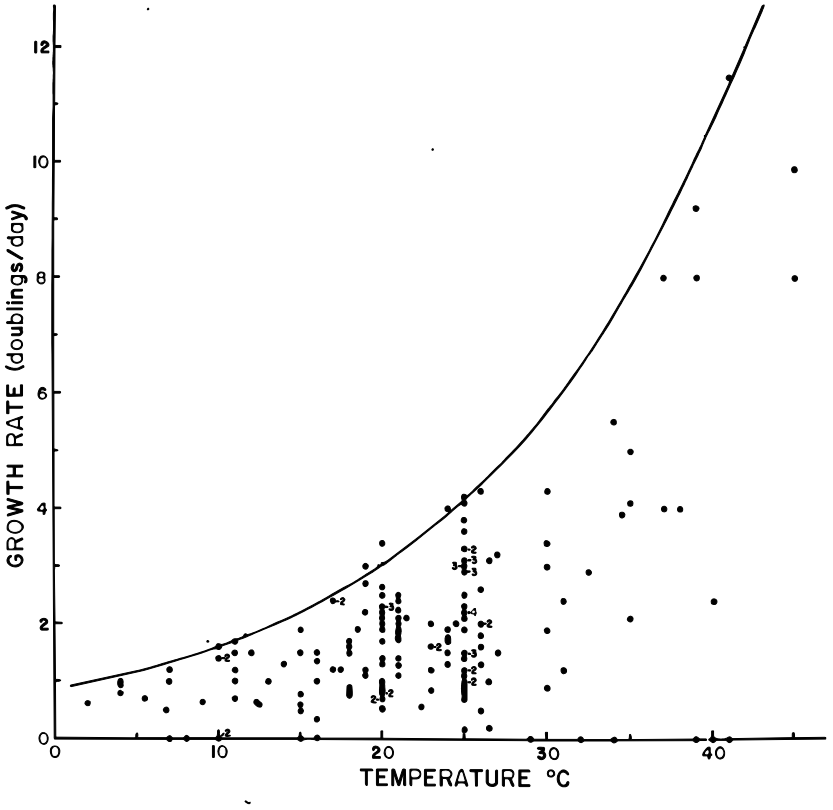

Fig. 118. Variation in the specific growth rate (μ) of photoautotrophic unicellular algae with temperature.

Note: Data are all for laboratory cultures. Growth rate is expressed in doublings/day. Approximately 80 of the points are from the compilation of Hoogenhout and Amesz (1965). That listing is restricted to maximum growth rates observed, largely in continuous light. The figure also includes additional data, mostly for cultures of marine phytoplankton, from the following sources: Lanskaya (1961), Eppley (1963), Castenholz (1964, 1969), Eppley and Sloan (1966), Swift and Taylor (1966), Thomas (1966), Paasche (1967, 1968), Hulburt and Guillard (1968), Jorgensen (1968), Smayda (1969), Bunt and Lee (1970), Guillard and Myklestad (1970), Ignatiades and Smayda (1970), Polikarpov and Tokaeva (1970). The latter papers include about 50 strains of marine phytoplankton. The line is the maximum expected growth rate. Small numbers by points indicate the number of values which fell on the points. (This graph is adopted from Eppley, 1972).

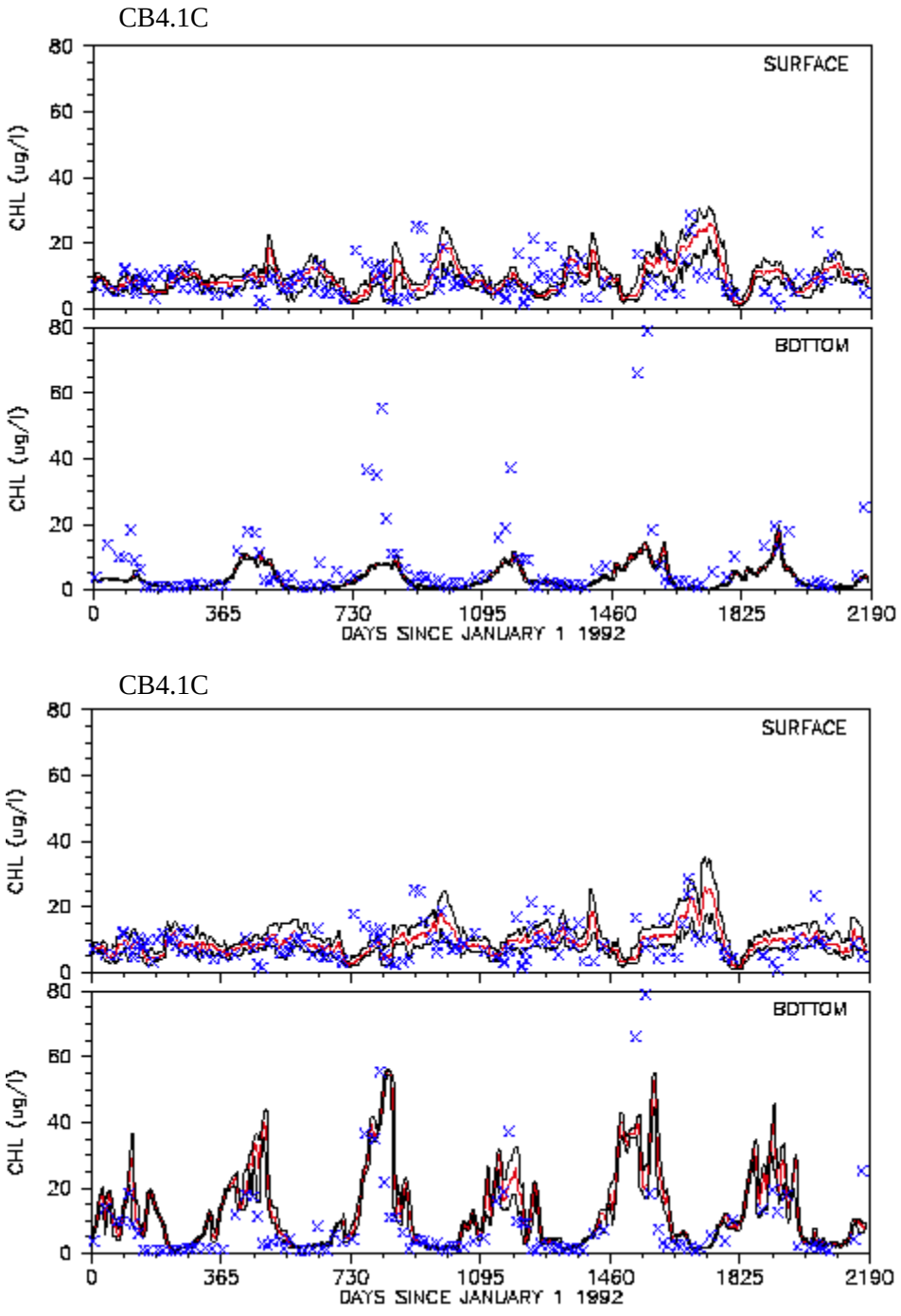

Fig. 119. Comparison of model results for chlorophyll a before (upper) and after (lower) implementing resuspension in the Upper Chesapeake Bay

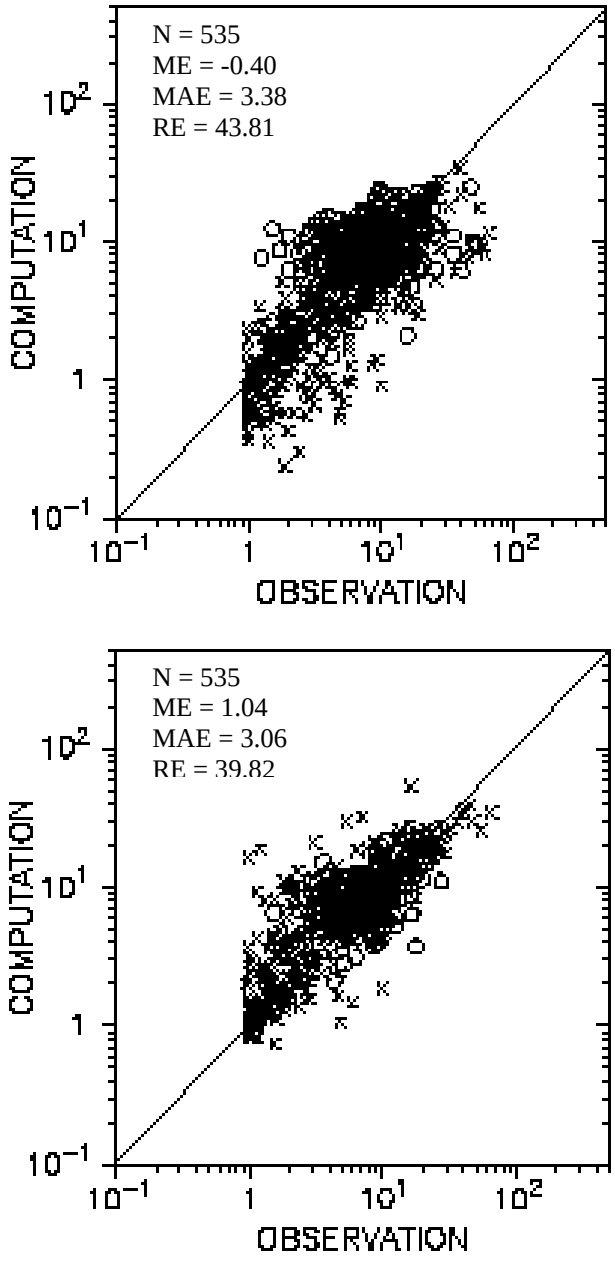

Fig. 120. Scatter plots of computed versus observed results for chlorophyll a before (upper)and after (lower) implementing resuspension in the Upper Bay

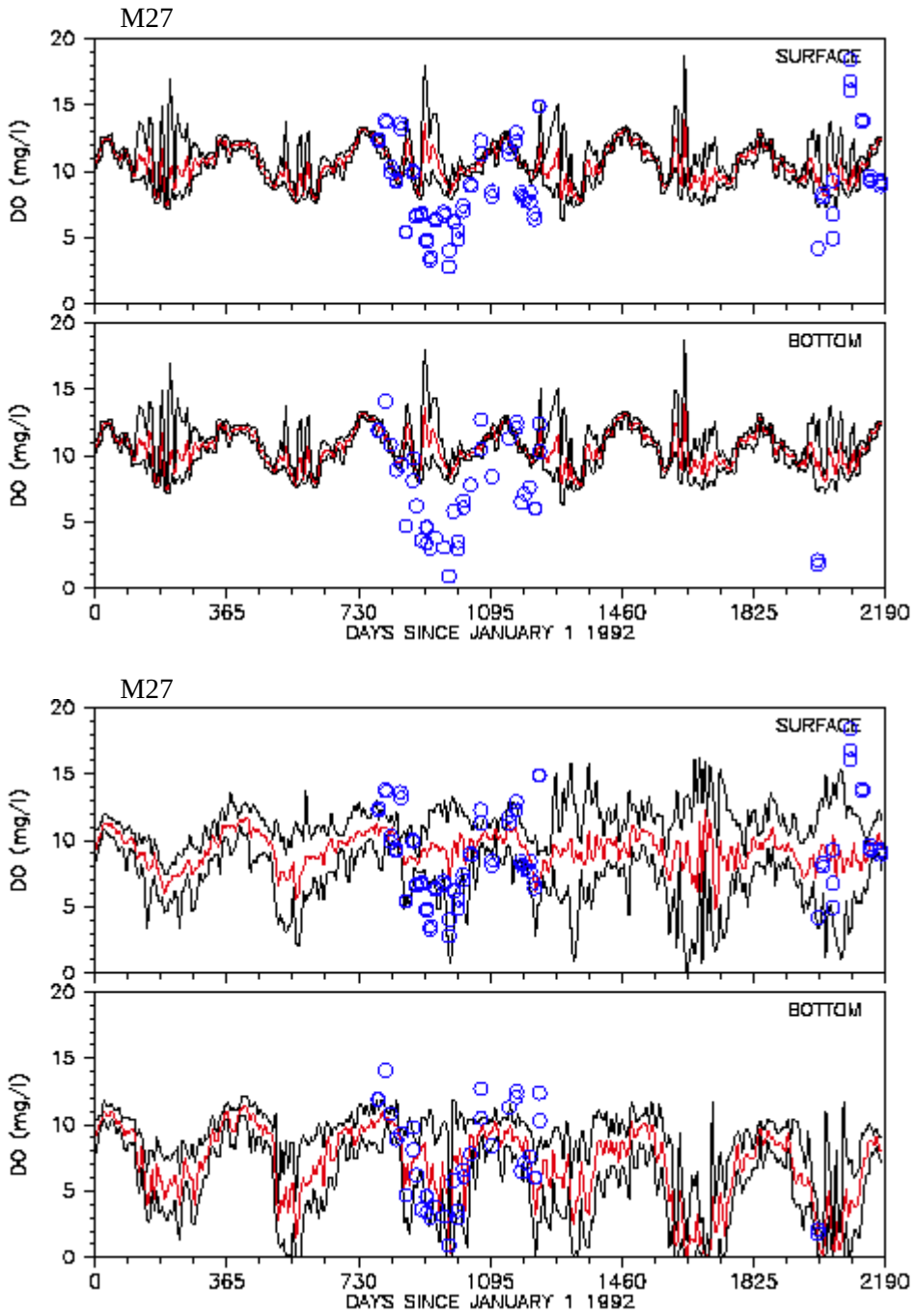

Fig. 121. Comparison of model results for DO before (upper) and after (lower) geometry change

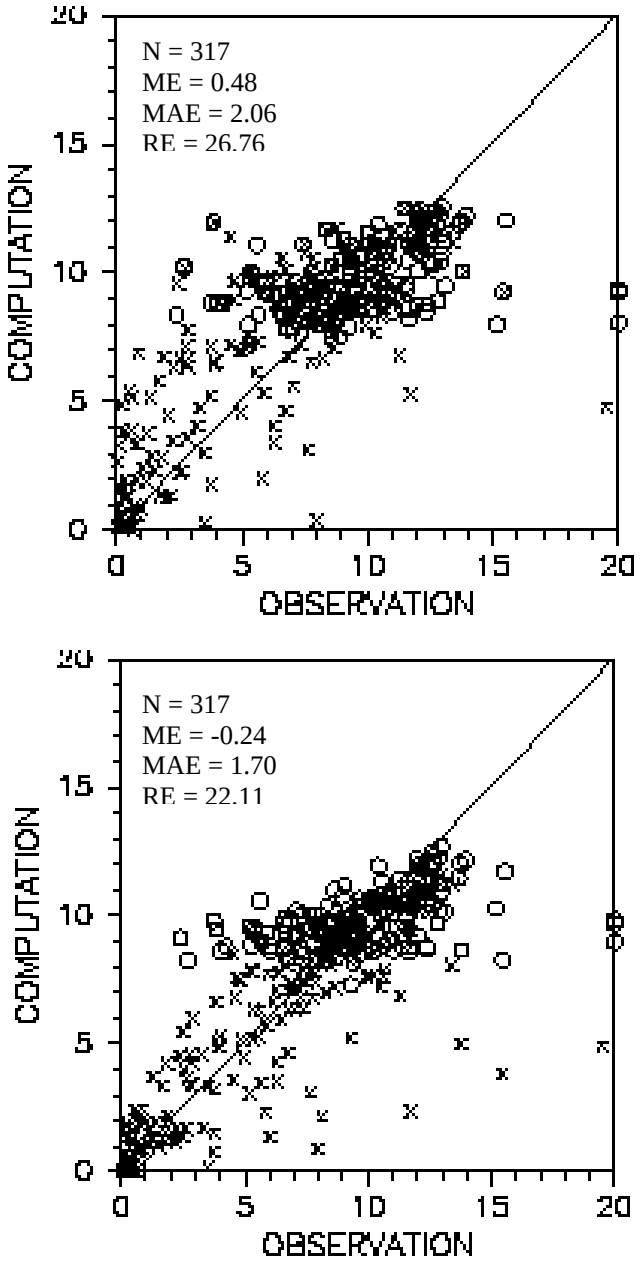

Fig. 122. Scatter plots of computed versus observed results for dissolved oxygen before (upper) and after (lower) geometry change in Baltimore Harbor

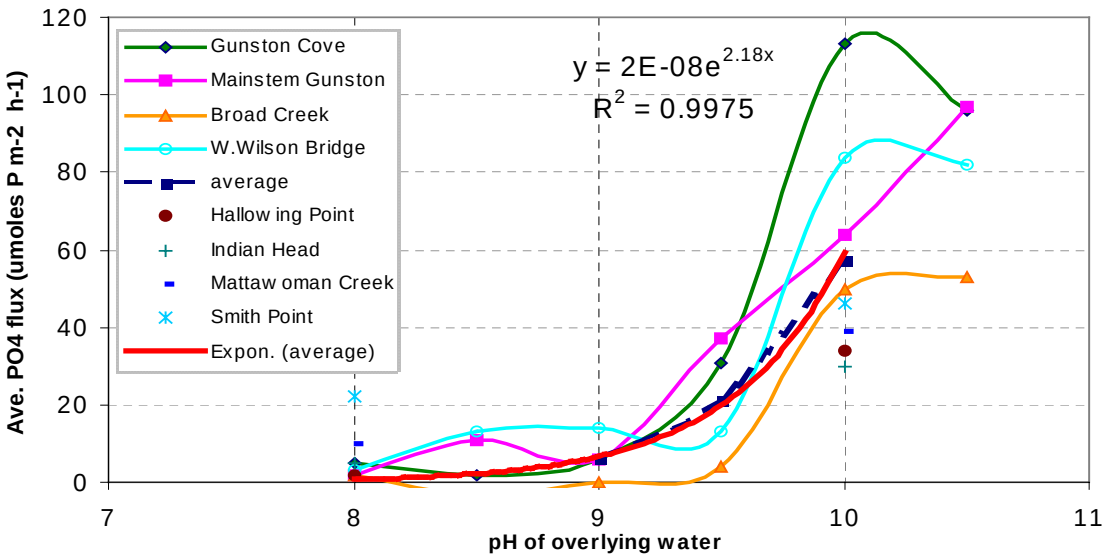

Figure 123. PO_4 fluxes versus pH values measured at different stations in Potomac Estuary

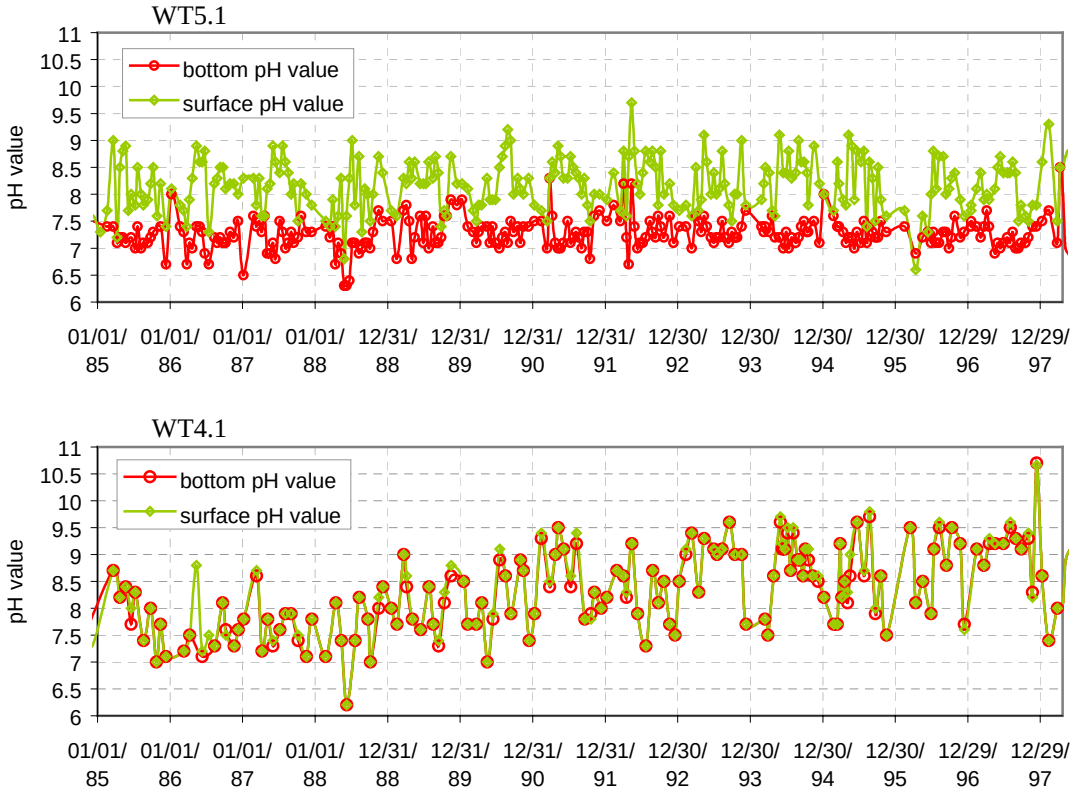

Fig 124. Measured pH values in Baltimore Harbor at WT5.1and Back River at WT4.1

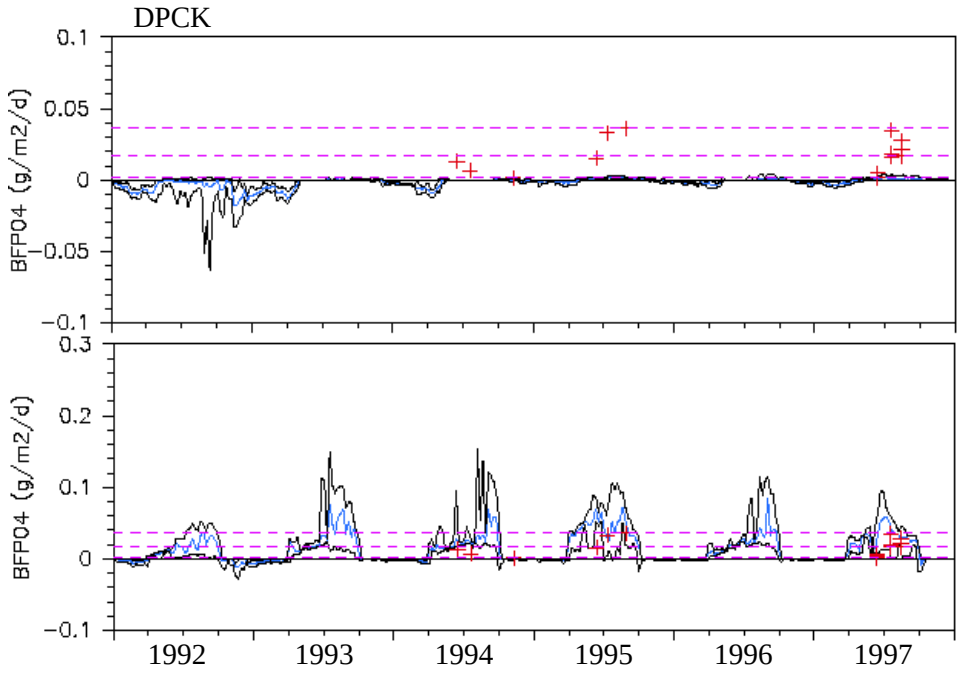

Fig. 125. Sediment phosphorus flux (model and data) before (upper) and after (lower) implementing pH function at DPCK in Back River

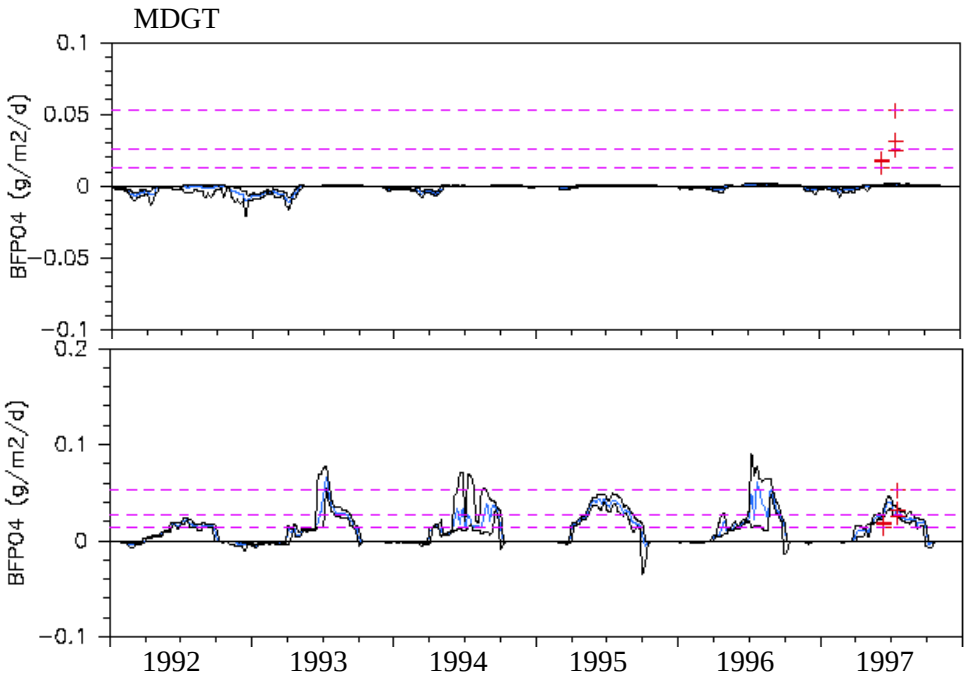

Fig. 126. Sediment phosphorus flux (model and data) before (upper) and after (lower) implementing pH function at MDGT in Back River

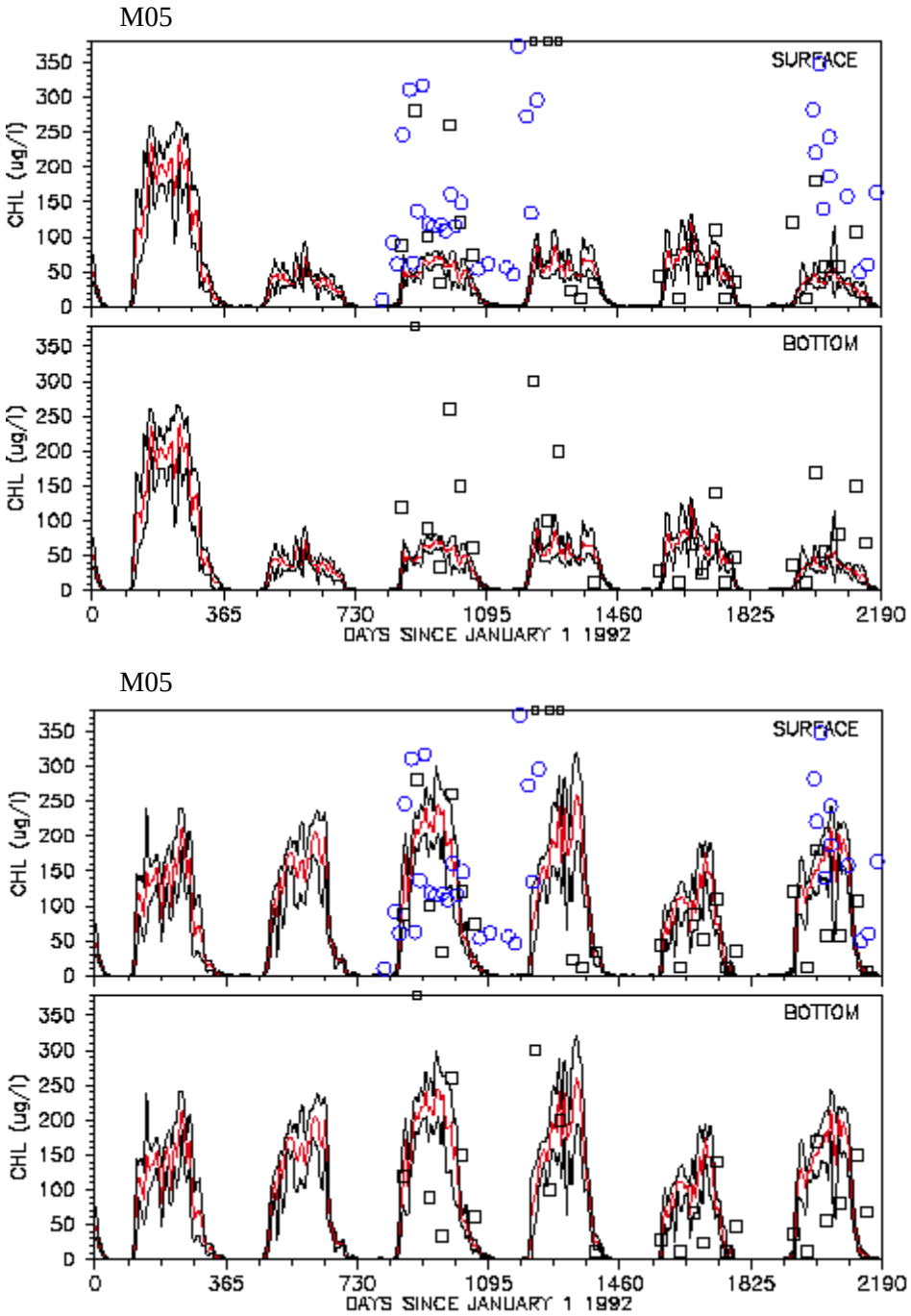

Fig. 127. The model results for chlorophyll a before (upper) and after (lower) implementing pH function at the station M05 in Back River

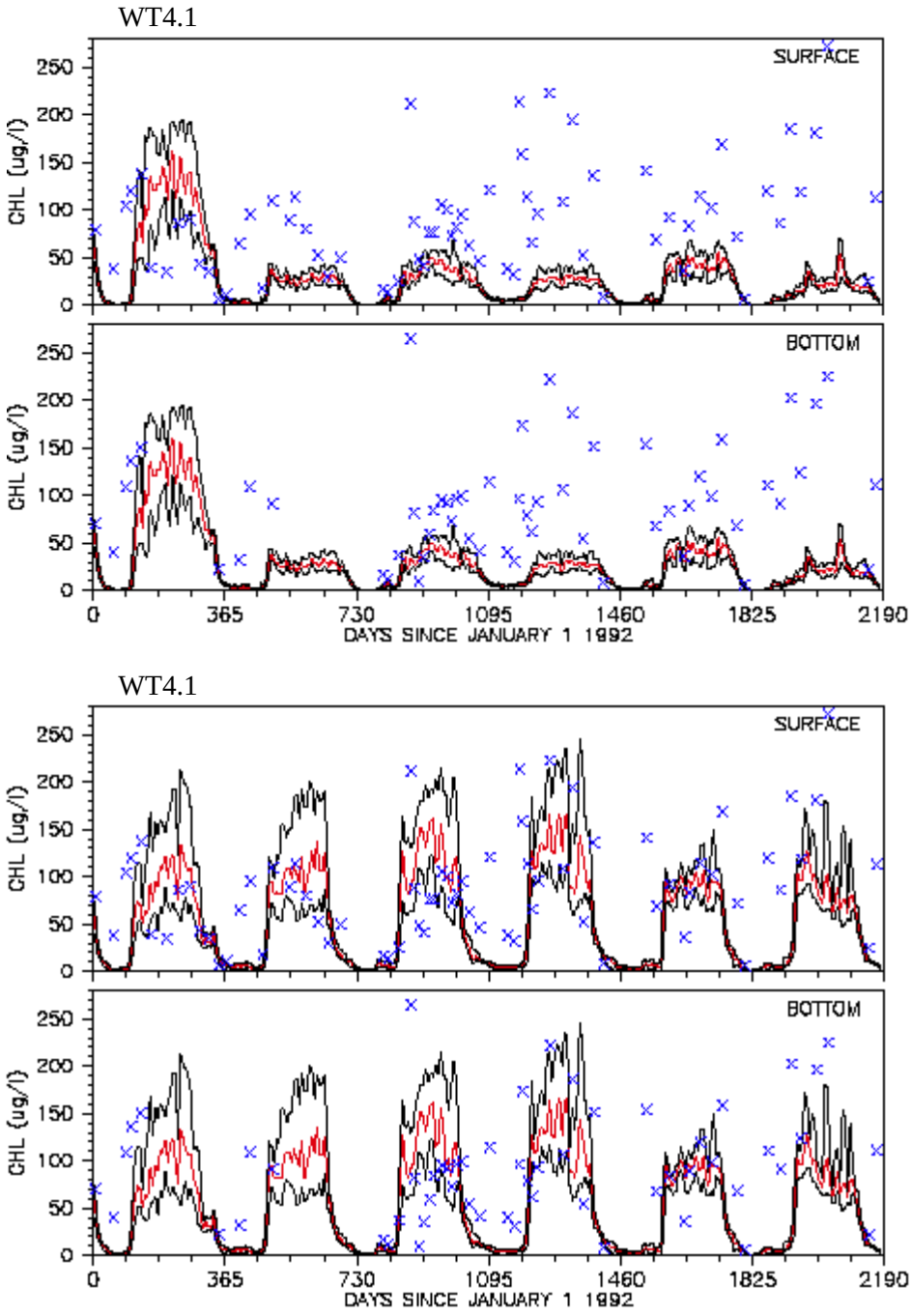

Fig. 128. The model results for chlorophyll a before (upper) and after (lower) implementing pH function at the station WT4.1 in Back River

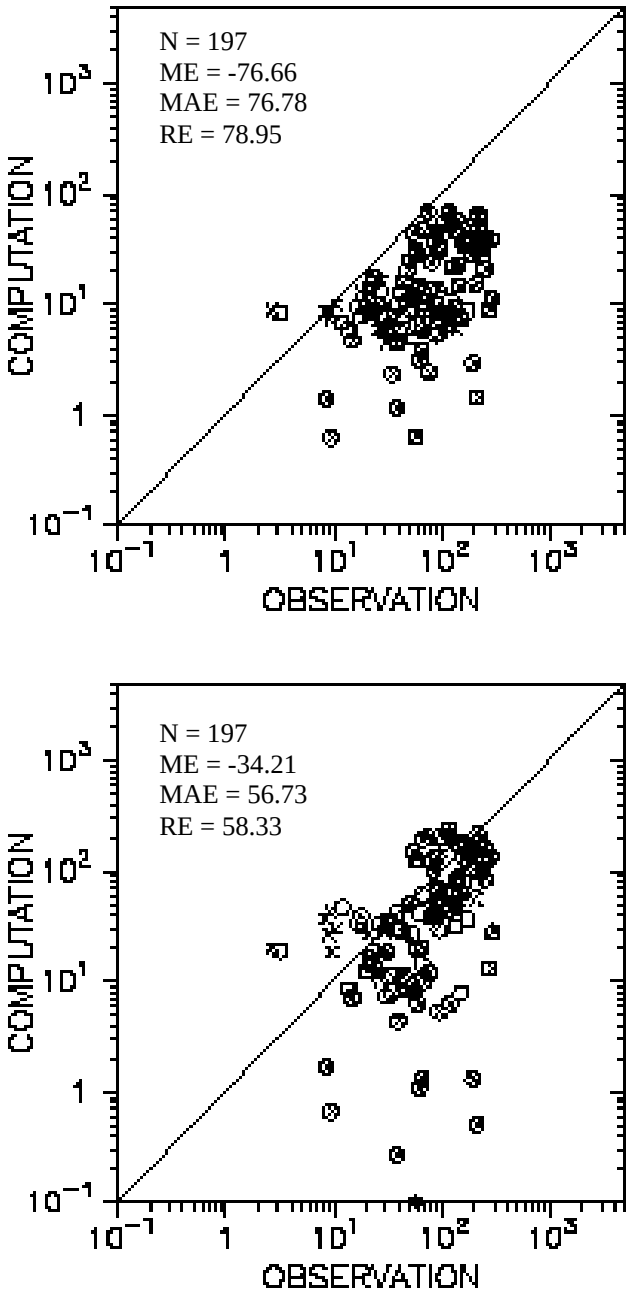

Fig. 129. Scatter plots of computed versus observed results for chlorophyll a before (upper) and after (lower) implementing pH function in Back River

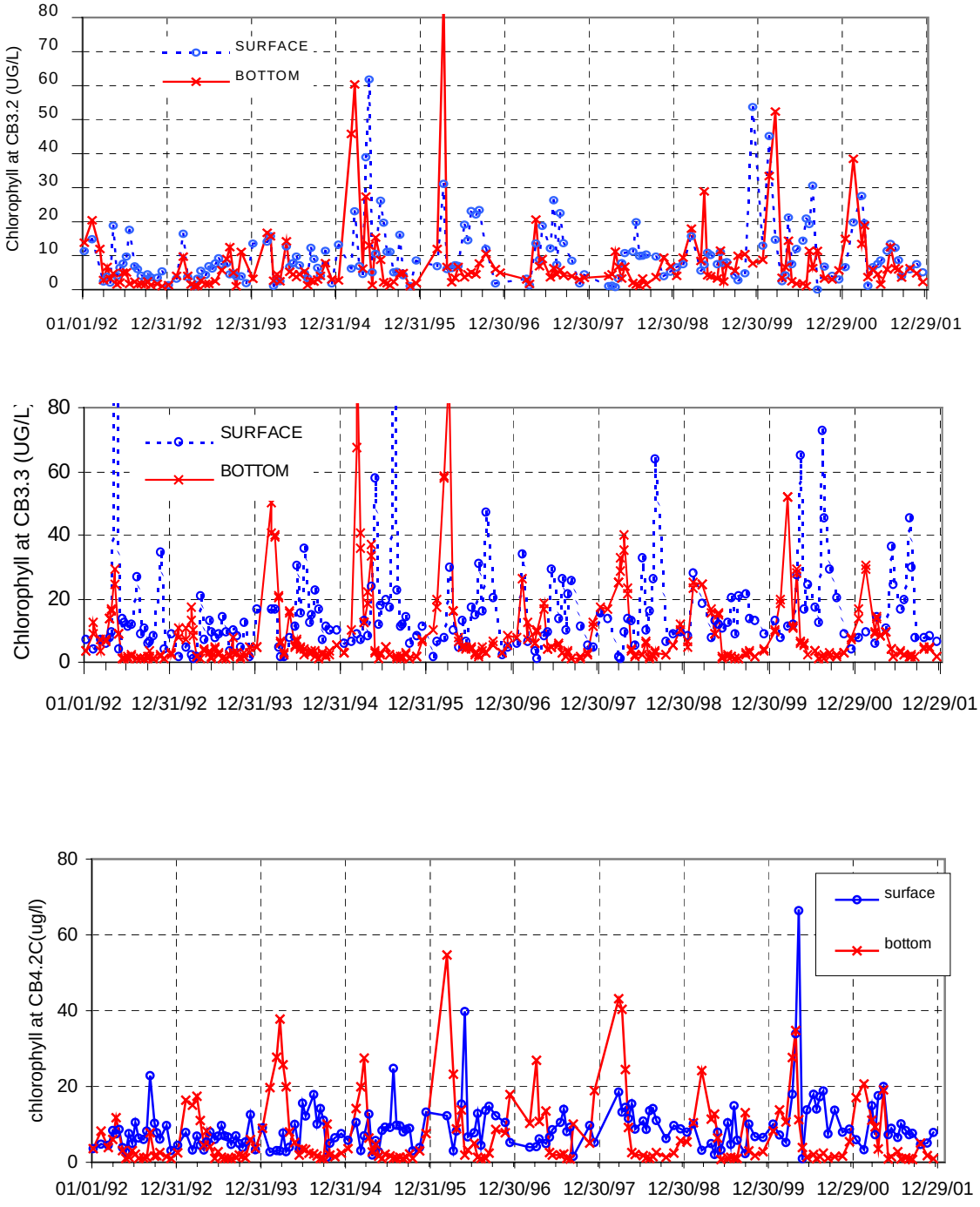

Fig 130. Surface and bottom chlorophyll a concentrations at CB3.2, CB3.3C, and CB4.2C, respectively

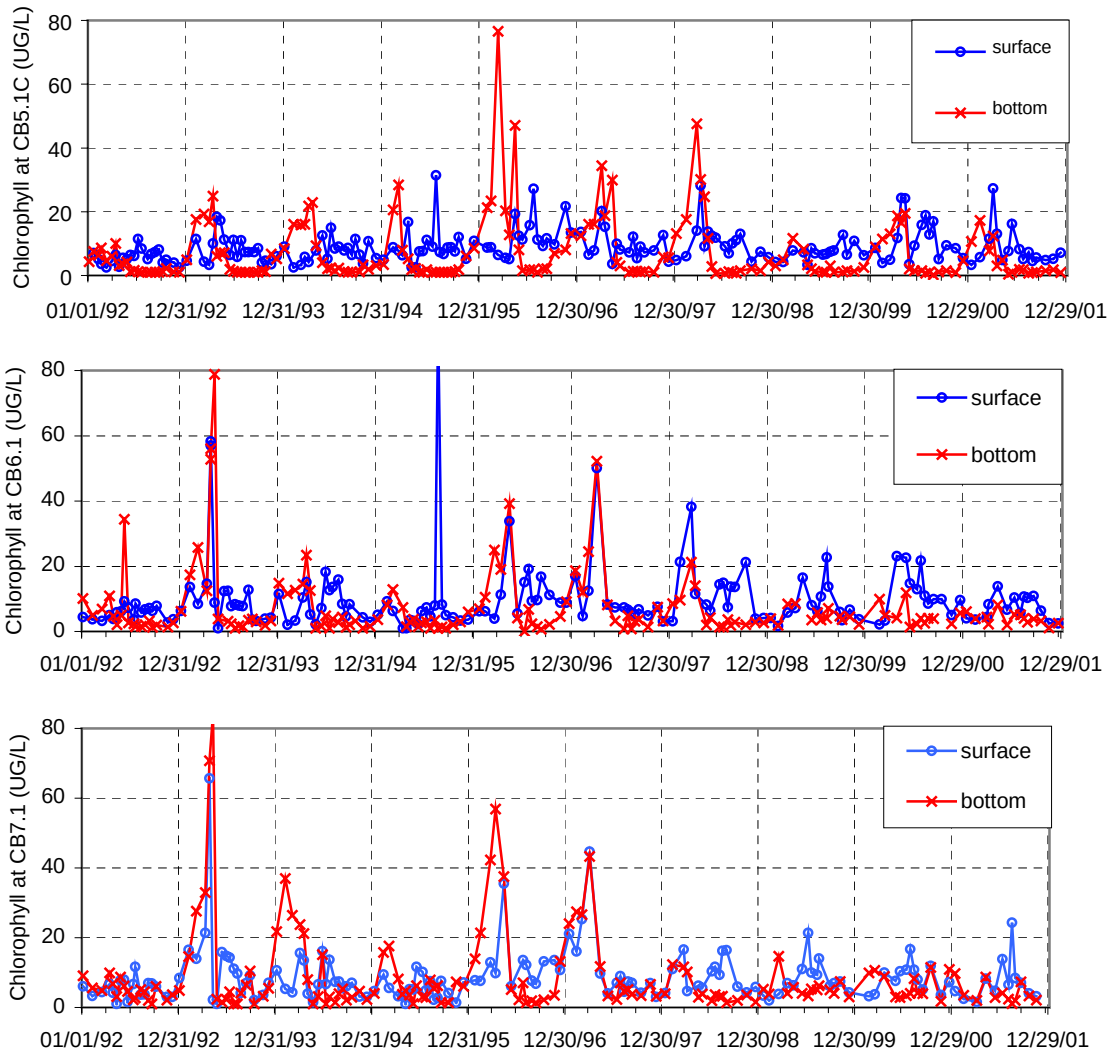

Fig 131 Surface and bottom chlorophyll a concentrations at CB5.1, CB6.1, and CB7.1, respectively

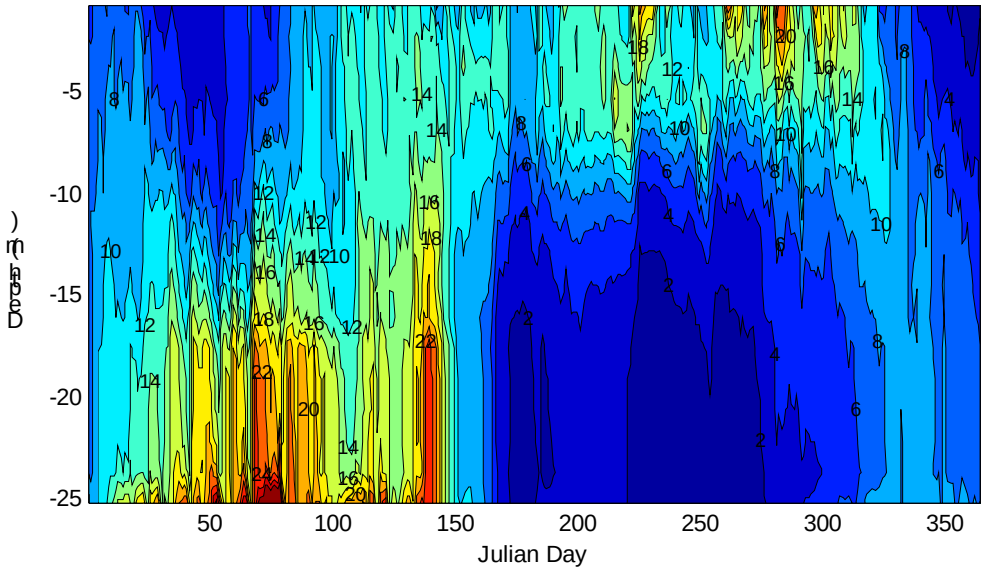

Fig. 132.Vertical distribution of chlorophyll a at CB4.2C in 1996

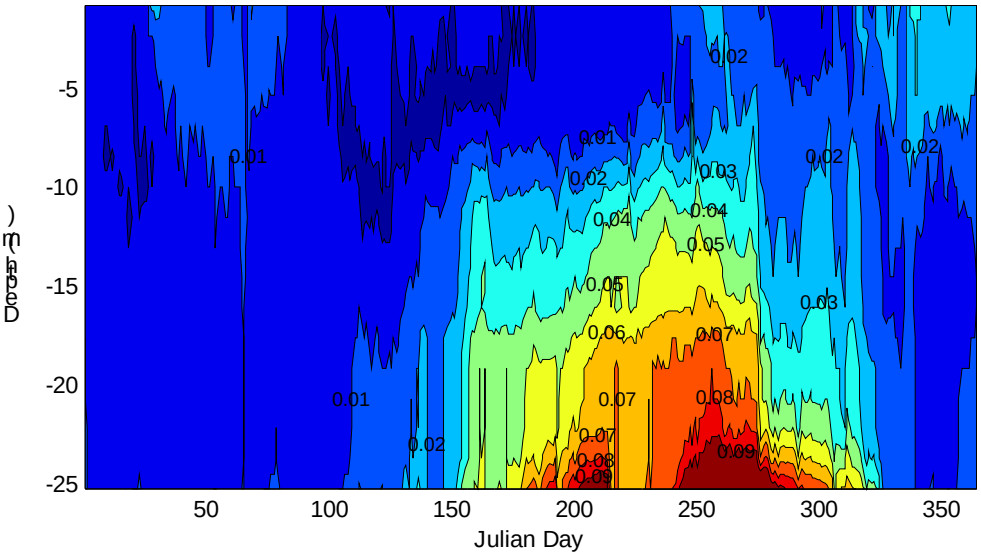

Fig. 133. Vertical distribution of dissolved phosphate at CB4.2C in 1996

APPENDIX A. SUPPLEMENTAL DESCRIPTION OF CONVENTIONS USED IN FIGURES

There are many figures presented in the report. The contents range from the descriptive graphics of the study domain, the observed water column and sediment flux data, the loading from the watersheds, to time series plots comparing modeled versus measured data. Most of the key information was provided in the legends and captions associated with the individual figure(s). However, for completeness, a supplemental description has been included to cover the diversity and the scope of the water quality parameters. Hopefully, this will prove to be useful for the initial inspection and interpretation of the figures.

1. Station naming convention:
   CB1.0 –CB4.4 was used by the EPA Chesapeake Bay Program (CBP) for naming the main stem monitoring stations. For certain stations, an additional character was attached to indicate its lateral location; for example, “CB3.3C” represents the center of CB3.3, “CB3.3W” the west and “CB3.3E” the east. Additional CBP stations used for the report include WT4.1 in the Back River and WT5.1 in Baltimore Harbor. M01 – M28 are used by MDE for naming its water quality monitoring stations. The sediment flux stations are marked by WCPT, MDGT, and DPCK in the Back River, and RVBH, HMCK, CTBY, FYBR, and INHB in Baltimore Harbor (**Figures: 2-10, 17-26, 28, 30-36, 38-50, 51-52, 54-57, 59-64, 66-82).
2. Symbols for observed data:
   The following designated symbols are used for distinguishing data from different sources: x: CBP water quality monitoring data; o: MDE water quality monitoring data; +: MDE sediment flux data, and □: City of Baltimore water quality monitoring data

** Figures relevant to each description

(Figures: 6, 8-10, 17-26, 30-36, 38-50, 56-57, 59-64, 66-70).

3. Model output convention:

   Since the monitoring data are collected on a weekly, bi-weekly or monthly frequency depending on the monitoring season, the model outputs were averaged over a one-week interval in order to make a sensible comparison of model versus observed data. Three lines were shown on the figures: the red solid line represents the weekly averaged value whereas the 2 black solid lines above and below represent the maximum and minimum.

   (Figures: 17-26, 30-36, 38-50, 56-57, 59-64, 66-70).

4. Interpretation of surface and bottom depths:

   The model surface layer represents 3.5 feet (1.067 m) below the free surface. For the observed data, its collection is at 1 meter below the free surface in most cases; however, occasionally, the observed data collected at 0.5 meters were also included as the surface values. For both the model and the observed data, the bottom differs from one station to another. The model depths for stations used in the thesis are as follows: CB4.4 (90 feet), CB4.3C (75 feet), CB4.2C (85 feet), CB4.1C (95 feet), CB3.3C (75 feet), CB3.2 (30 feet), M01 (15 feet), M02 (10 feet), M04 (5 feet), M05 (5 feet), WT4.1 (5 feet), M08 (45 feet), M16 (45 feet), WT5.1 (45 feet), M27 (15 feet), M28 (45 feet). (Figures: 17-26, 30-36, 38-50, 56-57, 59-64, 66-70).

5. Explanation of benthic flux data:

   Due to the sparse nature of the benthic flux measurement, the data do not show a clear pattern. In order to increase the readability, three dashed lines (maximum, mean and minimum) were generated for the available measured data from 1992-1997. The unit used is gram/m**2/day, which is the area-based measurement (Figures: 9-10, 54-55).

6. Explanation of nutrient limitation:

   The nutrient limitation figure is a plot of the Michaelis and Menton relationship for the uptake of nitrogen, phosphorus, and silica, respectively, by phytoplankton. The vertical axis represents the normalized phytoplankton uptake (by its maximum value). It is a reflection of the effect by nutrient limitation on maximum growth rate. For

example, if the value is 1, that indicates there is no limitation by the nutrient; in contrast, if the value approaches 0, it indicates a severe limitation by the nutrient on the maximum growth rate. When the three limiting functions co-exist, the minimum of the three will be the ultimate limiting factor. For details, see equation (IV-13) on page 29. (Figures: 51 and 71).

7. Explanation of statistics used to assess modeled versus observed results
Quantitative assessments of model performance are desirable to render the evaluation of the model application. Among numerous measures of model performance, employed in the present study are scatter plots with mean errors, mean absolute errors, and relative errors.

Three measures of errors for model-data comparison are utilized in this study. The mean absolute error (MAE), a measure of the absolute deviation of the model results from the data on the average, is defined as:

$$MAE = \frac{1}{N}\sum_{n=1}^{N}\left|P_n - O_n\right|$$

where P_n and O_n = corresponding model result and data; N = number of observations. The MAE of zero is ideal. Since the MAE cannot be used to discern the overestimation or underestimation, another measure is desirable. The mean error (ME) is defined as:

$$ME = \frac{1}{N}\sum_{n=1}^{N}(P_n - O_n)$$

Positive ME indicates the model's overestimation of the data on the average and negative ME indicates the model's underestimation of the data on the average, with zero ME being ideal. The relative error (RE) is defined as:

$$RE = \frac{\sum\left|P_n - O_n\right|}{\sum O_n}$$

The RE is the ratio of the MAE to the mean of the data, indicating the magnitude of the MAE relative to the data on the average. (Figures: 29, 37, 58).

LITERATURE CITED

Andersen, J.M. (1971). Nitrogen and Phosphorus budgets and the role of the sediments in six shallow Danish lakes. Archiv fur Hydrobiologie 74, 528-550.

Bienfang, P., Harrison, P., and L. Quarmby (1982). Sinking rate response to depletion of nitrate, phosphate, and silicate in flur marine diatoms. Marine Biology, 67, 295-302.

Bieri, R.H., Hein, C., Huggett, R. J., Shou, P., Slone, H., Snith, C., and S. Chih-Wu (1982). Toxic Organic Compounds in Surface Sediments from the Elizabeth and Patapsco Rivers and Estuaries. Virginia Institute of Marine Science, Gloucester Point, VA, 136 pp.

Boicourt, W.C. and P. Olson (1982). A hydrodynamic study of the Baltimore Harbor system. Tech. Rep. 82-10. Chesapeake Bay Institute, The Johns Hopkins University, MD.

Boicourt, W.C. (1992). Influence of circulation processes on dissolved oxygen in Chesapeake Bay. In: Smith D. Leffler M, Mackiernan G (eds) Oxygen Dynamics in Chesapeake Bay: a synthesis of recent research. University of Maryland Sea Grant College Publ., College Park, MD, 7-95 pp.

Bowie, G.L., Mills, W.B., Porcella, D.B., Campbell, C.L., Pagenkopf, J.R., Rupp, G.L., Johnson, K.M., Chan, P.W.H., Gherini, S.A. and C.E. Chamberlin (1985). Rates, constants and kinetics formulations in surface water quality modeling (2^{nd} edition). EPA/600/3-85/040, Environmental Research Lab., US Environmental Protection Agency, Athens, GA, 455 pp.

Boynton, W.R., Kemp, W. M. and C.W. Keefe (1982). A comparative analysis of nutrients and other factors influencing estuarine phytoplankton production. In : Kennedy VS(ed) Estuarine comparisons. Academic Press, New York,

69-90 pp.

Boynton, W.R., Burger, N.H., Stankelis, R.M., Rohland, F.M., Hagy III, J.D., Frank, J..M., Matteson, L.L. and M.M. Weir (1998). An environmental evaluation of Back River with selected data from Patapsco River. Prepared for Baltimore City Department of Public Works for Project 613, Comprehensive Wastewater Facilities Master Plan, University of Maryland Center for Environmental Science, Chesapeake Biological Lab., MD, 90 pp.

Canale, R. and A.Vogel (1974). Effects of temperature on phytoplankton growth, Journal of the environmental engineering Division, 100, 231-241.

Cerco, C.F. and T.M. Cole (1994). Three-dimensional eutrophication model of Chesapeake Bay: Volume 1, main report. Technical Report EL-94-4, US Army Engineer Waterways Experiment Station, Vicksburg, MS.

Cerco, C.F. and T.M. Cole (1995). User's guide to the CE-QUAL-ICM three-dimensional eutrophication model. Technical Report EL-95-15, US Army Engineer Waterways Experiment Station, Vicksburg, MS.

Chen, H., Hyer, P., and Y. Unkulvasapaul (1984). Summary report on calibration of water quality models of the Chesapeake Bay system. Virginia Institute of Marine Science, Gloucester Point, VA.

Coastal Environmental Services (1995). Patapsco/Back Rivers watershed study: ambient conditions, pollutant loads and recommendation for further action. Prepared for Maryland Department of the Environment, Coastal Environmental Services, Inc., Linthicum, MD.

Collins, C.D. and J.H. Wlosinski (1983). Coefficients for the US Army Corps of Engineers reservoir model, CE-QUAL-R1. Technical Report E-83-15, US Army Engineer Waterways Experiment Station, Vicksburg, MS, 120 pp.

Conley, D.J. and T.C. Malone (1992). Annual cycle of dissolved silicate in Chesapeake Bay: implications for the production and fate of phytoplankton biomass. Mar Ecol Prog Ser 81: 121-128.

DiToro, D. M. and J. Fitzpatrick (1993). Chesapeake Bay sediment flux model. Contract Report EL-93-2, US Army Engineer Waterways Experiment Station, Vicksburg, MS, 316 pp.

DiToro, D. M., S. Lowe, and J. Fitzpatrick (2001). Application of a water column-sediment eutrophication model to a mesocosm experiment I. Calibration. J. Environ. Engr. ASCE.

Dortch, M.S. (1990). Three-dimensional, Lagrangian residual transport computed from an intratidal hydrodynamic model. Technical Report EL-90-11, US Army Engineer Waterways Experiment Station, Vicksburg, MS.

Dortch, M.S., Chapman, R.S., and S.R. Abt (1992). Application of three-dimensional Lagrangian residual transport. Journal of Hydraulic Engineering, ASCE, 118(6): 831-848.

Dzombark, D.A., and F.M.M. Morel (1990). Surface complexation modeling. Hydrous Ferric Oxide. John Wiley & Sons, New York, NY.

Edinger, J.E.; Brady, D.K.; and J.C. Geyer (1974). Heat exchange and transport in the environment. Report No. 14, Johns Hopkins University, Baltimore, MD, 125 pp.

Environmental Resources Management (1997). Baltimore Harbor/Back River monitoring program: field sampling plan. W.O. No. F7103, Comprehensive Wastewater Facilities Master Plan, Project No. 613, Department of Public Works, City of Baltimore, MD, 35 pp.

Environmental Resources Management (1999). Database report for water quality tasks. Comprehensive Wastewater Facilities Master Plan, Project No. 613, Department of Public Works, City of Baltimore, MD, 23pp .

Environmental Technologies Associates, Inc. (1998). Baltimore City comprehensive wastewater facilities master planning project, Task 202, stream sampling data. Prepared for Baltimore City Department of Public Works.

Eppley, R. W. (1972): Temperature and Phytoplankton growth in the Sea. Fishery Bulletin: vol. 70, p1063-1085.

Ferguson, J.F. and D. Simmons (1974). The fate of nutrients in Back River. CRC Publication No. 32, Chesapeake Research Consortium, Inc., The Johns Hopkins University, MD, 27 pp.

Fisher, T.R., Harding, L.W., Stanley, D.W., and L.G. Ward (1988). Phytoplankton, nutrients, and turbidity in the Chesapeake, Delaware, and Hudson estuaries. Estuarine, Coastal and Shelf Science 27: 61-93.

Fisher, T.R., Peele, E.R., Ammerman, J. W. and L. W. Harding (1992). Nutrient limitation of phytoplankton in Chesapeake Bay. Marine Ecol Prog Ser 82: 51-63.

Fisher, T.R., Gustafson, A.B., Sellner, K., Lacouture, R., Haas, L.W., Wetzel, R.L., Magnien, R., Everitt, B. and R. Karrh (1999). Spatial and temporal variation of resource limitation in Chesapeake Bay. Marine Biology 133: 763-778.

Flemer, D., Biggs, R., and V. Tippie (1983). Chesapeake Bay: A Profile of Environmental Change. U.S. Environmental Protection Agency, Region III. Philadephia, PA.

Garland, C.F. (1952). A study of water quality in Baltimore Harbor. Publication No. 96, Chesapeake Biological Laboratory, Department of Research and Education, Solomons Island, MD.

Genet, L., D. Smith, and M. Sonnen (1974). Computer program documentation for the dynamic estuary model, U.S. Environmental Protection Agency, Systems Development Branch, Washington, DC.

Glibert, P., M., Conley, D.J., Fisher, T.R., Harding, L.W. Jr , and T. Malone (1995). Dynamics of the 1990 winter/spring bloom in Chesapeake Bay. Marine Ecology Progress Series 122: 27-43.

Harding, L.W. Jr, M. Leffler, and G.B. Mackiernan (1992b). Dissolved oxygen in the Chesapeake Bay: a scientific consensus. Maryland Sea Grand College, Publication No. UM-SG-TS-92-03, College Park, MD.

Hutchinson, G. (1967). A treatise on limnology, Volume II, John Wiley and Sons, New York, 245-305.

HydroQual (1991). Water quality modeling analysis of hypoxia in Long Island Sound. HydroQual Inc., Mahwah, NJ.

Istvanovics, V. (1988). Seasonal variation of phosphorus release from the sediments of shallow Lake Balaton (Hungary). Water Research 22, 1473 -1481.

Johnson, B. H., Heath, R.E., and Bernard B. Hsieh (1991). User's guide for a three-dimensional numerical hydrodynamic, salinity, and temperature model of Chesapeake Bay. Technical Report HL-91-20, US Army Engineer Waterways Experiment Station, Vicksburg, MS.

Jordan, T.E., Correll, D.L., Miklas, J., and D.E. Weller (1991a). Nutrients and Chlorophyll at the interface of a watershed and an estuary. Limnol. Oceanogr. 36: 251-267.

Jordan, T.E., Correll, D.L., Miklas, J., and D.E. Weller (1991b). Long-term trends in estuarine nutrients and chlorophyll, and short-term effects of variation in watershed discharge. Marine Ecology Progress Series 75:121-132.

Kamp-Neilsen, L. (1974). Mud-water exchange of phosphate and other ions on undisturbed sediment cores and factors affecting the exchange rates. Archiv for Hydrobiologie 73, 218-237.

Kemp, W.M., and W.R. Boynton (1984). Spatial and temporal coupling of nutrient inputs to estuarine primary production: the role of particulate transport and decomposition. Bull. Mar. Sci. 35: 242-247.

Liu, Hui (2002): The development of a water quality model in Baltimore Harbor, Back River, and the adjacent Upper Chesapeake Bay. Master Thesis, Virginia Institute of Marine Science, The College of William and Mary. pp 144.

Magnien, R.E., D.K. Austina, and B.D. Michael (1993). Chemical /Physical

Properties Component. Level 1 Data Report (1984-1991). Maryland Department of the Environment, Baltimore, MD.

Malone, T.C. (1992). Effects of water column processes on dissolved oxygen, nutrients, phytoplankton, and zooplankton. In: Smith D.E., Leffler M, Mackiernan G.(eds), Oxygen dynamic in the Chesapeake Bay, a synthesis of recent research. MD Sea Grant UM-SG-TS-92-01. College Park, Maryland, pp 61-112.

Malone, T.C., Falkowski, P. G., Hopkins, T. S., Rowe, G. T. and T. E. Whiteledge (1983). Mesoscale response of diatom populations to a wind event in the plume of the Hudson River. Deep Sea Research 30: 149-170.

Malone, T.C., L.H.Crocker, S.E. Pike, and B.W. Wendler (1988). Influence of river flow on the dynamics of phytoplankton production in a partially stratified estuary. Marine Ecology Progress Series, Vol. 48: 235-249.

Maryland Environmental Service (1974). Seminar on Water Pollution in the Baltimore Area. Maryland Environmental Service, Annapolis, MD.

Monod, J. (1949). The growth of bacterial cultures. Annual Review of Microbiology 3: 115-130.

Mortimer, C. H. (1941). The exchange of dissolved substances between mud and water. I and II. J. Ecol., 29:29:280-329.

Mortimer, C. H. (1942). The exchange of dissolved substances between mud and water in lakes. III and IV. J. Ecol., 30:147-201.

Newcombe, C. L. and W. A. Horne (1938). Oxygen-poor waters in the Chesapeake Bay. Science 88: 80-81.

Nixon, S.W. (1981). Remineralization and nutrient cycling in coastal marine ecosystems. In : Neilson, B.J.,Cronin, L.E. (eds). Estuaries and Nutrients. Humana Press, Clifton, New Hersey, 111-138.

Officer, C.B., Biggs, R.B., Taft, J.L., Cronin, L.E., Tyler, M. and W.R. Boynton (1984). Chesapeake Bay anoxia: Origin, development, and significance. Science 223: 22-27.

Park, K., Kuo, A.Y., Shen, J., and J.M. Hamrick (1995). Hydrodynamic-

eutrophication model (HEM-3D): Description of water quality and sediment process submodels. SRAMSOE No. 327, VIMS, College of William and Mary, VA.

Patapsco/Back Rivers Watershed Study (1995). Coastal Environmental Services, Inc. Linthicum, MD.

Pritchard, D.W., and J.H. Carpenter (1960). Measurements of turbulent diffusion in estuarine and inshore waters. Bull. Inter. Assoc. Sc. Hydrol. 20, 37 pp.

Riebesell, U. (1989). Comparison of sinking and sedimentation rate measurements in a diatom winter/spring bloom, Marien Ecology Progress Series, 54: 109-119.

Rhoads, D.C., Tenore, K. and M. Browne (1973). The role of resuspended bottom mud in nutrient cycles of shallow embayments. Estuarine Research, pp563-579.

Richardson, T., and J. Cullen (1995). Change in buoyancy and chemical composition during growth of a coastal marine diatom: ecological and biogeochemical consequences, Marine Ecology Progress Series, 128, 77-90.

Robertson, P.G. (1977). Back River- An Assessment of Water Quality and Related Fish Mortalities. Maryland Department of Natural Resources, Water Resources Administration, Water Quality Service, Annapolis, MD. 133 pp.

Sanford, L.P., Chao, S.Y., Halka, J.P., Maa, J.P.Y., Suttles, S.E., Wu, S., Ortt, R., and M.L. Chang (1996). Suspended sediment transport in Baltimore Harbor. The university of Maryland center for environmental and estuarine studies (UMCEES), Horn Point environmental laboratory (HPEL), Cambridge, MD.

Schubel, J. R. and D. W. Pritchard (1986). Estuaries. Vol.9, No. 4A, 236-249 pp.

Seitzinger, S. P. (1986). The Effect of pH on the Release of Phosphorus from Potomac River Sediment, Div. Env. Res., Academy of Natural Sciences of Philadelphia.

Seliger, H.H, J.A. Boggs, and W.H. Biggley (1985). Catastrophic anoxia in the Chesapeake Bay in 1984. Science 228: 70-73.

Seliger, H.H., McKinley, K.R., Biggley, W.H., Rivkin, R.B., and K.R.H. Aspden (1981). Pytoplankton patchiness and frontal regions. Marine Biology 61: 119-131.

Sellner, K.G., Sellner, S.G., Lacouture, R.V. and R.E. Magnien (2001). Excessive nutrients select for dinoflagellates in the stratified Patapsco River estuary: Margalef reigns. Mar Ecol Prog Ser. Vol. 220: 93-102.

Sinex, S.A. and G.R. Helz (1982). Entrapment of Zinic and Other Trace Elements in a Rapidly Flushed Industrialized Harbor. Environ. Sci. Technol., 16: 820-825.

Stroup, E.D., Pritchard, D.W. and J.H. Carpenter (1961). Final Report Baltimore Harbor Study. Chesapeake Bay Institute Tech. Rep. XXVI, 79 pp.

Stumm, W. and J. J. Morgan (1981). Aquatic chemistry. John Wiley and Sons, Inc, New York, 580 pp.

Taft, J.L., Hartwig, E.O., and R. Loftus (1980). Seasonal oxygen depletion in Chesapeake Bay. Estuaries 3: 242-247.

Thomann, R. V., Jaworski, N. J., Nixon, S. W., Pearl, H. W. and J. Taft (1985). Executive summary: the1983 algal bloom in the Potomac estuary. March 14, 1985.

Titman, D., and P. Kilham (1976). Sinking in freshwater phytoplankton: some ecological implications of cell nutrient status and physical mixing processes. Limnology Oceanography. 21:409-417.

Tyler, M.A. and H.H. Seliger (1978). Annual subsurface transport of a red tide dinoflagellate to its bloom area: water circulation patterns and organism distributions in the Chesapeake Bay. Limnology and Oceanography, 23(2): 227- 246.

Waite, A., Thompson, P., and P. Harrison (1992). Does energy control the sinking rates of marine diatoms? Limnology and Oceanography, 37(3), 468-477.

Wang, H.V., Sin, Y., and S.-C. Kim (in press) The development of a water

quality model for Baltimore Harbor, Back River and the adjacent Upper Chesapeake Bay, I: biological, chemical and physical characteristics of the Baltimore Harbor (Patapsco River) and Back River in the Upper Chesapeake Bay. SRAMSOE No. xxx, VIMS, College of William and Mary, VA.

Weaver, B.J. (1995). Sediment-water oxygen and nutrient exchange in the tidal Patapsco /Baltimore Harbor and Back River tributaries, University of Maryland center for environmental and estuarine studies (UMCEES). Reference No. [UMCEES]CBL 95-170. Chesapeake Biological Laboratory, Solomons, MD.

Wezernak, C. and J. Gannon (1968). Evaluation of nitrification in streams, Journal of the Sanitary Engineering Division, 94(SA5), 883-895.

Wilson, R. E. (1970). A Study of the Dispersion and Flushing of Water-borne materials in the Northwest Branch of Baltimore Harbor, and the Relationship Between These Physical Processes and the Water Quality of the Inner Harbor. Chesapeake Bay Institute Tech. Rep. 64, 75 pp.